Experimental and Analytical Evaluation of the Strength of Selected Truss Members from the Approach Spans of the Winona Bridge

Jason B. Lloyd, Leslie E. Campbell,
Francisco J. Bonachera Martín, Robert J. Connor

S-BRITE Center
PURDUE UNIVERSITY

JOINT TRANSPORTATION RESEARCH PROGRAM
Discovery with Delivery
Since 1937
JTRP

INDIANA DEPARTMENT OF TRANSPORTATION
INDOT

PURDUE UNIVERSITY

RECOMMENDED CITATION

Lloyd, J. B., Campbell, L. E., Bonachera Martín, F. J., & Connor, R. J. (2019). *Experimental and analytical evaluation of the strength of selected truss members from the approach spans of the Winona Bridge.* West Lafayette, IN: Purdue University. https://doi.org/10.5703/1288284316925

AUTHORS

Jason B. Lloyd
Purdue University

Leslie E. Campbell
Purdue University

Francisco J. Bonachera Martín
Purdue University

Robert J. Connor
Purdue University

ACKNOWLEDGMENTS

This project was funded by the Transportation Pooled Fund (Study Number TPF-5(281)). Participating agencies included the Minnesota Department of Transportation and Federal Highway Administration. This project benefited from substantial material donations provided by Steel Dynamics Inc., SSAB Americas, and Nucor Plate. In addition, the authors acknowledge the essential contributions from staff professionals and graduate students at Purdue University throughout this research.

NOTICE

ABSTRACT

The following report details a research project comprised of two phases. Phase I included the full-scale experimental testing of two built-up truss chord members removed from service. The members were installed into a reaction frame and loaded to failure to determine remaining capacity in the presence of pack rust, as well as after-failure load redistribution behavior mimicking the member in a state following complete fracture of half the cross section. Phase I also included a finite element–based parametric study calibrated by the experimental work. The study was focused on two-channel axially loaded members for the purpose of developing closed-form solutions intended for evaluation of internal member redundancy. During Phase II of the project, a small round-robin-style inspection and load rating study was performed with certified bridge inspectors and practicing load rating engineers. The purpose was to investigate the variability in the inspection and evaluation of severely corroded steel tension members. This process evaluated two separate, but related, sources of variability within the inspection and load rating process. The variability in each task was controlled such that variability in the load ratings was not compounded by variability in the inspection findings.

CONTENTS

LIST OF TABLES

LIST OF FIGURES

1. INTRODUCTION

The research project was comprised of two distinct phases. Phase I included the experimental and analytical studies of the bridge specimens, involving a parametric study of two-channel members for purposes of developing closed-form solutions intended for evaluation of internal member redundancy and after-fracture stress range calculations. Phase II included a round-robin study investigating variability of inspection results for corrosion damaged members, as well as the variability of load rating resulting from inspection data for corrosion damaged members. This report details Phase I activities, performed on truss members from approach span 16 of the Winona Bridge. The research was conducted at Purdue University's Robert L. and Terry L. Bowen Laboratory for Large-Scale Civil Engineering Research. The final report for Phase II is forthcoming.

The Research Team (RT) received several individual truss members from the bridge in late summer of 2017. Figure 1.1 and Figure 1.2 show the general condition of the specimens in the as-delivered condition. The condition of the rolled channels included some minor section loss along the top interior edges resulting from corrosion. Areas of significant pack rust were evident between the channels and the cover plates along much of the length of the chords to a depth equal to the first row of stitching rivets. The gusset connections for the L2–L6 tension chord sections had some very light corrosion damage, as well. No fatigue or fracture damage was visually detected by the RT. However, severe section loss at localized areas of the channel cover plates that resulted in crack-like defects were noted by the RT. These are briefly discussed later in the report.

1.1 Modification to Original Scope of Work

As was presented during discussion following the submission of Interim Report #1 with the Minnesota Department of Transportation (MNDOT) and the Federal Highway Administration (FHWA) personnel, a modest change to the scope of the project was made to Task 1 "Member Capacity Testing," which is part of Phase I work.

The specific changes were as follows:

- Since only two primary chords were received, only testing on two components was possible.
- Upon inspection, it was concluded that the section loss on these two members was not very significant. In fact, as will be discussed, the section loss and pack out that were present did not appear to reduce the capacity of the member. Since the overall capacity of the member appeared to be unaffected by the corrosion in the as-received condition, the Research Team (RT) determined there was little reason to conduct additional capacity testing on other smaller components that have similar or less corrosion damage.
- In lieu of the portion of the original scope of work that could not be completed as discussed above, the RT performed alternative testing to evaluate the internal redundancy of the members. There is considerable interest

Figure 1.1 Winona Bridge Specimens as they arrived.

Figure 1.2 View of corrosion damage resulting in section loss and pack rust.

in the topic of internal redundancy of truss-type FCMs and these alternative tests have greatly contributed to the efforts of moving recently adopted AASHTO provisions forward.

2. MATERIAL TESTING

Material was removed from a cover plate, a channel web, and two gusset plates in order to test for Charpy V-notch energy (for estimation of the material toughness), yield strength, tensile strength, and chemical composition. All material testing was performed according to requirements of ASTM E415, ASTM E8, and ASTM E23. Table 2.1 provides the results of the chemistry test showing element percentages that are within the relatively loose standards of the ASTM A7 steel that likely would have been specified at the time of the construction of the Winona Bridge in the late 1930s. This is compared to the 1949 issue of ASTM A7, which was the earliest issue available to the RT at the time of this report and likely similar to the current issue at the time of the Winona Bridge fabrication. ASTM A36 standard did not become a dominant steel in construction until the early 1960s. The mechanical properties shown in Table 2.2 are also consistent with minimums shown in the ASTM A7 (issued in 1949). ASTM A7 required a minimum 24% elongation in 2 inches, a minimum yield strength of 33 ksi, tensile strength of 60 to 75 ksi for shapes of all thicknesses, and tensile strength of 60 to 72 ksi for plates up to 1.5 inches thick. The tests revealed the steel demonstrated considerably more elongation over the 2-inch gauge length than the minimum specified value, suggesting higher ductility. Two samples were taken from each of two gusset plates. One sample was oriented parallel with the longitudinal axis of the tension chord ("Horizontal") and one sample was oriented perpendicular to the longitudinal axis of the tension chord ("Vertical"). This was done in order to observe whether differences in the material properties exist between the perpendicular directions, since often times the rolling direction of gusset plates cannot be visually detected. With one exception, differences of less than 2% were measured between opposing directions suggesting uniform, orthotropic mechanical properties. The one exception was the *elongation in 2 inches* for the two directions of Gusset Plate 2, where a *difference* of 13% was measured.

Although some limited chemical specifications and tensile capacity minimums were typically provided in early steel specifications, toughness was not. Toughness is a material property that quantifies the ability of a material to resist fracture in the presence of a crack. Direct measurement of toughness requires costly testing and relatively large piece of material. As a result, an economical alternative often used is the Charpy V-notch Impact (CVN) test. These tests are not a direct measure of toughness, rather a measure of energy absorption. Using accepted correlation methods, actual fracture toughness can be estimated from CVN data.

Typically, many CVN impact specimens are tested in an effort to fully characterize the full temperature transition curve, establishing the lower shelf, transition, and upper shelf regions of the material. A minimum of three specimens are normally tested at each temperature to characterize inherent scatter in the data. Eighteen CVN specimens were obtained from a rolled channel web and from a cover plate (36 specimens, total) in an effort to develop a complete CVN temperature transition curve

TABLE 2.1
Chemical composition of the Winona Specimens

Element	Channel Web	Cover Plate	Gusset Plate 1	Gusset Plate 2
Carbon (%)	0.23	0.24	0.25	0.26
Manganese (%)	0.49	0.5	0.42	0.63
Phosphorus (%)	0.016	0.016	0.009	0.024
Sulfur (%)	0.015	0.016	0.030	0.046
Silicon (%)	0.05	0.05	0.02	<0.005
Nickel (%)	0.04	0.04	0.03	0.03
Chromium (%)	0.05	0.05	0.02	0.04
Molybdenum (%)	0.01	0.01	0.01	0.01
Copper (%)	0.04	0.04	0.02	0.03

TABLE 2.2
Mechanical properties of the Winona Specimens

	Channel Web	Cover Plate	Gusset Plate 1: Horizontal Orientation	Gusset Plate 1: Vertical Orientation	Gusset Plate 2: Horizontal Orientation	Gusset Plate 2: Vertical Orientation
Tensile Strength (ksi)	66.1	69.6	63.7	64.0	70.7	69.9
Yield Strength @ 0.2% Offset (ksi)	38.6	40.5	36.1	35.2	41.4	42.6
Elongation in 2 inches (%)	37.5	31.2	34.3	33.5	30.2	26.7

(see Figure 2.1). However, the more data for each test temperature, the more reliable the estimate of toughness becomes. Therefore, more specimens were tested at selected temperature, such as 40°F and 70°F. Due to the single-digit energy measurements observed at 10°F, it was determined unnecessary to test at any cooler temperatures. The warmest temperature tested was 100°F at which the CVN data appear to remain in the transition region, but may also be approaching the upper shelf portion of the curve.

As noted in the figure, the specimens from the cover plate were "sub-size." A standard CVN specimen is 10 mm × 10 mm × 40 mm long. However, because the cover plate is only 3/8 inch thick (9.5 mm), a full-size CVN could not be machined and thinner, or sub-size specimens, measuring 7.5 mm × 10 mm × 40 mm long were required. Standardized testing of sub-size CVN specimens can be performed. The smaller thickness dimension of a sub-size specimen can influence the results in two ways. First, the thinner material has a reduced cross sectional area, which reduces its ability to absorb energy. This means the absorbed energy of a sub-size specimen will be less than that of a standard size specimen. Second, the reduced thickness of a sub-size specimen reduces the tri-axial constraint against plastic flow. This means that the sub-size specimen will be more ductile making cleavage fracture less likely to occur. This effect results in fracture mode transition temperatures that are lower for sub-size specimens than for standard size specimens. As a result, the American Petroleum Institute (API) Fitness-For-Service manual (API 579-1/ASME FFS-1, 2007) provides guidance for the adjustment of the measured CVN energy absorbed and the test temperature at which the sub-size specimens are tested. These adjustments account for the two effects of the sub-size specimen, which is reflected in the data plotted in Figure 2.1 and listed in Table 2.3. In other words, the data in the table and the figure have been converted to "full-size" equivalent values.

Using the Master Curve Method, the fracture toughness was estimated from CVN impact energy data. Correlation of CVN data was performed for the Winona Bridge Specimens using the British Standard 7910:2013, *Guide to Methods for Assessing the Acceptability of Flaws in Metallic Structures*, Annex J. There is no North American equivalent of this standard, and it is often referenced within the United States for estimation of fracture toughness and fitness-for-service (FFS) evaluations. Equation (2.1) below is Equation J.4 from this standard and is used to correlate CVN data to fracture toughness. Each parameter is explained below.

$$K_{mat} = 20 + \{11 + 77e[0.019(T - T_0 - T_K)]\}\left(\frac{25}{B}\right)^{\frac{1}{4}} \left[Ln\left(\frac{1}{1-P_f}\right)\right]^{\frac{1}{4}} \quad \text{(Eq. 2.1)}$$

Where:

$\boldsymbol{K_{mat}}$ = Material toughness measured by stress intensity factor (MPa-$\sqrt{m}$)

$\boldsymbol{T}$ = the temperature at which K_{mat} (material toughness) is to be determined (°C)

$\boldsymbol{B}$ = Thickness of the material for which an estimate of K_{mat} is required (mm)

$\boldsymbol{T_K}$ = 25°C. The term T_K can be thought of as the term intended to reflect the scatter (in terms of variation in temperature) at which one could expect an impact

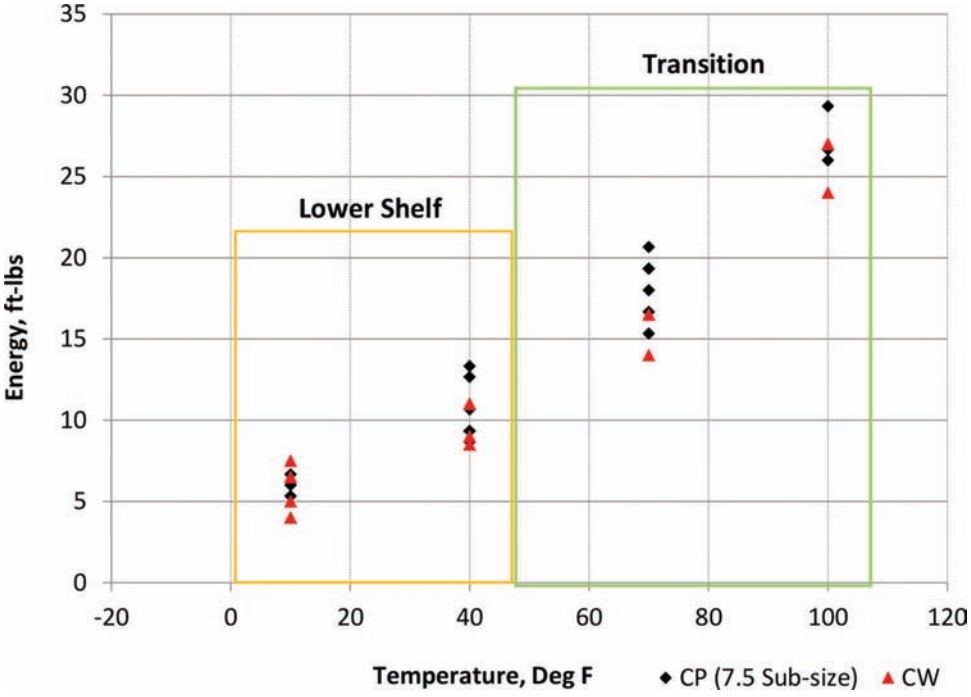

Figure 2.1 Plot of CVN impact energy vs. temperature: cover plate (CP) and channel web (CW).

TABLE 2.3
Estimated toughness values at 5% and 50% probability of failure

Test Temperature (°F)	Average CVN for Winona Channel (ft-lbs)	Average CVN for Winona Cover Plate (ft-lbs)	Channel Web		Cover Plate	
			Estimated K_{mat}, P_f=5% (ksi-√in)	Estimated K_{mat}, P_f=50% (ksi-√in)	Estimated K_{mat}, P_f=5% (ksi-√in)	Estimated K_{mat}, P_f=50% (ksi-√in)
70	16.0	18.2	54	87	59	97
40	10.0	10.7	46	71	50	79
10	6.8	6.0	40	60	43	66

energy of 27J. The value of 25°C is related to a 15°C standard deviation and 90% confidence. BS 7910:2013 (British Standards Institute, 2013) does allow for a lower value of T_K to be used if supported by experimental data for the material of interest. Lacking such data, the RT has used T_K = 25°C. (°C)

$\boldsymbol{T_{27J}}$ = 24°C (for cover plate), 28°C (for channel web). T_{27J} is the temperature at which 27J is measured for a standard 10 mm × 10 mm CVN specimen. This value is used in estimating the T_0 temperature. T_{27J} (and T_{40J}, which is similar in purpose) are used in BS7910 because they correspond to typical requirements in steel specifications. (°C)

$\boldsymbol{T_0}$ = 6°C (for cover plate), 10°C (for channel web). T_0 refers to a reference temperature at which the material of interest has a fracture toughness of 91 ksi-√in (100 MPa-√m). The Master Curve is based on a hypothesis that states that all grades and heats of ferritic steel will only vary in the temperature value T_0. This variable can be thought of as an "anchor" point for the specific steel that is being evaluated. Some suggest that the lower bound CVN data should be used when establishing T_{27J} because this value is used to calculate T_0, as seen in Equation (2.2), which is Equation J.2 in BS 7910:2013. However, it is also recognized that such an approach can be overly conservative when also using T_K = 25°C, which already accounts for scatter in the CVN data. Hence, considering these factors it was decided to use the average CVN data to obtain T_0, combined with T_K = 25°C in Equation (2.1) (°C)

$$T_0 = T_{27J} - 18°C \qquad \text{(Eq. 2.2)}$$

$\boldsymbol{P_f}$ = 5% and 50%. P_f is the probability of the actual K_{mat} (material toughness) being less than estimated. 5% and 50% were both used for separate estimates. Normally, for a FFS assessment where an existing structure is being evaluated and a level of conservatism is prudent in determining the safety of a structure that contains cracks, P_f = 5% is recommended (a 95% confidence limit). However, sometimes higher risk is acceptable in order to determine a reasonable estimate that is as accurate as possible without being too conservative. In these cases a P_f = 50% is more appropriate for estimating the material property. Both have been provided herein.

Table 2.3 contains a summary of the results of the CVN tests at the specified temperatures, which is based on the combined data set for all four angles tested. It also includes the estimated fracture toughness of the material as a function of temperature. The resulting estimated toughness values are not considered uncommon for bridge steels of the era of the Winona Bridge. Note that BS 7910:2013 is intended for lower shelf/transition behavior and advises that limits should be in place for Master Curve correlations to ensure that materials with low upper shelf Charpy energy are not overestimated. The upper limit for K_{mat} is more important when estimating fracture toughness of in-service structures rather than those removed from service. That said, it is the opinion of the RT that estimates of fracture toughness for the tested material at temperatures above 70°F (beginning of the transition region) may not be accurate and consequently have been excluded from the Charpy-toughness correlation. BS7910 includes upper-bound limits when estimating fracture toughness from CVN data, which would also limit the calculated values at these temperatures. The raw CVN data obtained from each component, as well as the Master Curve plots for 5% and 50% probability of failure, are included in Appendix A.

As a point of interest, Table 2.4 compares the modern CVN impact energy requirements from Section 6 of the *AASHTO LRFD Bridge Design Specification* with the average CVN impact energy test results for the Winona Bridge at the service temperature indicated. As can be seen, the only category for which the historic steel would meet the modern specification is *Zone 1 Nonfracture-critical. (It is noted that the bridge was located in Winona, Minnesota, which is classified as Minimum Service Temperature Zone 2 and would presently be required to meet the FCM CVN requirements.)* However, since no requirements were in place at the time the bridge was constructed, it is not surprising or uncommon for bridge steels like this not to meet modern ASTM specified minimums. Nevertheless, recent research at Purdue University for internal redundancy of mechanically fastened built-up members has unequivocally concluded that the toughness of steels for built-up members is not critical to the redundancy of the member (Hebdon, Korkmaz, Martín, & Connor, 2015; Lloyd, Bonachera Martín, Korkmaz, & Connor, 2018). A characteristic of built-up members referred to as cross-boundary fracture resistance (CBFR) enables the member to arrest running fractures at the boundaries between components stopping the fracture from propagating across the entire cross section,

TABLE 2.4
Comparison of CVN impact energy for Grade 36 steel

Service Temperature (°F)	AASHTO Fracture-Critical (ft-lbs)	AASHTO Nonfracture-Critical (ft-lbs)	Average for Winona Channel (ft-lbs)	Average for Winona Cover Plate (ft-lbs)
70 (Zone 1)	25	15	16.0	18.2
40 (Zone 2)	25	15	10.0	10.7
10 (Zone 3)	25	15	6.8	6.0

regardless of how poor the fracture toughness of the steel may be.

3. SETUP FOR EXPERIMENTAL TESTING

Two specimens cut from the tension chord of Span 16 were identified as candidates for the member capacity testing. A horizontally oriented self-reacting load frame was designed with capacity for 1.5 million pounds and was fitted with four hydraulic jacks, each having capacity for 300 kips, for a total payload of 1.2 million pounds. Two 60-foot-long W24 × 146 rolled wide flange beams were used in this frame and were sized and braced to ensure the frame possessed sufficient axial stiffness and buckling capacity. The reaction columns for the load frame were fabricated from these wide flange beams and can be seen in Figure 3.1.

Load and reaction boxes were fabricated at the Bowen Laboratory, along with connection and splice plate components, and all bracing components. Figure 3.2 shows the specimen placed between the reaction columns with the loading box attached. Figure 3.3 shows a top-down perspective of this area. The four hydraulic jacks pushed against the loading box, reacting against the reaction columns resulting in the specimen being loaded in axial tension. A reaction box identical to the loading box was connected to the

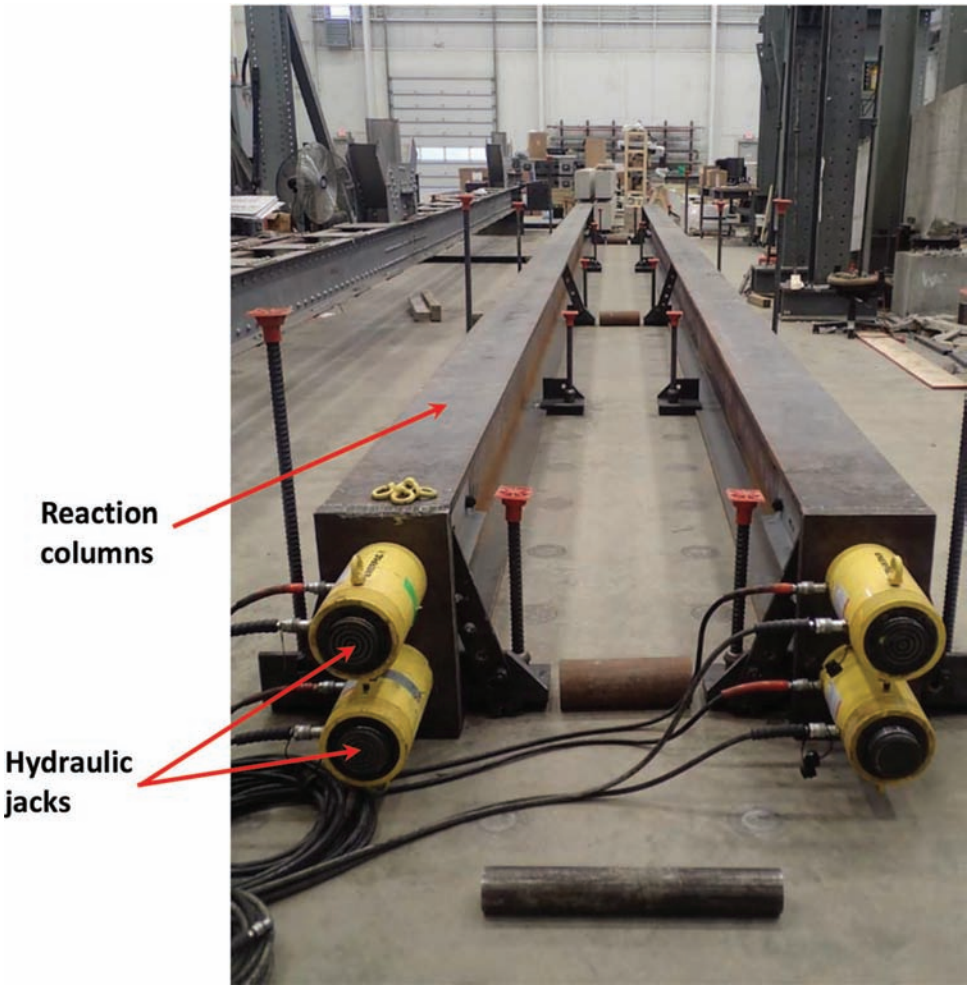

Figure 3.1 Self-reacting load frame with four hydraulic jacks.

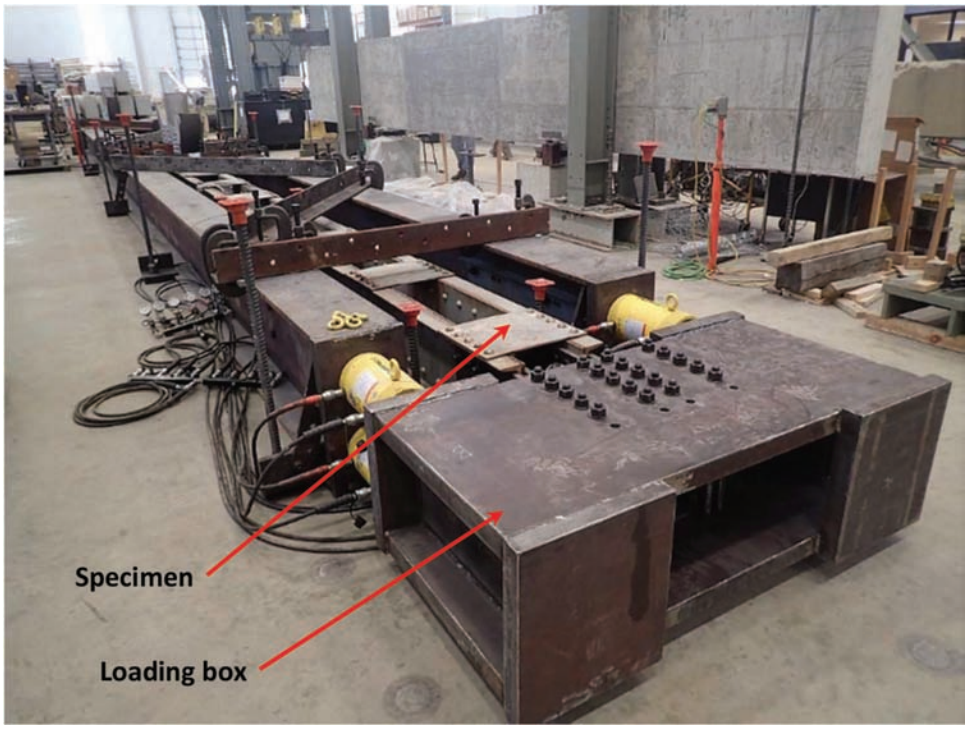

Figure 3.2 Load frame with specimen placed and ready for testing.

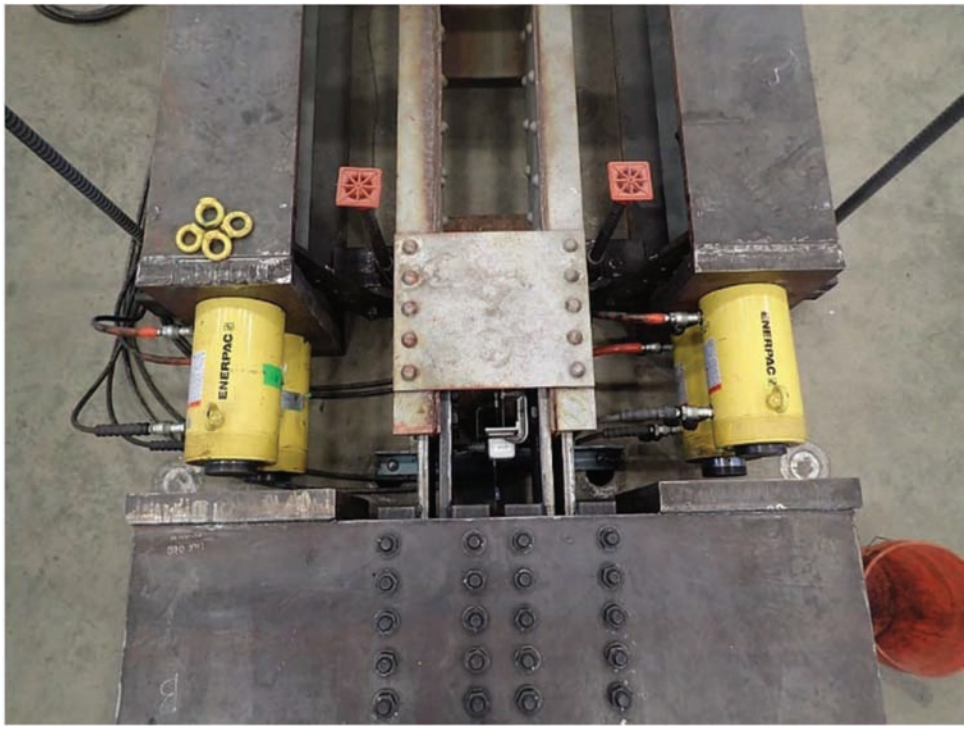

Figure 3.3 Top view of loading mechanism and specimen connection.

opposite end of the specimen providing a load path between the specimen and the reaction columns, seen in Figure 3.4. In this way the load was contained entirely within the load frame. Two connection plates clamped each of the two built-up channels at both ends of the specimen, being connected in bearing with high-strength bolts. The connection plates were welded to connection angles, which in turn were bolted to the load and reaction boxes, transferring load through fastener bearing.

Figure 3.4 Reaction box connection to the reaction columns.

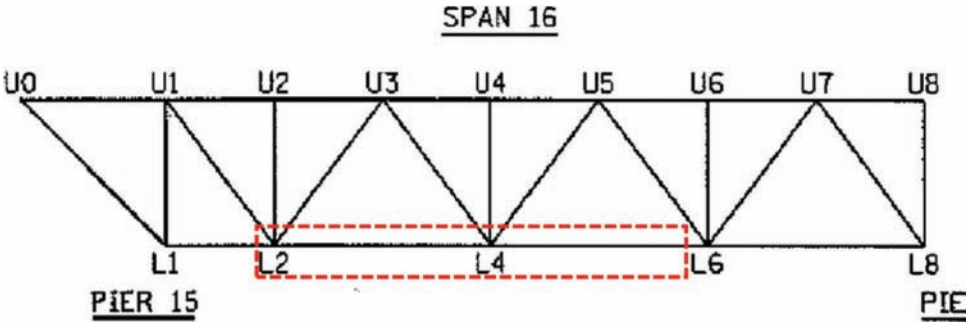

Figure 3.5 Winona Bridge Span 16 framing elevation.

Steel rollers can be seen along the length of the load frame in Figure 3.1. Smaller rollers are also placed along the length of the two reaction columns allowing the entire frame to effectively float without transferring load into the floor. This allowed the specimens to strain under tension and the reaction columns to strain under compression without preventing their relative movements. This aspect of the load frame was important because displacements of the long specimens were significant. For example, at the peak test load the specimens reached 1+ inch of axial extension.

Specimen 1 and Specimen 2 were two full-length tension chords removed from Span 16, as indicated in Figure 3.5 with the dashed red rectangle. Specimen 1 was from the east truss line chord and Specimen 2 was from the west truss line chord. The specimens were approximately 65 feet long upon arrival. Preparation of the specimens for testing included trimming each end to the length required to make the connection to the load frame. The final length of each of the specimens was 740.5 inches (61.7 feet). Rivets were removed at each end and bolt holes were drilled for connection to the load frame. The cross sectional area between L1 and L2 reduced to only the rolled channel, thus, to be able to test the full capacity of the larger cross section between L2 and L6, the RT installed an A992 Grade 50 splice plate near the L2 gusset plate and connection into the reaction box. The strengthening plate can be seen in Figure 3.6 where it is shown shortly after installation and prior to placing the specimen inside the load frame. All connections were bearing-type connection using ASTM F3125 Grade A325 high strength bolts. This allowed the RT to significantly reduce the number of required bolts, as well as the size of the loading and reaction boxes. It also made "shake down," explained later, an important part of the testing sequence.

Figure 3.6 Connection at the reaction end of the specimen showing the additional plate added to allow for strength testing of the main section of the specimen.

4. RESULTS OF STRENGTH TESTS

Strength tests were performed on Specimen 1 and Specimen 2 of the Winona Bridge Span 16 tension chords in the "as-delivered" condition. Following minor adaptation of the specimens described above to connect them into the loading frame, axial load was applied to the specimens to approximately 220% of the original design load. In addition, a section of Specimen 2 was later cooled and loaded to attempt brittle failure at a location deemed to be most susceptible to fracture due to existing corrosion damage. This test and the damage is detailed below. Data were collected during tests using bondable foil resistance strain gages that were installed on the cover plate, channel web, and channel flanges along the length of the specimen. A calibrated pressure transducer was placed in-line with the hydraulic system to measure load. Calibrated string potentiometers, which measure linear displacement, were installed at each end of the specimen. Two string "pots" were used so that relative displacement between the reaction and loading ends could be measured since the frame and specimen were free to move in either direction along the rollers. Thus, the actual axial elongation of the member could be calculated. Several load cycles were carried out on the first specimen to ensure settlement of the load frame and specimen connections. This is often referred to in laboratory testing as "shake down." Next, the specimen was incrementally loaded and then slowly released. The strains, load, and displacements were recorded for all tests.

Figure 4.1 plots the load-displacement curve for the final load cycles of Specimen 1, which was repeated two times (Test 5 and Test 6). The peak load was 1150 kips. The solid blue line is the estimated, or nominal, load-displacement curve based on a simple mechanics of materials equation for displacement of an axially loaded body (i.e., $\delta = PL/AE$). The measured curves correlated well with the nominal estimation and indicated a linear-elastic response to the load. The peak load of 1150 kips surpassed the original design load by 222% and effectively reached the capacity of the hydraulic jacks.

Figure 4.2 plots the load-displacement curve for the final load cycle of Specimen 2, which was not repeated until it after the section was cooled. The peak load was 1108 kips, however, some non-linear response can be seen to begin around 1060 kips. This most likely was either bolt slip or local yielding at fasteners connecting the specimen to the loading frame. No signs of yielding along the length of the specimen could be detected and all recorded net section stresses remained slightly below the measured yield strengths. Moreover, when the test was repeated (two times) later to a peak load of 1135 kips with a section of the member cooled, the specimen responded elastically indicating either fully seated bolts (most likely case), or possibly local strain hardening where yielding may have occurred in the previous test.

As was mentioned, an additional test was performed on Specimen 2 in which a section of Specimen 2 was cooled to a temperature of -30°F using a cooling chamber and liquid nitrogen, and then was loaded twice to the peak load of 1135 kips. Figure 4.3 shows the insulated wooden cooling chamber with liquid nitrogen being piped to all four surfaces of the member (two outside surfaces and two interior surfaces). The cooling chamber surrounded the two channels allowing the full cross section to be cooled. Temperature was monitored using two calibrated thermocouples. Note that at 10°F the specimen had merely single-digit CVN impact energy values (see Figure 2.1). It was cooled beyond 10°F to allow testing of the specimen prior to warming up. The section that was cooled was chosen because it had the greatest amount of corrosion damage, making it the most vulnerable to brittle failure. Figure 4.4 shows one side of the section that was cooled with two crack-like defects in the cover plate labeled *(Note that the specimen has been "white washed" to help observe yielding during*

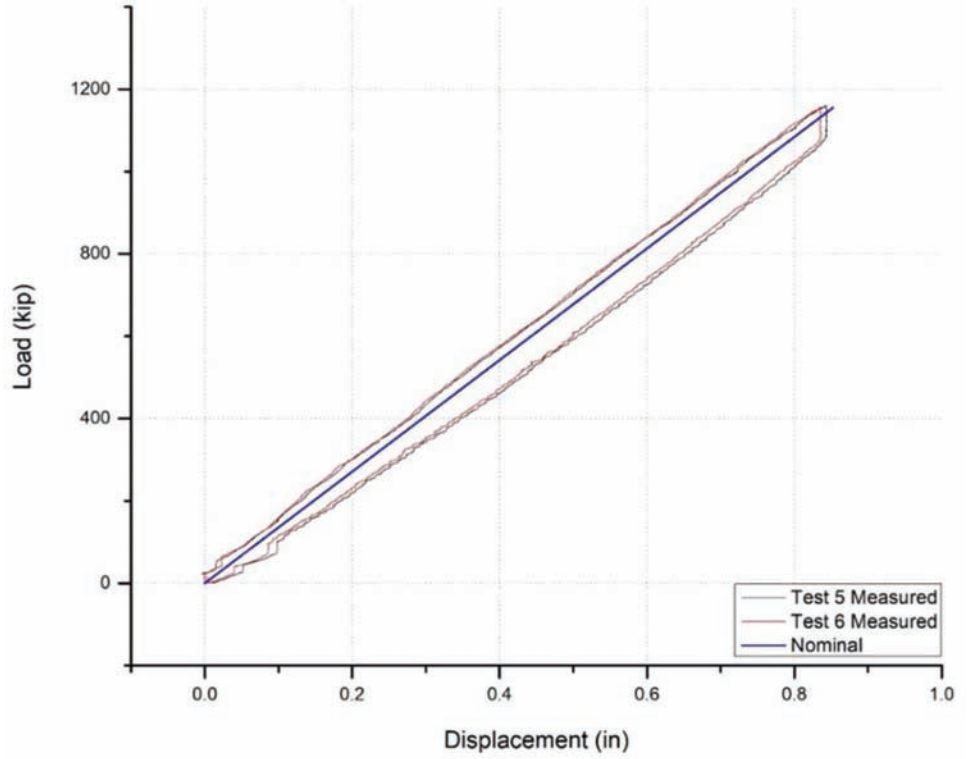

Figure 4.1 Plot of axial load vs. axial displacement for Specimen 1.

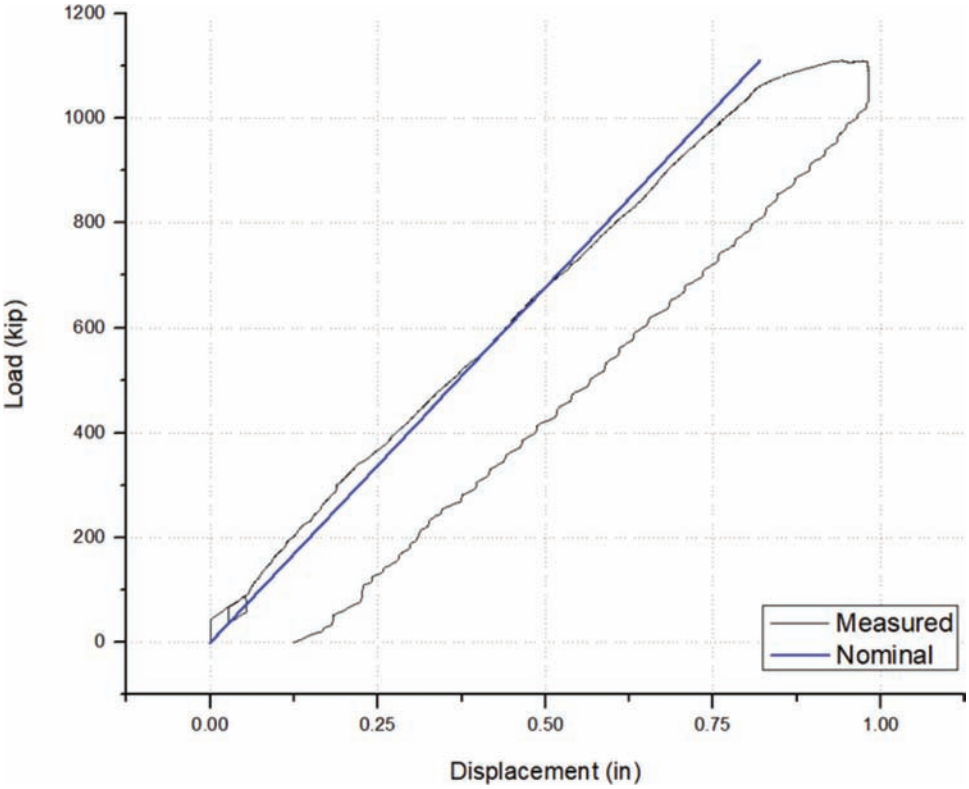

Figure 4.2 Plot of axial load vs. axial displacement for Specimen 2.

Figure 4.3 Cooling chamber used to cool section of Specimen 2 prior to testing.

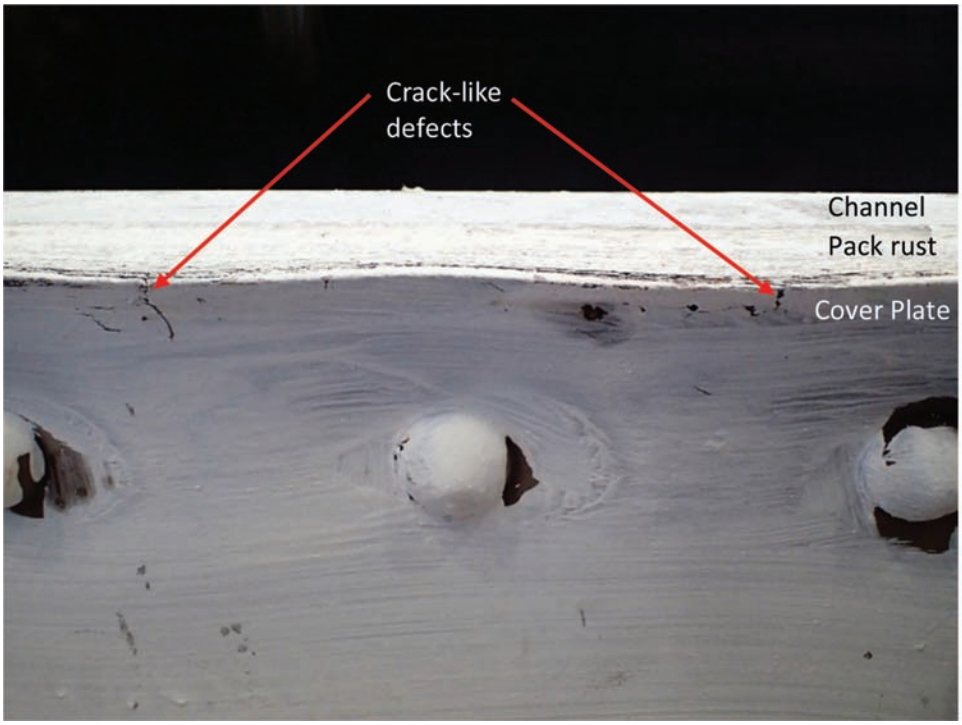

Figure 4.4 Section of Specimen 2 that was cooled for strength testing.

testing. Also, the opposite side (not pictured) has a small area of complete section loss of the cover plate near the top rivets.) These crack-like defects were identified prior to any testing; hence, it is clear that they did not result from testing. The research team believes these crack-like defects were the result of the cover plate section loss combined with the outward bending from the pack rust that caused a local failure. In other words, the thickness was reduced by corrosion and due to the pressure from the pack out between the plies,

TABLE 4.1
Summary of strength tests compared to nominal strength calculations

	Specimen 1	Specimen 2
Gross Area (in^2)	34.6	34.6
Net Area (in^2)	28.9	28.9
Original Design Load (kip)	517	517
Nominal Gross Section Yield (kip)	1,143	1,143
Nominal Net Section Fracture (kip)	2,023	2,023
Peak Test Load @ Room Temperature (kip)	1,150	1,108
Peak Test Load @ Cooled Temperature (kip)	–	1,135

simply cracked the plate. Upon closer inspection, no other cracks, such as due to fatigue, were detected in either member.

Table 4.1 summarizes the preliminary outcomes alongside the nominal strength calculations and original design load for the L2–L6 tension chord. *The term "nominal" refers to the loads and stresses calculated using the published ASTM A7 yield and tensile strengths of the steel.* It should be noted that the nominal gross section yield and net section fracture calculations do not take into account any capacity reductions for corrosion-related damage, such as section loss and pack out deformation. These calculations assume nominal, undamaged cross-sectional areas. That said, Specimen 1 slightly exceeded the nominal gross section yield load, reaching the capacity of the load frame hydraulic system, and coming to within 9% of the actual gross section yield capacity of the member. *The term "actual" refers to the loads and stresses calculated using the measured yield and tensile strengths of the steel, obtained through physical testing of the material.* Specimen 2 reached a peak load of just over 99% of the nominal gross section yield load, coming to within 10% of the actual gross section yield capacity of the member. This is remarkable considering that the actual and nominal estimates do not account for corrosion damage. Furthermore, it is estimated that due to the elastic response, the specimens would likely have reached the actual gross section yield capacity of about 1270 kips. Based on these results, it was concluded that the pack rust and minor section loss did not reduce the member strength limits in any observable way.

5. RESULTS OF INTERNAL MEMBER REDUNDANCY TESTS

Internal redundancy of mechanically-fastened built-up steel members has been a focus of several research projects at Purdue University. Numerous full-scale fatigue and fracture tests were performed for flexural members, as well as several full-scale fracture tests for axial members (Hebdon et al., 2015; Lloyd et al., 2018). However, the research was missing data on the behavior of continuous built-up axially loaded members that extended beyond a single span, or a single panel length. In other words, the RT was interested in understanding the load redistribution in long truss members as they span from panel point to panel point. Furthermore, the effects of component failures adjacent to a gusset plate or within the span of the members and the associated potential benefits that continuity across joints has with respect to restraining out-of-plane bending could be explored. The Winona Bridge members were excellent candidates for this type of testing providing the missing data needed to add to guide specifications that were recently adopted by AASHTO. The proposed specifications were also lacking criteria for two-component members, such as those comprised of two rolled channels connected through lattice or stay plates. The Winona Bridge members provided much-needed data to research this behavior by simply severing one entire half of the tension chord (cover plate and rolled channel) allowing the RT to collect data on the load redistribution behavior resulting from one half of the member failing. It should be noted that the RT has conducted research showing that it is not possible for a fracture of one component of a built-up member to propagate to an adjacent component. This is a characteristic of mechanically fastened built-up members referred to as cross-boundary fracture resistance (CBFR) (Lloyd et al., 2018). Thus, for the internally redundant member (IRM) testing of the Winona Bridge members, the components were severed using a thermal cutting procedure rather than by brittle fracture. Then the specimens were statically loaded allowing observation of load redistribution behavior. Thus, this process was not intended to test the dynamic response resulting from a fracture, rather the long-term, quasi-static load redistribution behavior of member after the fracture has already occurred.

5.1 Chronology of IRM Tests Conducted

First, half of Specimen 1 was completely severed at location "A," centered between the two gusset plates (see Figure 5.1 and Figure 5.2). In this faulted condition the specimen was loaded within the linear-elastic range, which was confirmed by strain gage data. Next, the cut at location "A" was spliced back together and the specimen was cut near the gusset plate at location "B," as can be seen in Figure 5.3. Then, in the faulted condition the specimen was loaded into the non-linear range plastically deforming the intact built-up channel.

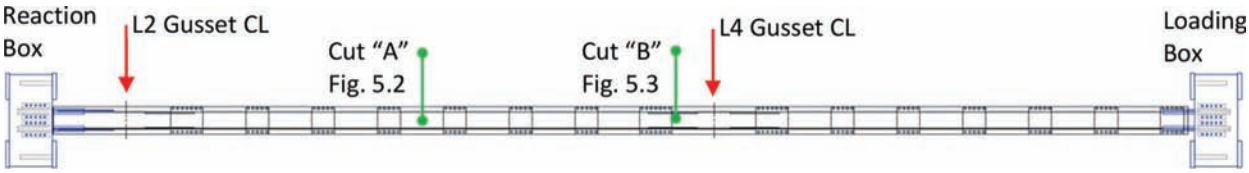

Figure 5.1 Plan view sketch of Winona Bridge Specimens showing locations of the member cuts.

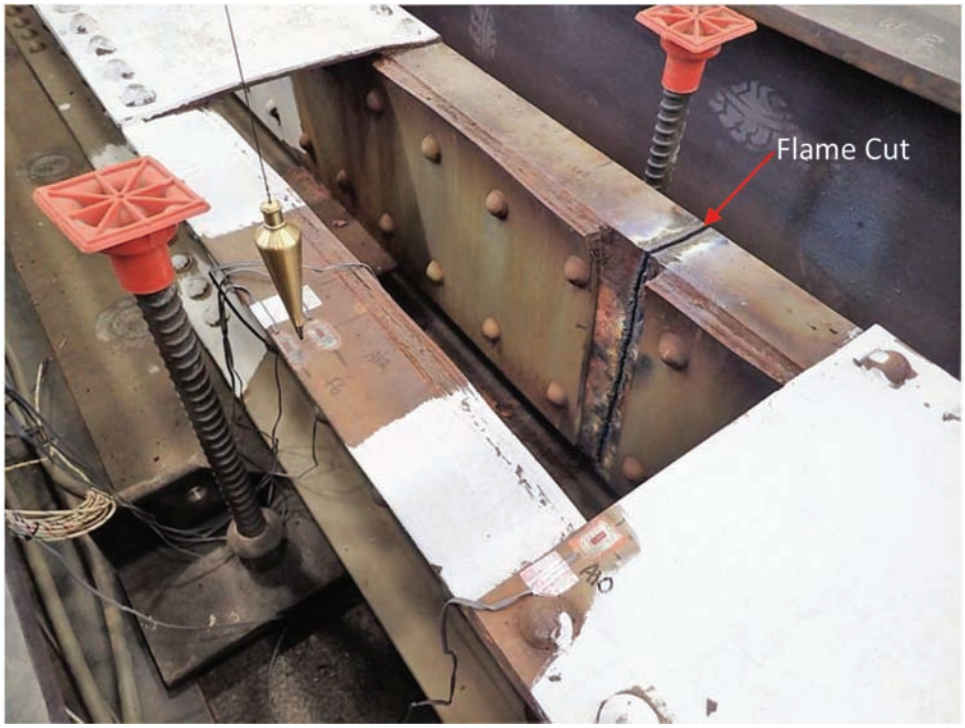

Figure 5.2 Example of component cut made at location "A" (see Figure 5.1).

Specimen 2 was tested with a complete cut at location "A" (identical to that for Specimen 1), as seen in Figure 5.2, and then loaded into the non-linear range, which was confirmed by strain gage data. Data from both sets of tests were used to calibrate finite element models allowing for parametric studies of two-component, truss-type built-up members.

5.2 Summary of IRM Test Results

Specimen 1 was initially severed at location "A," as described above in the chronology of testing. This was done to enable the RT to compare results to the elastic range of testing for Specimen 2. The results were consistent with that of Specimen 2 and therefore are not discussed in detail herein. Instead, the results for Specimen 2 are discussed for a member failure centered between gusset plates. Additionally, general behaviors and results are discussed in this section. Results specifically used to calibrate finite element models used in the parametric study of two-channel members are discussed in Section 6.1.

Three primary observations resulted from the laboratory IRM tests.

1. A second order moment resulting from load redistribution around the failure caused a global flexural response in the member. This moment is due to the shift in the centroid of the cross-section in the immediate portion of the member where the component was cut. The direction of bending was out-of-plane toward the failed component(s). This behavior was anticipated. Quantifying the second order moment and developing closed-form solutions for the calculation of the moment were core objectives of the parametric study that followed experimental testing.
2. Both specimens in the faulted condition were able to carry loads exceeding the calculated gross section yield loads (based on nominal ASTM A7 yield strength) despite the additional flexural stresses resulting from the second order moment.
3. Axial stiffness of the members in the faulted condition was reduced, as was expected. While this behavior is overtly obvious, it is mentioned here simply because it should be noted that it was ignored for development of the closed-form solutions making the results of the parametric study conservative in nature. Load shed due to a loss of axial stiffness in an actual truss bridge reduces the load demands in the member. In other words, it is conservative to assume the original dead load remains in the member between panel points. The same is also true for live load. This will also result in the actual fatigue stress ranges

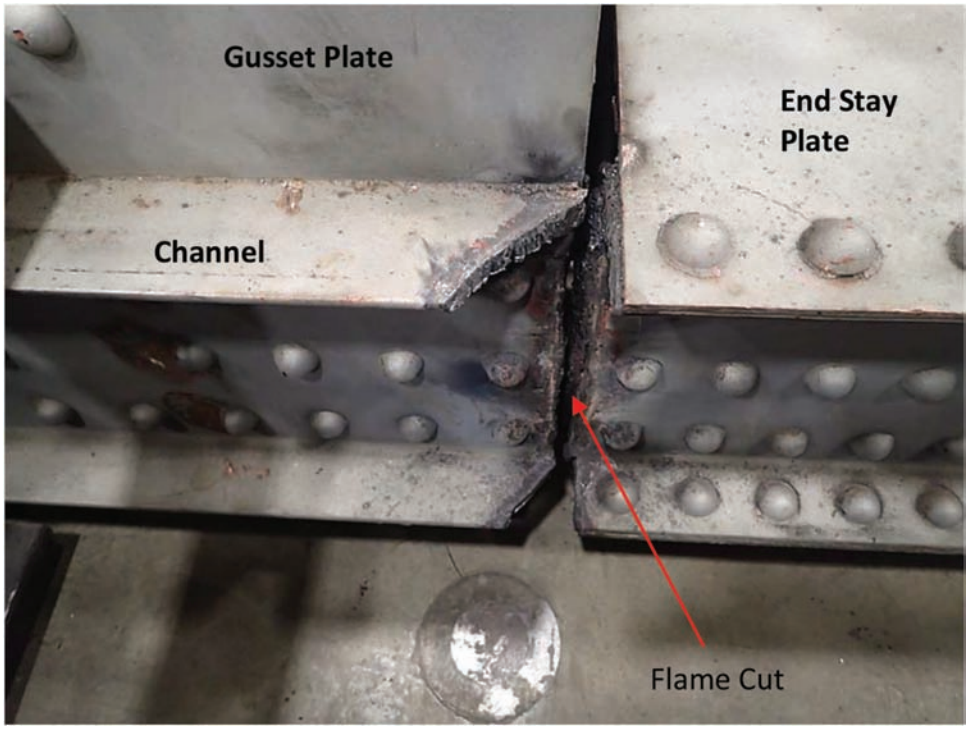

Figure 5.3 Cut at location "B" on Specimen 1 near the gusset plate (see Figure 5.1).

being lower than would be predicted by assuming the live load in the member remains unchanged before and after half of the member has failed.

5.2.1 Specimen 1 IRM Test Results

With Specimen 1 spliced at location "A" and severed at location "B," several load cycles were applied, including a final cycle up to 800 kips, as plotted in Figure 5.4. A calculated load-displacement curve has also been labeled as "Unfaulted" and plotted on the figure for the linear-elastic range, which *does not* take into account the loss of half the cross section. The "Unfaulted" curve is the same curve shown as "Nominal" on Figure 4.1 where it can be seen that in the unfaulted condition the behavior of the specimen was consistent with nominal predictions. The "Unfaulted" curve Figure 5.4 is also based on the equation for elastic displacement of an axially loaded body (i.e., $\delta = PL/AE$), where A is the gross area equal to the undamaged member, just as it was for Figure 4.1. However, in this case it is not equal comparison because the measured curve represents the member in the faulted condition with only half of its cross section at location "B" where localized slip and yielding reduced axial stiffness. As would be expected, the nominal calculation in the unfaulted condition estimated a stiffer load-displacement response then was measured. The difference in this case was about 18%. As discussed, in reality, this loss of axial stiffness would result in the member shedding some load to the stiffer adjacent members, such as cross members, diagonals, other chords etc. Similar behavior was observed by Diggelmann (2012) during testing on the Milton-Madison deck truss bridge. In this case, when half of a lower chord fabricated as a built-up channel member was severed, the stress measured in cross members, as well as in the truss line opposite the severed member were observed to increase. This is an important observation simply because all evaluation methods developed in this research conservatively assume the entire load originally carried by the faulted member remains in the faulted member. Some minor load shed from the damaged member should be expected and would improve performance of the damaged member by reducing fatigue load demands.

Table 5.1 provides the nominal (based on published ASTM A7 material properties) and actual (based on measured material properties) section capacity calculations for the specimen in the faulted state. The area calculations for Specimen 1 assume the cross section included the 1/2-inch splice plate and the rolled channel. This is because the channels were continuous through the joint, but the cover plates terminated at the gusset plate where 1/2-inch splice plates were used to carry the load across the discontinuity. This left the smallest net area near the gusset plate to be comprised of the splice plate and rolled channel. It can be seen in Figure 5.4 that the onset of yielding occurred around 600 kips, which was notably less than the actual gross section yield on the faulted section, calculated to be 754 kips. However, a yield load based on the net section was calculated to be approximately 625 kips. Although this was not actually observed, the research team believes that the specimen began to yield at fastener holes, most likely the first set of rivets shared by the splice plate and

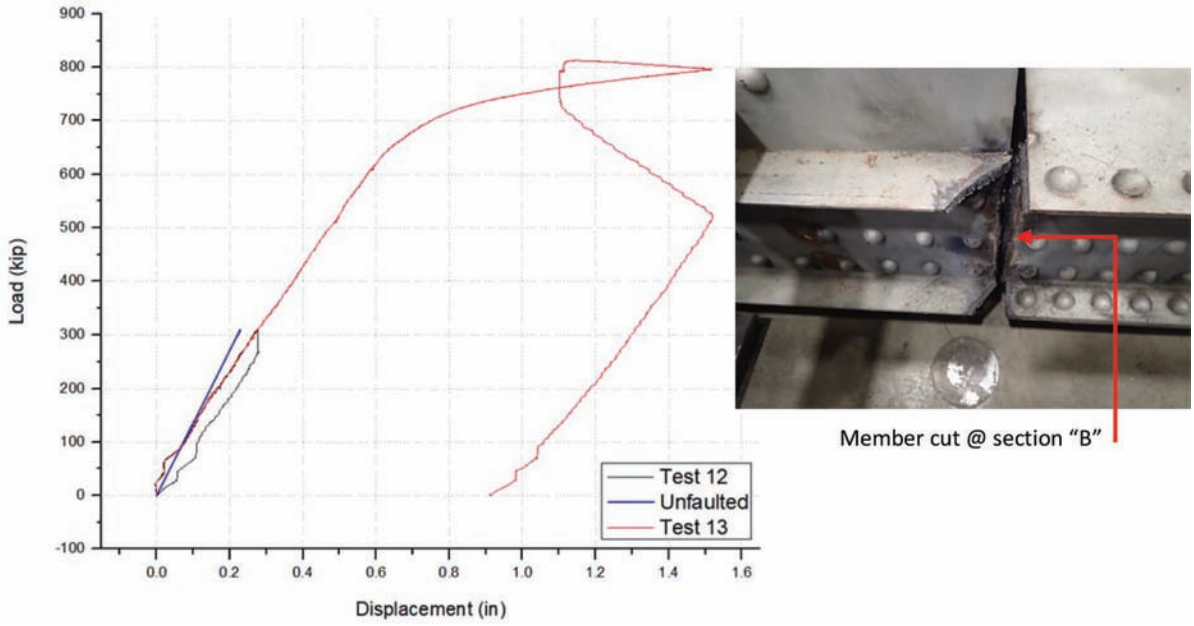

Figure 5.4 Load vs. displacement curve for Specimen 1 severed at location "B" (at gusset plate).

TABLE 5.1
Specimen 1 cross-sectional area and capacity calculations

	Specimen 1 (@ Location "B")
Gross Area (in^2)	19.2
Net Area (in^2)	15.9
Nominal Gross Section Yield (kip)	632
Actual Gross Section Yield (kip)	754
Nominal Net Section Fracture (kip)	954
Actual Net Section Fracture (kip)	1073
Peak Test Load (kip)	800

cover plate or gusset plate. These are also the locations of observed rivet slip in the final load cycle for Specimen 1. What is most important to notice, however, is that the faulted specimen exceeded the original design load of 517 kips (obtained from the original design drawings) by 15–20% before the onset of yielding and was able to reach about 1.5 times the design load before gross section yielding began to shed load. This is remarkable considering that the specimen was in the faulted state with only half of the original cross section intact. Furthermore, the specimen reached this load while also resisting additional flexural stress resulting from after-fracture second order moments at the location of the failure.

5.2.2 Specimen 2 IRM Test Results

With Specimen 2 severed at location "A," several load cycles were applied in order to perform a "shakedown" on the connections and ensure the specimen was seated into the load frame properly. Several additional static load cycles were applied up to a peak load of 647 kips. A few of these have been plotted in Figure 5.5 where cycles up to 300 kips remained linear-elastic and later cycles reaching loads of 600 kips or more produced permanent plastic deformation. The calculated nominal load-displacement curve of the member in the unfaulted condition has also been plotted as reference. In this case, the axial stiffness of the specimen in the faulted condition was reduced by 45% within the elastic range of loading, which would have resulted in load shed to adjoined members in an actual structure. This is notably more loss as compared to Specimen 1, likely due to the fact that Specimen 1 had the benefit of mutiple members and plates within the vicinity of the failure (cross member stubbs connecting gusset plates, bracing, etc.) helping to provide stiffness and load transfer. Table 5.2 provides the nominal (based on published A7 material properties) and actual (based on measured material properties) section capacity calculations for the specimen in the faulted state. Similar to Specimen 1, Specimen 2 experienced onset of what was likely a net section yeilding at about 500 to 550 kips, which is less than the calculated gross section yielding load of 679 kips. The 550 kip load closely corresponded with a yield load calculated on the net section of 565 kips. Once again, the faulted specimen was able to achieve loads in excess of the original design load, in this case by just over 25%, in addition to resisting the after-fracture second order moments induced by resdistribution of loads around the failure.

In both cases, the stay plates showed no sign of permanent deformation at the peak loads. This was surprising, particularly when considering that both specimens possessed considerable amounts of pack rust that had initiated out-of-plane deformation of the stay plates that would reduce their buckling capacity. An example of this is shown in Figure 5.6, which was taken

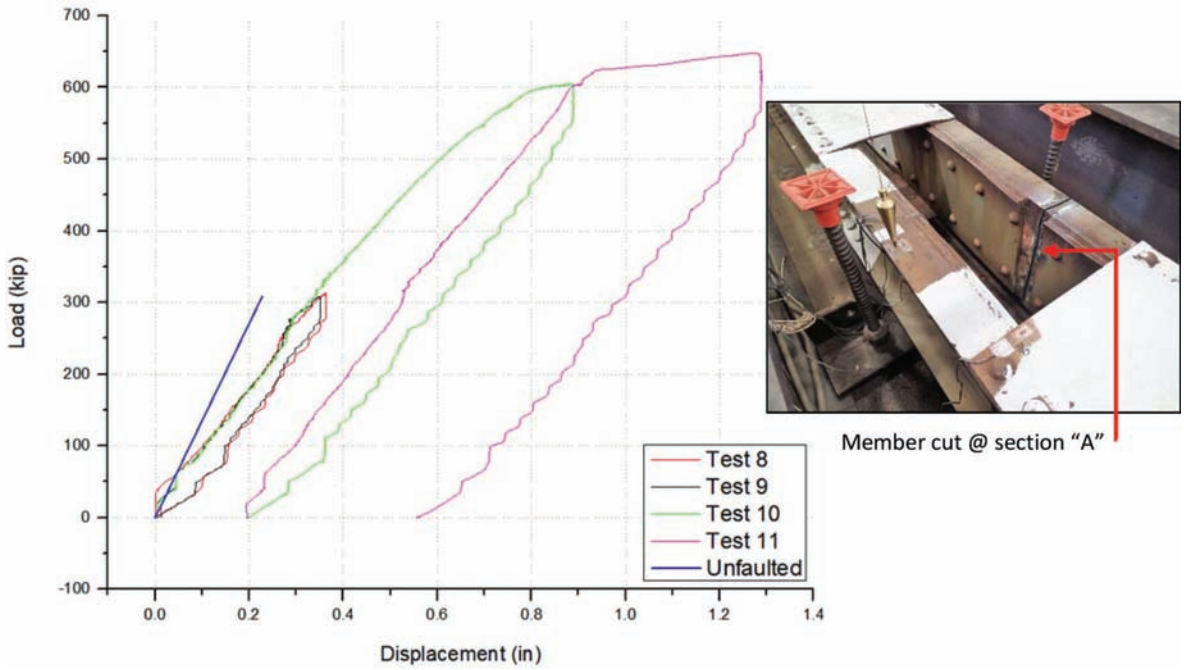

Figure 5.5 Specimen 2 load-displacement curves with severed section at location "A" (mid-panel cut).

TABLE 5.2
Specimen 2 cross-sectional area and capacity calculations

	Specimen 2 (@ Location "A")
Gross Area (in^2)	17.3
Net Area (in^2)	14.5
Nominal Gross Section Yield (kip)	571
Actual Gross Section Yield (kip)	679
Nominal Net Section Fracture (kip)	870
Actual Net Section Fracture (kip)	972
Peak Test Load (kip)	647

prior to testing. The deformation has been highlighted with dashed lines. Figure 5.7 shows Specimen 1 after testing has been completed where it can be seen that the channel flange buckled, slip occurred at the rivets, and the end stay plate rotated in-plane. Slip at the rivets indicates that either the rivet has yielded or the plate has yielded locally at the rivet hole, or both. The in-plane rotation of the stay plate shown in the figure was indicated at the corner of the end stay plate where a small, unpainted section of the channel was exposed. The stay plates resisted opening of the severed channel through horizontal in-plane shear action. This put part of the stay plate in tension and part of the plate in compression, the capacity of which would theoretically be controlled by the buckling capacity of the plate. However, in both experimental cases, and as was later confirmed in the parametric study, the faulted member capacity was not limited by the stay plate thickness (and thus buckling capacity), which was found to have no effect on the internal redundancy analysis. The plates for Specimen 1 and 2 were 3/8 inch thick—a common thickness for riveted built-up members and which can be considered a typical minimum thickness for stay plates.

Figure 5.6 Specimen 1 end stay plate prior to testing showing pack rust-induced bending.

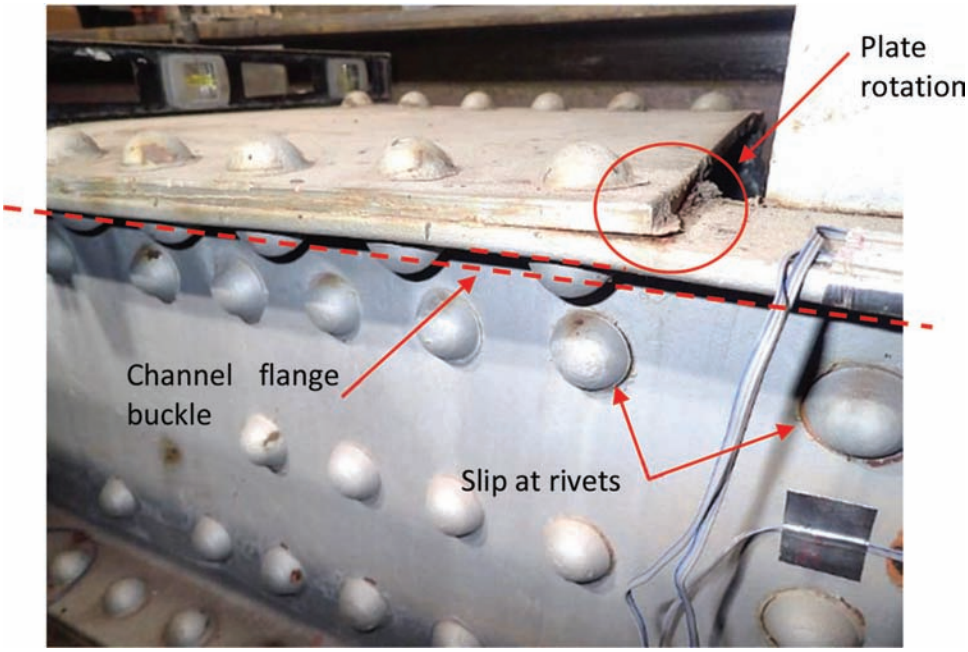

Figure 5.7 Specimen 1 after testing was completed showing buckled channel flange, slip at the rivets, and rotated end stay plate.

6. PARAMETRIC STUDY OF INTERNAL REDUNDANCY OF TWO-CHANNEL MEMBERS

Global behavior of two-channel type members resulting from a single failed component was examined using the Abaqus software suite. The parametric study resulted in several closed-form solutions intended to be used to calculate second order moments, which are combined with redistributed axial loads to estimate the live load stress range in the unbroken component.

6.1 Two-Channel Member FEM Calibration and Specifications

Finite element models for the two-channel member parametric study were calibrated using the lab benchmark test data from Specimen 1 and 2, the Winona Bridge tension chord specimens discussed previously. Following FEM calibration, a parametric study including numerous three-dimensional member geometries were created and evaluated using linear elastic, static

implicit analysis in which large deformation effects (finite strain theory) were included. The geometries studied included stay-plated members and double-latticed members with the intersection of the lattice bars connected. All geometries were subjected to concentrated axial tensile loads away from the failure site using reference points and kinematic coupling constraints. Plates and channels were modeled using four-node doubly curved shell elements with reduced integration and hourglass control (Abaqus designation S4R) and a structured quadrilateral mesh. The global size of the mesh size was 1/2 inch with five integration points through the thickness of the shells (Simpson integration rule). Lattice bars were modeled using two-node linear beam elements (Abaqus designation B31) with a 1-1/2-inch mesh size. A shell element mesh convergence study was performed halving the mesh density (1-inch elements), and then doubling the mesh density (1/4-inch elements) at locations adjacent to the failure sites. It was found that the results were insensitive to the mesh size up to at least 1 inch. However, the 1/2-inch element size facilitated the integration of nodal forces at locations of interest without significant increase in computational cost. Figure 6.1 is a zoomed-in image of a gusset plate connection on the 60-foot-long Winona Bridge Specimen showing a typical mesh for the models. The components of the specimens are differentiated by color: stay plates are light blue, gusset plates are dark blue, diagonal and vertical stubs are gray, channels are green, and cover plates (or redundant web plates) are yellow. The geometries of the rivets were not explicitly modeled. Non-linear connector elements were utilized initially, which were calibrated to single fastener shear test data obtained from Ocel (2013). However, the stress outcomes did not change significantly in comparison to simpler approaches and hence the use of connector elements was not carried forward into the parametric study. Rather, plates and channels were connected using surface-to-surface tie constraints. Lattice bars were connected to channel flanges and at center points of lattice bar intersections using kinematic tie coupling constraints that allowed rotation about what would be the fastener longitudinal axis.

For the benchmark FEM, an elastic-plastic isotropic material was defined for the channels and plates having a yield strength of 40.5 ksi—equal to the actual cover plate yield strength of Specimen 1 and 2 (material test results are presented in Section 2). The modulus of elasticity was defined as 29,000 ksi and a Poisson's Ratio of 0.3. Following calibration of the shell element models, the material definition was simplified to linear-elastic for the parametric study.

Data collected during the laboratory testing of Specimen 1 and 2 were compared to the benchmark finite element model to calibrate the model parameters and ensure accurate solutions. Strain, load, and displacement sensors used during the experimental testing provided data for comparison. Figure 6.2 and Figure 6.3 show load-displacement curves for each of the specimens compared to load-displacement results obtained from the benchmark FEM. While the load-displacement relationship was not necessarily the output of interest for purposes of the parametric study, it was considered a useful indicator of overall behavior and response to load in comparison of the laboratory test results to the FEM results. Figure 6.2 plots data for Specimen 2, where the member was cut at location "A"—the mid-panel point centered between truss nodes. Several elastic load cycles were applied, followed by two large load cycles resulting in permanent plastic deformation. It can be seen in Figure 6.2 that the FEM results compared relatively well with the laboratory results, particularly within the linear-elastic range up to about 400 kips. The FEM load-displacement curve showed reasonable non-linear behavior, as well. The same can be said for Figure 6.3 comparing FEM results to Specimen 1, which was cut at location "B"— between the gusset plate and end stay plate. The goal of this process was to simplify the FEM as much as possible while achieving reasonable and acceptable accuracy that could be carried forward into the parametric study of two-channel members. The divergence at peak loads

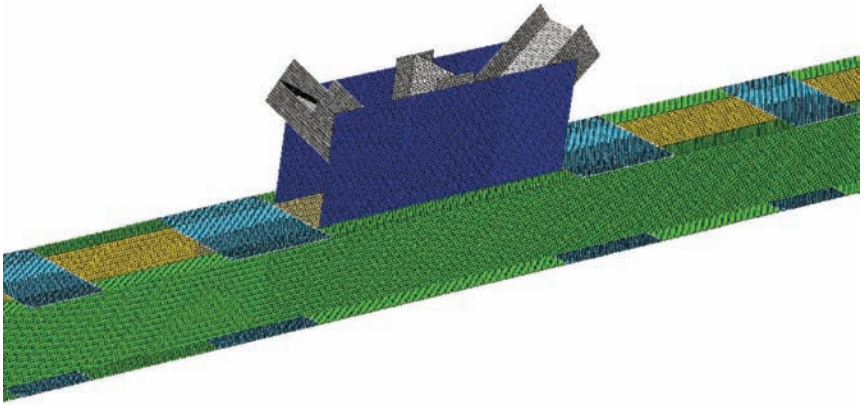

Figure 6.1 Typical 1/2-inch shell element mesh used for FEM validation and two-channel member parametric study.

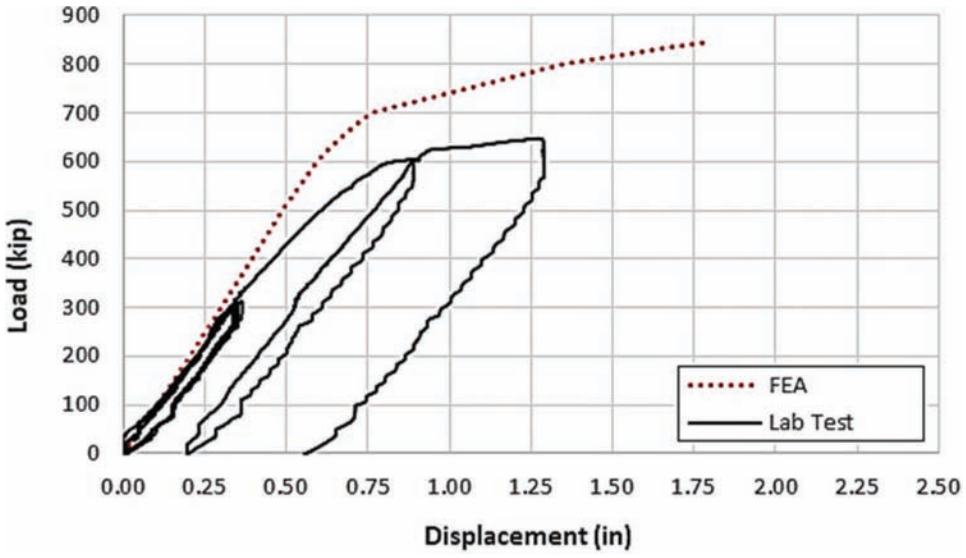

Figure 6.2 Benchmark data comparing FEA results to lab test data for Specimen 2 in faulted condition with severed member at mid-panel (Cut "A," Figure 5.1).

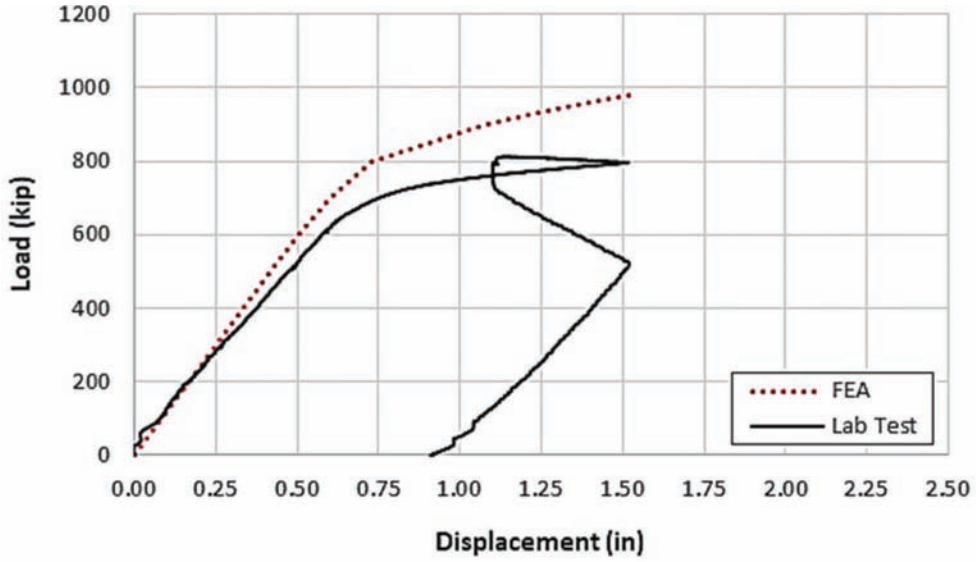

Figure 6.3 Benchmark data comparing FEA results to lab test data for Specimen 1 in faulted condition with severed member near the gusset (Cut "B," Figure 5.1).

seen in the plots is attributed to the modeling simplifications regarding component connections. For example, at peak loads the physical test experienced some slip at rivets very approximate to the location of failure, slip at bolted connections used to attach the specimen to the load frame, in-plane rotational slip of the stay plate pair closest to the member cut, as well as fastener hole deformation at extreme loads. These sources of additional axial displacement would not be captured by the simplified FEM, but were not considered necessary for the parametric study either, which focused on linear-elastic behavior that would be used for fatigue-based stress range calculations and subsequent fatigue life estimates.

Strain gages were placed at several cross sections along the full length of the specimens, as shown in the gage plans in Appendix C. The benchmark FEM generated longitudinal stress results within 10% or less of laboratory results at all critical areas, such as near the points of severed members, and within 15% or less of all other measured data. Figure 6.4(a) shows a cross-sectional view of the benchmark FEM at the site of the "failure" of Specimen 2. Symbols are sketched at approximate locations where the strain gages were installed, corresponding to the stress plots in Figure 6.4(b)–(d). Figure 6.4(b)–(d) plot stress on the vertical axes and transverse position on the component on the horizontal axes. Dashed lines are also sketched on Figure 6.4(a),

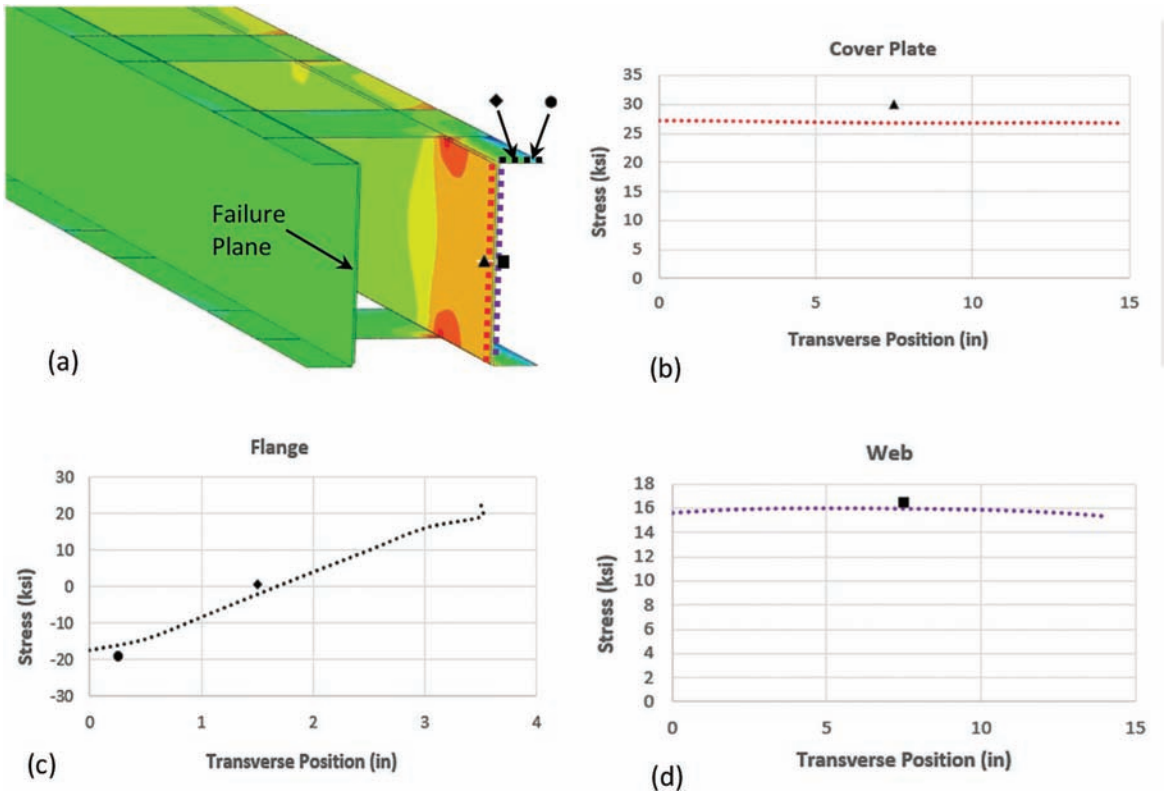

Figure 6.4 Benchmark data comparing FEA results to measured data at the location of failure.

corresponding to the path across which the stress outputs were obtained from the FEM. Figure 6.4(b) shows longitudinal normal stress across the width of the cover plate. The triangle indicates the location of the strain gage, which was centered between the edges of the cover plate, as well as between the adjacent stay plates, directly across from the severed half of the member. Figure 6.4(c) shows longitudinal normal stress across the width of the channel flange. Two strain gages were installed on the flange, one (shown as a diamond) was located 1-1/2 inches from the edge of the flange and the other (shown as a circle) was 1/2 inch from the edge. Both of these gages were centered between the adjacent stay plates directly across from the severed half of the member. Figure 6.4(d) plots longitudinal normal stress across the width of the channel web. The square indicates the location of the strain gage, which was directly opposite the strain gage installed on the cover plate. The applied load was 300 kips. All FEM results in this location were within 10% or less of laboratory measurements and considered acceptable. Figure 6.5 shows a side view of the same FEM, where the severed half can be seen, along with the stress hotspots at the corners of the stay plates. The strain gage symbols have also been placed on Figure 6.5 to illustrate their approximate positions. Note that the cover plate gage (triangle) is out of view. Stresses carried by the intact half of the member included the full axial load applied to the member, as well as secondary flexural moments resulting from load redistribution around the discontinuity. Stay plates provided load paths for the redistribution carrying load through in-plane shear, helping resist opening of the severed half of the member. This caused the intact member to displace inward (toward the severed member). Out-of-plane displacements of the FEM at the location of "failure" matched laboratory specimen measurements to within 5% at peak loads.

Pinned and fixed boundary conditions were also applied to the FEM in an effort to understand the effect it may have on the benchmark results. It was found that boundary conditions had a negligible effect likely due to benefits attributed to the member being continuous, meaning more than a single panel length. Boundary conditions and their effect on resulting stress within the context of the parametric study are discussed further in Section 6.3.

The benchmark shell element model, as described in herein, was found to be acceptably accurate, particularly within the linear-elastic range. Stresses and displacements at locations of highest interest were found to be within 10% of that measured in the laboratory tests and therefore the procedures used to construct the benchmark FEM were used as the basis for FEMs used in the parametric study of two-channel members.

6.2 Geometric Parameters Varied for Two-Channel Members

The parametric study was divided into four subgroups: continuous stay-plated, continuous laced,

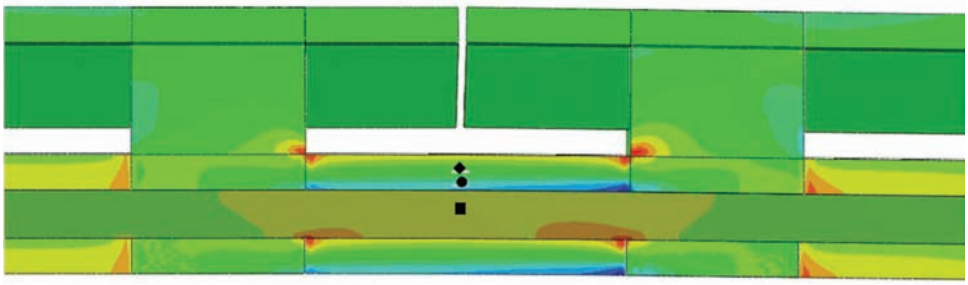

Figure 6.5 Benchmark FEM showing location of the severed half and stress hotspots at load equal to 300 kips.

non-continuous stay-plated, and non-continuous laced. Continuous stay-plated members were two-channel members where the channels were connected using intermittent stay plates and made continuous through multiple panel points. Continuous laced members were two-channel members with the channels connected using lattice bars and made continuous through multiple panel points. The non-continuous stay-plated members were two-channel members connected using intermittent stay plates and extending between two panel points, such as would be the case for a diagonal member. The non-continuous laced members were the same as non-continuous stay-plated members, except that the channels were connected using lattice bars instead of stay plates. Each of these subgroups was studied for effects of equivalent applicable parameters, but were divided into subgroups due to the differences in after-fracture load redistribution behavior.

The current AASHTO LRDF Bridge Design Specification is silent on the sizing and spacing of stay plates and lattice bars for built-up tension members. It does provide guidance on the design of built-up compression members, including single-angle members. Many existing built-up members, however, were constructed long before the modern design specification. The earliest AASHTO design specification that could be referenced for this work was *The Standard Specifications for Highway Bridges* adopted by AASHO in 1935 (later changed to AASHTO in 1973). Later design standards maintained nearly identical built-up member provisions. The 1935 specifications provided design guidance for built-up tension and compression members. It states that separate segments of tension members composed of shapes may be connected by stay plates or end stay plates and lacing. End stay plates were required to be sized the same as compression members. Intermediate stay plates were required to be sized at a minimum of three-quarters of that specified for compression member intermediate stay plates. This would require the following:

- End stay plates for tension members must be a minimum of 1.25 times the distance between the inner lines of rivets connecting them to the flanges.
- Intermediate stay plates for tension members would be a minimum of 0.75 × 1.25 times the distance between the inner lines of rivets connecting them to the flanges, equaling 0.9375 times the distance between the inner line of rivets connecting them to the flanges.
- Thickness of all stay plates must not be less than 1/50 of the distance between inner rivet lines connecting them to flanges.

Finally, the clear distance between stay plates was limited to no more than 36 inches. Lacing bars could be flats or shapes and were limited to a minimum width that was based on the diameter of the rivets connecting them to the member flanges. For example, a minimum of 2-1/2-inch-wide flat bar would be required for a 7/8-inch diameter rivet. Thickness of the bars was set at a minimum of 1/40 of the distance between connections for single lacings, and 1/60 for double lacing, but not less than 5/16 inch. The angle between the lacing bars and the longitudinal axis of the member was limited to "approximately 45 degrees" for double lacing and 60 degrees for single lacing. Double lacing was required for any member whose distance between connecting lines of rivets was equal to or greater than 15 inches. Finally, two rivets were required to connect each end of a lacing bar if the flanges were 5 inches or wider.

As a point of comparison, the current AREMA Chapter 15 provides guidance on design of these elements, as well. It states that built-up members shall be connected by stay plates or lacing bars with end stay plates. It goes on to specify that tension members shall have stay plates sized to a minimum of two-thirds the lengths specified for stay plates on primary compression members. This would require the following:

- End stay plates for tension member must be a minimum of 0.67 × 1.25 × the distance between the lines of connection to the outer flanges, equaling 0.833 times the distance between lines of connection to the outer flanges.
- Intermediate stay plates shall not be less than three-quarters of the end stay plate size. This means the tension member intermediate stay plates would be 0.67 × 0.75 times the distance between lines of connection to the outer flanges, equaling 0.5 times the distance between lines of connection to the outer flanges. Thus, intermediate stay plates would be sized at about 60% of the length of end stay plates on tension members.
- Thickness of all stay plates must not be less than γ_{50} of the distance between lines of connection to the outer flanges for main members, or γ_{60} for bracing members.

Lacing bars for tension members where the distance between connection lines in the flanges is greater than 15 inches and a bar less than 3-1/2 inches wide is used,

the lacing configuration shall be double and connected at the intersections. The angle and thickness of the lacing bars was similar to the requirements of the 1935 AASHO Standard Specifications. AREMA Chapter 15 also requires a similar minimum bar width and double fastener requirements for flanges of 5 inches or wider.

The parametric study included a variety of models that followed the requirements of the 1935 AASHTO Standard Specification, a few geometries that would not have met the minimums, and many geometries that would have exceeded the minimums. While it is likely that most bridges would have been built to the minimal design requirements, it cannot be said conclusively that some were not. Furthermore, it cannot be said that the minimums would have been different for bridges designed using earlier specifications or dissimilar design standards that were not available for reference for the current study. It was also preferred to develop a simplified method of analysis that would be inclusive of all possible designs, including those that were designed per the 1935 AASHO provisions and those designed per the more modern AREMA provisions, albeit the differences between the two specifications are marginal.

6.2.1 Parameters Evaluated for Two-Channel Members

Due to the size of the tables, the specific combinations of geometric parameters have been tabulated in Appendix B. Table B.1 lists geometries for continuous stay-plated two-channel members. Table B.2 shows geometries for continuous laced two-channel members. Table B.3 contains the parameters studied for non-continuous stay-plated two-channel members and Table B.4 is for non-continuous laced two-channel members. Many of the parameters evaluated for the two main types of members, stay-plated and laced, were similar. However, there were several parameters unique to each type of two-channel member. The parameters evaluated for stay-plated members included

- end boundary conditions (fixed vs. pinned),
- channel section,
- channel spacing,
- panel length—referring to the distance between two adjacent gusset joint centerlines,
- stay plate thickness,
- stay plate length,
- stay plate clear spacing,
- gusset plate thickness (for non-continuous only), and
- location of failures (next to the gusset vs. centered between gussets at mid-panel).

The laced members were modeled with end stay plates. Based on results for the stay-plated members, the thickness and length parameters of the end stay plates were not varied. Additionally, results for the stay-plated members also showed that gusset plate thickness for the non-continuous members had negligible effect and therefore was not varied for the laced members. The parameters considered for laced members included

- end boundary conditions (fixed vs. pinned),
- channel section,
- channel spacing,
- panel length—referring to the distance between two adjacent gusset joint centerlines,
- lacing bar thickness,
- lacing bar length,
- lacing bar spacing—referring to the distance between connecting rivets to the channel flange, which determined the lacing angle relative to the channel, and
- location of failures (Next to the gusset vs. centered between gussets at mid-panel).

End boundary conditions were applied to the non-continuous, as well as continuous members, evaluating effects of fixed and pinned end boundary conditions. Furthermore, a pinned boundary condition was applied to interior panel points on continuous members allowing rotation at the joints, but constraining against translation out-of-plate to the truss line. This is consistent with expected behavior in an actual bridge where floorbeams, diagonals, and bracing elements would provide resistance to out-of-plane translation. Boundary conditions were found to have a significant effect on results, which is discussed in greater detail in Section 6.3. Three sizes of rolled channels were considered, however not all sections were considered for all combinations of parameters. They were the C15 × 50, C15 × 40, and C8 × 11.5, which are sketched to scale in Figure 6.6 to give a sense of relative sizes. C15 × 50 is the largest rolled channel section currently available, so it was selected to investigate the effects of varying other parameters between it and the next size smaller. C15 × 40 was chosen because it appeared to be the most commonly used channel section for main tension chords in legacy bridges. This was the channel size used to construct the Winona Bridge from which two test specimens, Specimen 1 and 2, were obtained for the present research. It was necessary to consider channel section size effects, if any. The C8 × 11.5 was selected as a channel that is most likely

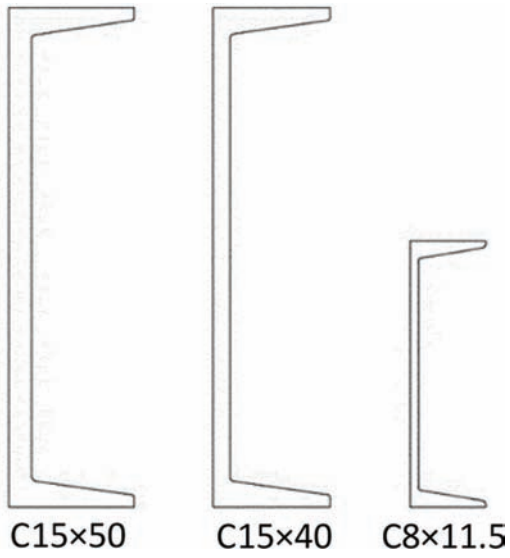

Figure 6.6 Channel sections included in the parametric study.

representative of the smallest size rolled channel used on bridges for any tension member, such as diagonals and hangers. While this size channel would not likely be found on railroad bridges, it would be very possible for shorter-span highway bridges.

Panel lengths were varied from 20 ft. to 40 ft. for continuous and non-continuous members of both stay-plated and laced types. The thickness of the tie elements, such as stay plates and lattice bars, varied from 1/8 inch up to 3/4 inch for lattice bars, and from 3/8 inch up to 7/8 inch for stay plates. Spacing of the tie elements was also examined, varying from 1/2 the depth of the channel to two times the depth of the channel for lattice bar spacing, and from 18 inches up to 148 inches for stay plate clear distances. Gusset plates were modeled for the non-continuous members, as is explained further in Section 6.3. The thickness of the gussets was modeled at 3/8 and 7/8 inch. Finally, the location of the failure within a member was also examined for the effect on results. Two locations were studied for all geometries, which included one at the mid-panel location centered between the gusset connections, and the other was adjacent to gusset plates located between the end stay plate and the gusset connection. This was considered for the continuous as well as the non-continuous types.

6.2.2 Definition of Eccentricity Parameter, e

Figure 6.7 illustrates the dimension "*e*" used in the post processing of data from the parametric study. 2*e* represents the distance between the centroids of individual channels that make up a two-channel member, or in other words, the channel spacing. Hence, *e* would simply be half of 2*e*, or the distance from the unfaulted *member centroid* to the centroid of an individual channel. The figure demonstrates how the eccentricity for two members that are comprised of the same size of channels with the same web-to-web spacing, but in reversed orientation, would be calculated and may differ from each other. The parametric study included channels in both orientations. All results discussed in the following used the appropriate theoretical *P e* to normalize the second order moment resulting from failure of a single channel, where *P* was the total load in the member. In this way, a simplified method was developed to calculate the resulting moments in two-channel members as a percentage of *P e*.

6.3 Rotational Stiffness of Joints for Continuous and Non-Continuous Two-Channel Members

Applied end boundary conditions proved to be the most influential parameter affecting the resulting second order moments in non-continuous two-channel members in the faulted condition. The applied end boundary conditions were effectively inconsequential to continuous members due to rotational stiffness provided by the continuity of the channels. Figure 6.8 plots selected data for several models where the length of stay plates parameter was being evaluated, which is used here only to illustrate the effect of end boundary conditions. A single channel was failed at the mid-panel location (centered between panel points). The vertical axis plots the resulting moment normalized by *P e*, or the percent of *P e.* The horizontal axis plots the length of a stay plate over the depth of a channel. Varying end boundary conditions were applied to each geometry, including a non-continuous member with pinned ends, a non-continuous member with fixed ends, a three-span continuous member with pinned ends, and a three-span continuous member with fixed ends. The dashed lines represent the continuous members. The percent *P e* for the non-continuous member with pinned boundary conditions differed as much as 10 × more than the same geometry with fixed boundaries. Figure 6.8 also shows that results for continuous members were very similar to non-continuous fixed members and that end boundary conditions on the continuous member had negligible effect on outcomes. This plot demonstrates that the rotational stiffness of the member at panel points

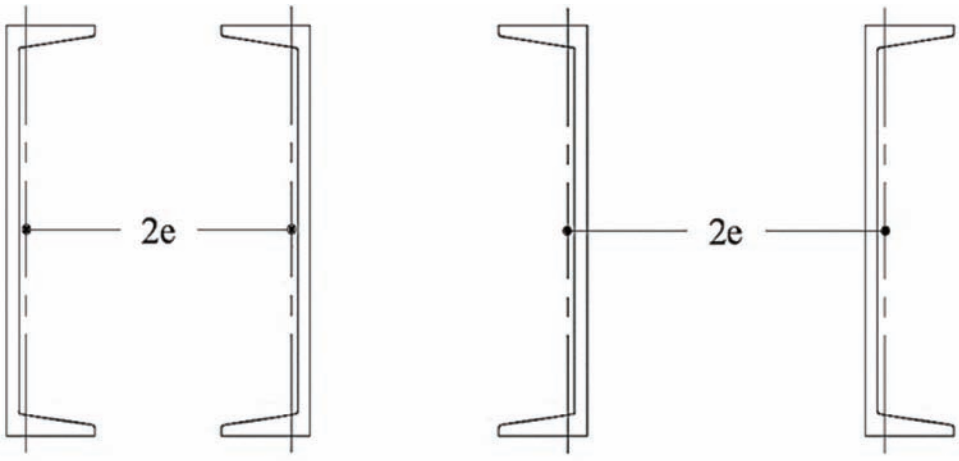

Figure 6.7 Illustrations showing eccentricity *e* used in development of the simplified evaluation method for two-channel members.

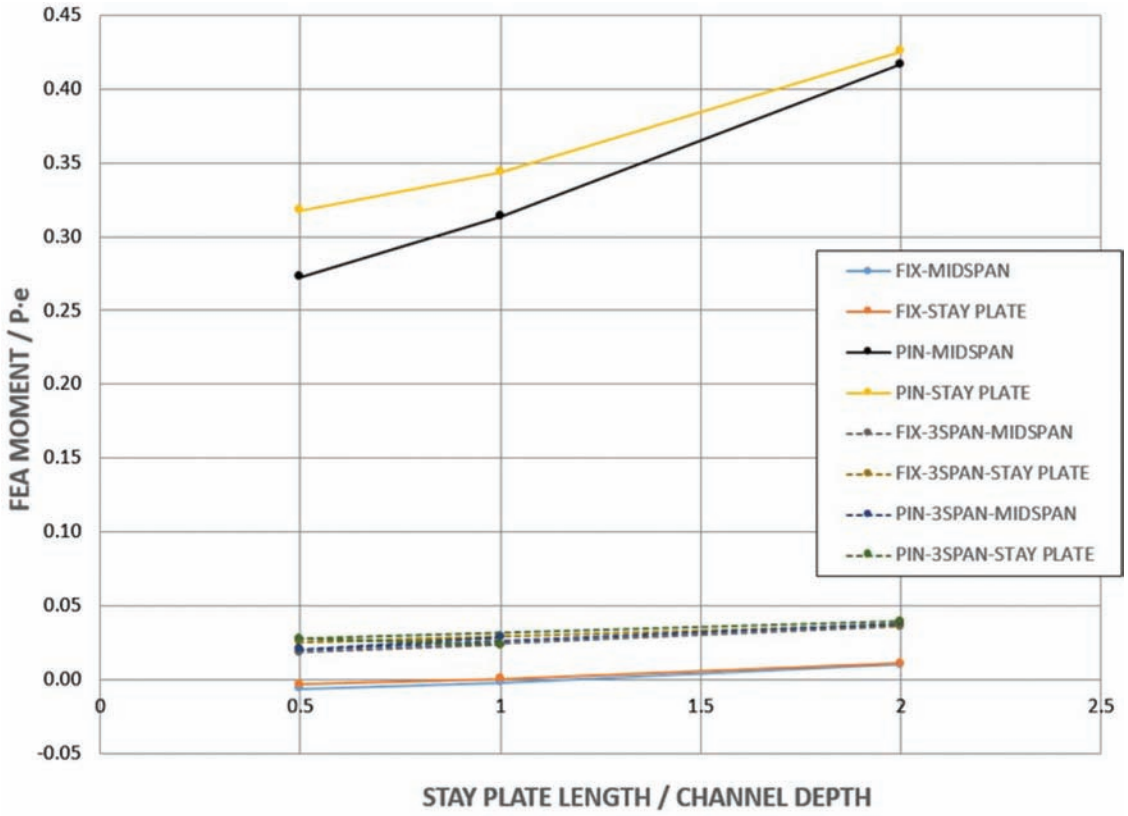

Figure 6.8 FEM results demonstrating effect of boundary conditions and member continuity.

has a large impact on results. Continuity of the channels through the panel points provided rotational constraint that approached fixed boundary conditions. No additional rotational constraints were placed at the interior panel points of the three-span member. However, they did have displacement constraints simulating constraints that would exist on an actual bridge to prevent out-of-plane displacement.

Primary and secondary members, including chords, floorbeams, diagonals, lateral braces, sway braces, and bearings, tie into panel points on a truss that are connected together using gusset plates. Chords or diagonal members will contribute some level of restraint for the joint against rotation. Other members such as lateral bracing and sway bracing may also help to restrain against rotation of the gusset connection. Floorbeams, often with connections as deep as the floorbeam themselves, increase rotational constraint of the connection. And in some cases bearings that are fixed, or even guided expansion bearings designed to only displace longitudinally, offer further resistance to rotation for the gusset connections. The combined restraint provided by all of these members is difficult to estimate without finite element analysis of each individual bridge and member geometry, which would not be feasible for most bridge owners, nor was it the desired outcome of this research. However, the effect of the rotational stiffness on the internal redundancy of two-channel members was apparent. It was clear that pinned conditions would not exist in actual bridges. However, it would be difficult to justify perfectly fixed conditions, as well.

Diagonal and vertical two-channel members typically are "deeply" connected into gusset plates; often they would be trimmed such that they fit tightly into the connection to within a few inches of the other intersecting primary members. An example of this is shown in Figure 6.9, which shows a removed railroad deck truss joint with diagonal two-channel members connected into the gusset plates to within a couple inches of the tension chords. Due to the rotational stiffness of the connection as a whole, for reasons previously stated, it was estimated that most of the rotation that a two-channel member would experience would likely be due to local flexure of the gusset plates near or at the edges of the gusset plates and that the plates themselves would behave as fixed toward the center of the connection. This concept was modeled by tying the channels to a set of gusset plates and then applying fixed boundary conditions to the free edges of the gusset plates. By doing this, generous flexibility of the gusset plate was allowed while simultaneously providing a reasonable level of rigidity that may be present in the gusset plate due to the interaction of intersecting members within the joint.

To fully explore the effects of various assumptions on this approach to simulate rotational stiffness, a separate parametric study was carried out to determine how best to model the boundary conditions of the

Figure 6.9 Example of deeply set diagonal members connected into a gusset plate.

non-continuous members without over-estimating joint rotational stiffness. The parameters considered in the study included the effective portion of the gusset plate, the member embedment depth into the gusset plate, the gusset length beyond the member, and the gusset plate thickness. Figure 6.10 shows an illustration of these parameters. Two different effective areas of gusset were examined, a simple rectangular shape shown on the left and a Whitmore Section-like shape, shown on the right. The member embedment depth was evaluated looking at depths ranging from half the channel depth to two times the channel depth. The gusset plate length beyond the member, labeled L on the figure, also ranged from half the channel depth up to two times the channel depth.

Figure 6.11 plots the results of the rotational stiffness parametric study. Green dots represent values resulting from mid-panel failures. Black dots represent values resulting from failures near the gusset connections, such as those shown in Figure 6.10. The rectangular and Whitmore-like effective gusset plate shapes are both represented. The chart on the left plots the percent of P e on the vertical axis and the member embedment depth into the gusset plate, normalized by the channel depth, on the horizontal axis. The chart on the right plots the same vertical axis and the gusset plate length, L, on the horizontal axis normalized by the channel depth. By quadrupling the embedment depth, the percent P e only increased by 2% for failures near the gusset plate and by less than 1% for mid-panel failures. By quadrupling the gusset plate length, L, the percent P e increased by less than 1% for both failure locations. The final parameter considered was the thickness of the gusset plates. Gusset plates of 3/8-inch thick are the thinnest plates used in bridges. The thickest plate is unknown and would not vary much from 3/8 inch for legacy bridges, but for new designs thicker gussets plates could be used, particularly on long span trusses. For these reasons it was necessary to understand if the thickness of the gusset plates would influence the finite element solution. Several non-continuous models were analyzed varying only the gusset plate thickness from 3/8 inch to 7/8 inch. It was found that results differed by 3% or less and therefore was concluded that the gusset plate thickness was not an essential geometric parameter.

The non-continuous member boundary condition study concluded that outcomes were insensitive to the shape of the gusset assumed to be engaging in rotational constraint, the member embedment depth, the gusset plate length L, and the gusset plate thickness. As a result, non-continuous FEMs were modeled in the comprehensive parametric study using 3/8-inch thick rectangular gusset plates with embedment depths and gusset plate lengths equal to the channel depth.

Finally, when percent P e results in Figure 6.11 are compared back to Figure 6.8 it can be seen that by adding the gusset plates to the non-continuous members, percent P e falls between results for pinned and fixed boundary conditions, more closely resembling that of fixed boundary conditions, and comparable to the continuous members. It is believed that this method of analysis reasonably and conservatively simulated typical boundary conditions on actual bridges for the non-continuous two-channel members, which was found to significantly affect the internal redundancy evaluation.

6.4 Results for Parametric Study of Two-Channel Members

The largest resulting second order moments were always located in the intact member directly across from the location of failure. The largest of these

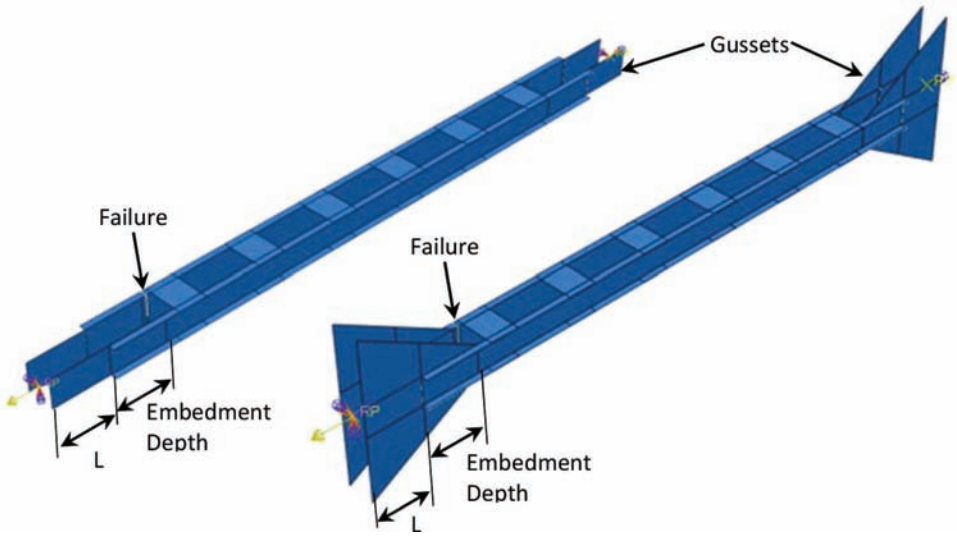

Figure 6.10 Example of FEMs used to study gusset connection parameters (left) rectangular gusset, (right) Whitmore gusset.

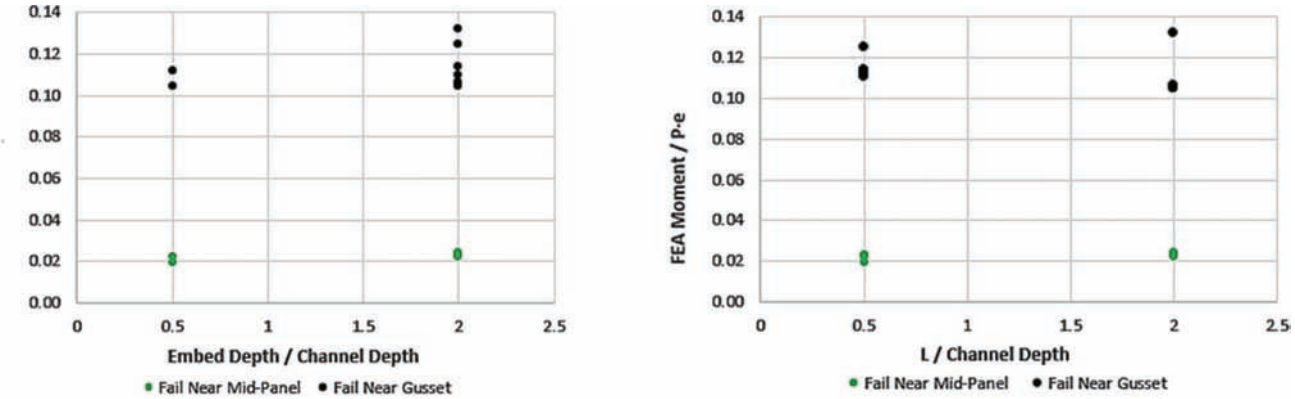

Figure 6.11 FEA results showing effects of the member embedment length (left) and gusset length, L (right) (see Figure 6.10).

moments nearly always resulted from a failure between the gusset plate and end stay plate, particularly for stay-plated members. Figure 6.12 shows the plan view of several FEMs with exaggerated deflections to illustrate general global behavior. Two were failed at the mid-panel, (a) and (b), and two were failed between the gusset plate and end stay plate, (c) and (d). Overall, global behavior was relatively similar between these two member types when they had failures at the same location. Mid-panel failures allowed moment distribution along the length of the intact channel via lattice bars or stay plates helping to distribute load more gradually around the failure. It was also observed that the end stay plates of the laced members contributed to load redistribution. Gusset-end stay plate failures, however, forced much of the resulting moment to be resisted by the intact channel within a smaller localized area. These failures were purposefully placed between the end stay plates and the gusset plates in order to force a worst-case scenario for the surviving channel, which was forced to resist the secondary moment within a relatively short length. Deflections across the remainder of the member were relatively gradual, as can be seen in Figure 6.12(c) and (d).

Moments integrated at the mid-panel of members with gusset-end stay plate failures were found to be very small compared to the moment at the end stay plate near the failure. Stay-plated members were also observed to experience localized reverse curvature at the edges of the stay plates that produced hot spots of stress and amplified moments. All moments reported in the following sections were taken near the edges of stay plates, when applicable, in order to capture the largest resultant moment. Figure 6.13 illustrates the reverse curvature of stay-plated members in which deformations are amplified with a very large load applied in order to make the structural behavior obvious. The opening of the fracture plane was resisted through in-plane shear in the stay plates. Laced members also benefited from in-plane shear resistance provided by end stay plates.

The size of the channel was found to have negligible effect on the outcomes. This makes sense when considering that loads were proportioned to the area of the

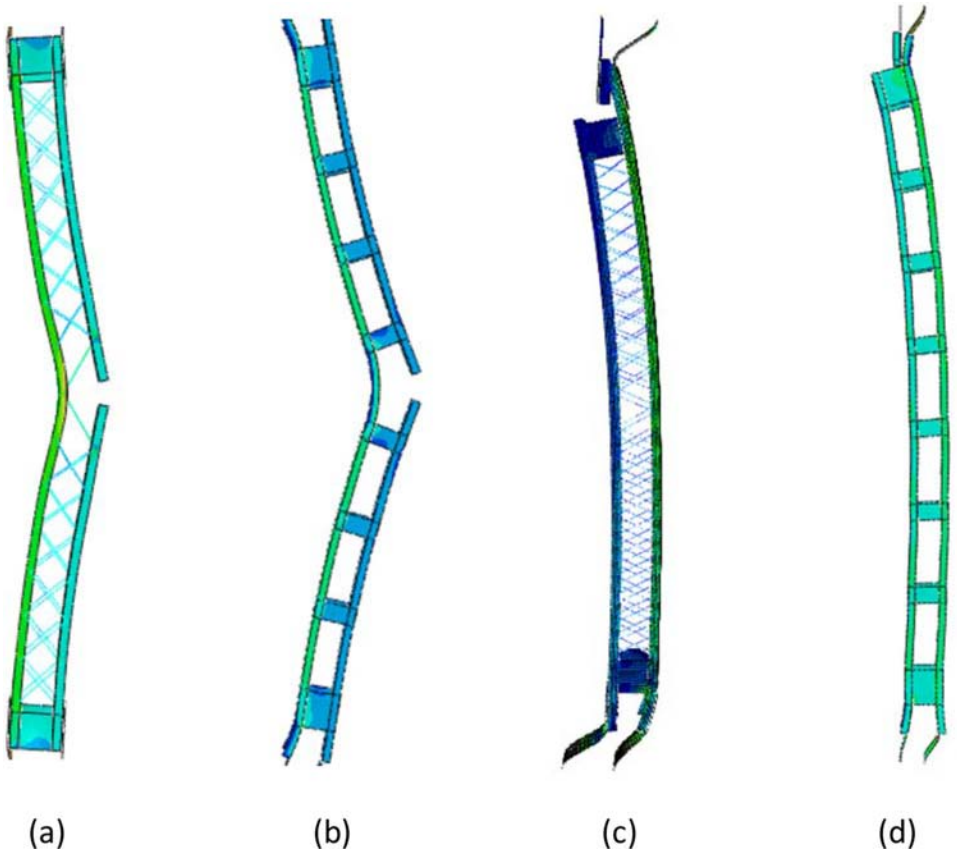

Figure 6.12 Non-continuous FEM results with deformations amplified 50× for clarity. (a) Laced with mid-panel failure; (b) Stay-plated with mid-panel failure; (c) Laced with end failure near gusset; (d) Stay-plated with end failure near gusset.

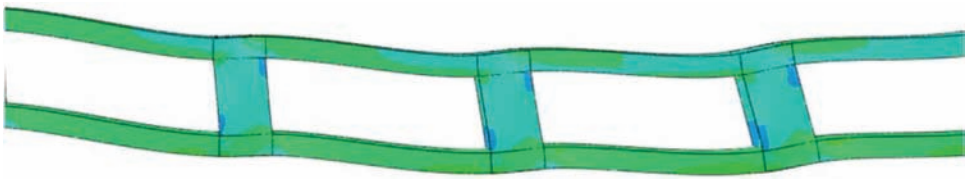

Figure 6.13 Close-up of stay-plated member with deformations amplified 50× showing reverse curvature of the channels.

member and that second order effects resulting from load redistribution were a function of eccentricity created when half the member was severed. Thus, a smaller channel carried proportionally smaller loads and would be proportionally spaced, as well, causing similar behavior but on a smaller scale. This means that when the results were plotted as a ratio of the second order moment (caused by the load redistribution) to the theoretical moment, $P\ e$ (where P is the load and e is the member eccentricity explained in Section 6.2.2), the results for the larger and smaller channel sections were nearly indistinguishable. This was the result for both continuous and non-continuous members.

In addition to channel size, the spacing between channel pairs was also examined. This parameter ranged from a spacing equal to half the depth of the channel up to two times the depth of the channel. When resulting second order moments were normalized by the theoretical moment, $P\ e$, then it appeared that as the spacing increased the resulting moment was reduced. However, when the second order moments were not normalized, and absolute magnitudes were compared for geometries having different channel spacing, then it became clear that channel spacing had minimal effect on the results. The larger theoretical moment was simply reducing the ratio of FEA moment to theoretical moment, due to the larger eccentricity, e.

This observation goes against the assumption that some have had toward two-component members, and even some designs for multi-component members, that when one of the components fails, the resulting second order moment is equal to the original load times the faulted member eccentricity. The present parametric study found that such an assumption would be overly conservative for any two-channel geometry; and as the

spacing between components increased, that assumption would become increasingly overly conservative.

The panel length, which refers to the distance taken from centerline of a panel point to centerline of the next panel point for continuous members or the length of the channels themselves for non-continuous members, was found to have minimal effect on the after-fracture moment. Due to the localized curvature of the channels at the edges of stay plates that generated hotspots in the intact channel, longer spans having similar clear distances between stay plates were observed to have negligible effect. For laced members, there were marginal increases in the resulting moments with longer spans. For example, doubling the span in some cases increased the after-fracture moment by a mere 2%.

Thickness and length of the stay plates had negligible effect on the results. The thickness of the plates ranged from 3/8 to 7/8 inch. The lengths of the plates ranged from half the depth of the channel to two times the depth of the channel. This range included a mixture of end and intermediate stay plates that would have violated and exceeded known minimum design provisions. However, the results were insensitive to these changes in stay plate parameters. The design provisions also state that each plate must be fastened to the flanges of primary components with a minimum of three rivets. This type of connection would offer in-plane rotational constraint engaging the stay plates in resisting opening of the failed component, transferring load around the discontinuity. The connection was modeled using surface-to-surface tie constraints between shell elements, which constrained displacements and rotational degrees of freedom. Hence, modeled rotational constraint would be similar to that found on real structures, though slightly stiffer since slip at the highest loads on a riveted connection would not be allowed with the tie constraint such as was observed to occur on Specimen 1 in the laboratory test. The consequence of having stiffer stay plate connections is a larger localized transferal of moment into the intact channel. This means any minimal error in the FEM results caused by stiffer stay plate connections would be conservative in nature. However, it is important to keep in mind that laboratory testing of the Winona Bridge chord, Specimen 1 and 2, showed that slip at the stay plates did not occur until near peak loads were reached, well beyond original design loads, and only for Specimen 1 when cut near the gusset connection. Specimen 2 showed no evidence of yielding and very minor evidence of slip at completion of testing in the stay plates adjacent to the failure location. The effectiveness of the stay plates in load redistribution is directly dependent upon the rotational constraint. This implies that stay plates have a minimum length to remain effective, but anything equal to or greater than half the depth of the channels to which they are attached with a minimum of three fasteners will effectively redistribute load. End stay plates were found to slightly reduce moments near the gusset connections for laced members, but did not affect the moment at the mid-panel location for mid-panel failures.

The number of stay plates within a given panel length was also studied. When clear distances were maintained constant and the number of stay plates was increased, this forced a longer panel length, for which the number of stay plates had no effect on results. However, if the panel length was maintained constant and the number of stay plates was increased, this forced smaller and smaller clear distances between the plates. The result was a slight increase in second order moments resulting from members having more stay plates within a given length. This is illustrated in Figure 6.14 where results for pinned, fixed, and continuous models have been plotted together as a function of the number of stay plates within a fixed panel length. The solid lines are single-span members and the dashed lines are 3-span continuous members. The legend indicates the boundary condition and the location where the moment was integrated in the FEM. The location of failure was mid-panel for all of the models shown in this figure. The effect was that as the number of stay plates increased, the bending stiffness of the member increased. This was most notable for pinned boundary conditions, with only marginal increases for fixed and continuous members. Smaller clear distances between stay plates resulted in stiffer sections of channel between the stiffening elements (the stay plates), which transferred slightly more load and consequently increased moments.

Lacing bar thickness, length, and spacing were examined for their effect on laced two-channel members. Lattice bars sizes ranged from 1/8- to 3/4-inch thick. Lattice fastener spacing ranged from half of the channel spacing to two times the channel spacing. Early design provisions limited the lattice spacing to about 45 degrees, which would be equal to the channel spacing. The same provisions also called for a lattice thickness-to-length ratio of about γ_{60}. The parametric study varied this ratio from γ_{169} to γ_{28}. It was found that these parameters all had negligible effects. One model was also analyzed in which the lattice bars were completely removed so that it only had the end stay plates. When the failure was at the mid-panel location of the member, the resulting moment at the location of the failure was reduced by about half compared to the same geometry with lattice bars, but the moment at the end stay plate was unaltered. When the failure was located between the end stay plate and the gusset connection of the member without lattice bars, the resulting moment at the mid-panel location was unchanged and the moment at the location of failure was nearly doubled, going from 5% to about 9% of $P\ e$. This behavior suggests that while the lattice may support some limited load redistribution, they are not critical to performance of the member in the faulted condition. This also suggests that even though the parametric study focused on double lattice with fastened intersections, less robust systems of lattice, such as single lattice, would not be expected to affect results significantly. This comparison suggests that the simplified method of analysis resulting

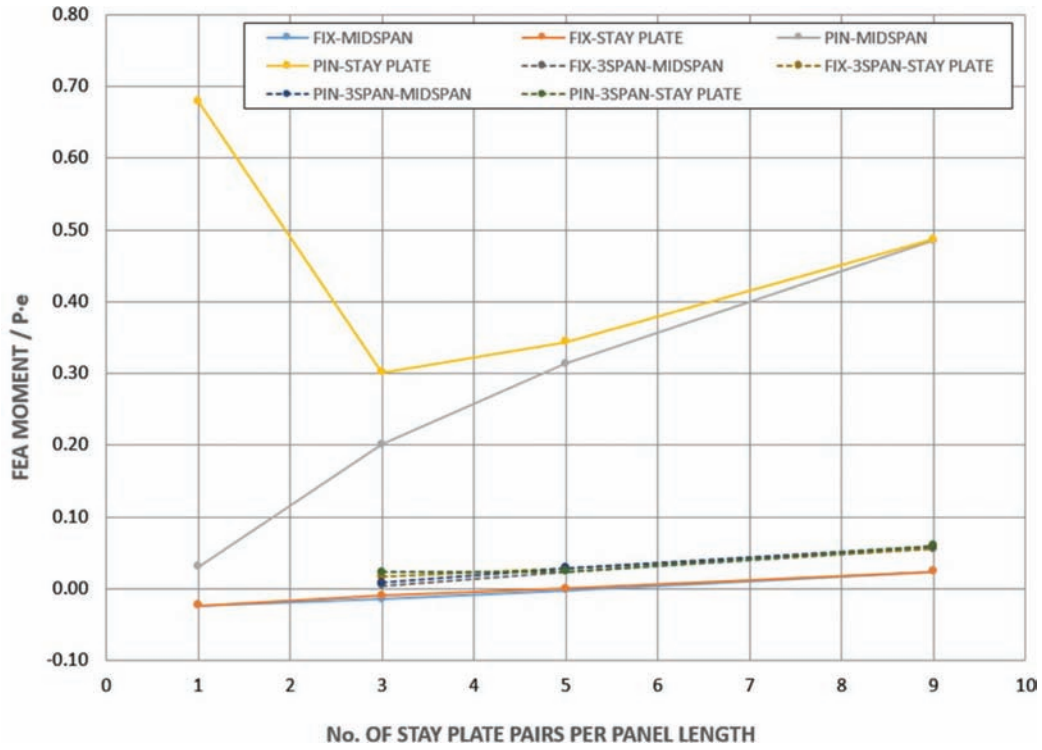

Figure 6.14 Plot showing the increase in moment resulting from more stay plates.

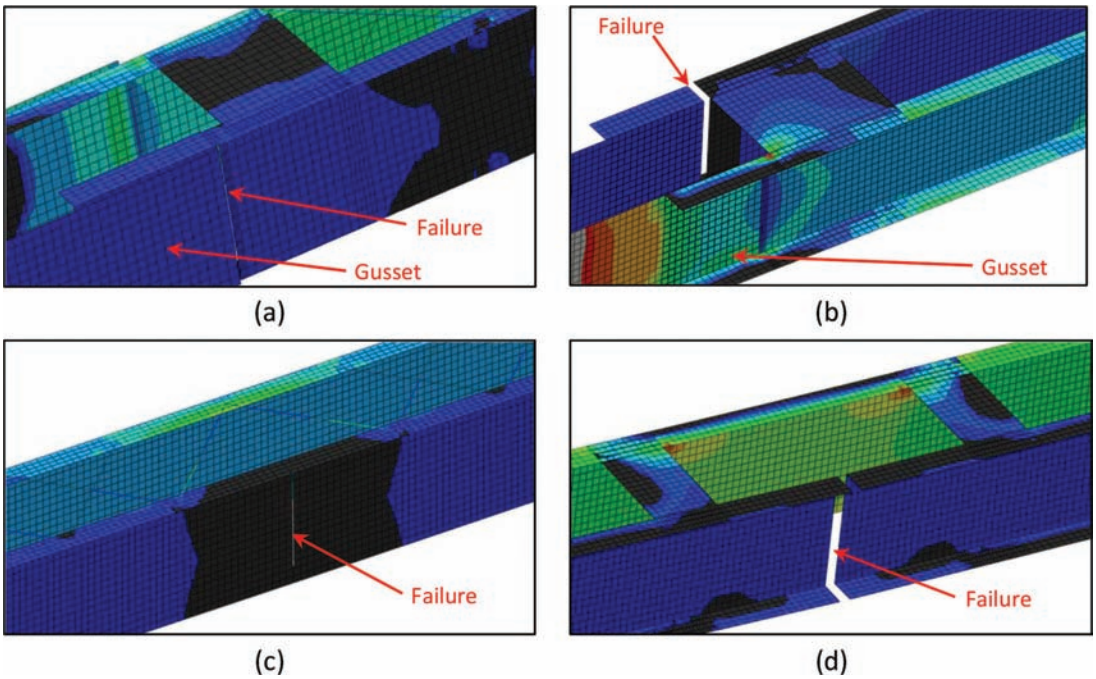

Figure 6.15 Images depicting failure locations for stay-plated and laced two-channel members.

from the parametric study can be used for laced members of all kinds, whether double or single lattice configurations.

The final parameter studied was the location of the failure. This was not necessarily geometric, but affected the response of the members and magnitude of the solution. It included the mid-panel location and between the end stay plate and the gusset plate connections. Figure 6.15 shows four examples, one from each of the locations for each type of member. Figure 6.15(a) shows failure between the end stay plate and gusset plate on a laced member. Figure 6.15(b) shows

failure between the end stay plate and gusset plate on a stay-plated member. Notice that in both cases the failure was placed between the gusset plate and the end stay plate. Figure 6.15(c) shows the mid-panel failure for a laced member where the two lattice bars that would have connected into the location of the failure have been removed to facilitate convergence of the finite element solution. This was done for all laced member mid-panel failure models. Figure 6.15(d) shows a typical mid-panel failure for the stay-plated members. The resulting moment in laced members was not significantly affected by the location of the failure. This means to say that the resulting moment was always largest at the location of failure, however, the magnitude was not necessarily larger for mid-panel failures versus failures near the gusset plate. The same cannot be said for stay-plated types, as it was found that failures near the gusset connection for both continuous and non-continuous stay-plated members resulted in moments that were two or three times larger than for the same geometry failed near the mid-panel length. There were a few exceptions to this observation, so most models were analyzed two times, once with a failure at each location to ensure the worst-case scenario was captured for a given geometry. Plots of the percent of $P\ e$ in the following sections include results for both failure locations, which is the primary source of the data scatter.

6.4.1 Results for Continuous Stay-Plated Two-Channel Members

Figure 6.16 compiles the results for all continuous stay-plated models analyzed. The vertical axis is the finite element analysis moment divided by the theoretical moment, $P\ e$. The horizontal axis is a combination of geometric properties used to correlate the results. The correlation includes the number of stay plate pairs (meaning a pair of plates located at the top and bottom of the member at the same cross section) within a single panel length. This includes the two end stay plate pairs and all intermediate stay plate pairs on the section of the member being evaluated, multiplied by the ratio of the channel depth to the channel spacing.

Regression analysis was used to conservatively fit a line to the maximum values. Approximately 5% of the data exceeded the limit defined by the line, which was considered acceptable. The line is defined by Equation 6.1, which can be used to calculate the second order moment resulting from a failed channel in a continuous stay-plated two-channel member.

$$M_{AF} = \frac{P_u e}{120}\left[\frac{N_{SP} d_{CH}}{2e} + 3\right] = \frac{P_u N_{SP} d_{CH} + 6 P_u e}{240} \qquad (6.1)$$

Where:

M_{AF} After-fracture moment resulting from failure of a channel in a two-channel member (kip-in).

P_u Total factored axial load (kips).

e Distance measured from the centroid of the unfaulted two-channel member to the centroid of the intact channel in the faulted state (in; see Figure 6.7).

N_{SP} Number of stay plate pairs (1 pair equals the top and bottom stay plates at the same cross section) within the span of the member between the panel points.

d_{CH} Depth of the channels (in).

The resulting moment is inserted into Equation 6.5 to calculate the after-fracture net section stress used to determine the remaining fatigue life. All results for continuous stay-plated members have also been tabulated in Appendix B.

6.4.2 Results for Continuous Laced Two-Channel Members

Figure 6.17 compiles the results for all continuous laced models analyzed. The vertical axis is the finite

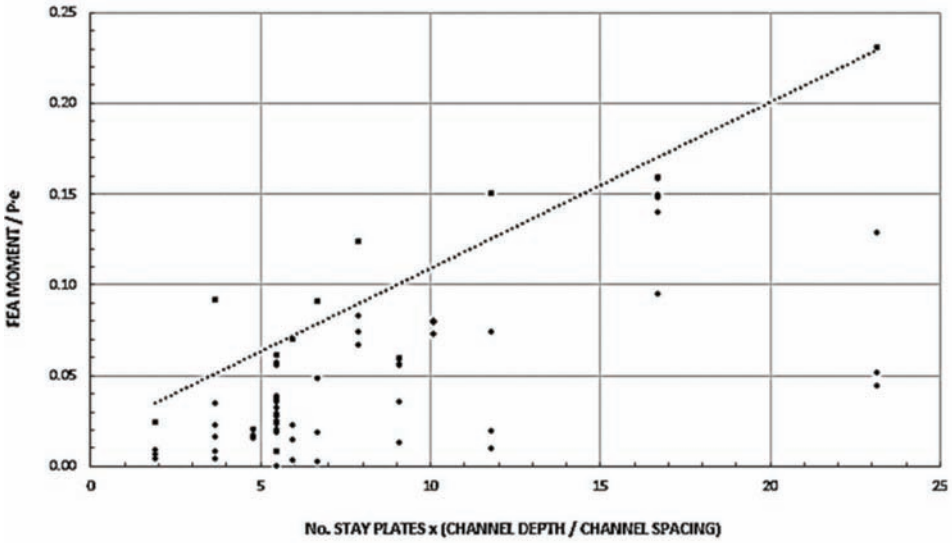

Figure 6.16 Plot of results for continuous stay-plated two-channel members.

element analysis moment divided by the theoretical moment, $P\ e$. The horizontal axis is a combination of geometric properties used to correlate the results. The correlation parameters includes the length (inches) from the centerline of a panel point to the centerline of the next panel point, times the ratio of the channel depth to the channel spacing.

Regression analysis was used to conservatively fit a line to the maximum values. Less than 5% of the data exceeded the limit defined by the line, which was considered acceptable. The line is defined by Equation 6.2, which can be used to calculate the second order moment resulting from a failed channel in a continuous laced two-channel member. The lattice bar configuration factor, γ_{LB}, accounts for the fact that single lattice bars will have twice the spacing of comparable double lattice bars. Equation 6.2 was derived using double lattice bar spacing. Based on results for members where the lattice was removed, the simplified method can be extended to single lattice configurations, as well. Thus, the lattice bar configuration factor reduces the spacing of single lattice bar members to an equivalent double lattice bar spacing such that the moment is not incorrectly doubled for single lattice members. Finally, as can be seen in Figure 6.17 the maximum moment reaches a plateau of less than 14% of Pe. Equation 6.2 limits the moment to $0.15Pe$, which is slightly above the maximum value observed for the continuous laced members.

$$M_{AF} = \frac{P_u e}{590}\left[\frac{L_{PL} d_{CH}}{\gamma_{LB} S_{LB} 2e} + 14\right] = \frac{P_u L_{PL} d_{CH} + 28 P_u e \gamma_{LB} S_{LB}}{1180 \gamma_{LB} S_{LB}} \leq 0.15 P_u e \quad \text{(Eq. 6.2)}$$

Where:

M_{AF} After-fracture moment resulting from failure of a channel in a two-channel member (kip-in).

P_u Total factored axial load (kips).

e Distance measured from the centroid of the unfaulted two-channel member to the centroid of the intact channel in the faulted state (in; see Figure 6.7).

L_{PL} Length of the panel measured between the centerlines of two panel points (in).

S_{LB} Spacing of the lattice bars measured longitudinally between centerlines of fasteners connecting the lattice bars to a channel flange (in).

d_{CH} Depth of the channels (in).

γ_{LB} Lattice bar configuration factor; 1.0 for double lattice, 0.5 for single lattice.

The resulting moment is inserted into Equation 6.5 to calculate the after-fracture net section stress used to determine the remaining fatigue life. All results for continuous laced members have also been tabulated in Appendix B.

6.4.3 Results for Non-Continuous Stay-Plated Two-Channel Members

Figure 6.18 compiles the results for all non-continuous stay-plated models analyzed. The vertical axis is the finite element analysis moment divided by the theoretical moment, $P\ e$. The horizontal axis is a combination of geometric properties used to correlate the results. It is the number of stay plate pairs (meaning a pair of plates located at the top and bottom of the member at the same cross section) along the entire length of the member, which includes the two end stay plate pairs and all intermediate stay plate pairs on the section of the member being evaluated, multiplied by the ratio of the channel depth to the channel spacing.

Regression analysis was used to conservatively fit a line to the maximum values. Less than 5% of the data exceeded the limit defined by the line, which was considered acceptable. The line is defined by Equation 6.3, which can be used to calculate the second order moment

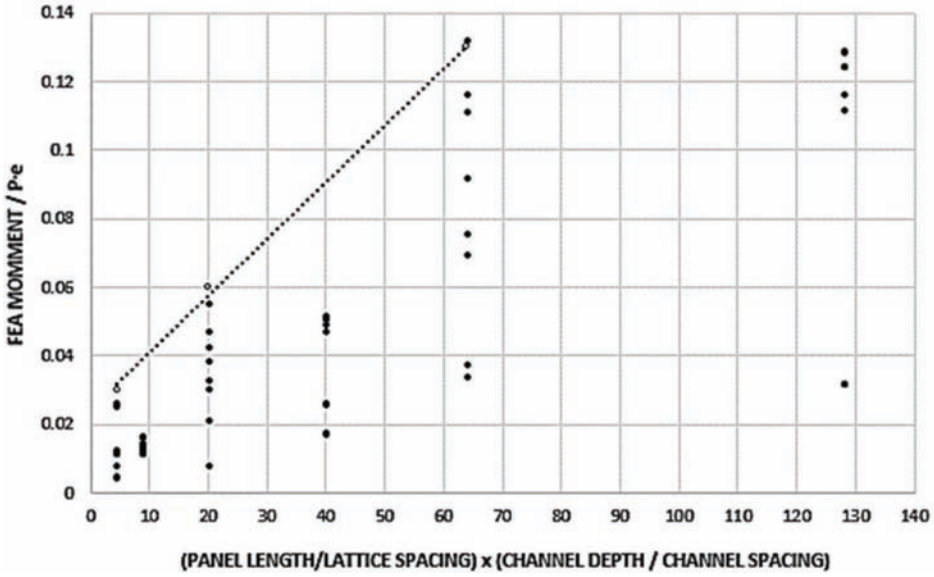

Figure 6.17 Plot of results for continuous laced two-channel members.

resulting from a failed channel in a non-continuous stay-plated two-channel member. The moment is limited to $0.35Pe$, which is slightly above the maximum value observed for the continuous laced members, as can be seen in Figure 6.18.

$$M_{AF} = \frac{P_u e}{22}\left[\frac{N_{SP} d_{CH}}{2e} + 1\right] = \frac{P_u N_{SP} d_{CH} + 2P_u e}{44} \leq 0.35Pe \quad \text{(Eq. 6.3)}$$

Where:

M_{AF} After-fracture moment resulting from failure of a channel in a two-channel member (kip-in).

P_u Total factored axial load (kips).

e Distance measured from the centroid of the unfaulted two-channel member to the centroid of the intact channel in the faulted state (in; see Figure 6.7).

N_{SP} Number of stay plate pairs (1 pair equals the top and bottom stay plates at the same cross section) within the span of the member between the panel points.

d_{CH} Depth of the channels (in).

The resulting moment is inserted into Equation 6.5 to calculate the after-fracture net section stress used to determine the remaining fatigue life. All results for non-continuous stay-plated members have also been tabulated in Appendix B.

6.4.4 Results for Non-Continuous Laced Two-Channel Members

Figure 6.19 compiles the results for all non-continuous laced models analyzed. The vertical axis is the finite element analysis moment divided by the theoretical moment, $P\,e$. The horizontal axis is a combination of geometric properties used to correlate the results. It is the length in inches of the channels, including the depth into the gusset plate at each end of the member, times the ratio of the channel depth to the channel spacing.

Regression analysis was used to conservatively fit a line to the maximum values. Five percent of the data exceeded the limit defined by the line, which was considered acceptable. The line is defined by Equation 6.4, which can be used to calculate the second order moment resulting from a failed channel in a non-continuous laced two-channel member. The lattice bar configuration factor, γ_{LB}, accounts for the fact that single lattice bars will have twice the spacing of comparable double lattice bars. Equation 6.4 was derived using double lattice bar spacing. Based on results for members where the lattice was removed, the simplified method can be extended to single lattice configurations, as well. Thus, the lattice bar configuration factor reduces the spacing of single lattice bar members to an equivalent double lattice bar spacing such that the moment is not incorrectly doubled for single lattice members.

$$M_{AF} = \frac{P_u e}{550}\left[\frac{L_{PL} d_{CH}}{\gamma_{LB} S_{LB} 2e} + 20\right] = \frac{P_u L_{PL} d_{CH} + 40 P_u e \gamma_{LB} S_{LB}}{1100 \gamma_{LB} S_{LB}} \quad \text{(Eq. 6.4)}$$

Where:

M_{AF} After-fracture moment resulting from failure of a channel in a two-channel member (kip-in).

P_u Total factored axial load (kips).

e Distance measured from the centroid of the unfaulted two-channel member to the centroid of the intact channel in the faulted state (in; see Figure 6.7).

L_{PL} Length of the panel measured between the centerlines of two panel points (in).

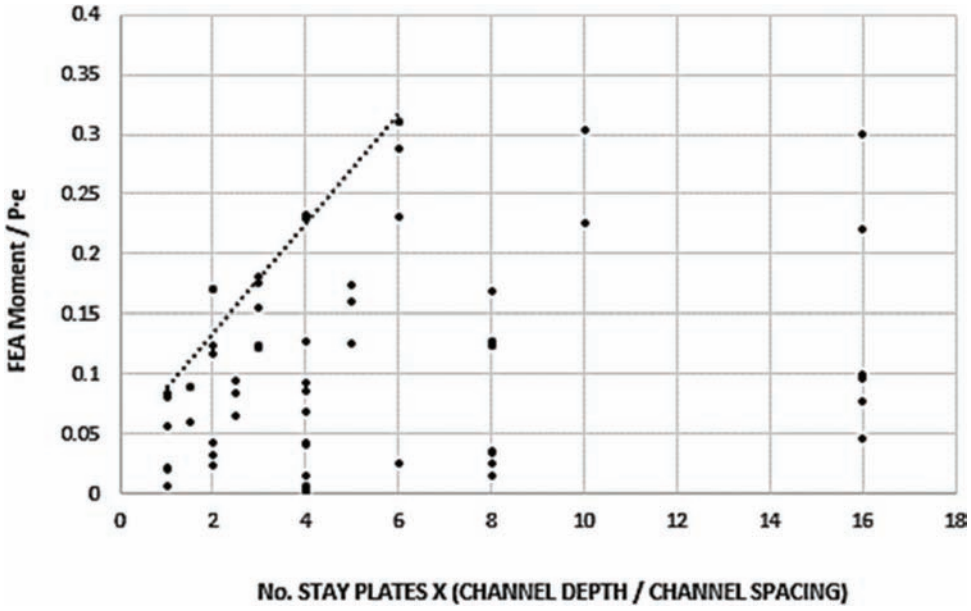

Figure 6.18 Plot of results for non-continuous stay-plated two-channel members.

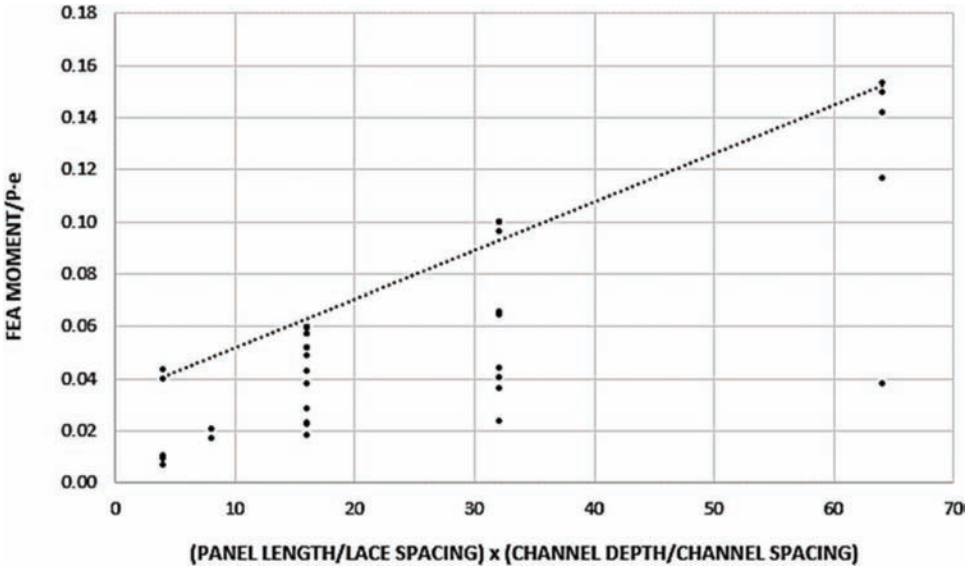

Figure 6.19 Plot of results for non-continuous laced two-channel members.

S_{LB} Spacing of the lattice bars measured longitudinally between centerlines of fasteners connecting the lattice bars to a channel flange (in).

d_{CH} Depth of the channels (in).

γ_{LB} Lattice bar configuration factor; 1.0 for double lattice, 0.5 for single lattice.

The resulting moment is inserted into Equation 6.5 to calculate the after-fracture net section stress used to determine the remaining fatigue life. All results for non-continuous laced members have also been tabulated in Appendix B.

6.5 Application of Parametric Study Findings for Two-Channel Members

The following sections describe implementation of the after-fracture moments, previously explained, in order to calculate the after-fracture net section stress resulting from failure of a channel in a two-channel member. A validation exercise is completed and further guidance is given for proper application of the simplified method.

6.5.1 After-fracture Net Section Stress Calculation

Following calculation of the after-fracture moment that results from failure of one of the two channels, Equation 6.5 is used to calculate the after-fracture net section stress. The equation combines the axial net section stress and second order flexural stress. The axial net section stress is simply the total factored load carried by the member in the unfaulted state, divided by the after-fracture net section. The flexural stress is the after-fracture moment calculated using one of Equations 6.1–6.4, as applicable for the member type, times the distance from the neutral axis to the point of interest, c, divided by the weak axis moment of inertia, I_y.

$$f_{AFN} = \frac{P_u}{A_{AFN}} + \frac{M_{AF}c}{I_y} \qquad \text{(Eq. 6.5)}$$

Where:

A_{AFN} Net section area of the member in the faulted state. This is equal to the net area of a single channel (in^2).

f_{AFN} Factored total net section stress in the faulted state (ksi).

P_uTotal factored applied tensile load (kip).

I_y Principle axis moment of inertia about the weak axis of a single channel (in^4).

c Distance from the centroid of the channel to the surface of stress calculation (in).

M_{AF} After-fracture moment resulting from failure of a channel in a two-channel member (kip-in).

The flexural stress calculation requires the input of the variable, c, which is the distance from the channel weak orientation neutral axis to the spot on the channel for which the stress calculation is being made. Failure of a channel will result in the intact channel bending inward toward the failed channel, or toward the center of the member. This means that the highest combination of tensile axial and flexural stress will result at the interior surface of the intact channel. The stress should be estimated for the location of fasteners that are closest to the center of the member because they would likely be the most fatigue prone detail subjected to the greatest tensile stress range. For the case of the Winona Bridge Specimen 1, shown in Figure 6.20 where the channels were oriented with the flanges pointing away from the center of the member, this would be the inward surface of the cover plate where fasteners holes were located. Generally speaking though, two-channel members will only have fasteners in the flanges used for connection to lattice bars or stay plates. Therefore, the

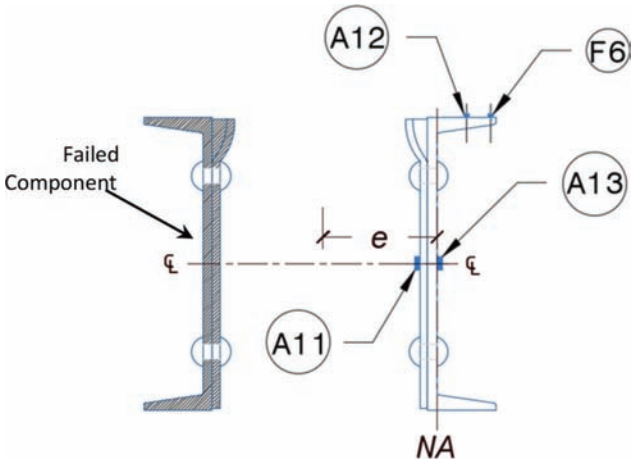

Figure 6.20 Cross sectional view of Winona Bridge Specimen 1, cut location "A."

flexural stress would be calculated for the centerline position of the fasteners in the channel flanges. If the channels were oriented with flanges pointed outward, this could mean that the fastener holes may be subjected to compressive flexural stresses.

Finally, Equations 6.1 through 6.5 are intended for use in the calculation of strength limit states, as well as fatigue. The residual dead load that redistributes following failure of a single channel will generate a residual secondary moment that is combined with the increased axial load demands on the remaining channel. Then the same equations are used for the factored live loads in order to estimate after-fracture net section stress range leading to evaluation of fatigue life.

6.5.2 Validation Exercise: Simplified Analysis of Two-Channel Members

Data collected on the Winona Bridge chord, Specimen 1, were used to validate the simplified analysis method for continuous stay-plated two-channel members. The Winona Bridge test specimen data were used to calibrate the finite element models utilized to perform the parametric study for two-channel members. However, the geometries used to develop the simplified method of analysis did not specifically include the Winona Bridge tension chord. This means it was reasonable to use the experimental data collected on the Winona Bridge Specimens to validate the simplified method. Moreover, the experimental data was preferred for a validation process because it was a physical measurement of stresses in a true bridge member, rather than an assumed and idealized geometry analyzed using finite element.

Although Specimen 1 was not two-channel member, it was treated as such by severing an entire half of the member. If the Winona Bridge chord, or one similar to it, were being evaluated in reality, it would be treated as a multi-component member due to the fact that the rolled channels each had redundant web plates that would prevent an entire half of the cross section from fracturing. Furthermore, prior to cutting of the channel on Specimen 1, the redundant web plate (or cover plate) was cut and the specimen was loaded measuring load, displacement and stress. It was observed that no second order moment was generated in the member, as it was for the case when an entire half of the member was severed. This observation supports the categorization of a member configured similar to the Winona Bridge tension chord as a "multi-component member" where load redistribution was managed within the portion of the member containing the failure component. However, solely for the purpose of validating the two-channel member simplified analysis methods, this member was treated as if there were only two components where one entire half has fractured leaving half of the original cross section to carry the full axial load and secondary moment resulting from load redistribution. Final conclusions from the FEM-based parametric study confirm that this approach was reasonable and effective.

Figure 6.20 shows the cross-sectional view of Specimen 1 at the location of the severed channel and cover plate. The channel and cover plate that were cut have been hatched with black lines. Strain gages are sketched on the intact cross section with blue rectangles at the exact locations they were installed on the test specimen, but are not to scale. Each gage is labeled with the channel identity prescribed to them during the experimental testing. Gage A11 was centered in the net section between the two rows of rivets that stitched the cover plate to the rolled channel. Gage A13 was directly opposite of A11 on the outward surface of the channel web. The eccentricity of the member, e, was calculated based on the composite section of the channel and redundant web plate. The weak orientation neutral axis is shown, labeled "NA," which was positioned very closely to the outward surface of the channel web. Stay plates were located in the foreground and background of the location of the cross section shown, but have been removed for clarity.

Table 6.1 lists the member properties that were used for the validation exercise. A_{AFN} was the after-fracture net section area, N_{SP} was the number of stay plate pairs within a panel length, e was the distance from the centroid of the member in the unfaulted state to the centroid of the member in the faulted state, d_{CH} was the depth of the channels, c_{A11} was the distance from the centroid (neutral axis) of the member in the faulted state to the location of gage A11, c_{A13} was the distance from the centroid (neutral axis) of the member in the

TABLE 6.1
After-fracture properties for Specimen 1

Member Property	Unit	Value
A_{AFN}	in^2	15.91
N_{SP}	–	8
e	in	5.96
d_{CH}	in	15
c_{A11}	in	0.845
c_{A13}	in	-0.03
I_y	in^4	12.8

faulted state to the location of gage A13, and I_y was the weak axis moment of inertia for the remaining half of the member.

Table 6.2 contains the results for the simplified method of analysis, as well as the measured stresses collected during two loading cycles, Test 9 and Test 10, for Specimen 1. P was the total axial load applied to the member, which is presented in increments of 50 kips. M_{AF} was the after-fracture moment calculated using Equation 6.1 for continuous stay-plated two-channel members. f_{bend} was the stress in the member due to the after-fracture moment, M_{AF}, calculated for the position of strain gage A11. f_{axial} was the after-fracture net section axial stress calculated by dividing P by the after-fracture net section area, A_{AFN}. f_{AFN} was the total after-fracture net section stress calculated using Equation 6.5, or simply adding f_{bend} to f_{axial}. The final two columns contain the experimental results measured with strain gage A11, located on the inward surface of the redundant web plate (see Figure 6.20). The following demonstrates the calculations made for Table 6.2 using the final load of 300 kips:

$$M_{AF} = \frac{P_u N_{SP} d_{CH} + 6P_u e}{240} = \frac{300kip(8)(15in) + 6(300kip)(5.96in)}{240} = 194.7kip{\cdot}in$$

$$f_{AFN} = f_{axial} + f_{bend} = \frac{P_u}{A_{AFN}} + \frac{M_{AF}c}{I_y} = \frac{300kip}{15.91in^2} + \frac{194.7kip{\cdot}in(0.845in)}{12.8in^4} = 18.9ksi + 12.9ksi = 31.7ksi$$

Table 6.3 contains the results for the simplified method of analysis, as well as the measured stresses collected during two loading cycles, Test 9 and Test 10, for Specimen 1. P was the total axial load applied to the member. M_{AF} was the after-fracture moment calculated using Equation 6.1 for continuous stay-plated two-channel members. f_{bend} was the stress in the member due to the after-fracture moment, M_{AF}, calculated for the position of strain gage A13. f_{axial} was the after-fracture net section axial stress calculated by dividing P by the after-fracture net section area, A_{AFN}. f_{AFN} was the total after-fracture net section stress calculated using Equation 6.5, or simply adding f_{bend} to f_{axial}. The final two columns contain the experimental results measured with strain gage A13, located on the outward surface of the channel web. As can be seen on Figure 6.20, gage A13 was installed very close to the weak direction neutral axis of the member in the faulted state, which is why the flexural stress component was nearly zero at all load steps.

Comparing results from strain gage A11 for Test 9 and Test 10 to f_{AFN} in Table 6.2 yields:

- the largest overestimation from the simplified method was 14% (1.3 ksi) for Test 10 at the 100-kip load step,
- the greatest under estimate was 5% (-0.5 ksi) for Test 9 at the 100-kip load step,
- the combined average error for all of Test 9 was an overestimation of 1%, and
- the combined average error for Test 10 was an overestimate of 6%.

Results shown in Table 6.2 would be used to determine the after-fracture net section stress and establish the remaining fatigue life of the member. However, to extend the validation exercise further, the data set collected for strain gage A13 on the channel web was also compared to the simplified method of analysis.

Weighing results from strain gage A13 for Test 9 and Test 10 against f_{AFN} in Table 6.3 yields

- the greatest overestimation from the simplified method was 25% (1.2 ksi) for Test 10 at the 50-kip load step,
- the largest underestimate was 19% (-0.7 ksi) for Test 9 at the 150-kip load step,
- the average error for all of Test 9 was an overestimation of 5%, and
- the average error for Test 10 was an overestimation of 13%.

The two experimental test results can also be averaged and then compared to the closed-form solutions. For stress at the location of gage A11

- the largest over estimate becomes 5.3% (1.4 ksi) at the 250-kip load step,
- there was no underestimation,
- the error at the peak load was a 5% (1.6 ksi) overestimation, and
- the combined average error was a 3% overestimation.

TABLE 6.2
Validation results for Specimen 1, gage A11 located on cover plate

Load, P (kip)	M_{AF} (kip-in)	f_{bend} (ksi)	f_{axial} (ksi)	f_{AFN} (ksi)	Test 9, Gage A11 (ksi)	Test 10, Gage A11 (ksi)	Test Average (ksi)	% Error
50	32.4	2.1	3.1	5.3	5.1	5.2	5.2	1.9
100	64.9	4.3	6.3	10.6	11.1	9.3	10.2	3.8
150	97.3	6.4	9.4	15.9	15.8	15.3	15.6	1.9
200	129.8	8.6	12.6	21.1	21.3	20.8	21.1	0
250	162.2	10.7	15.7	26.4	25.3	24.7	25.0	5.3
300	194.7	12.9	18.9	31.7	30.2	30.0	30.1	5

TABLE 6.3
Validation results for Specimen 1, gage A13 located on the channel web

Load, P (kip)	M_{AF} (kip-in)	f_{bend} (ksi)	f_{axial} (ksi)	f_{AFN} (ksi)	Test 9, Gage A13 (ksi)	Test 10, Gage A13 (ksi)	Test Average (ksi)	% Error
50	32.4	-0.1	3.1	3.0	3.8	2.5	3.2	-6.6
100	64.9	-0.2	6.3	6.1	5.6	4.9	5.3	13.1
150	97.3	-0.2	9.4	9.2	8.1	10.0	9.1	1
200	129.8	-0.3	12.6	12.3	11.3	10.9	11.1	9.7
250	162.2	-0.4	15.7	15.3	13.9	13.3	13.6	11.1
300	194.7	-0.5	18.9	18.4	17.0	16.5	16.7	9.2

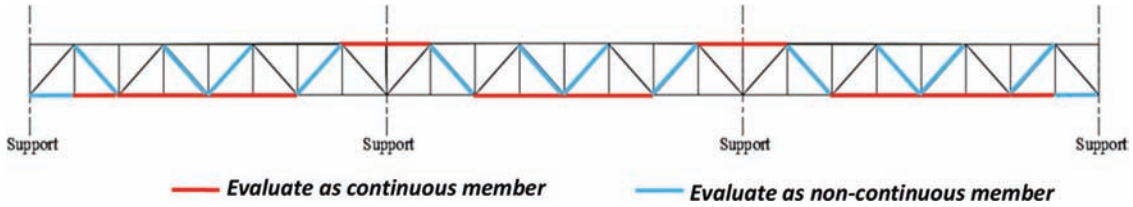

Figure 6.21 Sketch illustrating correct application of Equations 6.1–6.4 on continuous trusses.

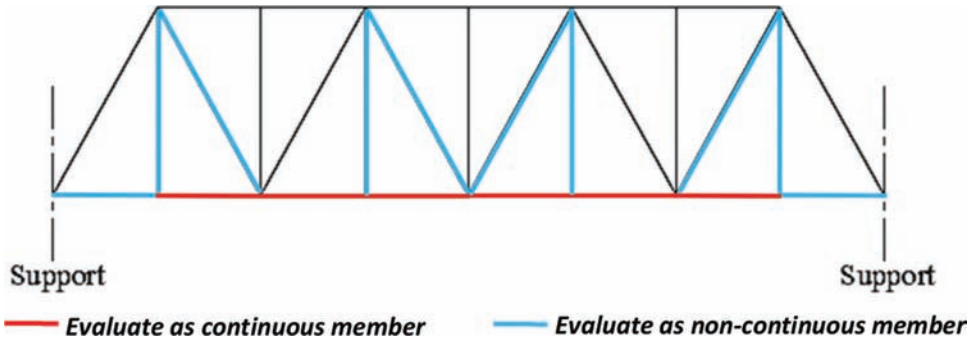

Figure 6.22 Sketch illustrating correct application of Equations 6.1–6.4 on simple span trusses.

For stress at the location of gage A13

- the largest over estimate became 13.1% (0.8 ksi) at the 100-kip load step,
- the largest under estimation became -6.6% (-0.2 ksi) at the 50-kip load step,
- the error at the peak load was a 9.2% overestimation, and
- the combined average error was a 6.2% overestimation.

It was anticipated that results of the closed-form solution for the location of gage A13 could have larger margins of error due to the fact that it was located very close to the estimated neutral axis of bending. However, overall the results agreed well. The simplified method was able to predict the after-fracture net section stress for the controlling fatigue detail to within acceptable margins of error at multiple load steps.

6.5.3 Guidance for Use of Closed-form Solution for Two-Channel Members

The simplified method of analysis was developed taking into account failures at mid-panel and near the gusset connections capturing the largest resulting moments for the geometries analyzed. This means that a single after-fracture moment calculation and net section stress calculation need to be performed for each member. There is no need to repeat this calculation multiple times for different cross sections of the same member. Figure 6.21 and Figure 6.22 illustrate two typical types of trusses where two-channel members could be used. Figure 6.21 shows a generic three-span continuous deck truss structure. Figure 6.22 depicts a generic single-span through-truss structure. Each figure has been highlighted with red and blue lines. The red lines indicate members that would be analyzed using either Equation 6.1 (stay-plated) or 6.2 (laced) for continuous members. The blue lines designate members that would be evaluated using either Equation 6.3 (stay-plated) or 6.4 (laced) for non-continuous members. Members that are *not* highlighted, or which appear black, are compression members that would not need to be evaluated for internal redundancy. Reversal zones that are subjected to both tensile and compressive live load stresses need to be evaluated. Notice that the terminating bottom chord of each truss is evaluated using equations for non-continuous members. Due to

the lack of continuity beyond the abutment at each end of a truss, the last panel must be analyzed using equations developed for non-continuous members. This was confirmed during the parametric study as the correct application of the equations for terminating members.

7. DETAILED INSPECTION AND LOAD RATING ROUND-ROBIN STUDY

During Phase II of the project, a small round-robin style inspection and load rating study was performed with certified bridge inspectors and practicing load rating engineers. The purpose was to investigate the variability in the inspection and evaluation of severely corroded steel tension members. This process evaluated two separate, but related, sources of variability within the inspection and load rating process. The variability in each task was controlled such that variability in the load ratings was not compounded by variability in the inspection findings.

7.1 Inspection Round-Robin

A small pool of bridge inspectors was invited to perform a detailed inspection of Specimen 1 between, but not including, the two gusset plates, as shown in Figure 7.1. Inspectors were directed to use typical inspection procedures to evaluate the condition of the chord and provide the necessary thickness measurements to support a load rating calculation. The inspection was divided into three separate tasks to gain insight into the individual inspection strategies employed by the inspectors but also to provide consistent data that could be directly compared to evaluate variability. The variability was evaluated by comparing the inspector measurements to each other and to the reference measurements determined by the RT.

7.1.1 Inspector Demographics

Five inspectors (four males and one female) participated in the inspection round-robin. Two of the inspectors were from federal agencies, one was from a state department of transportation, and two worked for a private engineering and inspection firm. The inspectors ranged in age from 25 to 59 and their experience varied from 1 year to 18 years. The average experience of the group was 7.2 years. Four of the five inspectors possessed a post-secondary degree in engineering and were either an engineer-in-training or a professional engineer. Four of the five inspectors had completed the FHWA/NHI 2 week course *Safety Inspection of In-service Bridges*. Only one inspector had received additional training specific to estimating section loss in steel members. The inspectors had performed between 0 and 60 fracture critical inspections during the 12 months prior to their participation in the study and the percentage of time spent performing inspections ranged from less than 1% to 95%. Inspector characteristics and inspection conditions are summarized in Table 7.1.

7.1.2 Inspection Scenario

The inspections were completed outside at Bowen Laboratory in West Lafayette, IN between April 2018 and July 2018. The inspections were completed from the ground adjacent to the truss chord and no specialized access equipment was required. The average temperatures on the days of the inspections ranged from 47 degrees to 80 degrees. Figure 7.2 shows two of the inspectors taking thickness measurements during this hands-on inspection. During the inspection, the proctor recorded the weather conditions, the start and end time for each task, the tools used by the inspector, and general firsthand observations of the inspector's

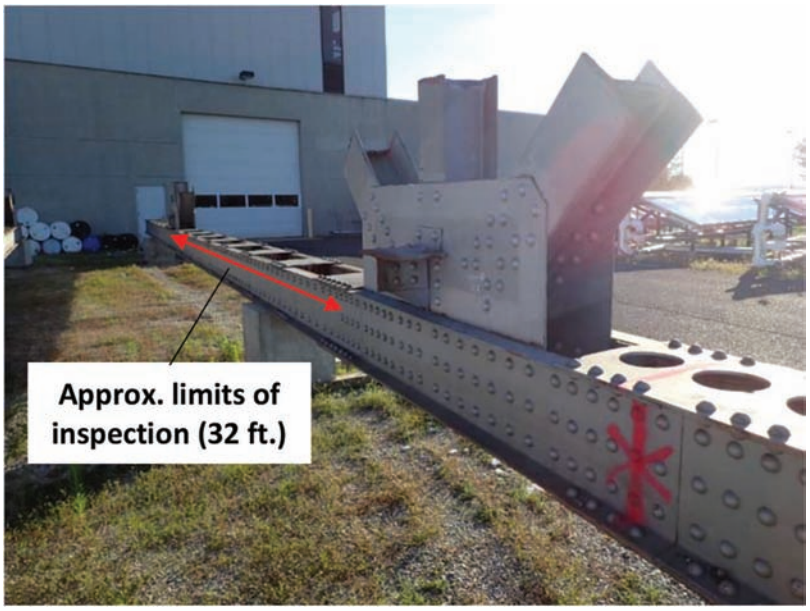

Figure 7.1 Truss chord elevation view (looking from joint L4 to L2).

TABLE 7.1
Inspector characteristics and inspection conditions

	Inspector 1	Inspector 2	Inspector 3	Inspector 4	Inspector 5
Inspection Date	23-Apr-18	24-Apr-18/ 26-Apr-18	27-Jun-18	16-Jul-18	16-Jul-18
Temperature (°F)	55	55/47	75	80	80
Weather	Overcast, light rain	Clear	Overcast, humid	Hot, humid	Hot, humid
Age	59	29	45	27	25
Gender	Male	Female	Male	Male	Male
Employer	Federal Agency	Federal Agency	State Agency	Private Consultant	Private Consultant
Years of Inspection Experience	10	1	18	5	2
No. of Routine Inspections in Previous 12 Months	4	1	80	20	30
No. of Hands On Inspections in Previous 12 Months	4	0	60	4	1
Professional Licensure	PE	FE	None	FE	FE
Education	Master's Degree	Bachelor's Degree	Bachelor's Degree	Bachelor's Degree	Bachelor's Degree

Figure 7.2 Two inspectors taking thickness measurements of the truss chord.

activities. After the inspection, the inspector was asked to complete a written exit survey to gather information on their education, experience, training, etc. All inspectors were read the same set of instructions and provided with a set of blank inspections forms. These documents are provided in Appendix D.

In addition to the inspection forms and procedures, the following information about the structure was given to the inspectors:

- This member was removed from a bridge constructed in the early 1940s in the upper Midwest region of the US.
- This member was a part of the bottom chord of the deck truss.
- This member is fracture critical.

The inspection was divided into three separate tasks. Before beginning each task, the proctor read the same set of instructions to the inspector and answered any questions. Task 1 was the most unstructured task. The inspectors were asked to identify the critical section for measuring section loss within the inspection limits. The inspectors were allowed to use any tools that they brought with them to complete this task and a time limit of 30 minutes was imposed. This time limit was intended to ensure that inspectors did not spend an unreasonable amount of time taking measurements at multiple locations. In Task 2, the inspectors were asked to estimate the remaining thickness of the truss chord at the two locations. The locations were identified on the

inspection forms and on the chord, itself. The inspectors were allowed to use any tools they brought with them to complete the task and no time limit was imposed. In Task 3, the inspectors were asked to indicate the critical section for measuring section loss within a 28-inch segment of the chord spanning between two adjacent batten plates. The inspectors did not need to record the remaining thickness at this location, but could use any tools they brought with them to complete the task. No time limit was imposed. The three tasks were designed to yield inspection results that could be compared among the inspectors, while also providing a realistic representation of the variability in inspection strategies.

7.1.3 Inspection Results

Determining the remaining member area based on the inspectors' recorded thickness measurements was not a straightforward task. In many cases, the RT had to make assumptions about the intentions of the inspectors since the inspectors often just noted measurements on the sketches without providing dimensions. The inspectors explained that common practice is to take the measurements in the field and then calculate section loss in their office, so they may not be accustomed to making their field notes intelligible to others. For consistency in this study, a numerical approximation similar to the middle Riemann sum method was used to calculate the remaining area from the thickness measurements. Each recorded thickness measurement was assumed to be the measurement at the center of a rectangular shaped increment as shown in Figure 7.3 and the total remaining area of the member was calculated by summing the areas of the increments. As the number of increments increases, the length of the increments gets shorter and the sum of the areas eventually approaches the true area of the member. The number and length of the increments was determined based on the number of thickness measurements recorded by the inspector; more thickness measurements resulted in shorter increments. When the exact location of the measurements was not provided, they were assumed to be evenly spaced, and when thickness measurements were not provided, the design thickness of the component was used to calculate the remaining area. The rivet holes were ignored during all area calculations.

7.1.3.1 Task 1. As mentioned previously, in Task 1, the inspectors were asked to identify the most critical section for estimating the remaining capacity of the tension chord within the inspection limits. Four of the five inspectors successfully completed Task 1. The remaining inspector provided various thickness measurements along the length of the chord, but did not provide enough detail to determine the remaining section at any single location. A summary of the results for this task is shown in Table 7.2. Based on the measurements provided, the remaining area estimates ranged from 32.4 in^2 to 35 in^2. Assuming an original gross cross section of 34.7 in^2 based on the construction plans, the percent "loss" estimates range from -6.4% to +0.9%.

The quickest inspector completed Task 1 in 17 minutes and the slowest inspector required 47 minutes. Although a time limit of 30 minutes had been set for this task, two inspectors were allowed to exceed this to provide useable data. All of the inspectors used an ultrasonic thickness gauge to complete this task. Four of the five inspectors used a measuring device (folding ruler or tape measure) and a camera during this task. One inspector used digital calipers and another inspector used a hammer.

Figure 7.4 shows the locations along the chord that the inspectors identified as the most critical section for

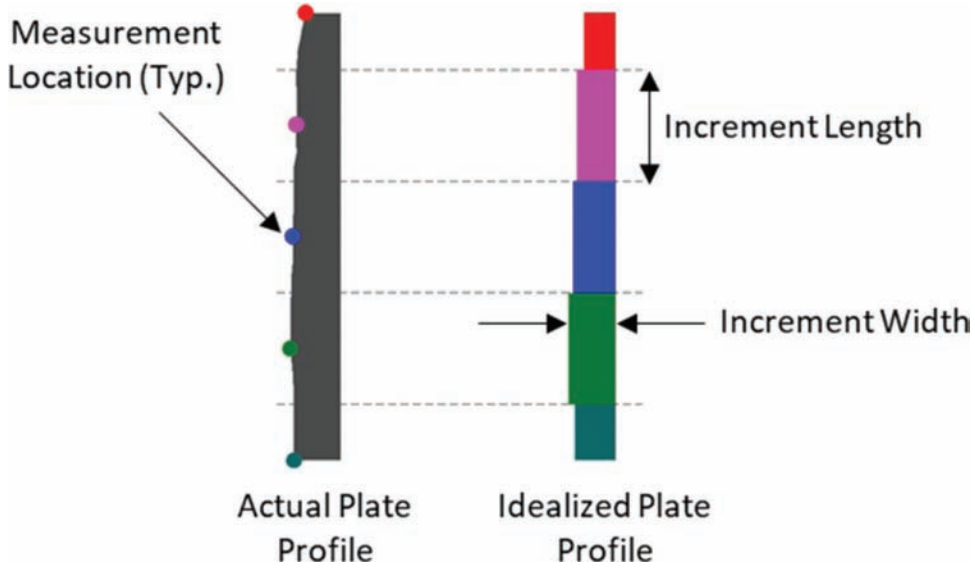

Figure 7.3 Method used to calculate remaining member area from field measurements.

TABLE 7.2
Summary of Task 1 results

	Inspector 1	Inspector 2	Inspector 3	Inspector 4	Inspector 5
Remaining Member Area (in^2)	32.4	Incomplete	34.6	33.1	35
Duration (min.)	47	30	24	39	17
Location of Critical Section (in inches measured from Joint L2)	129	Incomplete	17.25	130	120

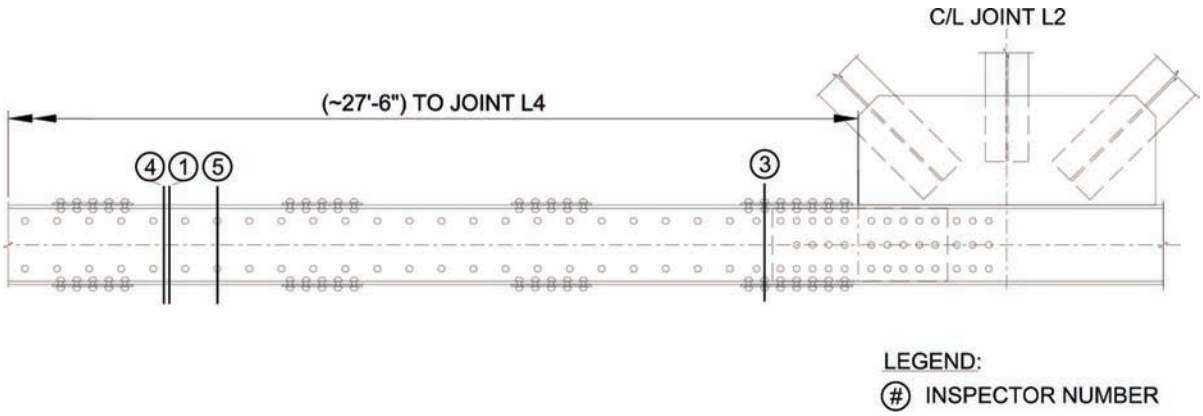

Figure 7.4 Critical section locations identified in Task 1.

determining remaining capacity. Three of the four inspectors that successfully completed Task 1 identified a critical section within a 10-inch region of the chord. This region of the chord had experienced significant section loss and distortion due to pack rust at the top of one of the cover plates as shown in Figure 7.5. The fourth inspector determined that the critical section was beneath the batten plate closest to joint L2.

One of the largest sources of variability within this task was the location and quantity of thickness measurements recorded by the inspectors. Only two of the five inspectors recorded thickness measurements on all four components (2 channels and 2 cover plates) of the built-up chord. Inspector 1 provided measurements at approximately 1-inch intervals along the depth of each component and inspector 3 provided measurements at approximately 2-1/2-inch intervals along the components. In contrast, Inspector 4 provided seven thickness measurements along just one of the channels and one of the cover plates and Inspector 5 provided three thickness measurements along just one of the channels. Since the amount of section loss in the chord is relatively small, especially in the channel components, the lack of measurements had a limited influence on the remaining area calculations. However, in members with more severe section loss, this may cause the remaining area to be significantly over- or underestimated.

Although not the focus of this phase, only two of the five inspectors provided notes or measurements related to the distortion in the cover plate. In the vicinity of the critical sections selected by Inspectors 1, 4, and 5, the thickness of the pack rust is more than 1 inch at the top and bottom of the member. For tension members, distortion due to pack rust is typically ignored during the engineering evaluations since design standards allow for areas of localized yielding and tension members are self-stabilizing (Kulicki, Prucz, Sorgenfrei, Mertz, & Young, 1990). Therefore, the lack of measurements or notes would likely not affect the load rating. However, for compression members, the distortion could pose more significant issues (Kulicki et al., 1990) and may need to be accounted for by the load rating engineer. Distortion in the cover plates may reduce their effectiveness and lower the overall capacity of the member. In this case, the inspector should include more detailed notes, photos, and measurements. For this inspection, the inspectors were not explicitly told that this was tension member but were told it was a fracture critical lower truss chord, which implies that it is a tension member. It is possible they understood that the distortion measurement was not needed for the load rating of a tension member or it is possible that they were not aware of its importance for any loading type. In general, inspectors should be instructed to err on the side of providing too much information and allow the rating officials to determine what condition information should be included in their analysis.

7.1.3.2 Task 2. In Task 2, the inspectors were instructed to provide thickness measurements for the truss chord at the two locations shown in Figure 7.6.

Following the inspections, reference values were developed by the research team after disassembling the chord. Measurements were taken with an ultrasonic thickness gauge at 1/2-inch increments along each cover plate and channel and the remaining area was

Figure 7.5 Region identified as the critical section by three of the inspectors.

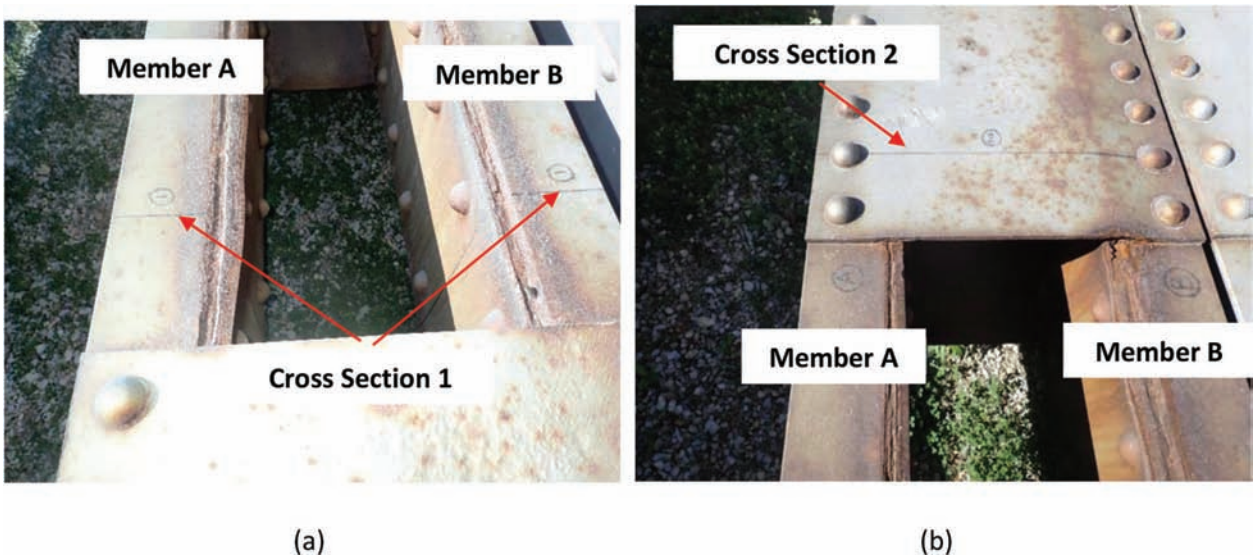

Figure 7.6 Truss chord at (a) Cross Section 1 and (b) Cross Section 2.

calculated using the middle Riemann sum approach discussed above. A summary of the results from the RT measurements is provided in Table 7.3. Reference measurements were taken at 6 or 7 locations along each flange, 28 locations along the channel web, and 31 or 32 locations along the cover plate. The remaining area determined from the thickness measurements was 33.27 in^2 at Cross Section 1 and 33.63 in^2 at Cross Section 2. The disassembled pieces of the truss are shown in Figure 7.7.

All five inspectors successfully completed this task. A summary of the results for this task is shown in Table 7.4. At Cross Section 1, the remaining area estimates ranged from 33.42 in^2 to 35.66 in^2. At Cross Section 2, the remaining area estimates ranged from 34.16 in^2 to 35.70 in^2. Compared to the reference values developed by the RT, all inspectors overestimated the remaining area at both locations as shown in Figure 7.8. The reference area calculated based on the RT measurements is shown on the x-axis and the measured area calculated based on the inspectors' measurements is shown on the y-axis. The diagonal 1-to-1 reference line represents exact agreement between the reference area and the measured area. All of the measured areas plot above the 1-to-1 line indicating that the measured area exceeds the reference area. The percent error ranged from 0.5% to 7.2% at Cross Section 1 and from 1.0% to 6.2% at Cross Section 2.

TABLE 7.3
Summary of RT results

Member Description	Cross Section 1		Cross Section 2	
	Member A Areas (in^2)	Member B Areas (in^2)	Member A Areas (in^2)	Member B Areas (in^2)
Web	7.70	8.01	8.09	8.05
Top Flange	1.83	1.83	1.85	1.83
Bottom Flange	1.81	1.83	1.84	1.83
Channel (Web + Flanges)	11.33	11.68	11.78	11.71
Cover Plate	4.99	5.27	5.24	4.90
Channel + Cover Plate	16.32	16.94	17.02	16.61
Total Cross Section	33.27		33.63	

Figure 7.7 Disassembled pieces from Cross Sections 1 and 2.

The duration of this task ranged from 5 minutes to 31 minutes. The average time to complete this task was 19 minutes. The quickest inspector measured the remaining thickness at Cross Section 2 as part of Task 1, and so they did not repeat that as part of Task 2. All of the inspectors used an ultrasonic thickness gauge to complete this task. Four of the five inspectors used a measuring device (tape measure or folding ruler) during this task and only one inspector used a flashlight to complete this task.

Similar to Task 1, the location and number of thickness measurements varied significantly from inspector to inspector. Again, Inspector 1 provided measurements at approximately 1-inch intervals along the depth of each component and Inspector 3 provided measurements at approximately 2-1/2-inch intervals. Inspector 2 took measurements at approximately 5-inch intervals along the channels and 2-1/2-inch intervals along the cover plates. Inspector 4 recorded the thickness of the channels at 1-1/2-inch intervals but took only one measurement along the cover plates. Inspector 5 recorded the thickness of the channels and cover plates at only a single location.

Considering the components separately provides a clearer look at the variability in the measurements. Measurement statistics for the cover plates are provided from Cross Section 1 in Table 7.5 and Cross Section 2 in Table 7.6. The variability in remaining area, as indicated by the standard deviation, was largest at Cover Plate B in Cross Section 2 where the smallest estimate of the remaining area of this member was 4.9 in^2 and the largest estimate was 6.27 in^2. The average of the measurements was 5.4 in^2 and the standard deviation was 0.61 in^2. This cross section was difficult to inspect because it was beneath the batten plate near Joint L2 and this plate had experienced complete section loss near the top edge as shown in Figure 7.9. Conversely, the variability in remaining area was smallest at Cover Plate A in Cross Section 2. The remaining area estimates ranged from 5.3 in^2 to 5.75 in^2 with a mean of 0.5 in^2 and a standard deviation of 0.15 in^2. Although this plate was also obscured by the batten plate, it was in relatively good condition and inspectors were able to provide a reasonable estimate of the remaining thickness without performing a careful visual inspection.

TABLE 7.4
Summary of Task 2 results

	Inspector 1	Inspector 2	Inspector 3	Inspector 4	Inspector 5	Reference
Cross Section 1 (in^2)	33.42	34.34	34.62	35.66	35.12	33.27
Cross Section 2 (in^2)	34.25	34.92	34.58	35.70	33.96	33.63
Duration (min.)	29	31	5	19	13	N/A

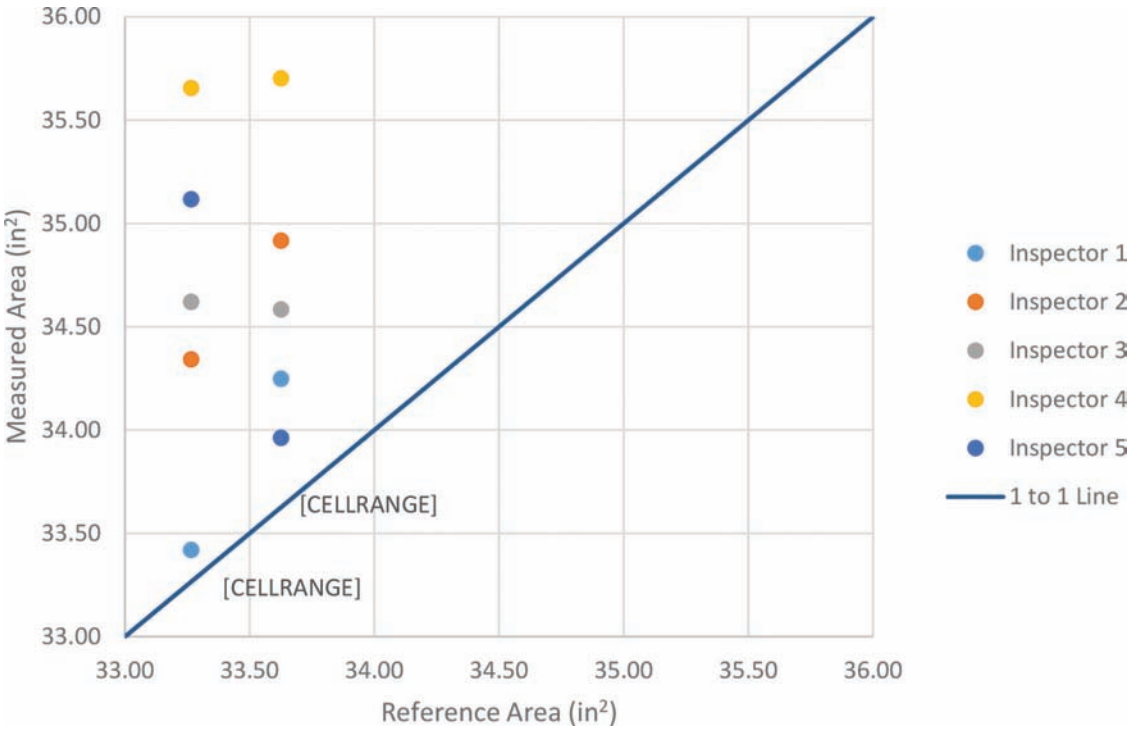

Figure 7.8 Measured area versus reference area for both cross sections.

TABLE 7.5
Measurement statistics for the cover plates at Cross Section 1

	Inspector 1	Inspector 2	Inspector 3	Inspector 4	Inspector 5	Reference
Calculated Area, in^2 (Plate A/Plate B)	5.11/4.92	5.1/5.29	5.19/5.36	5.63/5.63	5.58/5.81	4.99/5.27
Min. Thickness Measurement, in (Plate A/Plate B)	0.04/0.13	0.16/0.265	0.207/0.329	0.375/0.375	0.378/0.394	0.116/0.26
Number of Measurements (Plate A/Plate B)	16/16	6/6	6/6	1/1	1/1	31/32

TABLE 7.6
Measurements statistics for the cover plates at Cross Section 2

	Inspector 1	Inspector 2	Inspector 3	Inspector 4	Inspector 5	Reference
Calculated Area, in^2 (Plate A/Plate B)	5.36/4.9	5.3/5.4	5.52/4.73	5.63/5.63	5.65/6.27	5.24/4.9
Min. Thickness Measurement, in. (Plate A/Plate B)	0.31/0.16	0.305/0.275	0.329/0	0.375/0.375	0.383/0.425	0.298/0
Number of Measurements (Plate A/Plate B)	16/16	6/5	6/6	1/1	1/1	31/31

Figure 7.9 Cover plate condition at Cross Section 2.

TABLE 7.7
Percent area for cover plates area*

	Inspector 1	Inspector 2	Inspector 3	Inspector 4	Inspector 5
Cover Plate A, Cross Section 1 (%)	2.4	2.3	4.0	12.8	11.8
Cover Plate B, Cross Section 1 (%)	-6.6	0.3	1.7	6.8	10.3
Cover Plate A, Cross Section 2 (%)	2.3	1.1	5.2	7.3	7.8
Cover Plate B, Cross Section 2 (%)	0.1	10.2	-3.5	14.8	28.0
Average Absolute Error (%)	2.8	3.5	3.6	10.4	14.5

*Errors exceeding 5% shown in red.

Table 7.7 shows the percent error for each inspector considering only the cover plates. As expected, the area calculated from the inspectors' measurements approach the reference area as the number of measurements increase. In general, Inspectors 1, 2, and 3 provided sufficient thickness measurements such that the remaining area could be calculated within 5% of the reference value while Inspectors 4 and 5 did not provide such information. Of note, only one of the five inspectors recorded the depth of the cover plates, 14-3/4 inches, on the inspection forms. Although the construction plans call for 15 × 3/8-inch web plates, the measured depth of these plates in their current condition is between 14-3/4 and 14-7/8 inches. If no depth dimension was recorded, the plan dimension was used to calculate the remaining area.

Table 7.8 through Table 7.12 present the descriptive statistics for the member areas estimated from the inspectors' measurements. These tables include the reference area, along with the average area estimated from the sample, standard deviation from the sample, coefficient of variation (COV) from the sample, the minimum and maximum estimated areas, and the number of inspectors that provided thickness measurements (n). In all but one instance, the average area from the sample exceeds the reference area.

A one-sample *t*-test was used to determine if the average areas estimated from the inspectors' measurements were statistically different from the reference areas. The *t*-test was used to test the null hypothesis that the sample mean is equal to the reference value. The results of this test are summarized in Table 7.13. "Fail" indicates that the null hypothesis can be rejected, meaning that the average area determined based on the inspection results is different from the reference area calculated based on the measurements from the research team at the 5% significance level. "Pass" indicates that the null hypothesis could not be rejected and the average area determined based on the inspection results is not different from the reference area at the 5% significance level. Based on the results from this test, this population of inspectors incorrectly estimated the area of the cover plate at two locations and the area of the channel at one location. Additionally, this population of inspectors incorrectly estimated the area of the chord at both locations.

TABLE 7.8
Descriptive statistics for Member A at Cross Section 1

	Cover Plate	Channel Web	Channel Top Flange	Channel Bottom Flange	Total Channel	Total Member
Reference Area (in^2)	4.99	7.70	1.83	1.81	11.33	16.32
Average Area (in^2)	5.32	8.07	1.91	1.94	11.93	17.25
Standard Deviation of Area (in^2)	0.26	0.22	0.13	0.07	0.16	0.38
COV	0.05	0.03	0.07	0.04	0.01	0.02
Minimum Area (in^2)	5.10	7.86	1.70	1.83	11.80	16.90
Maximum Area (in^2)	5.63	8.33	2.03	2.03	12.20	17.83
n	5	5	5	5	5	5

TABLE 7.9
Descriptive statistics for Member B at Cross Section 1

	Cover Plate	Channel Web	Channel Top Flange	Channel Bottom Flange	Total Channel	Total Member
Reference Area (in^2)	5.27	8.01	1.83	1.83	11.68	16.94
Average Area (in^2)	5.40	8.10	1.95	1.93	11.98	17.38
Standard Deviation of Area (in^2)	0.34	0.24	0.06	0.09	0.25	0.52
COV	0.06	0.03	0.03	0.05	0.02	0.03
Minimum Area (in^2)	4.92	7.69	1.87	1.79	11.59	16.51
Maximum Area (in^2)	5.81	8.30	2.03	2.03	12.20	17.83
n	5	5	5	5	5	5

TABLE 7.10
Descriptive statistics for Member A at Cross Section 2

	Cover Plate	Channel Web	Channel Top Flange	Channel Bottom Flange	Total Channel	Total Member
Reference Area (in^2)	5.24	8.09	1.85	1.84	11.78	17.02
Average Area (in^2)	5.49	8.20	1.85	1.85	11.90	17.39
Standard Deviation of Area (in^2)	0.15	0.11	0.26	0.27	0.48	0.44
COV	0.03	0.01	0.14	0.14	0.04	0.03
Minimum Area (in^2)	5.30	8.07	1.38	1.37	11.07	16.72
Maximum Area (in^2)	5.65	8.31	2.03	2.03	12.21	17.84
n	5	5	5	5	5	5

TABLE 7.11
Descriptive statistics for Member B at Cross Section 2

	Cover Plate	Channel Web	Channel Top Flange	Channel Bottom Flange	Total Channel	Total Member
Reference Area (in^2)	4.90	8.05	1.83	1.83	11.71	16.61
Average Area (in^2)	5.38	8.25	1.81	1.84	11.91	17.29
Standard Deviation of Area (in^2)	0.61	0.12	0.35	0.25	0.53	0.42
COV	0.11	0.01	0.19	0.14	0.04	0.02
Minimum Area (in^2)	4.73	8.12	1.19	1.39	10.98	16.88
Maximum Area (in^2)	6.27	8.40	2.03	1.96	12.24	17.86
n	5	5	5	5	5	5

7.1.3.3 Task 3. In Task 3, the inspectors were asked to indicate the critical section for measuring section loss within the region of the chord shown in Figure 7.10. The inspectors were not required to report any thickness measurements at this location, although they could take measurements to identify the section. A summary of the results for this task is shown in Table 7.14. The duration of this task ranged from 2 minutes to 11 minutes. All of the inspectors used an ultrasonic thickness gauge and a measuring device (folding ruler or tape measure) to complete this task. One inspector used a broom during this task.

Each inspector identified a different section as the critical section, as shown in Figure 7.11. One inspector

explained that they picked the section that they did because the rivets appeared to be stretched and there was a gouge in the web of the channel at the same location. Another inspector selected the critical section based on the amount of distortion at the top of the cover plate. A third inspector asserted that there was not much difference in thickness through the identified region, so they selected the center because it would be the worst case for buckling (note the inspector was told to assume that this was a fracture critical bottom chord, implying that it is a tension member). The proctor observed that the majority of the inspectors only considered the distortion and thickness loss near the top of the cover plate. However, since this is fairly consistent through the region, it was not a particularly effective or efficient way to identify the section with the most section loss. Nevertheless, the inspectors should have considered the thickness along the bottom of the cover plates as this varied between 0.28 inches and 0.375 inches. Since greater distortion generally indicates more section loss, this could have been identified without taking thickness measurements. The research team determined the critical section to be located 25 inches from Batten Plate D similar to the section identified by Inspector 2.

It is interesting to note that although this task was limited to 28 inches of the chord, the results do not reflect increasing agreement among the inspectors as compared to Task 1. In both tasks, three inspectors identified critical sections within a 10-inch region. This suggests that inspectors applied the same general reasoning to identify the critical region of the specimen, but their precise reasoning, used to identify the exact location, differed. For instance, in Task 1, the inspectors identified the critical region based mainly on the degree of section loss and/or distortion along the top edge of the web plates. However, in Task 3, the distortion and section loss was relatively uniform, and so this reasoning was less effective. Instead, inspectors applied additional considerations, such as the likely failure mechanism or condition of the rivets and channel member, to identify the exact location of the critical section.

TABLE 7.12
Descriptive statistics for the truss chord member

	Cross Section 1	Cross Section 2
Reference Area (in^2)	33.27	33.63
Average Area (in^2)	34.63	34.68
Standard Deviation of Area (in^2)	0.84	0.67
COV	0.02	0.02
Minimum Area (in^2)	33.42	33.96
Maximum Area (in^2)	35.66	35.70
n	5	5

TABLE 7.13
T-test results at 5% significance level for average estimated areas by component

Location	Cover Plate	Channel Web	Channel Top Flange	Channel Bottom Flange	Total Channel	Total Member
Cross Section 1				***Fail***		
Member A	Fail	Fail	Pass	Fail	Fail	Fail
Member B	Pass	Pass	Fail	Pass	Pass	Pass
Cross Section 2				***Fail***		
Member A	Fail	Pass	Pass	Pass	Pass	Pass
Member B	Pass	Fail	Pass	Pass	Pass	Fail

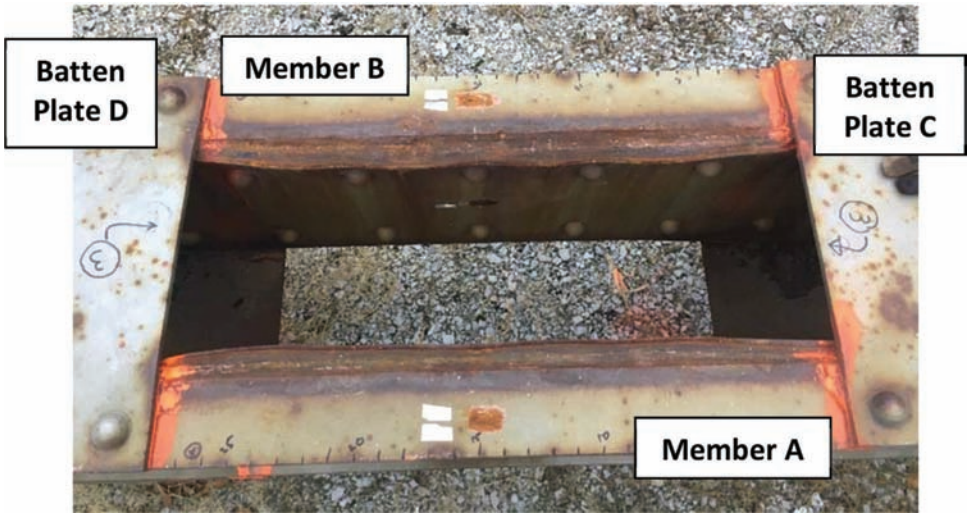

Figure 7.10 Limits of inspection for Task 3 (between Batten Plates C and D).

TABLE 7.14
Summary of Task 3 results

	Inspector 1	Inspector 2	Inspector 3	Inspector 4	Inspector 5
Location of Critical Section (in inches measured from Batten Plate C)	15	27	9	6	18.5
Duration (min.)	10	11	3	6	2

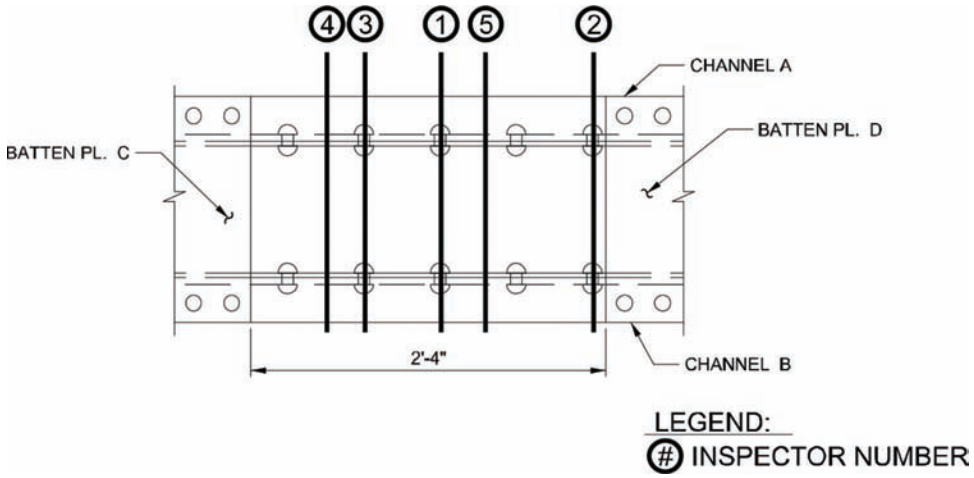

Figure 7.11 Critical section locations identified in Task 3.

7.1.4 Summary and Recommendations

Five inspectors from diverse backgrounds were invited to perform a hands-on inspection of a portion of Specimen 1 to investigate the variability in thickness measurements recorded during inspections of corroded steel bridge members. Inspectors were directed to use typical inspection procedures to evaluate the condition of the chord and provide the necessary thickness measurements to support a load rating calculation. The variability was evaluated by comparing the inspector measurements to each other and to the reference measurements determined by the RT. In Task 1, three of the five inspectors determined that the critical section was located within a 10-inch region of the specimen. This level of agreement indicates some consistency in the methods used by inspectors to identify where the most section loss has occurred along a bridge member. In Task 2, inspectors provided thickness measurements at two pre-determined locations. All five of the inspectors provided thickness measurements that overestimated the remaining member area and two of the inspectors did not record a sufficient number of measurements to provide a reasonably accurate estimate of the area (less than 5% error). In Task 3, all five inspectors identified a different critical section within the region of interest. Although this task was limited to 28 inches of the chord, the results do not reflect increasing agreement among the inspectors as compared to Task 1. In both tasks, three inspectors identified critical sections within a 10-inch region. Overall, the level of detail in the findings recorded by some of the inspectors suggests a general uncertainty about what information is needed from the field to support a load rating analysis. This uncertainty may result in the need for follow-up inspections to gather the necessary information. The following recommendations to improve the consistency and quality of visual inspections of corroded steel bridge members were developed based on the results from this round-robin:

- Inspectors should receive training specific to corrosion inspection and evaluation. Instructions on how to properly calibrate and use an ultrasonic thickness gauge should be provided. Inspectors need improved instructions on what information is required by load rating engineers, and how these requirements vary based on bridge and member type. Illinois DOT has developed a clear and concise training that includes much of this information and is available online here: http://www.idot.illinois.gov/doing-business/procurements/engineering-architectural-professional-services/Consultants-Resources/bridge-management-and-inspections.
- Thickness measurement of members with moderate deterioration should be taken at intervals not to exceed 3 inches. Additional thickness measurements will be needed for critical members or members with more severe deterioration. Inspectors should clearly record the location of each measurement or the distance between measurements on their inspection forms.
- Inspectors should record dimensional measurements or all members to verify construction plans. Nominal (no deterioration) thickness measurements should also be recorded for reference.
- Before recording thickness measurements, inspectors should visually inspect the full length of the member.

The inspector should use typical inspection tools, including a flashlight, to perform this inspection. After this general inspection, they should focus on areas that are prone to corrosion and pack rust or are showing the most signs of deterioration.

7.2 Load Rating Round-Robin

A small pool of load rating engineers was invited to load rate Specimen 1 between, but not including, the two gusset plates. This is the same portion of the chord that was used in the inspection round-robin. A benchmark set of inspection data was established by the RT and provided to each of the load raters ensuring that each engineer was working from the same information. The load raters were asked to determine the inventory level load rating factor for the Strength I limit state and the remaining fatigue life based on the information provided. The load raters' calculations were compared to the theoretical load rating derived by the RT and to each other to evaluate the variability in interpreting inspection findings and applying code requirements.

7.2.1 Load Rater Demographics

Four engineers (three males and one female) participated in this study. Two of the load raters were from federal agencies, one was from a state department of transportation, and one worked for a private engineering firm. The inspectors ranged in age from 29 to 56 and their load rating experience varied from 0 years to 10 years. All four load raters were professional engineers with post-secondary degrees in civil engineering. Three of the four load raters had completed the FHWA/NHI 4-day course *Fundamentals of LRFR and Applications of LRFR for Bridge Superstructures*. The engineers had performed between 0 and 50 load ratings during the 12 months prior to their participation in the study and the percentage of work time spent performing load ratings ranged from 0% to 90%. Three of the four load raters had previously load rated a steel truss bridge, although for one of the participants, this was the only bridge that they had ever load rated. In addition to load rating experience, two of the load raters also had inspection experience and/or experience designing steel bridges for new construction. Load rater characteristics are summarized in Table 7.15.

7.2.2 Load Rating Scenario

The load ratings were completed at the participants' convenience between June 2018 and August 2018. The load raters were provided with the same load rating procedure, inspection report, construction plans, exit form, and results worksheet via e-mail. These documents are provided in Appendix D. After completing the load rating, the load rater was asked to complete a written exit survey to gather information on their education, experience, training, etc. The engineers were also asked to record and report the amount of time they spent on the evaluation. The load rating report, calculations, and exit form were returned to the RT via e-mail.

The evaluation was divided into two separate tasks that could be completed in any order. In Task 1, the load raters were asked to calculate the inventory level load rating factor for the Strength I limit state in the as-built (undamaged) condition and the as-inspected (damaged) condition. In Task 2, the load raters were asked to calculate the remaining fatigue life in the as-inspected condition. The load rating procedures specified that the load rating was to be completed using the load and resistance factor rating method in accordance with the second edition of the *AASHTO Manual for Bridge Evaluation* (MBE), including the 2016 interim revisions. The load raters were allowed to use any other references or computer software available to them.

A partially completed load rating summary report was provided so that all inspectors would record their final results in a consistent manner. Inspectors were asked to show all work necessary to support these results, however standardized forms for the calculations were not provided by the RT.

The background information provided to the participants consisted of a mock bridge inspection report and relevant sheets from the construction plans. The inspection report was populated by the RT with information from the National Bridge Inventory and the inspection findings from Inspectors 1 and 2 in the inspection round-robin. This report included detailed measurements of metalwork losses at three locations along the chord.

In addition to the construction plans and the inspection report, the following information about the structure was given to the load raters:

TABLE 7.15
Load rater characteristics

	Load Rater 1	Load Rater 2	Load Rater 3	Load Rater 4
Load Rating Date	27-Jun-18	15-Jul-18	18-Jul-18	11-Aug-18
Age	40	42	56	29
Employment Sector	Federal Agency	Federal Agency	State Agency	Private Consultant
Years of Load Rating Experience	0	10	8	4
Professional Licensure	PE (Civil)	PE (Civil)	PE (Civil)	PE (Civil)
Education	PhD (Civil Engineering)	MS (Civil Engineering)	BS (Civil Engineering)	MS (Civil Engineering)

- the bridge was constructed in 1941 in the upper Midwest region of the United States;
- the member under evaluation is the bottom truss chord in Span 16 between joints L2 and L4;
- the member is fracture critical;
- P_{DC} = 335 kips, P_{DW} = 0 kips, P_{LL+IM} = 322 kips (design truck with lane load);
- P_{LL+IM} = 134 kips (fatigue truck);
- these loads are unfactored. They include the distribution factor and dynamic load allowance;
- $(ADTT)_{SL}$ = 1500 and it is assumed that $(ADTT)_{SL}$ is constant through the life of the bridge.

The loads were determined by the RT using a 2D SAP2000 model of Span 16, as shown in Figure 7.12. The total dead load was calculated from the construction plans and applied at the top chord joints. The predicted dead load in member L_2L_4 was 320 kips. This compared well with the design dead load of 335 kips specified on the construction plans. For consistency, the design dead load was used in this exercise. Influence lines were used to determine the live load effects on member L_2L_4. The predicted Strength I and Fatigue live loads for HL-93 loading were 322 kips and 104 kips, respectively. The fatigue live load was artificially increased to 134 kips for this exercise to produce a finite fatigue life. To validate the model, the live load effects from the H-20 loading were determined in accordance with the 1931 *AASHO Standard Specifications* since this was the governing specification at the time of design (Kulicki & Mertz, 2006). The predicted live load was 150.7 kips and the predicted impact load was 30.1 kips. These values are nearly identical to the design live loads of 150.3 kips and the design impact load of 29.7 kips specified on the construction plans. Complete calculations are provided in Appendix D.

7.2.3 Load Rating Results

The reference load rating was developed by the RT in accordance with the second edition of the MBE and the seventh edition of the *AASHTO LRFD Bridge Design Specifications* (LRFD BDS). All four participants also used the MBE and the LRFD BDS to complete this load rating. One load rater used the third edition of the MBE instead of the second edition. Additionally, one load rater also referenced a state specific load rating manual and class notes. Three of the load raters used Microsoft Excel to complete the load rating and one used PTC Mathcad.

The load raters were asked to self-report the amount of time they spent on this evaluation. Three of the participants reported that it took them 8 hours or less to complete the evaluation. One load rater reported that the load rating took 50 hours. This load rater also reported that they used SAP2000 to verify the loads provided by the RT. Therefore, it is likely that the load rating portion of the exercise required only a small percentage of the total reported time, although this is not known for sure.

7.2.3.1 Material Strength Assumptions. The load raters were required to make an assumption regarding the material strength (yield and ultimate) of the truss chord members. The material type was not specified on the construction plans and the engineers were not provided with the results from the material tests performed

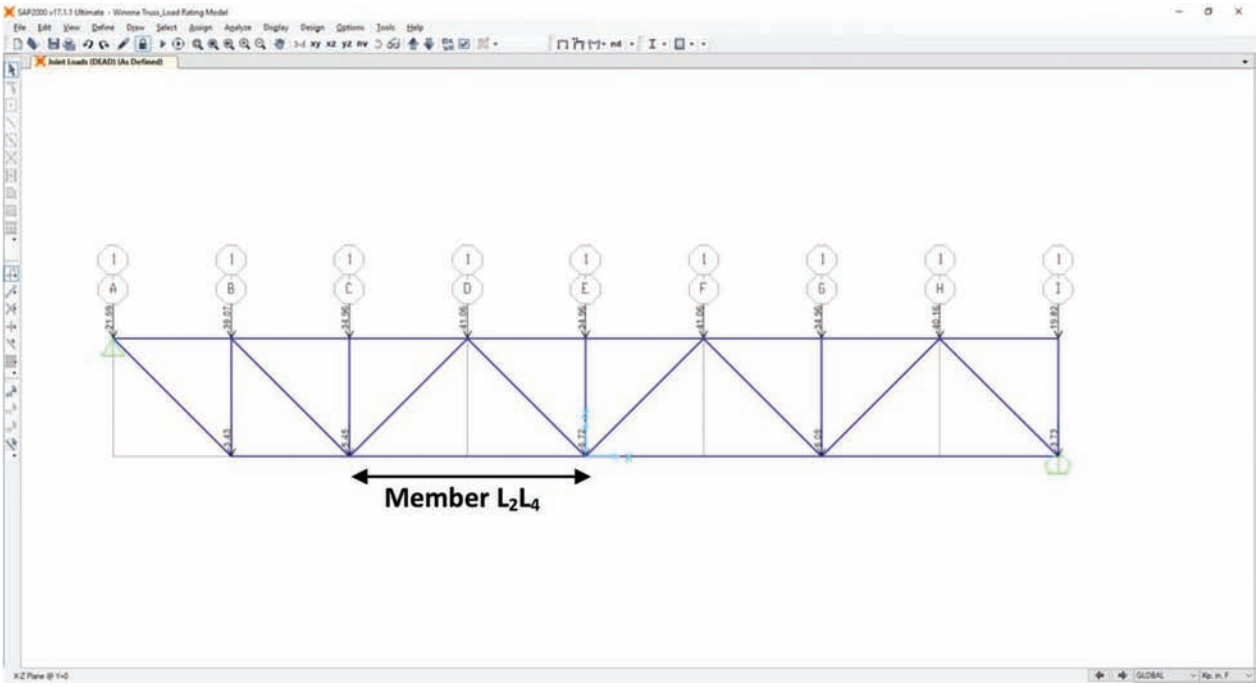

Figure 7.12 2D SAP model of Span 16.

by the RT. It was expected that the load raters would use the year of construction to determine the minimum mechanical properties of the steel. This information is available from a variety of sources including the MBE, the *AISC Rehabilitation and Retrofit Guide, and* withdrawn ASTM specifications. The RT assumed a yield strength of 33 ksi and an ultimate strength of 66 ksi based on Table 6A.6.2.1-1 in the MBE for construction between 1936 and 1963.

The material strengths assumed by the load raters are summarized in Table 7.16. All of the participants assumed a yield strength of 33 ksi, while the assumed ultimate strength varied between 52 ksi and 66 ksi. Only two of the load raters provided a reference to support their assumption with one citing the MBE and the other citing the 1939 version of ASTM A7. Of note, the engineer that referenced the MBE assumed an ultimate strength of 52 ksi, which corresponds to construction before 1905.

7.2.3.2 Gross and Net Section Calculations. Before calculating the load rating factors and the remaining fatigue life, the load raters needed to determine the gross section and net section areas of the truss chord. In the as-built condition, this is relatively straightforward and can be calculated from the construction plans and handbook properties. In the as-inspected condition, the load raters were required to consider the inspection findings provided in the inspection report to determine the appropriate section areas.

The gross and net section areas in the as-built condition are summarized in Table 7.17. Estimates for the gross section area varied from 34.7 in^2 to 118.3 in^2 and estimates of the net section area varied from 27.3 in^2 to 33.2 in^2. The reference values were 34.7 in^2 and 29.0 in^2 for the gross section area and the net section area, respectively.

There is reasonable agreement among the areas calculated by the load raters, with the exception of the gross section area reported by Load Rater 2. The gross section area determined by Load Rater 2 is more than three times the reference value, but since Load Rater 2 did not provide any calculations to support this value, the cause of the discrepancy could not be identified. The following list summarizes some of the other sources of variability in these values. No distinction is made between assumptions or inaccuracies that yield a conservative estimate of member area and those that lead to an unconservative estimate.

- *Channel Area*. Two load raters used an area of 11.8 in^2 for the C15 × 40 channel. This is the value given in current steel handbooks, but is slightly larger than the value given in steel handbooks at the time of construction. The other load raters and the RT used an area of 11.7 in^2 as specified in the third edition of the *AISC Steel Construction Manual,* originally released in 1937.
- *Number of holes in the net section*. The number of rivet holes through the cross section varies along member L_2L_4. The majority of the member includes four rivets connecting the cover plates to the channel webs. At the batten plates, there are an additional four rivets connecting the batten plates to the channel flanges. Near the joints, there is a section with six holes through the webs, but the partially developed 1/2-inch splice plates compensate for the two additional holes. Two-load raters assumed six holes through the web and four holes through the flange when calculating the net section area, but they did not include the developed portion of the splice plate. One load rater assumed a single hole through each web and no holes through the flange. The final load rater and the RT calculated the net section based on eight holes through the cross section (four holes through the flanges and four holes through the webs).
- *Rivet and rivet hole diameter*. The construction plans specify a 7/8-inch diameter rivet for connections in the main truss members. Still, one load rater assumed the rivet diameter was 3/4 inch. Two load raters and the RT assumed the hole diameter was 1/16 inch greater than the rivet diameter. One load rater assumed the hole diameter matched the rivet diameter and another load rater assumed that the hole diameter was 1/8 inch greater than the rivet diameter.

The gross and net section areas in the as-inspected condition are summarized in Table 7.18. Estimates for the gross section area varied from 31.2 in^2 to 114.9 in^2 and estimates of the net section area varied from 25.3 in^2 to 28.7 in^2. The reference values were 32.5 in^2 and 27.9 in^2 for the gross section area and the net section area, respectively.

TABLE 7.16
Summary of assumed material strengths

	Load Rater 1	Load Rater 2	Load Rater 3	Load Rater 4	Reference
Assumed Yield Strength (ksi)	33	33	33	33	33
Assumed Tensile Strength (ksi)	60	66	60	52	66
Reference Cited	ASTM 7-39	Not Given	Not Given	MBE Table 6A.6.2.1-1	MBE Table 6A.6.2.1-1

TABLE 7.17
Summary of as-built gross and net section area estimates

	Load Rater 1	Load Rater 2	Load Rater 3	Load Rater 4	Reference
Gross Section Area (in^2)	34.7	118.3	34.9	35.3	34.7
Net Section Area (in^2)	28.8	28.7	33.2	27.3	29.0

TABLE 7.18
Summary of as-inspected gross and net section area estimates

	Load Rater 1	Load Rater 2	Load Rater 3	Load Rater 4	Reference
Gross Section Area (in^2)	32.9	114.9	31.2	32.3	32.5
Governing Cross Section Use to Determine Gross Section Area	Cross Section 1	Cross Section 1	Cross Section 1	Cross Section 1	Cross Section 1
Net Section Area (in^2)	27.3	25.3	Not Specified	28.7	27.9
Governing Cross Section Use to Determine Net Section Area	Cross Section 1	Cross Section 1	Not Specified	Cross Section 1	Cross Section 3

Again, there is reasonable agreement among the values determined by the load raters, with the exception of the gross section area determined by Load Rater 2. The error in the as-built calculation was carried forward as the losses reported at Cross Section 1 were simply subtracted from the as-built area. All four engineers used Cross Section 1 as the governing cross section, and two of the load raters provided calculations at all three locations to support this. The following list summarizes some of the other sources of variability in these values. No distinction is made between assumptions or inaccuracies that yield a conservative estimate of area and those that lead to an unconservative estimate.

- *Material losses in the cover plate.* The load raters employed different methods to account for the material loss and distortion in the cover plates. One load rater used the average of the thickness measurements to determine the remaining area, and two load raters used a weighted average of the thickness measurements. The final load rater assumed total section loss in regions where the cover plates had been deformed by pack rust. At Cross Section 1, this included the top and bottom 3 inches of Web Plate A and the top 3 inches of Web Plate B. This load rater did not account for the losses in other portions of the plates. The RT used the approach discussed in Section 7.1.3 to determine the remaining area of the cover plates.
- *Material losses in the channel.* The inspection report included thickness measurements for Channel B at Cross Section 1. In all other locations, no losses were reported. One load rater used the average of the thickness measurements to determine the remaining area of this channel, and one load rater used a weighted average of the thickness measurements. The other two load raters ignored the losses in the channel at Cross Section 1. The RT accounted for the losses in this channel similar to the cover plates, although the losses in this member were very small and likely within the mill tolerances for the rolled shape.
- *Number of holes in the net section.* Although all three-load raters that estimated the net section area in the as-inspected condition assumed that Cross Section 1 was the governing cross section, each assumed a different number of holes through the cross section. Load Rater 1 assumed eight holes (4 flange, 4 web), Load Rater 2 assumed ten holes (6 flange, 4 web), and Load Rater 3 assumed four holes (0 flange, 4 web). The RT calculated the net section area at Cross Sections 1 and 2 with four holes through the cross-section (0 flange, 4 web), while the net section area at Cross Section 3 was calculated with eight holes through the cross-section (4 flange, 4 web). The RT determined that smallest gross section occurred at Cross Section 1 and the smallest net section occurred at Cross Section 3.
- *Rivet and rivet hole diameter.* As discussed above.

7.2.3.3 Task 1. In Task 1, the load raters were asked to record the member capacity and inventory load rating factor for the Strength I limit state in the as-built and as-inspected conditions. Using their previous assumptions about material strength and the calculated gross and net section areas, the load raters were able to determine the member's resistance to yielding and fracture. All of the load raters used the equations given in Section 6.8.2.1 of the LRFD BDS to determine the tensile capacity of the member and the Equation 6A.4.2.1-1 from the MBE to calculate the load rating factor. The member capacity and rating factor results are summarized in Table 7.19 and Table 7.20 for the as-built and as-inspected conditions, respectively.

In the as-built condition, estimates for member capacity ranged from 923 kips to 1363 kips and estimates for the load rating factor varied from 0.9 to 1.68. The reference capacity was 978 kips and the corresponding rating factor was 0.99. Three of the four load raters determined that the capacity was governed by yielding on the gross section. Load Rater 2, who reported the greatest member capacity and highest rating factor, determined that fracture on the net section was the governing limit state. This was due to the previously discussed overestimation in the gross section area.

In the as-inspected condition, estimates for member capacity ranged from 732 kips to 1022 kips and estimates for the rating factor varied from 0.56 to 1.07. The reference capacity was 866 kips and the corresponding rating factor was 0.79. Three of the four load raters determined that the capacity was governed by yielding on the gross section. Again, there is reasonable agreement among the values determined by the load raters, with the exception Load Rater 2.

In addition to variability caused by the material strength and area estimates discussed above, the following list summarizes some of the other sources of variability in these values. No distinction is made between assumptions or inaccuracies that yield a conservative estimate of member capacity or rating factor and those that lead to an unconservative estimate.

TABLE 7.19
Summary of Task 1 results (as-built condition)

	Load Rater 1	Load Rater 2	Load Rater 3	Load Rater 4	Reference
Governing Limit State	Yielding on the gross section	Fracture on the net section	Yielding on the gross section	Yielding on the gross section	Yielding on the gross section
Member Capacity (kips)	923	1363	929	996	978
Inventory Rating Factor	0.9	1.68	0.9	1.02	0.99

TABLE 7.20
Summary of Task 2 results (as-inspected condition)

	Load Rater 1	Load Rater 2	Load Rater 3	Load Rater 4	Reference
Governing Limit State	Yielding on the gross section	Fracture on the net section	Yielding on the gross section	Yielding on the gross section	Yielding on the gross section
Member Capacity (kips)	877	1022	831	732	866
Inventory Rating Factor	0.81	1.07	0.73	0.56	0.79

- *Assumed value for R_P.* The equation for tensile resistance to fracture on the net section (LRFD BDS Eq. 6.8.2.1-2) includes a hole reduction factor, R_P, to account for reduced fracture resistance in the vicinity of holes that were punched full size. Two of the load raters assumed R_p was equal to 0.9, as specified for holes punched full size. One inspector assumed that R_p was equal to 1.0, as specified for holes that are drilled full size or sub-punched and reamed. One inspector did not include this factor in the equation and so a value of 1.0 was used by default. The RT assumed that R_p was equal to 1.0 based on a construction plan note which reads, "General reaming will be required as per M.H.D [Minnesota Highway Department] Specifications 2407 3E5a."
- *Assumed values for φ_C and φ_S.* The equation for member capacity in the strength limit state (MBE Eq. 6A.4.2.1-2) includes a condition state factor, φ_C, and a system factor, φ_S. These factors are applied along with the strength resistance factor from the LRFD BDS to the nominal member capacity. The condition factor takes a value between 0.85 and 1.0 and is intended to account for the increased uncertainty in the capacity of deteriorated members and the high likelihood of additional deterioration before the next inspection. The system factor also takes a value between 0.85 and 1.0 and is intended to account for reduced redundancy in specific superstructure types. Additionally, the MBE stipulates that the product of the condition factor and the system factor ($\varphi_C \times \varphi_S$) need not be taken as less than 0.85 (MBE Eq. 6A.4.2.1-3). The reference member capacity in the as-built condition was based on a condition factor of 1.0, specified for members in for good condition, and a system factor of 0.9, specified for riveted members in two-girder/truss/arch bridges. The reference member capacity in the as-inspected condition was based on a condition factor of 0.85, specified for members in poor condition, and a system factor of 0.9. Since the product of 0.85 and 0.9 is 0.77, a factor of 0.85 was instead applied to the design capacity in the as-inspected condition. The values assumed by the load raters for the factors are shown in Table 7.21. The only factor that the load raters were in complete agreement on was the condition factor in the as-inspected condition. For all the other factors, at least two different values were used by the load raters. Additionally, two load raters did not apply the lower limit to the product of the condition and system factors even though it was warranted.

7.2.3.4 Task 2. In Task 2, the load raters were asked to record the governing fatigue category, the effective stress range, and the remaining fatigue life of the member. This evaluation was only performed for the as-inspected condition. The results for this task are summarized in Table 7.22.

Estimates for the effective stress range varied from 2.9 ksi to 3.7 ksi and the reference value was 3.6 ksi. One load rater assumed Category A as the governing fatigue category, two load raters assumed Category C, and one load rater assumed Category D. The RT determined that Category D was the applicable fatigue category. Finally, three of the four load raters determined that the member had infinite remaining fatigue life, while one load rater determined that the remaining fatigue life was just under 30 years. The RT calculated a remaining fatigue life of 32 years.

While Fatigue Category A is not appropriate for this member since it applies only to base metal with minimum surface roughness, the distinction between Category C and Category D is less clear. For design, the LRFD BDS assigns base metal at the net section of non-pretensioned mechanically fastened joints to Category D (LRFD BDS Table 6.6.1.2.3-1). For evaluation, the MBE allows riveted connections to be considered as Category C details due to the internal redundancy of built-up members (MBE Sections 7.2.1 and C7.2.1). In the 2015 revisions to the second edition of the MBE, AASHTO included an additional stipulation stating that the increase in fatigue life is not warranted for riveted members in "poor physical conditions, such as with missing rivets or indications of punched holes" (MBE, Section 7.2.1). This forces the load rater to make

TABLE 7.21
Assumed condition and system factors

	Load Rater 1	Load Rater 2	Load Rater 3	Load Rater 4	Reference
Condition Factor, As-Built	0.85	1	0.85	1	1
System Factor, As-Built	1	0.9	0.85	0.9	0.9
Condition Factor, As-Inspected	0.85	0.85	0.85	0.85	0.85
System Factor, As-Inspected	1	0.9	0.85	0.85	0.9
Lower Limit, Applied?	N/A	No	Yes	No	Yes

TABLE 7.22
Summary of Task 2 results

	Load Rater 1	Load Rater 2	Load Rater 3	Load Rater 4	Reference
Governing Fatigue Category	D	C	A	C	D
Effective Stress Range (ksi)	3.7	3.7	2.9	3.5	3.6
Remaining Fatigue Life (years)	29.6	Infinite	Infinite	Infinite	32

a judgement call between Category C and Category D based on the condition of the member. Although the MBE does not mention section loss or damage from pack rust, the RT determined that the increase in fatigue life was not appropriate for this member and assumed Category D was the governing fatigue category.

In addition to variability caused by the material strength and area estimates discussed above, the following list summarizes some of the other sources of variability in these values. No distinction is made between assumptions or inaccuracies that yield a conservative estimate of remaining fatigue life and those that lead to an unconservative estimate.

- *Assumed value of R_R.* The equation for estimating total fatigue life (MBE Eq. 7.2.5.1-1) includes a factor related to the probability of fatigue crack initiation, R_R. The MBE includes four levels at which fatigue life can be estimated: minimum, Evaluation 1, Evaluation 2, and mean. The minimum expected fatigue life provides the most conservative estimate while mean fatigue life yields the statistically most likely fatigue life The Evaluation 1 and Evaluation 2 fatigue life estimates will fall between the minimum and the mean fatigue life estimates. The MBE provides only general guidance on selecting the appropriate fatigue life for evaluation, leaving the decision largely up to the engineer. In this study, Load Rater 1 reported the minimum fatigue life. Load Rater 2 elected to estimate the mean fatigue life, although they later determined the life to be infinite. The other two load raters did not provide any indication of which finite fatigue life level they would have used if they had found the member to have finite life. The RT reported the Evaluation 1 fatigue life. This corresponds to the evaluation life used in previous editions of the MBE and is the level recommended by MnDOT in the 2018 edition of the *Bridge Load Rating and Evaluation Manual.*
- *Application of R_p and R_s.* The equation for effective stress (MBE Eq. 7.2.2-1) includes a partial load factor, R_s and a multiple presence factor, R_p. Additionally, the partial load factor is included in the equation for maximum stress range (MBE Section 7.2.4). These factors are typically very close to 1.0, and so ignoring or misapplying them has negligible or no effect on the results. A few discrepancies in how these factors were applied were noted by the RT while reviewing the load raters' calculations and are noted here for completeness. One inspector had a minor typo in the equation for R_p, multiplying by the number of lanes instead of dividing. One load rater included R_s in the calculation for maximum stress range. One load rater assumed R_p was equal to 1.0 and two load raters did not include R_p or R_s in any of the stress range calculations. Since these factors are approximately or exactly equal to 1.0, none of these errors had a measurable effect on the results.
- *Area used to determine live load stress range.* One load rater used the gross section area instead of the net section area to determine live load stress range. The other three load raters and the RT used the net section area to determine live load stress range.
- *Typographical errors and different interpretations of the provided information.* A number of other small errors or misinterpretations of the provided information were noted in the Task 2 calculations. There may have been ambiguity in how the background information was presented or conveyed to the participants, although there was no common mistake among all the load raters pointing to an obvious omission. In practice, these calculations would be subject to review from a higher-level official, and it is likely that these errors would have been noticed and corrected. However, the fatigue life analysis is less straightforward than the strength evaluation, both in the process and communication, and so minor mistakes are likely to occur more frequently. One load rater used a fatigue truck load of 135 kips, instead of 134 kips, and another reduced the given fatigue truck load by the multiple presence factor for a single lane (1.2) even though this factor had not been included in the load provided by the RT. One load rater used the third edition of the MBE, which has adopted the larger load factors for the Fatigue I (0.8) and Fatigue II (1.75) limit states from the eighth edition of the LRFD BDS. One load rater used an area that did not match any of the previous calculations to determine the live load stress range. This area was similar to the net section areas in the as-built and as-inspected conditions. Another inspector assumed

a traffic volume growth rate of 2%, even though the load rating procedures stated that the load raters were to assume a constant ADTT throughout the life of the bridge. This resulted in an underestimation of the number of cycles that had already been applied to the structure and an overestimation of the remaining fatigue life.

7.2.4 Summary and Recommendations

Four engineers were invited to load rate a portion of Specimen 1 to investigate the variability in how inspection reports are interpreted and code requirements are applied for corroded steel bridge members. The load raters were provided with the same set of procedures and background information to complete their analysis. The variability in the results was evaluated by comparing them to each other and to the reference values calculated by the RT. In Task 1, three of the four inspectors reported a load rating factor within 10% of the reference value for the truss chord in the as-built condition. In the as-inspected condition, two of the load raters reported a rating factor within 10% of the reference value. In Task 2, three of the four load raters reported an effective stress range within 5% of the reference value for the truss chord in the as-inspected condition. However, due to variability in determining the governing fatigue category, only one of these inspectors determined that the truss chord had a finite fatigue life. The following recommendations to improve the quality and consistency of load rating evaluations of corroded steel bridge members were developed based on the results from this round-robin:

- Load raters should receive instruction specific to determining the gross section and net section areas in the as-inspected condition. A single method should be used by all load raters to ensure that results from one load rater can be compared to the results from another. This guidance should clearly state how the thickness measurements are used to determine remaining area (average, weighted average, etc.) and whether load raters should assume that the thickness measurements may apply anywhere along the member or at a specific location. The method used to calculate member area should inform how the inspectors' collect and record measurements in the field.
- Load raters should be required to clearly document and cite all assumptions. If questions or discrepancies arise in the future, this information will make it easier to validate previous evaluation. Additionally, load raters should be encouraged to include sketches to support the area calculations. Sketches would be especially helpful in identifying where the net section area was calculated.
- State DOT manuals should provide clear guidance on issues not directly specified in the MBE, such as how to determine the appropriate fatigue category for riveted members or the recommended fatigue life evaluation level.
- Load raters should have access to historical standards and specifications, both federal and state specific, and be encouraged to use these when load rating older structures. Load raters should be encouraged to include the relevant pages from the historic documents, including the construction plans, in their calculation packages for future reference.
- The fatigue life evaluation method presented in the MBE is complicated. Small mistakes are common and so fatigue life evaluations should be carefully reviewed by a senior load rater. Load raters should be encouraged to familiarize themselves with the theory behind the equations and factors; simply "plugging and chugging" with the code equations may lead to mistakes.

REFERENCES

British Standards Institute. (2013). *Guide to methods for assessing the acceptability of flaws in metallic structures* (BS 7910:2013). London, UK: BSI Standards Limited.

Diggelmann, L. M. (2012). *Evaluation of member and structural redundancy on the US-421 bridge over the Ohio River* (Master's thesis, Purdue University, West Lafayette, IN). Retrieved from https://docs.lib.purdue.edu/dissertations/AAI10156265/

Hebdon, M. H., Korkmaz, C., Martín, F. J. B., & Connor, R. J. (2015). *Member-level redundancy of built-up steel girders subjected to flexure*. West Lafayette, IN: Purdue University. https://doi.org/10.5703/1288284316728

Kulicki, J. M., Prucz, Z., Sorgenfrei, D. F., Mertz, D. R., & Young, W. T. (1990). *Guidelines for evaluating corrosion effects in existing steel bridges* (NCHRP Report 333). Washington, DC: Transportation Research Board. Retrieved from http://onlinepubs.trb.org/onlinepubs/nchrp/nchrp_rpt_333.pdf

Kulicki, J. M. & Mertz, D. R. (2006). Evolution of vehicular live load models during the interstate design era and beyond. In *50 years of interstate structures: Past, present and future* (Transportation Research Circular No. E-C104). Washington, DC: Transportation Research Board. Retrieved from http://onlinepubs.trb.org/onlinepubs/circulars/ec104.pdf

Lloyd, J. B., Bonachera Martin, F. J., Korkmaz, C., & Connor, R. J. (2018). *Member-level redundancy of built-up steel axially loaded members*. West Lafayette, IN: Purdue University. https://doi.org/10.5703/1288284316997

Ocel, J. M. (2013). *Guidelines for the load and resistance factor design and rating of riveted and bolted gusset-plate connections for steel bridges* (NCHRP Web-Only Document 197). Washington, DC: The National Academies Press. https://doi.org/10.17226/22584

APPENDICES

Appendix A. Charpy V-Notch Impact Test Results

Appendix B. Tabulated Results for Parametric Study

Appendix C. Gage Plans

Appendix D. Inspection and Load Rating Documents

APPENDIX A – CHARPY V-NOTCH IMPACT TEST RESULTS

CVN Test Data & Master Curve for the Channel Web:

Table A.1 CVN test data results for the channel web

Test Temperature (°F)	Energy (ft-lbs)	K_{mat} (ksi-√in) P_f = 5%	K_{mat} (ksi-√in) P_f = 50%
100	27	66	109
100	27		
100	24		
70	16.5	54	87
70	16.5		
70	14		
40	11	46	71
40	11		
40	9		
40	11		
40	8.5		
40	11		
10	6.5	40	60
10	6.5		
10	7.5		
10	5		
10	4		
10	4		

Inputs for Table A.1 K_{mat} *Estimate:*

- Mean T_{27J} = 28°C
- T_0 = 10°C
- T_k = 25°C

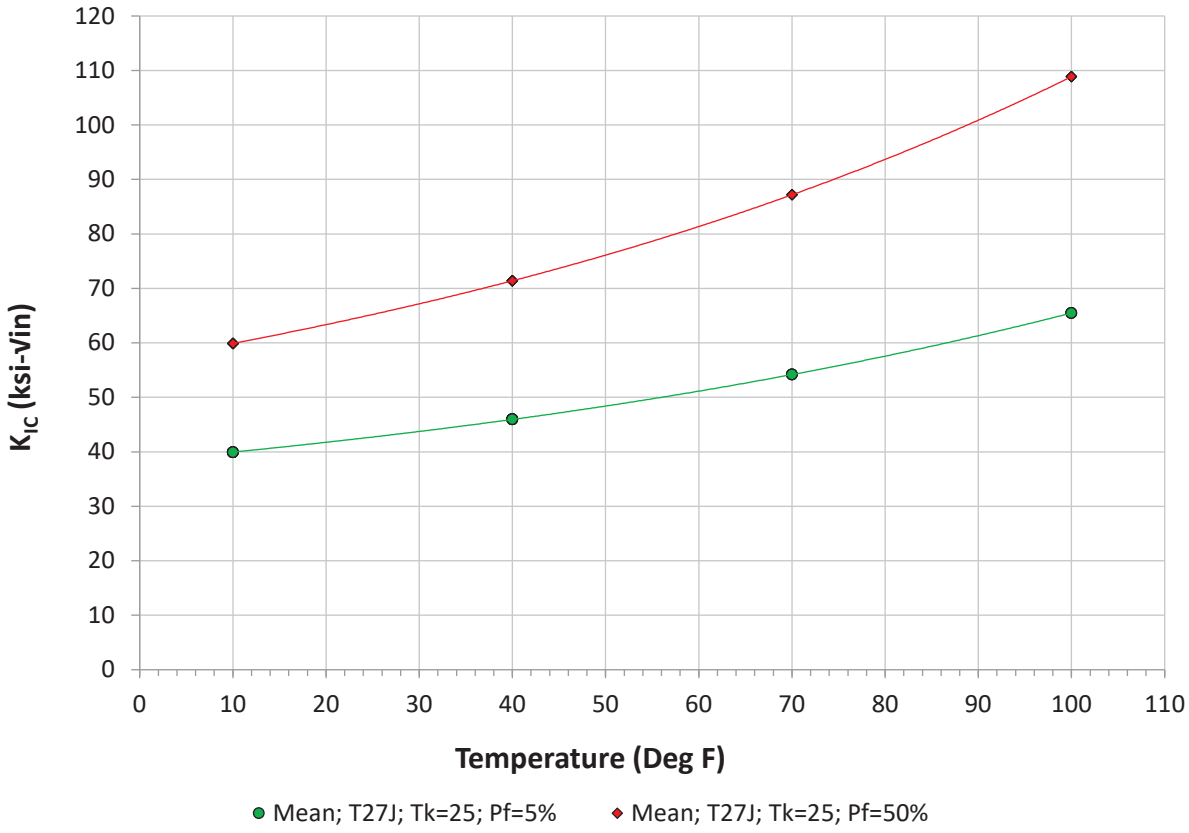

Figure A.1. Master Curve results for the channel web

CVN Test Data & Master Curve for the Cover Plate:

Table A.2. CVN test data results for the cover plate

Test Temperature (°F)	*Energy (ft-lbs)	K_{mat} (ksi-√in) P_f = 5%	K_{mat} (ksi-√in) P_f = 50%
100	26	73	122
100	29.33		
100	26.67		
70	15.33	59	97
70	16.67		
70	19.33		
70	20.67		
70	19.33		
70	18		
40	8.67	50	79
40	13.33		
40	9.33		
40	9.33		
40	12.67		
40	10.67		
10	5.33	43	66
10	6		
10	6.67		

* Equivalent standard size CVN impact energy, including geometric and temperature adjustments

Inputs for Table A.2 *K_{mat} Estimate:*

- Mean T_{27J} = 24°C
- T_0 = 6°C
- T_k = 25°C

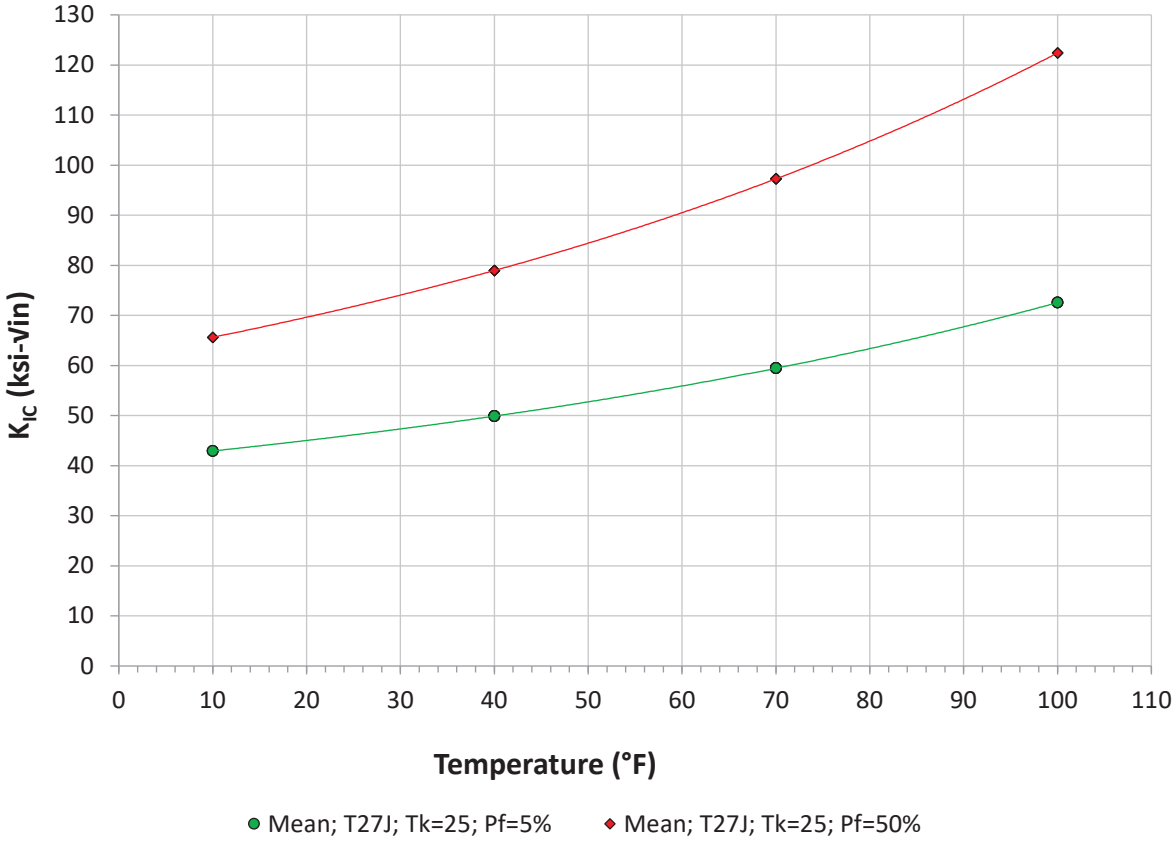

Figure A.2. Master Curve results for the cover plate

APPENDIX B – TABULATED RESULTS FOR PARAMETRIC STUDY

Table B.1 Moment ratio results for continuous stay-plated two-channel members

Model ID	Failure Location	No. SP x (CD/CS)	FEA Moment @ Adjacent Stay Plate (kip-in)	FEA Moment @ Midpoint of Adjacent Stay Plates (kip-in)	*P·e* (kip-in)	Ratio @ Stay Plate	Ratio @ Midpoint
C-SP1	Mid-Panel	5.45	58.0	48.3	2062.5	0.03	0.02
C-SP2	Mid-Panel	5.45	48.5	59.6	2062.5	0.02	0.03
C-SP3	Gusset	5.45	114.5	126.5	2062.5	0.06	0.06
C-SP4	Mid-Panel	5.45	52.3	38.2	2062.5	0.03	0.02
C-SP5	Mid-Panel	5.45	56.5	41.9	2062.5	0.03	0.02
C-SP6	Mid-Panel	5.45	77.0	74.3	2062.5	0.04	0.04
C-SP7	Mid-Panel	5.45	80.9	78.1	2062.5	0.04	0.04
C-SP8	Gusset	5.45	78.4	16.5	2062.5	0.04	0.01
C-SP9	Mid-Panel	3.64	34.3	8.6	2062.5	0.02	0.00
C-SP10	Mid-Panel	3.64	47.7	17.8	2062.5	0.02	0.01
C-SP11	Gusset	3.64	188.9	72.5	2062.5	0.09	0.04
C-SP12	Mid-Panel	9.09	117.1	115.1	2062.5	0.06	0.06
C-SP13	Mid-Panel	9.09	122.9	121.7	2062.5	0.06	0.06
C-SP14	Gusset	9.09	73.9	27.2	2062.5	0.04	0.01
C-SP15	Mid-Panel	5.45	66.2	17.4	2062.5	0.03	0.01
C-SP16	Mid-Panel	5.45	66.9	17.7	2062.5	0.03	0.01
C-SP17	Gusset	5.45	117.9	0.9	2062.5	0.06	0.00
C-SP18	Mid-Panel	16.67	168.2	166.6	1125.0	0.15	0.15
C-SP19	Mid-Panel	16.67	179.7	178.2	1125.0	0.16	0.16
C-SP20	Gusset	16.67	157.7	106.6	1125.0	0.14	0.09
C-SP21	Mid-Panel	4.76	63.8	63.1	3937.5	0.02	0.02
C-SP22	Gusset	4.76	81.5	69.1	3937.5	0.02	0.02
C-SP23	Mid-Panel	4.76	63.7	62.9	3937.5	0.02	0.02
C-SP24	Mid-Panel	6.67	54.5	20.9	1125.0	0.05	0.02
C-SP25	Gusset	6.67	102.2	3.5	1125.0	0.09	0.00
C-SP26	Mid-Panel	1.90	26.7	36.3	3937.5	0.01	0.01
C-SP27	Mid-Panel	1.90	94.7	17.4	3937.5	0.02	0.00
C-SP28	Mid-Panel	7.85	34.1	27.6	412.1	0.08	0.07
C-SP29	Mid-Panel	11.77	30.7	4.0	412.1	0.07	0.01
C-SP30	Mid-Panel	23.12	27.0	9.3	209.9	0.13	0.04
C-SP31	Mid-Panel	5.94	18.6	2.9	816.5	0.02	0.00
C-SP32	Gusset	7.85	51.2	30.6	412.1	0.12	0.07
C-SP33	Gusset	11.77	62.0	8.1	412.1	0.15	0.02
C-SP34	Gusset	23.12	48.5	10.9	209.9	0.23	0.05
C-SP35	Gusset	5.94	57.2	12.0	816.5	0.07	0.01

*Note: *Ratios* are the FEA results divided by the theoretical moment *P·e* at the respective location

Table B.2 Moment ratio results for continuous laced two-channel members

Model ID	Failure Location	(PL/LS) x (CD/CS)*	FEA Moment @ Mid-Panel (kip-in)	FEA Moment @ End Stay Plate (kip-in)	*P·e* (kip-in)	Ratio @ Mid-Panel	Ratio @ End Stay Plate
C-L1	Mid-Panel	40	92.1	48.1	1822.5	0.05	0.03
C-L2	Mid-Panel	40	94.7	47.4	1822.5	0.05	0.03
C-L3	Gusset	40	32.1	85.5	1822.5	0.02	0.05
C-L4	Gusset	40	31.4	90.0	1822.5	0.02	0.05
C-L5	Mid-Panel	20	86.1	100.5	1822.5	0.05	0.06
C-L6	Mid-Panel	20	77.7	70.0	1822.5	0.04	0.04
C-L7	Gusset	20	15.0	55.6	1822.5	0.01	0.03
C-L8	Gusset	20	38.3	60.0	1822.5	0.02	0.03
C-L9	Mid-Panel	128	114.2	110.5	887.5	0.13	0.12
C-L10	Mid-Panel	128	114.4	110.5	887.5	0.13	0.12
C-L11	Gusset	128	28.4	103.2	887.5	0.03	0.12
C-L12	Gusset	128	28.4	98.9	887.5	0.03	0.11
C-L13	Mid-Panel	64	117.1	98.5	887.5	0.13	0.11
C-L14	Mid-Panel	64	103.3	61.5	887.5	0.12	0.07
C-L15	Gusset	64	30.0	66.9	887.5	0.03	0.08
C-L16	Gusset	64	33.1	81.5	887.5	0.04	0.09
C-L17	Mid-Panel	8.89	60.1	46.5	3700.0	0.02	0.01
C-L18	Mid-Panel	8.89	62.1	46.2	3700.0	0.02	0.01
C-L19	Gusset	8.89	42.0	49.8	3700.0	0.01	0.01
C-L20	Gusset	8.89	42.1	53.7	3700.0	0.01	0.01
C-L21	Mid-Panel	4.44	46.3	98.1	3700.0	0.01	0.03
C-L22	Mid-Panel	4.44	42.4	94.5	3700.0	0.01	0.03
C-L23	Gusset	4.44	19.3	29.0	3700.0	0.01	0.01
C-L24	Gusset	4.44	15.6	42.5	3700.0	0.00	0.01
C-L25	End Gusset	64	-	199.8	887.5	-	0.23
C-L26	End Gusset	20	-	147.7	1822.5	-	0.08

*Note: PL = Panel length (in.); LS = Lacing spacing (in.); CD = Channel Depth (in.); CS = Channel Spacing, or 2*e* (in.)
Ratios are the FEA results divided by the theoretical moment *P·e* at the respective location

Table B.3 Moment ratio results for non-continuous stay-plated two-channel members

Model ID	Failure Location	CD / CS*	FEA Moment @ Gusset (kip-in)	FEA Moment @ Mid-Panel	*P·e* (kip-in)	Ratio @ Gusset	Ratio @ Mid-Panel
N-SP1	Gusset	2	389.8	-	1675.8	0.23	-
N-SP2	Gusset	1	386.5	-	3329.6	0.12	-
N-SP3	Gusset	0.5	368.9	-	6637.1	0.06	-
N-SP4	Gusset	2	388.3	-	1675.8	0.23	-
N-SP5	Gusset	1	406.5	-	3329.6	0.12	-
N-SP6	Gusset	0.5	398.1	-	6637.1	0.06	-
N-SP7	Gusset	2	379.8	-	1675.8	0.23	-
N-SP8	Gusset	1	419.5	-	3329.6	0.13	-
N-SP9	Gusset	0.5	434.1	-	6637.1	0.07	-
N-SP10	Gusset	2	370.8	-	1675.8	0.22	-
N-SP11	Gusset	1	414.2	-	3329.6	0.12	-
N-SP12	Gusset	0.5	449.3	-	6637.1	0.07	-
N-SP13	Gusset	2	481.8	-	1675.8	0.29	-
N-SP14	Gusset	2	483.1	-	1675.8	0.29	-
N-SP15	Gusset	1	513.8	-	3329.6	0.15	-
N-SP16	Gusset	1	530.7	-	3329.6	0.16	-
N-SP17	Gusset	0.5	558.0	-	6637.1	0.08	-
N-SP18	Gusset	0.5	573.1	-	6637.1	0.09	-
N-SP19	Gusset	1	413.8	-	3329.6	0.12	-
N-SP20	Gusset	1	409.9	-	3329.6	0.12	-
N-SP21	Gusset	1	422.7	-	3329.6	0.13	-
N-SP22	Gusset	1	424.3	-	3329.6	0.13	-
N-SP23	Gusset	1	424.3	-	3329.6	0.13	-
N-SP24	Gusset	1	409.5	-	3329.6	0.12	-
N-SP25	Mid-Panel	2	104.3	136.8	3329.6	0.04	0.03
N-SP26	Mid-Panel	1	1.2	142.5	3329.6	0.04	0.00
N-SP27	Mid-Panel	0.5	44.3	35.8	6637.1	0.01	0.01
N-SP28	Mid-Panel	1	25.9	46.2	3329.6	0.01	0.01
N-SP29	Gusset	1	409.5	-	3329.6	0.12	-
N-SP30	Mid-Panel	1	55.8	81.4	3329.6	0.02	0.02
N-SP31	Gusset	1	405.2	-	3329.6	0.12	-
N-SP32	Mid-Panel	2	129.0	167.0	1675.8	0.10	0.08
N-SP33	Mid-Panel	1	81.8	111.8	3329.6	0.03	0.02
N-SP34	Mid-Panel	0.5	20.3	39.9	6637.1	0.01	0.00
N-SP35	Gusset	2	66.4	-	209.9	0.32	-
N-SP36	Gusset	1	70.2	-	412.1	0.17	-
N-SP37	Gusset	0.5	68.2	-	816.5	0.08	-
N-SP38	Gusset	2	65.2	-	209.9	0.31	-

N-SP39	Gusset	1	72.4	-	412.1	0.18	-
N-SP40	Gusset	0.5	73.2	-	816.5	0.09	-
N-SP41	Gusset	2	63.7	-	209.9	0.30	-
N-SP42	Gusset	1	71.9	-	412.1	0.17	-
N-SP43	Gusset	0.5	76.9	-	816.5	0.09	-
N-SP44	Gusset	2	62.9	-	209.9	0.30	-
N-SP45	Gusset	1	69.7	-	412.1	0.17	-
N-SP46	Gusset	0.5	76.3	-	816.5	0.09	-
N-SP47	Mid-Panel	2	1.29	8.9	209.9	0.04	0.01
N-SP48	Mid-Panel	1	12.9	10.0	412.1	0.02	0.03
N-SP49	Mid-Panel	0.5	17.5	16.1	816.5	0.02	0.02
N-SP50	Mid-Panel	2	9.6	20.2	209.9	0.10	0.05
N-SP51	Mid-Panel	1	5.7	15.0	412.1	0.04	0.01
N-SP52	Mid-Panel	0.5	3.7	2.4	816.5	0.00	0.00

*Note: CD = Channel Depth (in.); CS = Channel Spacing, or 2*e* (in.)
Ratios are the FEA results divided by the theoretical moment *P·e* at the respective location

Table B.4 Moment ratio results for non-continuous laced two-channel members

Model ID	Failure Location	(PL/LS) x (CD/CS)*	FEA Moment @ Mid-Panel (kip-in)	FEA Moment @ End Stay Plate (kip-in)	*P·e* (kip-in)	Ratio @ Mid-Panel	Ratio @ End Stay Plate
N-L1	Mid-Panel	16	119.0	79.6	2062.5	0.06	0.04
N-L2	Mid-Panel	4	27.6	41.6	3937.5	0.01	0.01
N-L3	Mid-Panel	64	172.8	159.6	1125.0	0.15	0.14
N-L4	Mid-Panel	8	68.5	82.6	3937.5	0.02	0.02
N-L5	Mid-Panel	32	133.2	91.8	2062.5	0.06	0.04
N-L6	Mid-Panel	32	206.4	84.4	2062.5	0.10	0.04
N-L7	Mid-Panel	16	123.1	89.2	2062.5	0.06	0.04
N-L8	Mid-Panel	16	58.7	101.5	2062.5	0.03	0.05
N-L9	Mid-Panel	16	118.7	199.7	2062.5	0.06	0.10
N-L10	Mid-Panel	-	54.8	81.8	2062.5	0.03	0.04
N-L11	Gusset	16	47.2	107.5	2062.5	0.02	0.05
N-L12	Gusset	4	37.5	171.9	3937.5	0.01	0.04
N-L13	Gusset	64	43.4	131.8	1125.0	0.04	0.12
N-L14	Gusset	8	40.9	108.8	1125.0	0.04	0.10
N-L15	Gusset	32	49.9	135.9	2062.5	0.02	0.07
N-L16	Gusset	32	48.4	108.0	2062.5	0.02	0.05
N-L17	Gusset	16	38.7	123.6	2062.5	0.02	0.06
N-L18	Gusset	-	50.7	185.0	2062.5	0.02	0.09

*Note: PL = Panel length (in.); LS = Lacing spacing (in.); CD = Channel Depth (in.); CS = Channel Spacing, or 2*e* (in.)
Ratios are the FEA results divided by the theoretical moment *P·e* at the respective location

APPENDIX C – GAGE PLANS

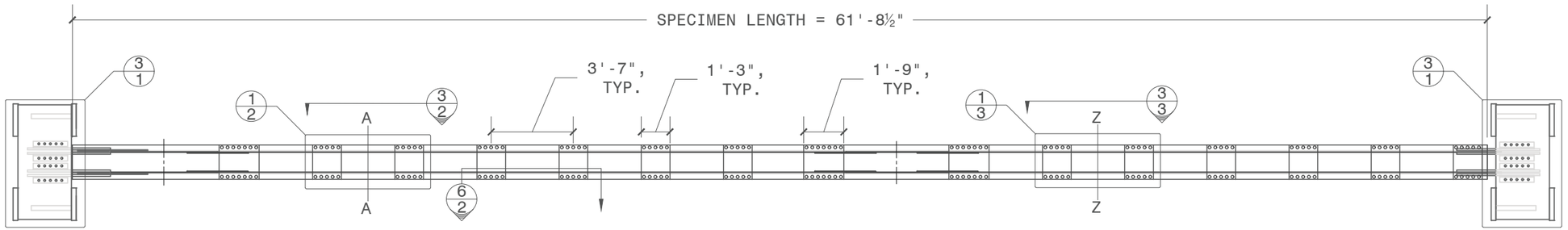

1/1 PLAN VIEW
SCALE: 3/16" = 1'-0"

LOAD (SOUTH)

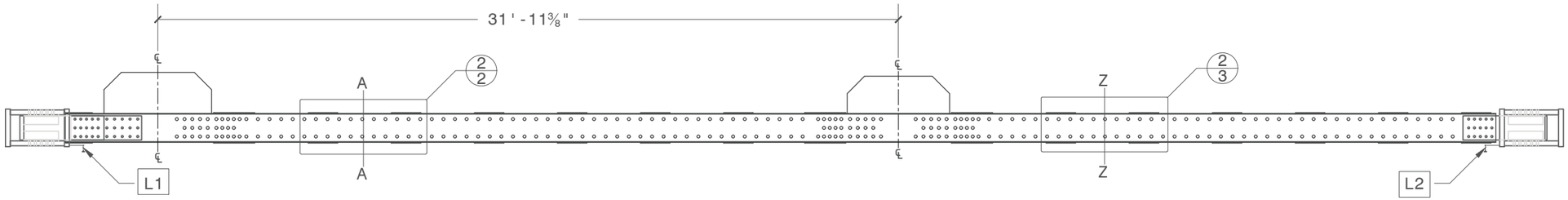

2/1 ELEVATION VIEW
SCALE: 3/16" = 1'-0"

LOAD (SOUTH)

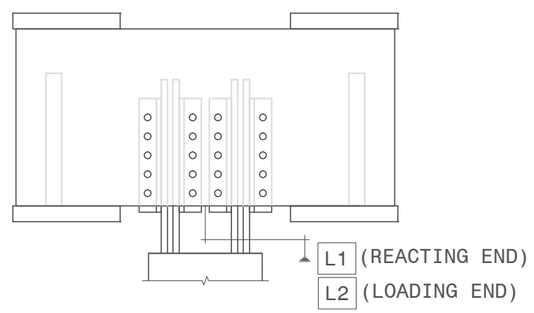

3/1 STRING POTENTIOMETERS
SCALE: 3/4" = 1'-0"

BOWEN LABORATORY
PURDUE UNIVERSITY

1040 SOUTH RIVER ROAD
WEST LAFAYETTE, IN 47906
P: 765-494-2227 F: 765-494-9886

PROJECT:
MNDOT Winona Truss Test Gage Plans

SHEET NOTES:

L1 Displacement sensor channels

A1 Strain gage channels

REVISIONS:

NO.	DATE	BY

DESIGNED BY: JBL
DRAWN BY: JBL
CHECKED BY:
DATE: 2017
PROJECT NO.:
SHEET TITLE:

SPEC. 1 OVERVIEW

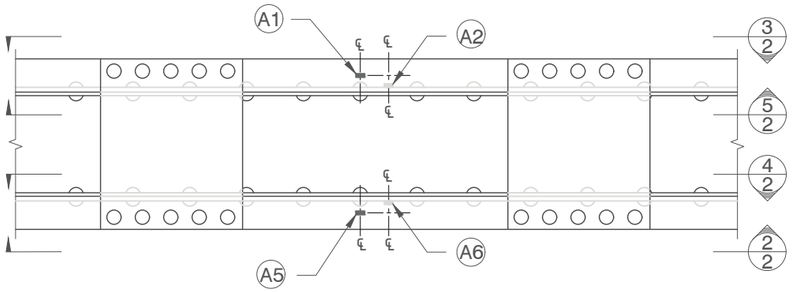

1/2 PLAN VIEW, TYP.
SCALE: 3/4" = 1'-0"

LOAD (SOUTH)

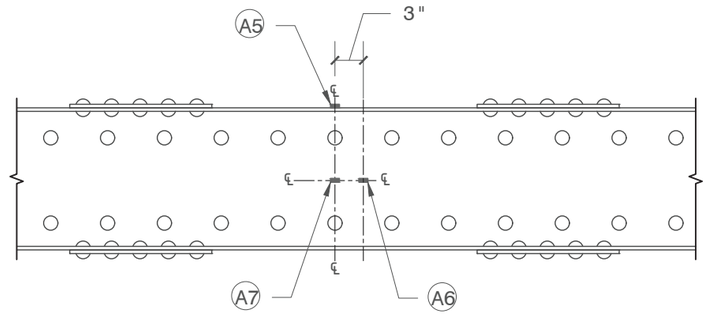

2/2 WEST EXT. ELEVATION
SCALE: 3/4" = 1'-0"

LOAD (SOUTH)

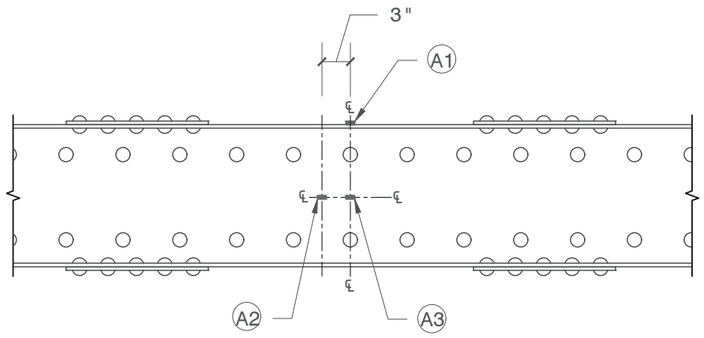

3/2 EAST EXT. ELEVATION
SCALE: 3/4" = 1'-0"

LOAD (SOUTH)

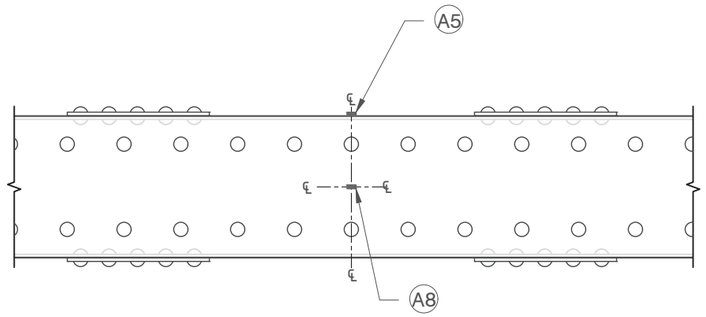

4/2 WEST INT. ELEVATION
SCALE: 3/4" = 1'-0"

LOAD (SOUTH)

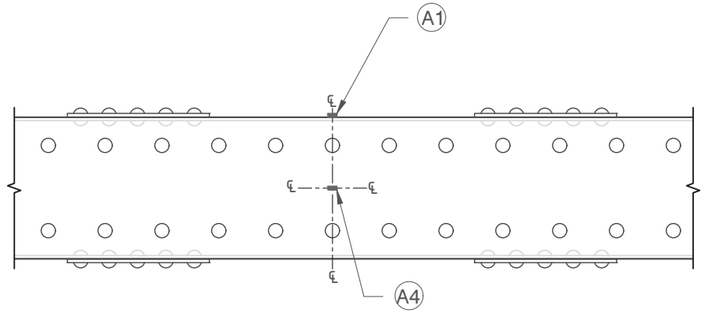

5/2 EAST INT. ELEVATION
SCALE: 3/4" = 1'-0"

LOAD (SOUTH)

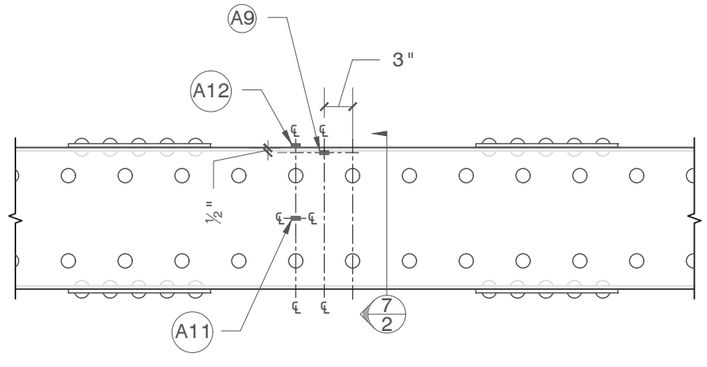

6/2 WEST INT. ELEVATION
SCALE: 3/4" = 1'-0"

LOAD (SOUTH)

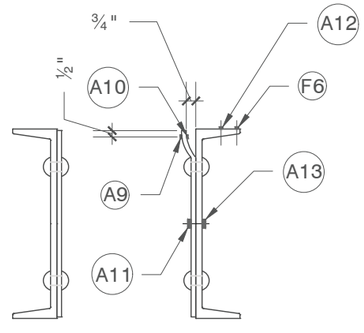

7/2 WEST CHANNEL CROSS-SECTION
SCALE: 1" = 1'-0"

BOWEN LABORATORY
PURDUE UNIVERSITY

1040 SOUTH RIVER ROAD
WEST LAFAYETTE, IN 47906
P: 765-494-2227 F: 765-494-9886

PROJECT:

MNDOT Winona Truss Test Gage Plans

SHEET NOTES:

L1 Displacement sensor channels

A1 Strain gage channels

REVISIONS:

NO.	DATE	BY

DESIGNED BY: JBL
DRAWN BY: JBL
CHECKED BY:
DATE: 2017
PROJECT NO.:
SHEET TITLE:

SPEC. 1 GAGE PLACEMENT DETAILS

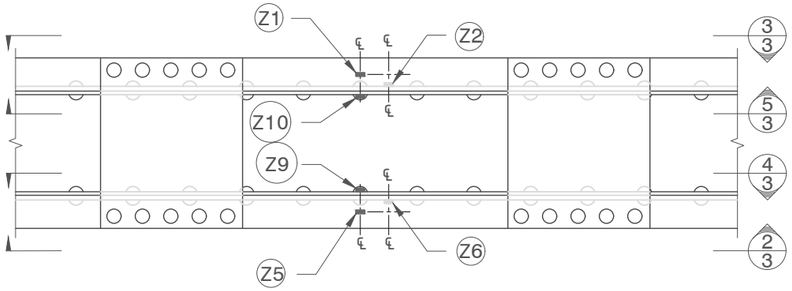

1/3 PLAN VIEW, TYP.
SCALE: 3/4" = 1'-0"

LOAD (SOUTH)

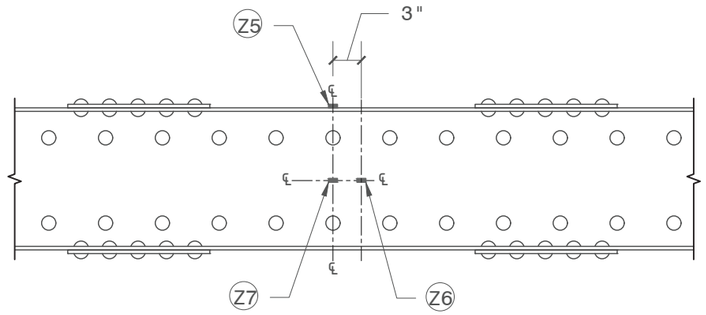

2/3 WEST EXT. ELEVATION
SCALE: 3/4" = 1'-0"

LOAD (SOUTH)

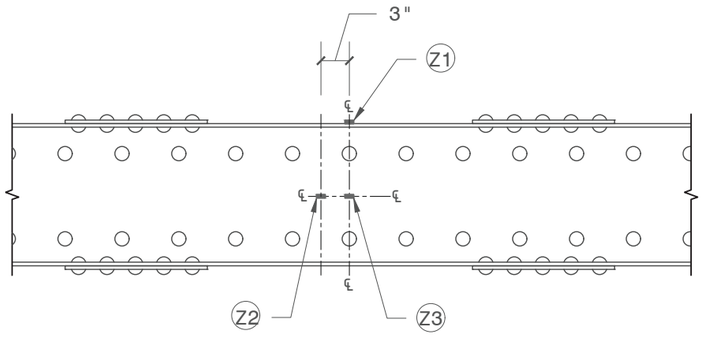

3/3 EAST EXT. ELEVATION
SCALE: 3/4" = 1'-0"

LOAD (SOUTH)

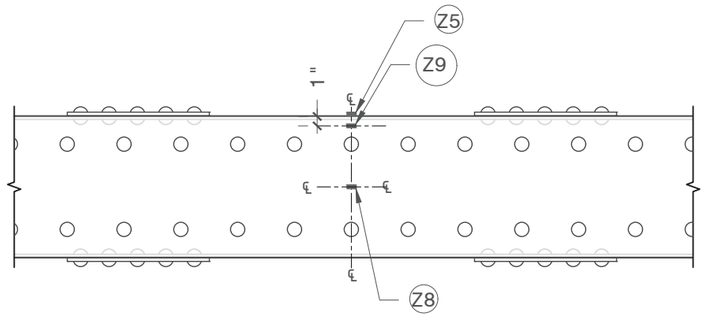

4/3 WEST INT. ELEVATION
SCALE: 3/4" = 1'-0"

LOAD (SOUTH)

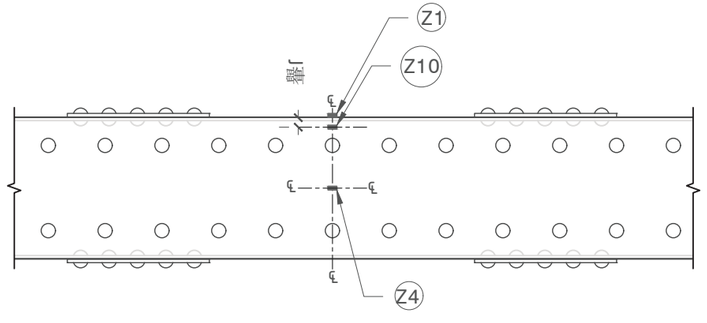

5/3 EAST INT. ELEVATION
SCALE: 3/4" = 1'-0"

LOAD (SOUTH)

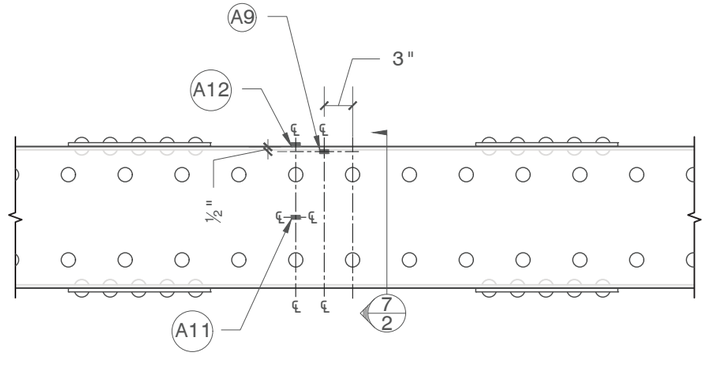

6/3 WEST INT. ELEVATION
SCALE: 3/4" = 1'-0"

LOAD (SOUTH)

BOWEN LABORATORY
PURDUE UNIVERSITY

1040 SOUTH RIVER ROAD
WEST LAFAYETTE, IN 47906
P: 765-494-2227 F: 765-494-9886

PROJECT:

MNDOT Winona Truss Test Gage Plans

SHEET NOTES:

L1 Displacement sensor channels

A1 Strain gage channels

REVISIONS:

NO.	DATE	BY

DESIGNED BY: JBL
DRAWN BY: JBL
CHECKED BY:
DATE: 2017
PROJECT NO.:
SHEET TITLE:

SPEC. 1 GAGE PLACEMENT DETAILS

SHEET NO.: 3 of 3

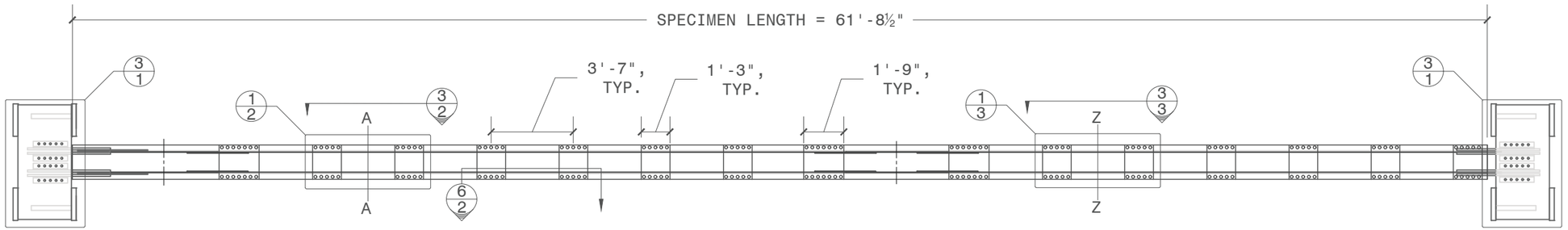

1/1 PLAN VIEW
SCALE: 3/16" = 1'-0"

LOAD (SOUTH)

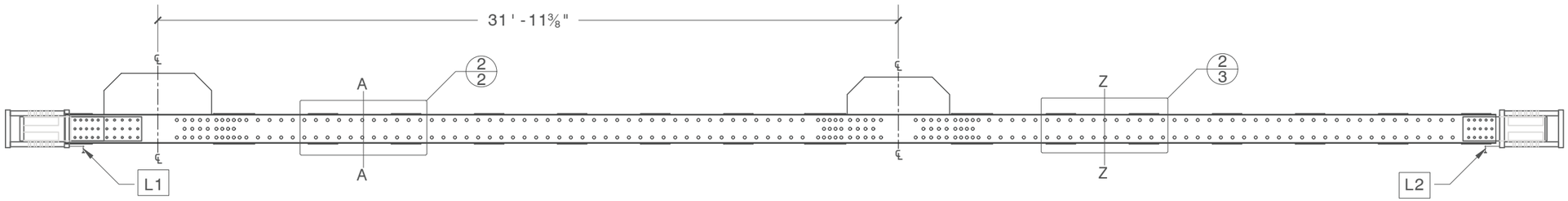

2/1 ELEVATION VIEW
SCALE: 3/16" = 1'-0"

LOAD (SOUTH)

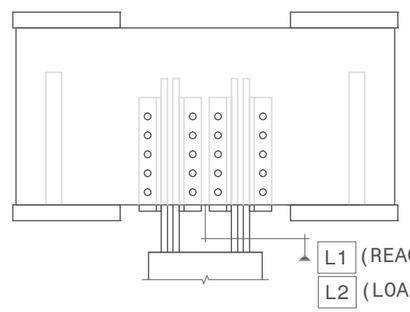

3/1 STRING POTENTIOMETERS
SCALE: 3/4" = 1'-0"

BOWEN LABORATORY
PURDUE UNIVERSITY

1040 SOUTH RIVER ROAD
WEST LAFAYETTE, IN 47906
P: 765-494-2227 F: 765-494-9886

PROJECT:
MNDOT Winona Truss Test Gage Plans

SHEET NOTES:

L1 Displacement sensor channels

(A1) Strain gage channels

REVISIONS:

NO.	DATE	BY

DESIGNED BY: JBL
DRAWN BY: JBL
CHECKED BY:
DATE: 2017
PROJECT NO.:
SHEET TITLE:

SPEC. 2 OVERVIEW

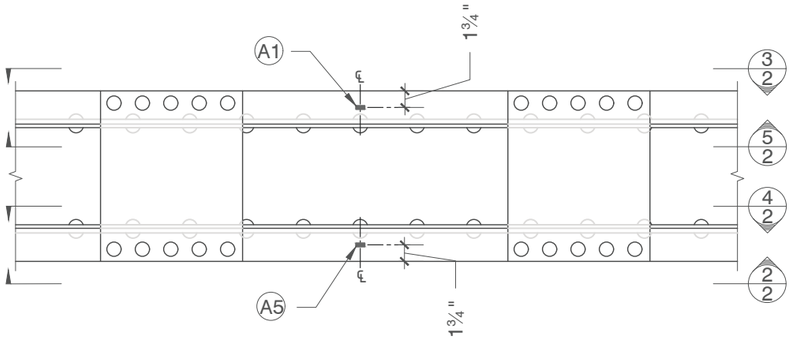

1/2 PLAN VIEW, TYP.
SCALE: 3/4" = 1'-0"

LOAD (SOUTH)

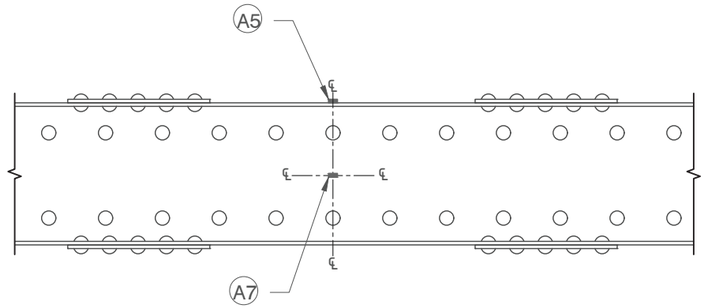

2/2 WEST EXT. ELEVATION
SCALE: 3/4" = 1'-0"

LOAD (SOUTH)

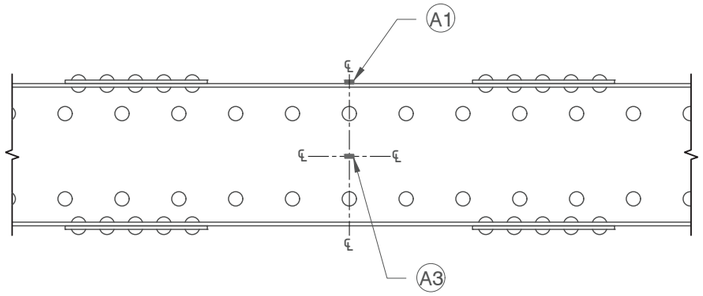

3/2 EAST EXT. ELEVATION
SCALE: 3/4" = 1'-0"

LOAD (SOUTH)

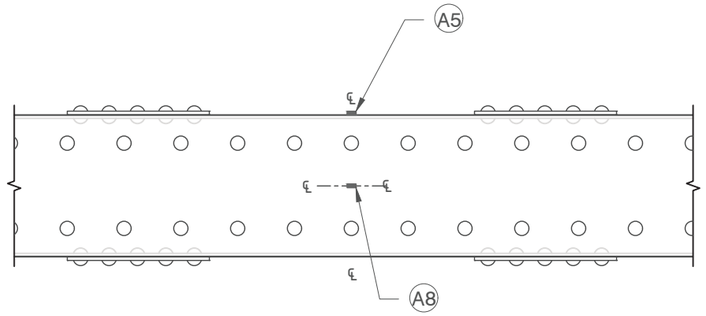

4/2 WEST INT. ELEVATION
SCALE: 3/4" = 1'-0"

LOAD (SOUTH)

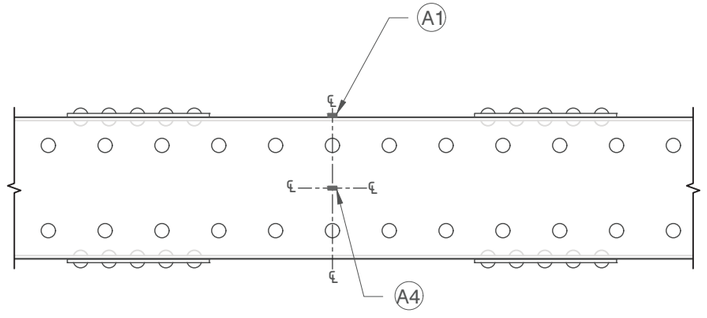

5/2 EAST INT. ELEVATION
SCALE: 3/4" = 1'-0"

LOAD (SOUTH)

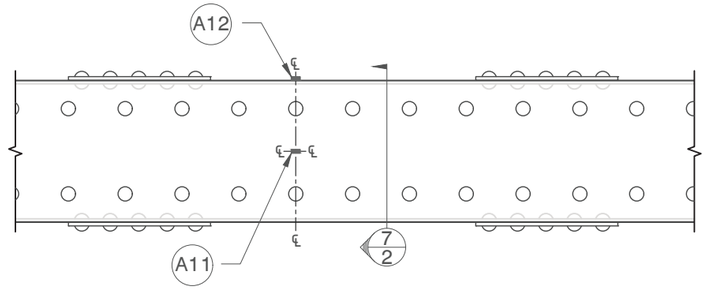

6/2 WEST INT. ELEVATION
SCALE: 3/4" = 1'-0"

LOAD (SOUTH)

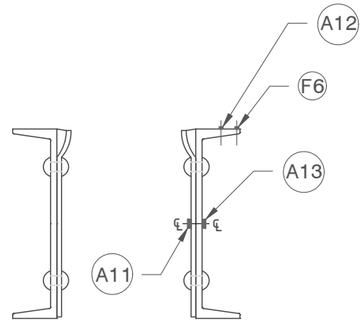

7/2 WEST CHANNEL CROSS-SECTION
SCALE: 1" = 1'-0"

BOWEN LABORATORY
PURDUE UNIVERSITY

1040 SOUTH RIVER ROAD
WEST LAFAYETTE, IN 47906
P: 765-494-2227 F: 765-494-9886

PROJECT:
MNDOT Winona Truss Test Gage Plans

SHEET NOTES:

L1 Displacement sensor channels

A1 Strain gage channels

REVISIONS:

NO.	DATE	BY

DESIGNED BY: JBL
DRAWN BY: JBL
CHECKED BY:
DATE: 2017
PROJECT NO.:
SHEET TITLE:

SPEC. 2 GAGE PLACEMENT DETAILS

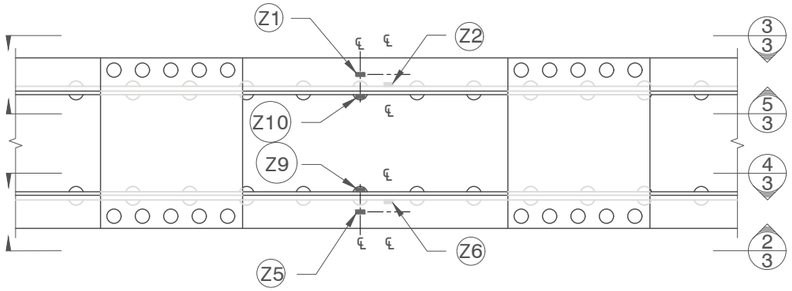

1/2 PLAN VIEW, TYP.
SCALE: 3/4" = 1'-0"

LOAD (SOUTH)

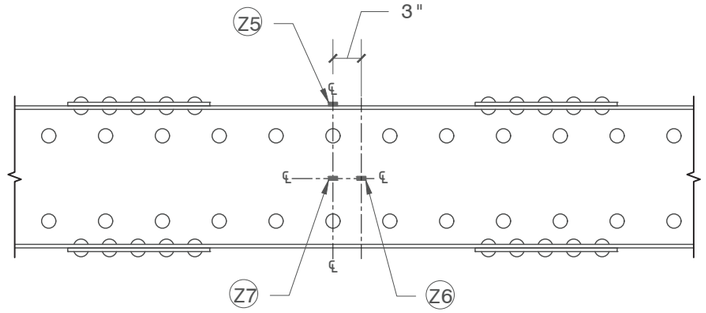

2/2 WEST EXT. ELEVATION
SCALE: 3/4" = 1'-0"

LOAD (SOUTH)

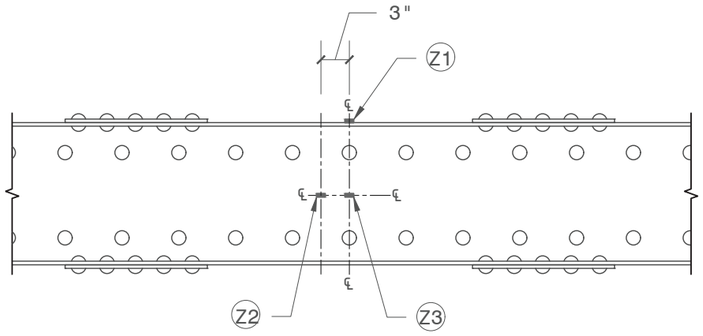

3/2 EAST EXT. ELEVATION
SCALE: 3/4" = 1'-0"

LOAD (SOUTH)

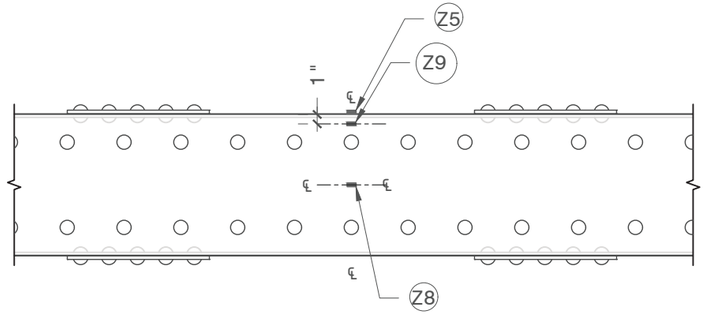

4/2 WEST INT. ELEVATION
SCALE: 3/4" = 1'-0"

LOAD (SOUTH)

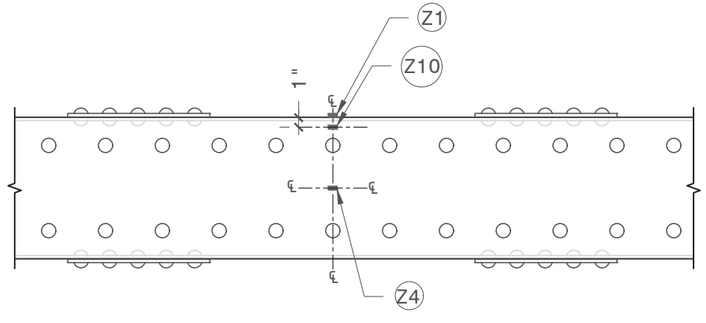

5/2 EAST INT. ELEVATION
SCALE: 3/4" = 1'-0"

LOAD (SOUTH)

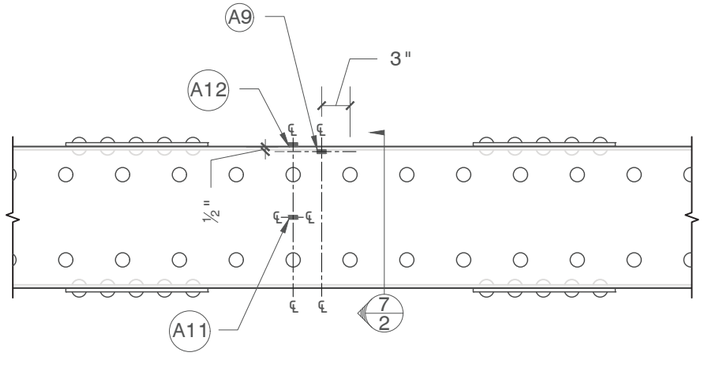

6/2 WEST INT. ELEVATION
SCALE: 3/4" = 1'-0"

LOAD (SOUTH)

BOWEN LABORATORY
PURDUE UNIVERSITY

1040 SOUTH RIVER ROAD
WEST LAFAYETTE, IN 47906
P: 765-494-2227 F: 765-494-9886

PROJECT:

MNDOT Winona Truss Test Gage Plans

SHEET NOTES:

L1 Displacement sensor channels

A1 Strain gage channels

REVISIONS:

NO.	DATE	BY

DESIGNED BY: JBL
DRAWN BY: JBL
CHECKED BY:
DATE: 2017
PROJECT NO.:
SHEET TITLE:

SPEC. 2 GAGE PLACEMENT DETAILS

SHEET NO.: 3 of 3

APPENDIX D – INSPECTION AND LOAD RATING DOCUMENTS

Appendix D1: Information provided to inspectors

Appendix D2: Information provided to load raters

Appendix D3: Research Team load rating calculations

Appendix D1: Information provided to inspectors

Inspection Participant:

Thank you for agreeing to participate in the Truss Chord Inspection Round Robin at Purdue University. This study is focused solely on the evaluation of corrosion and section loss, not the visual detection of cracks.

The study consists of the following inspection scenario:

Hands-on inspection of a built-up truss chord (ref. Figures 1 and 2 attached)

The inspection is estimated to require 2 to 4 hours to complete.

On the day of your participation, please bring any tools and personal protective equipment you would normally use for a hands-on visual inspection. At a minimum, please bring a hard hat, long pants, closed toe shoes, and safety glasses. All inspection activities will be completed from the ground beneath or adjacent to the member. Check the weather and dress appropriately, as all activities for this study are held outdoors.

It is critical to the study that all procedures and findings are kept confidential. If information regarding the study set-up or results are shared among inspectors, the results will become invalid. Likewise, your identity will remain confidential.

If you have any questions, please contact:

Dr. Robert J Connor
rconnor@purdue.edu

Thank you for your willingness to participate in this study. We look forward to working with you.

Dr. Robert J. Connor

Jason B. Lloyd, PE

Leslie E. Campbell, PE

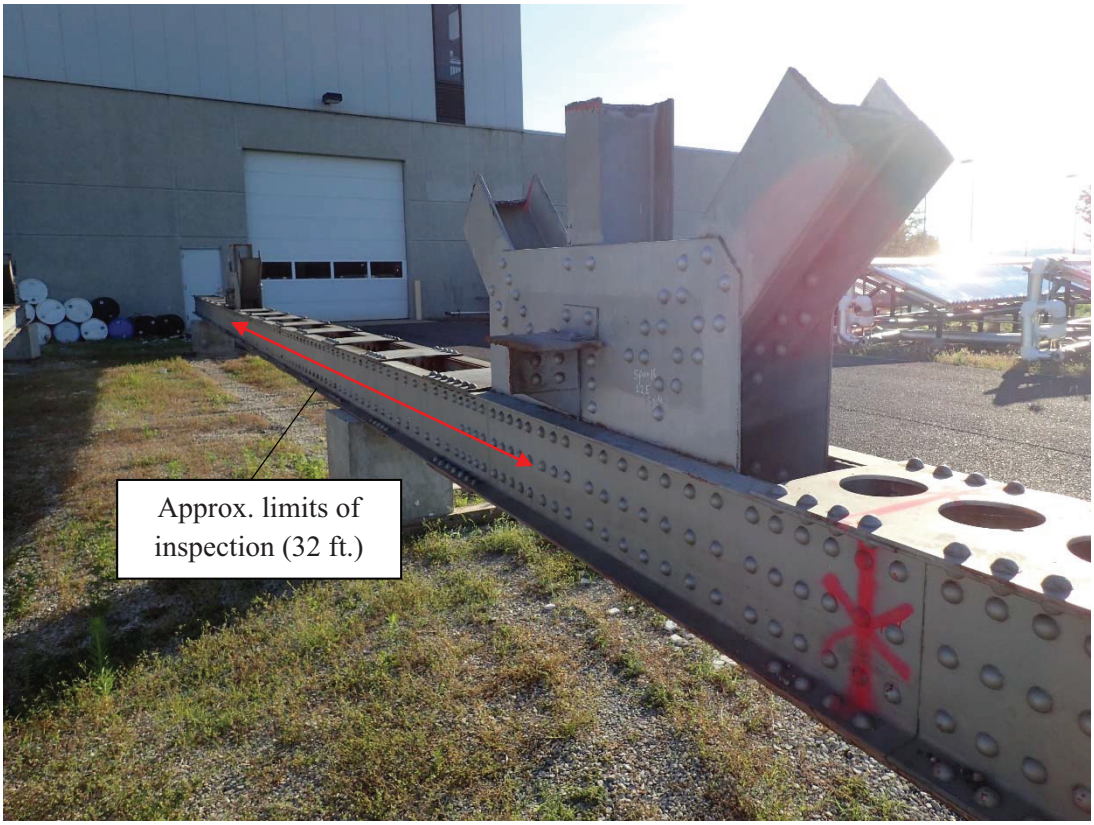

Figure 1. Truss chord elevation view (looking from joint L4 toward joint L2)

Figure 2. Truss chord plan view (looking from joint L4 toward joint L2)

Truss Chord Inspection Round Robin

Visual Inspection Testing Procedure
Purdue University
2018

This document provides the procedures and instructions for inspectors participating in the Truss Chord Inspection Round Robin at Purdue University.

Read these instructions to the inspector prior to the inspection -

Introduction:

You are about to participate in a study for visual inspection of steel bridges. It is critical to the study that all procedures and findings are kept **CONFIDENTIAL**. Likewise, your identity will remain confidential; the results from your specific participation will not be shared or be published.

The objectives of this portion of study are as follows:

1. Establish the variability in identifying the critical section and estimating section loss during hands-on, visual inspection of steel bridges
2. Establish methods for improving consistency in these measurements

Inspection Scenario:

This inspection is focused solely on the evaluation of corrosion and section loss in steel bridge members, NOT crack detection, although cracks may be present. You should conduct this inspection in the same manner and with the same care as normally implemented in the field. All inspection activities will be completed from the ground beneath or adjacent to the specimen. You may take breaks as needed throughout this inspection activity.

This inspection is divided into three separate tasks. The tasks must be completed in the specified order. Please notify the proctor when you complete each task so that the time may be recorded. At that time, the instructions for the next task will be provided.

At the end of your inspection, please submit the completed inspection forms to the proctor. Upon completion of the entire inspection course, please complete the Inspector Exit Form. Feel free to ask the proctor any questions related to the study procedures at any time during the inspection.

Member Background:

1. This member was removed from a bridge constructed in the early 1940s in the upper Midwest region of the US.
2. This member was a part of the bottom chord of the deck truss.
3. This member is fracture critical.

Truss Chord Inspection Round Robin

Visual Inspection Testing Procedure

Purdue University

2018

Inspection Tasks:

Task 1:

In Task 1, you are asked to identify the MOST critical location for determining remaining capacity along the full length of the member. At the critical location, you are asked to provide sufficient information (measurements, notes, sketches, photos, etc.) such that a load rating engineer could determine the load rating for this member. You may use any tools that you brought with you to complete this task. The location of the critical section and your inspection findings should be recorded on the forms provided. Photos may be taken with the camera provided. The time limit for this task is 30 minutes.

Task 2:

In Task 2, you are asked to estimate the remaining thickness of the member at the two (2) locations identified on your inspection form. You may use any tools that you brought with you to complete this task. If needed, please use the provided ultrasonic thickness gauge. Your measurements should be recorded in the tables provided. Please label the location of the measurements on the cross section sketches. There is no time limit for this task.

Task 3:

In Task 3, you are asked to identify the MOST critical location for determining remaining capacity within the region identified on your inspection form. The location of the critical section should be recorded on the inspection form. You do NOT need to record the remaining thickness at this location. You may use any tools that you brought with you to complete this task. An ultrasonic thickness gauge is available for your use, if needed. There is no time limit for this task.

Thank you for your participation and cooperation.

ELEVATION OF FULL BRIDGE

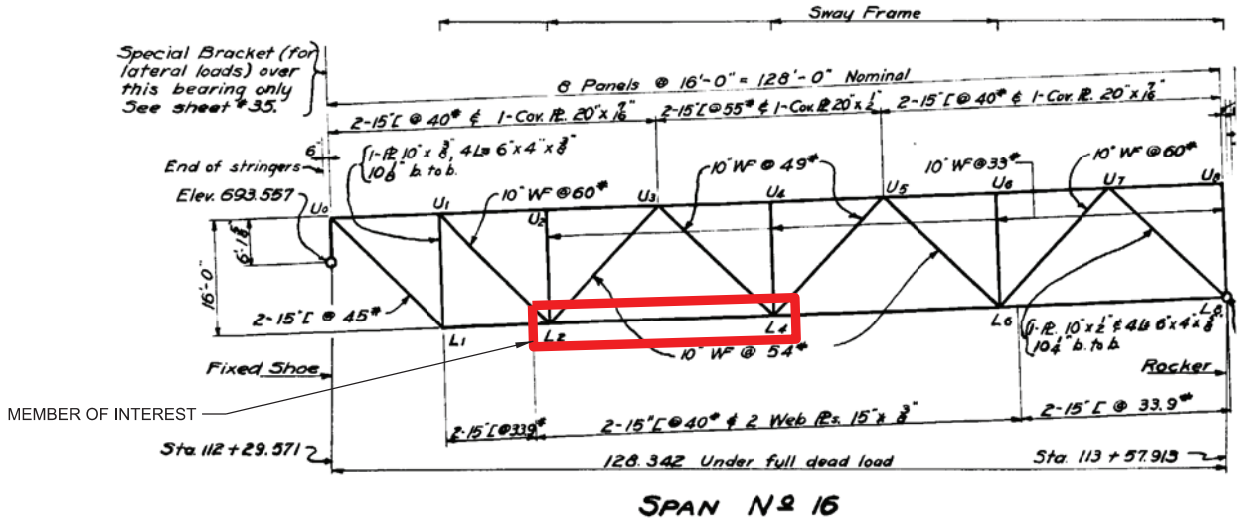

SPAN NO 16

ELEVATION OF SPAN OF INTEREST

BOWEN LABORATORY
PURDUE UNIVERSITY

1040 SOUTH RIVER ROAD
WEST LAFAYETTE, IN 47906
P: 765-404-2227 F: 765-494-9886

PROJECT:

TRUSS INSPECTION
ROUND ROBIN

INSPECTOR ID:
INSPECTION DATE:
PROCTOR INITIALS:

SHEET TITLE:

SHEET NO.:

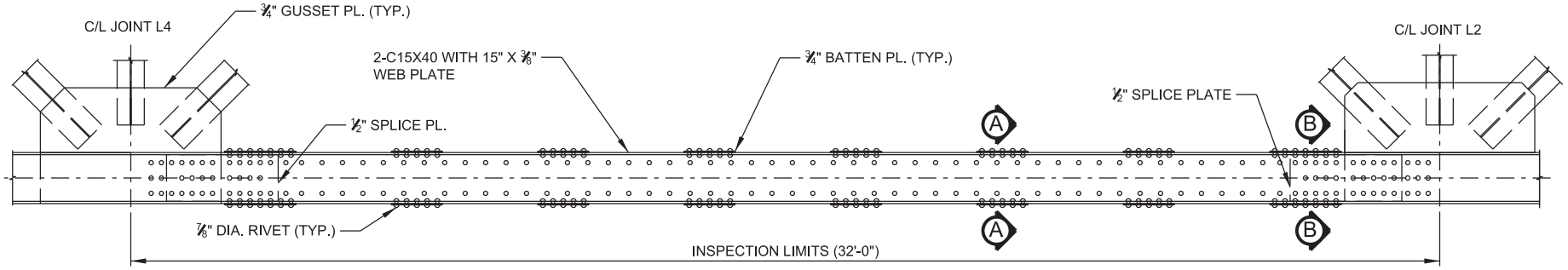

ELEVATION
SCALE: 1" = 4'

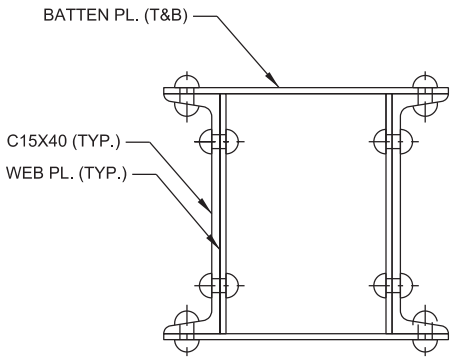

SECTION A
SCALE: 1" = 1'-0"

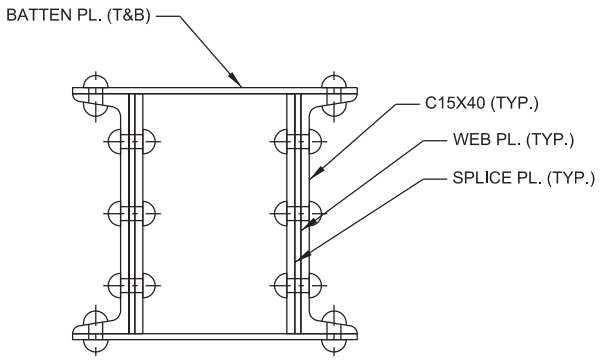

SECTION B
SCALE: 1" = 1'-0"

BOWEN LABORATORY
PURDUE UNIVERSITY

1040 SOUTH RIVER ROAD
WEST LAFAYETTE, IN 47906
P: 765-404-2227 F: 765-494-9886

PROJECT:

TRUSS INSPECTION ROUND ROBIN

INSPECTOR ID:
INSPECTION DATE:
PROCTOR INITIALS:

SHEET NOTES:

1. INDICATE THE LOCATION OF THE CRITICAL SECTION ON THE ELEVATION VIEW OF THE TRUSS CHORD (THIS SHEET).

2. PROVIDE MEASUREMENTS TO SUPPORT SECTION LOSS CALCULATIONS AT THIS LOCATION. SHEETS 1-2 THROUGH 1-3 MAY BE USED FOR RECORDING MEASUREMENTS, ADDITIONAL SKETCHES, ETC.

3. THE TIME LIMIT FOR THIS TASK IS 30 MINS.

SHEET TITLE:

TASK 1 SKETCHES

SHEET NO.: 1-1

BOWEN LABORATORY
PURDUE UNIVERSITY

1040 SOUTH RIVER ROAD
WEST LAFAYETTE, IN 47906
P: 765-404-2227 F: 765-494-9886

PROJECT:

TRUSS INSPECTION ROUND ROBIN

INSPECTOR ID:

INSPECTION DATE:

PROCTOR INITIALS:

SHEET NOTES:

1. INDICATE THE LOCATION OF THE CRITICAL SECTION ON THE ELEVATION VIEW OF THE TRUSS CHORD (SHEET 1-1).

2. PROVIDE MEASUREMENTS TO SUPPORT SECTION LOSS CALCULATIONS AT THIS LOCATION. SHEETS 1-2 AND 1-3 MAY BE USED FOR RECORDING MEASUREMENTS, ADDITIONAL SKETCHES, ETC.

3. THE TIME LIMIT FOR THIS TASK IS 30 MINS.

SHEET TITLE:

TASK 1 MEASUREMENTS

SHEET NO.: 1-2

BOWEN LABORATORY
PURDUE UNIVERSITY

1040 SOUTH RIVER ROAD
WEST LAFAYETTE, IN 47906
P: 765-404-2227 F: 765-494-9886

PROJECT:

TRUSS INSPECTION ROUND ROBIN

INSPECTOR ID:

INSPECTION DATE:

PROCTOR INITIALS:

SHEET NOTES:

1. INDICATE THE LOCATION OF THE CRITICAL SECTION ON THE ELEVATION VIEW OF THE TRUSS CHORD (SHEET 1-1).

2. PROVIDE MEASUREMENTS TO SUPPORT SECTION LOSS CALCULATIONS AT THIS LOCATION. SHEETS 1-2 AND 1-3 MAY BE USED FOR RECORDING MEASUREMENTS, ADDITIONAL SKETCHES, ETC.

3. THE TIME LIMIT FOR THIS TASK IS 30 MINS.

SHEET TITLE:

TASK 1 MEASUREMENTS

SHEET NO.: 1-3

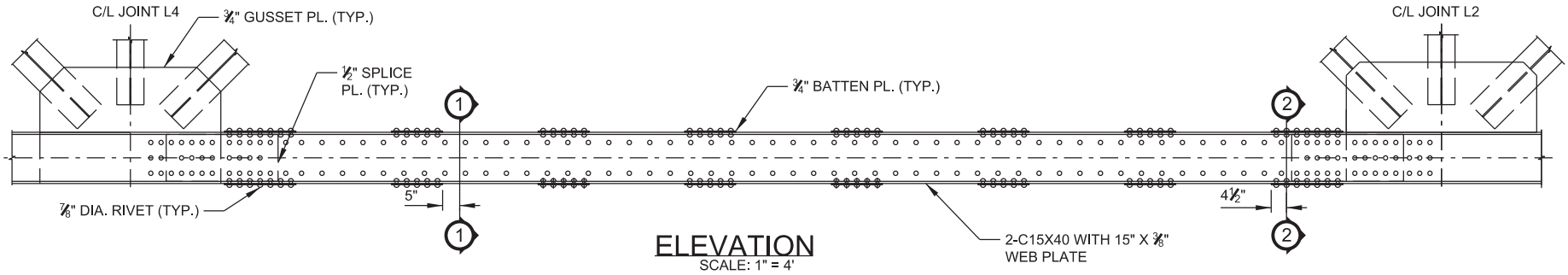

ELEVATION

SCALE: 1" = 4'

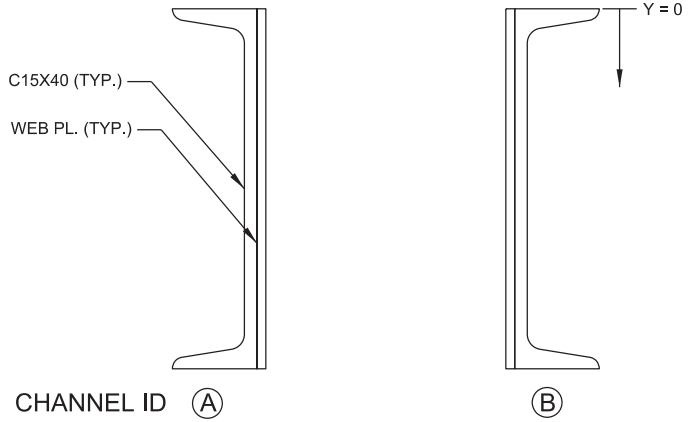

CROSS SECTION 1

SCALE: 1½" = 1'-0"

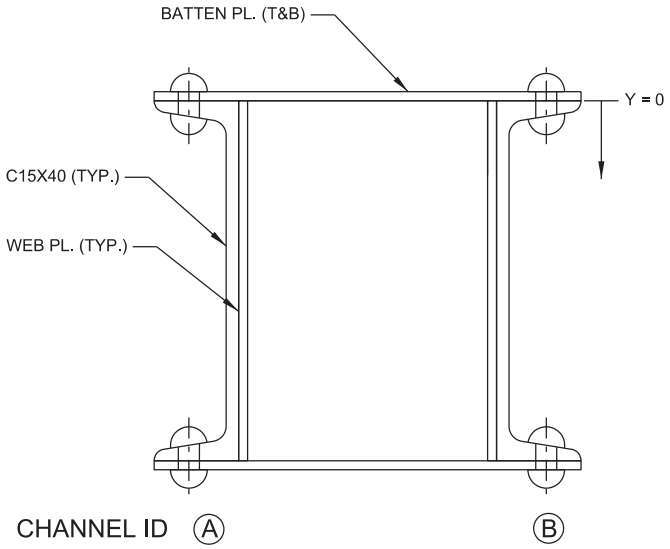

CROSS SECTION 2

SCALE: 1½" = 1'-0"

BOWEN LABORATORY
PURDUE UNIVERSITY

1040 SOUTH RIVER ROAD
WEST LAFAYETTE, IN 47906
P: 765-404-2227 F: 765-494-9886

PROJECT:

TRUSS INSPECTION ROUND ROBIN

INSPECTOR ID:

INSPECTION DATE:

PROCTOR INITIALS:

SHEET NOTES:

1. PROVIDE THICKNESS MEASUREMENTS AT CROSS SECTIONS 1 AND 2. RECORD YOUR FINDINGS ON SHEETS 2-2 AND 2-3 (IF NEEDED).

2. INDICATE THE LOCATION OF THE MEASUREMENTS ON THE CROSS SECTION SKETCHES (THIS SHEET).

SHEET TITLE:

TASK 2 SKETCHES

SHEET NO.: 2-1

CROSS SECTION NO.	CHANNEL ID	LOCATION LABEL	DISTANCE, Y, FROM TOP FLANGE (IN.)	THICKNESS MEASUREMENT (IN.)

CROSS SECTION NO.	CHANNEL ID	LOCATION LABEL	DISTANCE, Y, FROM TOP FLANGE (IN.)	THICKNESS MEASUREMENT (IN.)

BOWEN LABORATORY
PURDUE UNIVERSITY

1040 SOUTH RIVER ROAD
WEST LAFAYETTE, IN 47906
P: 765-404-2227 F: 765-494-9886

PROJECT:

TRUSS INSPECTION ROUND ROBIN

INSPECTOR ID:

INSPECTION DATE:

PROCTOR INITIALS:

SHEET NOTES:

1. PROVIDE THICKNESS MEASUREMENTS AT CROSS SECTIONS 1 AND 2. RECORD YOUR FINDINGS ON SHEETS 2-2 AND 2-3 (IF NEEDED).

2. INDICATE THE LOCATION OF THE MEASUREMENTS ON THE CROSS SECTION SKETCHES (SHEET 2-1).

SHEET TITLE:

TASK 2 SKETCHES

SHEET NO.: 2-2

BOWEN LABORATORY
PURDUE UNIVERSITY

1040 SOUTH RIVER ROAD
WEST LAFAYETTE, IN 47906
P: 765-404-2227 F: 765-494-9886

PROJECT:

TRUSS INSPECTION ROUND ROBIN

INSPECTOR ID:

INSPECTION DATE:

PROCTOR INITIALS:

SHEET NOTES:

1. PROVIDE THICKNESS MEASUREMENTS AT CROSS SECTIONS 1 AND 2. RECORD YOUR FINDINGS ON SHEETS 2-2 AND 2-3 (IF NEEDED).

2. INDICATE THE LOCATION OF THE MEASUREMENTS ON THE CROSS SECTION SKETCHES (SHEET 2-1).

SHEET TITLE:

TASK 2 SKETCHES

SHEET NO.: 2-3

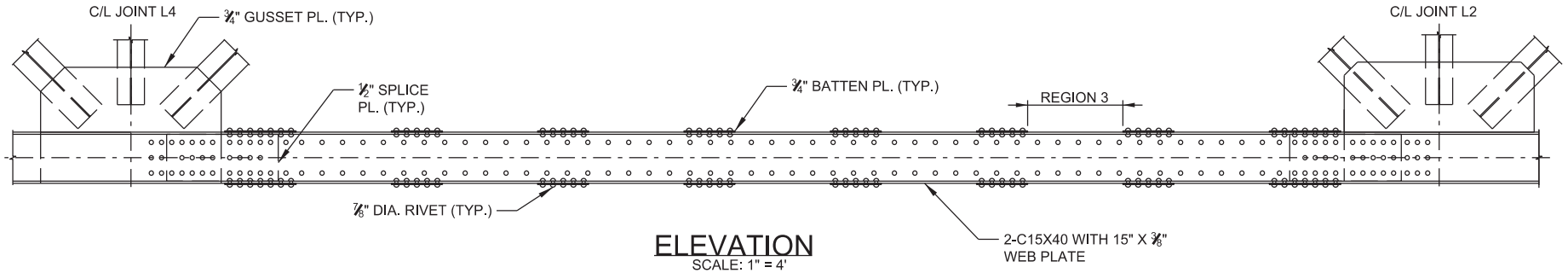

ELEVATION
SCALE: 1" = 4'

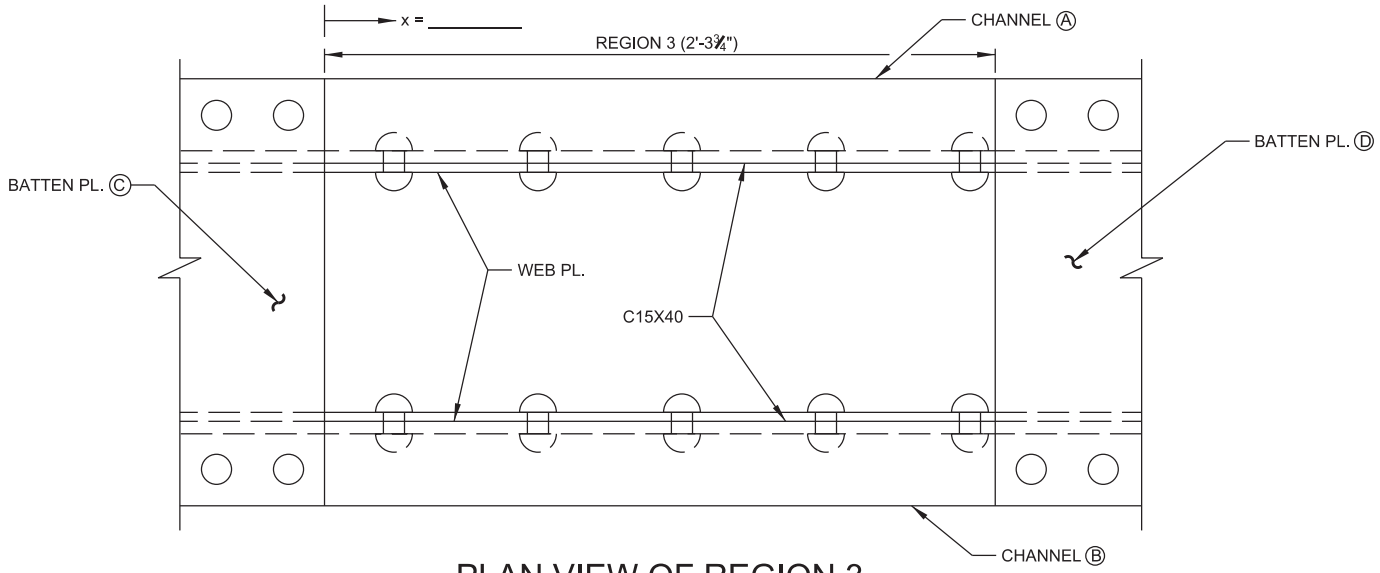

PLAN VIEW OF REGION 3
SCALE: 1½" = 1'-0"

BOWEN LABORATORY
PURDUE UNIVERSITY

1040 SOUTH RIVER ROAD
WEST LAFAYETTE, IN 47906
P: 765-404-2227 F: 765-494-9886

PROJECT:

TRUSS INSPECTION ROUND ROBIN

INSPECTOR ID:
INSPECTION DATE:
PROCTOR INITIALS:

SHEET NOTES:

1. INDICATE THE LOCATION OF THE CRITICAL SECTION WITHIN REGION 3 ON THE PLAN VIEW SKETCH. PROVIDE THE DISTANCE BETWEEN THE FACE OF BATTEN PLATE C AND THE CRITICAL SECTION (X = ____).

2. THICKNESS MEASUREMENTS DO NOT NEED TO BE PROVIDED AT THIS LOCATION.

SHEET TITLE:

TASK 3 SKETCHES

SHEET NO.: 3-1

Truss Inspection Round Robin
Inspector Information

BOWEN LABORATORY
PURDUE UNIVERSITY

Please complete the following form. All information collected is used for research purposes only.

Inspector ID:_____ Inspection Date:_____
Employer:_____ Years of Inspection Experience:_____
Age:_____ Gender:_____

1) Please list all tools you brought to complete this inspection.

2) Please list which tools you used during the inspection course.

3) Are there any additional tools you wish you would have had available?

3) Approximately how many hands-on, fracture critical inspections have you completed in the last 12 months?

4) Approximately how many routine inspections have you completed in the last 12 months? What percentage of these were performed on steel bridges?

5) Approximately what percentage of your work time (on a per week basis) is spent performing bridge inspections?

6) Please indicate which inspection training courses you have completed and the date of completion (estimates are acceptable for the dates):

Safety Inspection of In-Service Bridges (FHWA/NHI): _____
Bridge Inspection Refresher Training (FHWA/NHI): _____
Engineering Concepts for Bridge Inspectors (FHWA/NHI): _____
Underwater Bridge Inspection (FHWA/NHI): _____
Fracture Critical Inspection Techniques for Steel Bridges (FHWA/NHI): _____
Inspection and Maintenance of Ancillary Highway Structures (FHWA/NHI): _____
Introduction to Element Level Bridge Inspection (FHWA): _____
Inspecting Steel Bridges for Fatigue (Purdue/S-BRITE): _____
State Specific Bridge Inspection Refresher Training: _____

Others:

Truss Inspection Round Robin
Inspector Information

BOWEN LABORATORY
PURDUE UNIVERSITY

7) Are you qualified as a Team Leader?

Yes No

8) Have you received any training specific to estimating section loss in steel members? If yes, please provide a brief description.

Yes No

9) Are you a registered professional engineer or engineer-in-training?

Yes No

If yes, please indicate your license below.

SE PE (civil) PE (other) FE (civil) FE (other) Other

10) What is the highest educational level that you have completed?

_____ High School degree or equivalent

_____ Trade School Degree

_____ Associate's Degree

_____ Bachelor's Degree in CIVIL ENGINEERING? Or OTHER? (circle one)

_____ Master's Degree in CIVIL ENGINEERING? Or OTHER? (circle one)

_____ PhD in CIVIL ENGINEERING? Or OTHER? (circle one)

11) How did your effort level during this task compare to your effort level during a typical bridge inspection?

More effort Similar effort Less effort

12) How did your focus level during this task compare to your focus level during a typical bridge inspection?

More focused Similar focus Less focused

Appendix D2: Information provided to load raters

Load Rating Participant:

Thank you for agreeing to participate in the Truss Chord Load Rating Round Robin at Purdue University. The goal of this study is to assess the variability in load rating evaluations of built-up tension members with significant section loss.

The study consists of the following evaluation scenario:

Load rating of a built-up tension truss chord (ref. Figures 1 and 2 attached)

This review may be completed from your home or office. You will be provided with all necessary design information to determine the load rating factor. You will be responsible for interpreting the inspection results and incorporating the findings into your analysis. Computer software will not be required to complete this analysis, but may be used.

The evaluation is estimated to require 2 to 4 hours to complete.

It is critical to the study that all procedures and findings are kept confidential. If information regarding the study set-up or results are shared among engineers, the results will become invalid. Likewise, your identity will remain confidential.

Thank you for your willingness to participate in this study. If you have any questions, please contact:

Dr. Robert J Connor
rconnor@purdue.edu

Leslie E. Campbell, PE
campb270@purdue.edu

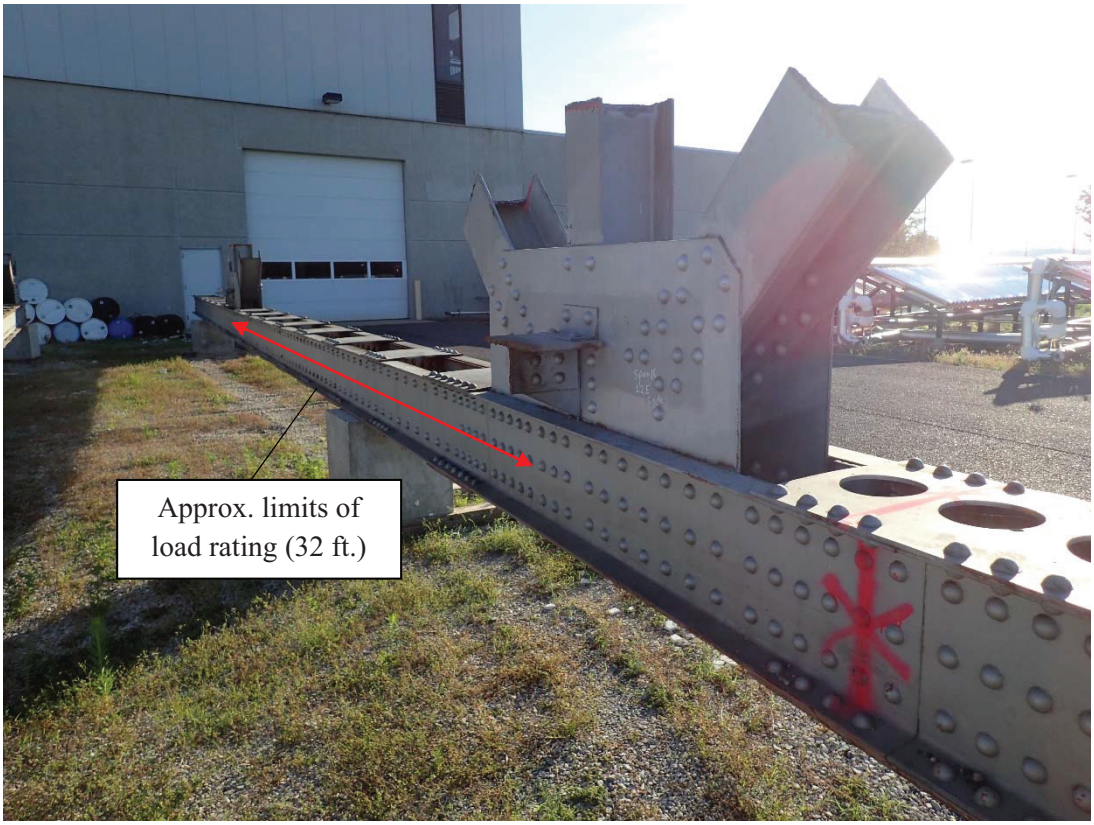

Figure 1. Truss chord elevation view (looking from joint L4 toward joint L2)

Figure 2. Truss chord plan view (looking from joint L4 toward joint L2)

Truss Chord Load Rating Round Robin

Evaluation Instructions
Purdue University
2018

This document provides the procedures and instructions for engineers participating in the Truss Chord Load Rating Round Robin at Purdue University.

Introduction:

You are about to participate in a study on corrosion evaluation of steel bridges. It is critical to the study that all procedures and findings are kept **CONFIDENTIAL**. Please do not share the inspection information or discuss your evaluation with other engineers or personnel in your office. Likewise, your identity will remain confidential; the results from your specific participation will not be shared or be published.

The objectives of this portion of study are as follows:

1. Establish the variability in load rating evaluations of steel bridge tension members with corrosion and section loss.
2. Investigate the various approaches load rating engineers use to interpret and apply inspection findings.
3. Identify methods for improving consistency in how the effects of corrosion are accounted for in load rating.

Load Rating Scenario:

The evaluation is focused on the load rating of the lower chord in Span 16 between joints L2 and L4 (Ref. Construction Plans, Sheet 33). The joints and gusset plates do not need to be load rated. The load rating should be completed using the load and resistance factor rating method in accordance with the 2nd Edition of the *AASHTO Manual for Bridge Evaluation*, including the 2016 interim revisions. The evaluation is divided into two separate tasks and may be completed in any order.

The unfactored dead and live loads are provided. The live load corresponds to the HL-93 loading. You will need to make an assumption regarding the material strength (yield and ultimate) and identify the governing fatigue category. The inspection report and relevant construction plans have been provided for your reference.

Bridge Data:

- The bridge was constructed in 1941 in the upper Midwest region of the United States.
- The member under evaluation is the bottom truss chord in Span 16 between joints L2 and L4.
- The member is fracture critical.
- P_{DC} = 335 kips, P_{DW} = 0 kips, P_{LL+IM} = 322 kips (design truck with lane load), P_{LL+IM} = 134 kips (fatigue truck)
- These loads are unfactored. They include the distribution factor and dynamic load allowance.
- $(ADTT)_{SL}$ = 1500 and it is assumed that $(ADTT)_{SL}$ is constant through the life of the bridge.

Truss Chord Load Rating Round Robin

Evaluation Instructions
Purdue University
2018

Evaluation Tasks:

Task 1:
Calculate the inventory level load rating factor for the Strength I limit state in the as-built (undamaged) condition AND the as-inspected (damaged) condition.

Task 2:
Calculate the remaining fatigue life in the as-inspected (damaged) condition.

A blank load rating report has been provided for recording your results. Please show all work to support your calculation of load rating, remaining fatigue life, member capacity, and effective stress range, including appropriate load and resistance factors. Reference applicable equations and provisions from the *AASHTO Manual for Bridge Evaluation*. After finishing the evaluation, please complete the Load Rater Exit Form. The load rating report, calculations, and exit form may be emailed to the Research Team (campb270@purdue.edu).

Thank you for your participation and cooperation. Please contact us with any questions.

Dr. Robert J. Connor
rconnor@purdue.edu

Leslie Campbell, PE
campb270@purdue.edu
(916) 803-2428

BRIDGE RATING REPORT

(Note: Load rater to complete all YELLOW fields)

Load Rater:	
Date:	
Rating Method:	Load and resistance factor

IDENTIFCATION

Structure Type:	Steel deck truss (approach span)
Description:	Two (2) parallel trusses/simple span
Year Built:	1941

GEOMETRY

Span Number:	16 (approach span)	O-to-O Coping:	35'-2"
Span Length:	128'-0"	Clear Roadway:	27'-0"
Truss Spacing:	32'-2"	Skew:	0°

STEEL SUPERSTRUCTURE

Structural Steel:

Steel Fy:		ksi
Steel Fu:		ksi

DESIGN LOADS (unfactored)

Dead Load:

P_{DC}	335	kips
P_{DW}	0	kips

Live Load: Strength I

P_{LL+IM}	322	kips

Live Load: Fatigue

P_{LL+IM}	134	kips

STRENGTH I RATING (as-built condition)

Vehicle Configuration:	HL-93	
Member Capacity:		kips
Inventory Rating Factor:		

STRENGTH I RATING (as-inspected condition)

Vehicle Configuration:	HL-93	
Member Capacity:		kips
Inventory Rating Factor:		

FATIGUE ANALSYIS (as-inspected condition)

Vehicle Configuration:	HL-93 (Fatigue Truck)	
Governing Fatigue Category:		
Effective Stress Range:		ksi
Remaining Fatigue Life:		years

*If infinite fatigue life remains, indicate such here.

CALCULATIONS

CALCULATIONS

CALCULATIONS

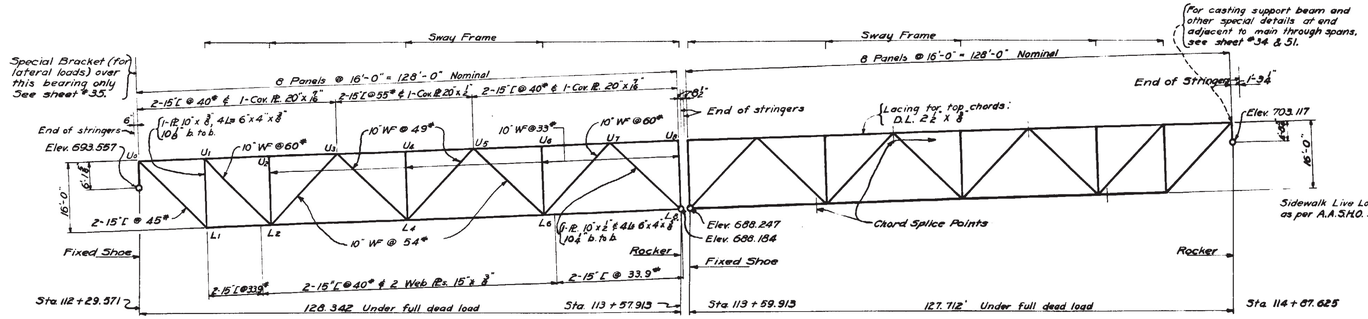

SPAN Nº 16

SPAN Nº 17

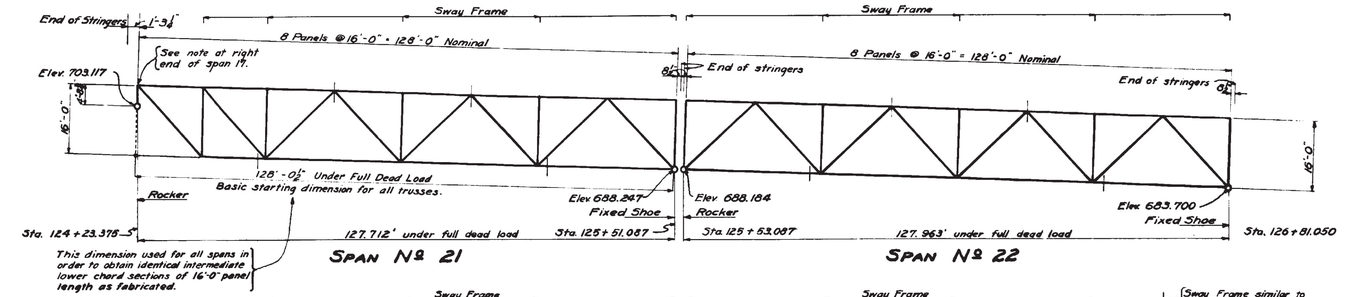

SPAN Nº 21

SPAN Nº 22

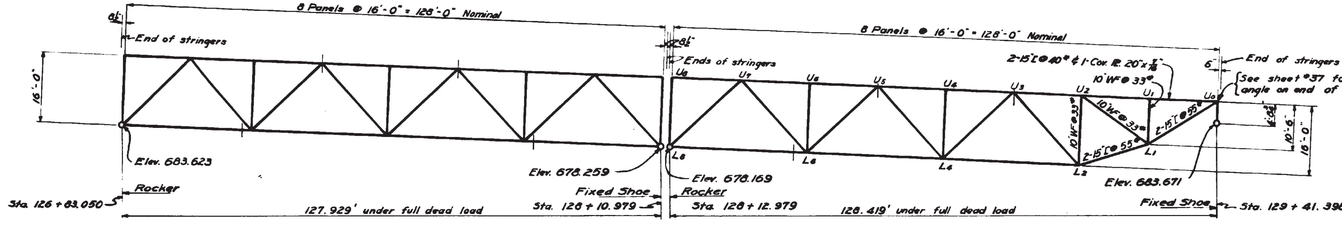

SPAN Nº 23

SPAN Nº 24

Sway Frame similar to that shown on sheet #34.

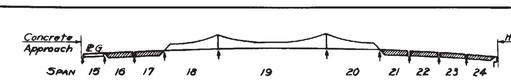

KEY SKETCH OF STEEL SPANS

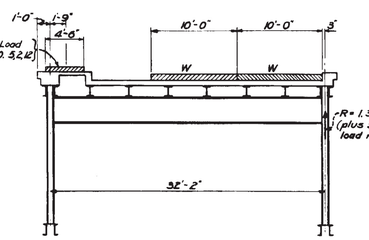

SKETCH SHOWING POSITION OF LIVE LOAD FOR MAXIMUM LOAD ON ROADWAY SIDE TRUSS

Analysis and design are for roadway side truss. Both trusses shall be made alike.

Roadway Live Load:
2 lanes of H-20 loading as per A.A.S.H.O. S.2.7. each lane occupying a 10 foot width with lanes placed in the roadway to produce maximum stress.

STRESS TABLE

Member	Dead Load (Kips)	Live Load (Kips)	Impact (Kips)	S.W. Load (Kips)	Total Axial (Kips)	Bending (Ft Kips)	Area Req'd	Area Used & Out	Holes
U₀U₁	-156.45	-70.16	-13.06	-0.90	-241.37	35.2		32.15	
U₁U₃	-268.20	-120.27	-23.77	-1.54	-413.78	22.9		32.15	
U₃U₆	-357.60	-160.36	-31.69	-2.05	-551.70	25.5		42.22	
U₆U₇	-268.20	-120.27	-23.77	-1.54	-413.78	22.9		32.15	
U₇U₈	0.0	0.0	0.0	0.0	0.0	52.4		32.15	
L₁L₂	+156.45	+70.16	+13.86	+0.90	+241.37	0.0	13.41	14.90	4 flange 6 web
L₂L₄	+335.25	+150.34	+29.71	+1.92	+517.22	0.0	28.75	28.94	4 flange 4 web
L₄L₆	+335.25	+150.34	+29.71	+1.92	+517.22	0.0	28.75	28.94	4 flange 4 web
L₆L₈	+156.45	+70.16	+13.86	+0.90	+241.37	0.0	13.41	14.90	4 flange 6 web
U₀L₁	+221.25	+112.70	+22.27	+1.27	+357.49	0.0	19.86	21.40	6 web
U₁L₁	-156.45	-79.70	-15.75	-0.90	-252.80	0.0	18.21	18.19	
U₁L₂	+158.03	+69.22	+20.18	+1.07	+268.50	0.0	14.92	14.93	4 flange
U₂L₂	-44.70	-44.88	-14.29	-0.40	-104.27	0.0	8.30	9.71	
U₂L₄	-94.82	-66.20	-16.63	-0.83	-180.48	0.0	14.83	15.88	
U₃L₄	+22.13 +31.61	-28.60 +49.61	-8.28 +13.13	-0.42 +0.62	-22.76 +102.56	0.0	5.69	12.17	4 flange
U₄L₄	-44.70	-44.88	-14.29	-0.40	-104.27	0.0	8.30	9.71	
L₄U₅	+32.13 +31.61	-28.60 +49.61	-8.28 +13.13	-0.42 +0.62	-22.76 +102.56	0.0	5.69	12.17	4 flange
U₅L₆	-94.82	-66.20	-16.63	-0.83	-180.48	0.0	14.83	15.88	
U₆L₆	-44.70	-44.88	-14.29	-0.40	-104.27	0.0	8.30	9.71	
L₆U₇	+158.03	+69.22	+20.18	+1.07	+268.50	0.0	14.92	14.93	4 flange
U₇L₈	-221.25	-112.70	-22.27	-1.27	-357.49	0.0	27.66	28.44	
U₀L₀	-22.35	-44.88	-15.94	-0.20	-83.34	0.0	6.66	9.71	
U₀L₁	+285.15	+145.25	+28.70	+1.63	+460.73	0.0	25.59	25.72	8 web
U₁U₂	-238.39	-106.90	-21.12	-1.37	-367.78	35.2		32.15	
U₁L₁	-44.70	-44.88	-14.29	-0.40	-104.27	0.0	7.52	9.71	
U₂L₁	-24.93 +35.62	+31.31 -39.82	+11.10 -8.13	+0.28 -0.46	+26.66 -260.90	0.0	7.76	9.71	
L₁L₂	+283.60	+127.18	+25.13	+1.62	+437.53	0.0	24.46	25.72	8 web
U₂L₂	-17.60 -25.14	+15.07 -36.00	+3.68 -12.10	+0.18 -0.46	-1.95 -76.38	0.0	6.09	9.71	

Special end portion of span Nº 24. Other members same as above.

Note:
North half of Span #16, south half of Span #17, north half of Span #21, both halves of Spans #22 and #23, and south half of Span #24 are identical except for bearings. See special camber for Span #24.
South half of Span #16, north half of Span #17, and south half of Span #21 are identical except for bearings and for special details at south end of span #16.
Design moments shown in the table are 75% of simple beam bending moments due to direct loads (52,400 #) reduced by moment of axial load x eccentricity. Critical section is considered to be at mid-panel.

CONSTRUCTION NOTES FOR STRUCTURAL STEEL FOR DECK TRUSSES

The Minnesota Highway Department's Specifications for Highway Construction dated July 1, 1938 shall apply on this project except as otherwise specifically noted.
Reference to specific sections of these specifications is made by number or by prefix M.H.D. and section number.
Four copies of the reports enumerated in M.H.D. 2407.3J1 will be required.
◇ General reaming will be required as per M.H.D. 2407.3E5a.
Rivets - ⅞ ϕ, except for ⅜ ϕ in laterals, sway frames, stringers, and as otherwise noted.
All field connections shall be riveted except where otherwise noted.
Paint:
Shop coat - Red - M.H.D. 3501
1st field coat - Gray - M.H.D. 3503
2nd field coat - Aluminum - M.H.D. 3505
Special or typical joint details at panel points U₁, U₂ shall be subject to the approval of the Minnesota Highway Dept. Layouts may or may not be furnished to the fabricator.
Gusset plates shall be ⅜" thick except where otherwise noted.
Fabricator to determine length of stringers and spacing of connections to floor beams, to allow for conformation of truss to vertical curve.
All double lacing shall be riveted at the intersection.

NOTE ON ERECTION:
Individual trusses may be partially or completely assembled and riveted up on the ground in order to reduce or eliminate falsework. See Special Provisions on this procedure and on falsework restrictions in spans 16 & 17.

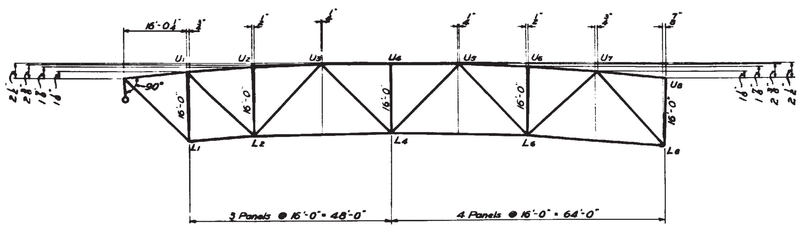

CAMBER BLOCKING DIAGRAM FOR SPANS Nº 16, 17, 21, 22, & 23

All members shall be fabricated to exact lengths between panel points as shown above.
Posts will be normal to the vertical curve at the panel points under full dead load.
Dead load deflection equals 1¼".
Residual camber equals 1½" (to conform to 18908' radius curve)

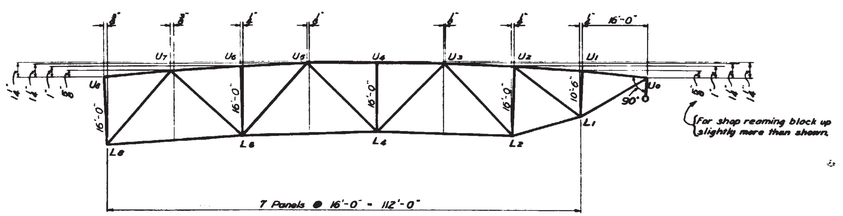

CAMBER BLOCKING DIAGRAM FOR SPAN Nº 24

See note on the left concerning fabrication.
Dead load deflection equals 1¼".
No residual camber.

STATE OF MINNESOTA
DEPARTMENT OF HIGHWAYS

BRIDGE Nº 5900
MISSISSIPPI RIVER CROSSING AT WINONA
DECK TRUSS SPANS
DESIGN SHEET
Approved Nov. 7, 1940.

E. J. Miller
Bridge Engineer

S.P. 8503-05 (T.H. 43 & 75) F.A.P. 912-A(3)

SHEET 33 OF SHEETS

5900

D.C.P. MW 1 1940

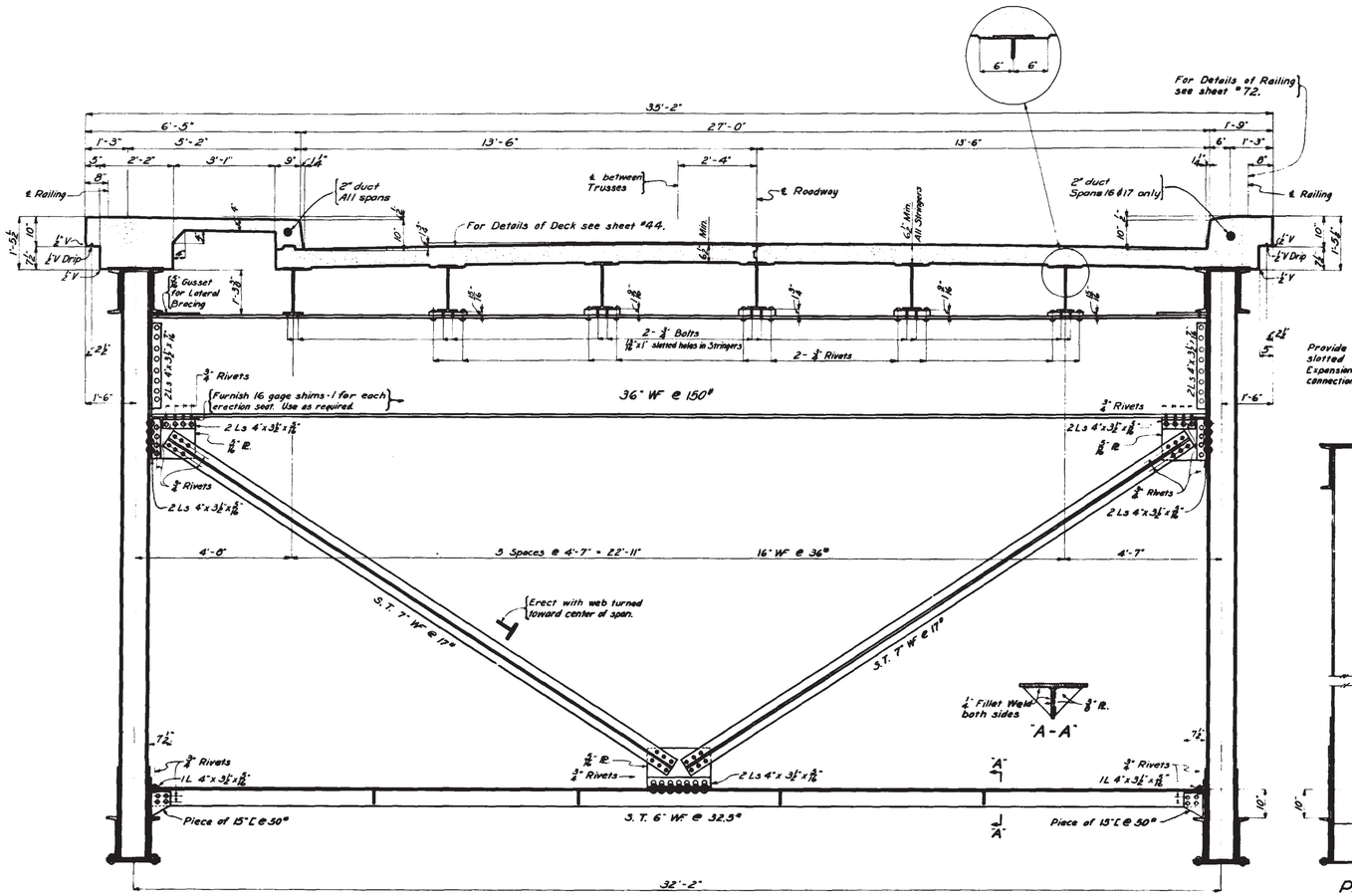

SECTION AT U4L4
Looking South

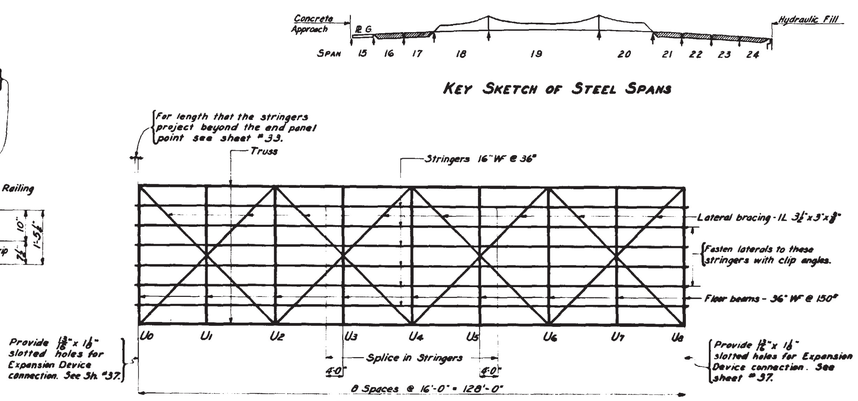

KEY SKETCH OF STEEL SPANS

FRAMING PLAN

Sway frames shall be at all panel points where there is a post. See sheet #33. Lateral system designed for erection purposes only.

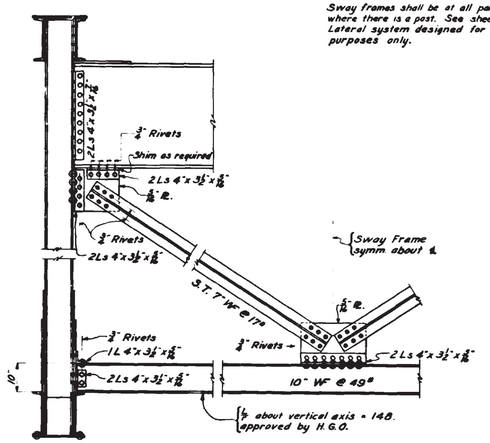

PART SECTION SHOWING SWAY FRAME AT PIERS 16, 21, 22 & 23.

Estimated Quantities Of Structural Steel	
Span No. 16	186,312 Lbs.
Span No. 17	188,538 Lbs.
Span No. 21	188,538 Lbs.
Span No. 22	186,768 Lbs.
Span No. 23	186,768 Lbs.
Span No. 24	184,846 Lbs.
Total	1,131,740 Lbs.

Note. 3% allowance as per M.H.D. 2407.42 1a is added on Sh. 47.

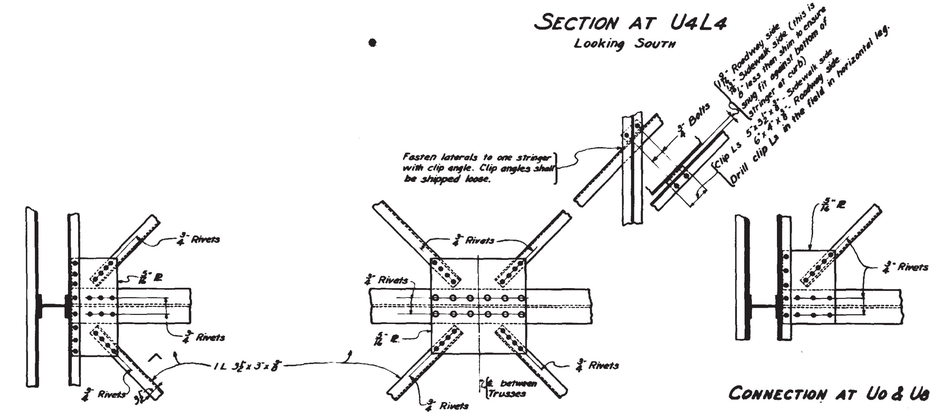

CONNECTION AT U2, U4 & U6

CONNECTION AT U1, U3, U5 & U7

LATERAL BRACING
(in plane of top of floor beams)

CONNECTION AT U0 & U8

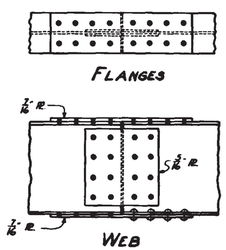

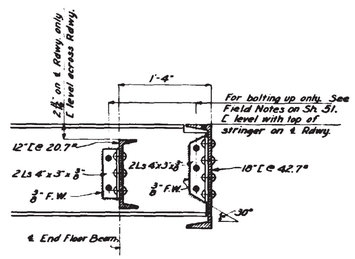

EXPANSION DEVICE HEADERS OVER PIERS 17 & 20.
For Plan and Elevation see sheet #51.

STATE OF MINNESOTA
DEPARTMENT OF HIGHWAYS

BRIDGE No. 5900
MISSISSIPPI RIVER CROSSING AT WABASHA
DECK TRUSS SPANS
CROSS-SECTION & DETAILS
Approved Nov. 7, 1940.

E. J. Miller
Bridge Engineer

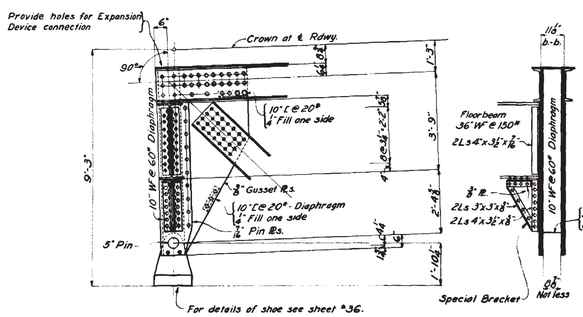

JOINT DETAIL OF END OF SPAN 16 OVER PIER 15

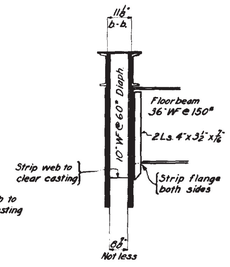

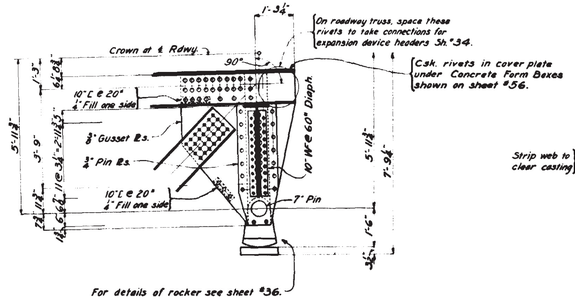

JOINT DETAIL OF ENDS OVER PIERS 17 & 20

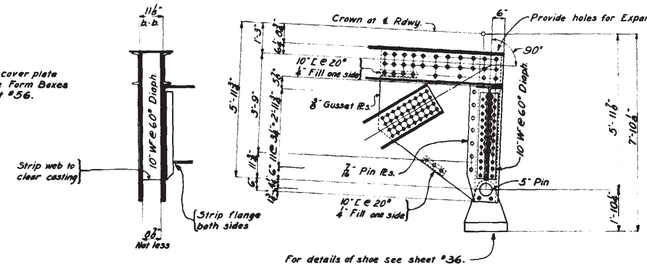

JOINT DETAIL OF END OF SPAN 24 OVER NORTH ABUTMENT

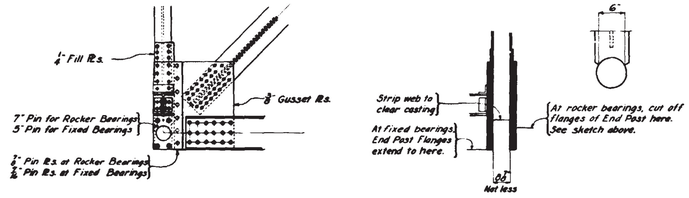

JOINT DETAIL OF ENDS OVER PIERS 16, 21, 22 & 23

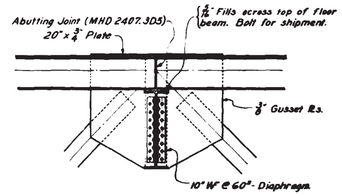

TYPICAL TOP CHORD JOINT DETAIL
AT PANEL POINTS WITHOUT POSTS

Top chord splice, as shown, is required at U8 & U8 only. See sheet #33.

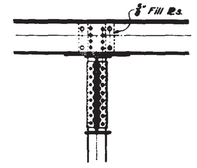

TYPICAL POST CONNECTION
No gusset plates required

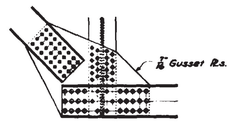

JOINT DETAIL AT L1
SPANS 16, 17 & 21

NOTES ON RIVETING

Spacing of rivets where shown in these plans is subject to minor modifications by the fabricator. Rivet groups shall be made as compact as possible. For holes out assumed in design, see note on sheet #33. Web members having excess sectional area shall be developed in the connections for the average of the calculated and permissible stresses, but not less than 75% of the latter.

For General Notes see sheet #3.

Contractor shall provide fills where required.

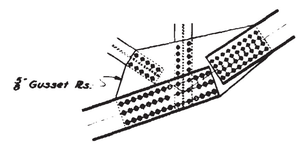

JOINT DETAIL AT L1
SPAN 24

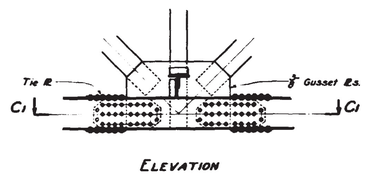

DETAIL OF JOINT L4
Typical for all spans

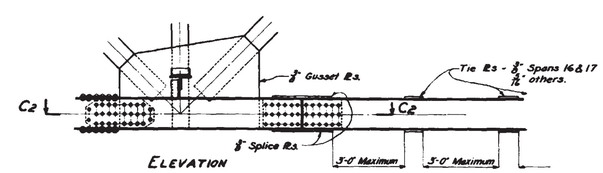

DETAIL OF SPLICE AND JOINT AT L2 & L6
Typical for all spans except joint at L2 in span 24.

Gusset plates are not to scale.

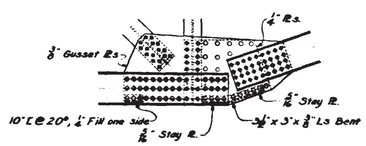

JOINT DETAIL AT L2
SPAN 24

STATE OF MINNESOTA
DEPARTMENT OF HIGHWAYS

BRIDGE No. 5900
MISSISSIPPI RIVER CROSSING AT WINONA
DECK TRUSS SPANS
JOINT DETAILS
Approved Nov. 7, 1940.

E. J. Miller
Bridge Engineer

S.P. 8503-05 (T.H. 43 & 75) F.A.P. 9/2-A(3)

SHEET 35 OF SHEETS

5900

DCP
DCR
H.A.S.

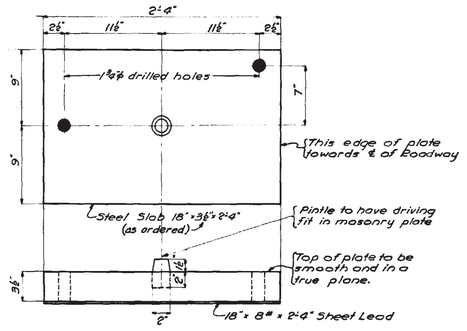

MASONRY PLATE

Make 6 thus mark M.P.B
Make 6 Rev. mark M.P.L
Furnish one pair each for Piers 16, 17, 20, 21, 22 & 23

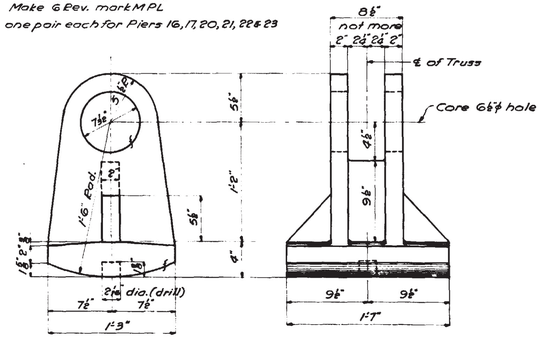

EXPANSION SHOE

Cast Steel as per M.H.D. 3323
Test bars as per M.H.D. 2407.3F3
Make 12 as shown

Note:
Piece mark as follows:
2 Shoes for Pier 16 Mk. 16-B1
2 Shoes for Pier 17 Mk. 17-B1
2 Shoes for Pier 20 Mk. 20-B1
2 Shoes for Pier 21 Mk. 21-B1
2 Shoes for Pier 22 Mk. 22-B1
2 Shoes for Pier 23 Mk. 23-B1

Note Z

Weights of Cast Steel are based on net dimensions plus allowances for finishing as per M.H.D. 2407.421b. 10% for fillets and overruns is added in the summary. Steel Shims and masonry plates to be included with and paid for at the same unit price as other structural steel items.

Furnish 12-7⅞ pins and nuts for expansion shoes as per M.H.D. 2407.3D7

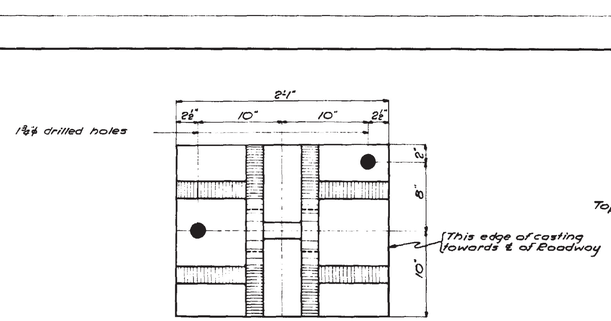

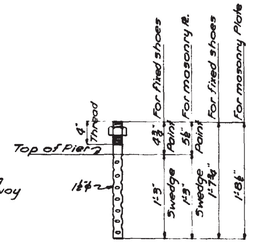

DETAIL OF ANCHOR BOLTS

Make 2a thus for Masonry Plates
Make 2a thus for Fixed Shoes

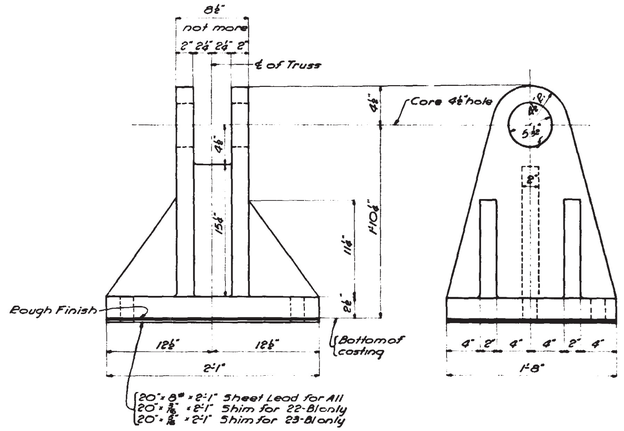

FIXED SHOE

Cast Steel as per M.H.D. 3323
Test bars as per M.H.D. 2407.3F3
Make 6 Thus
Make 6 Reverse

Note:
Piece mark as follows
One pair of Shoes for Pier 15 Mk. 15-B1
One pair of Shoes for Pier 16 Mk. 16-B1
One pair of Shoes for Pier 21 Mk. 21-B1
One pair of Shoes for Pier 22 Mk. 22-B1
One pair of Shoes for Pier 23 Mk. 23-B1
One pair of Shoes for North Abut. Mk. N.A.B1

Furnish 12-5⅞ Pins & nuts for fixed shoes as per M.H.D. 2407.3D7

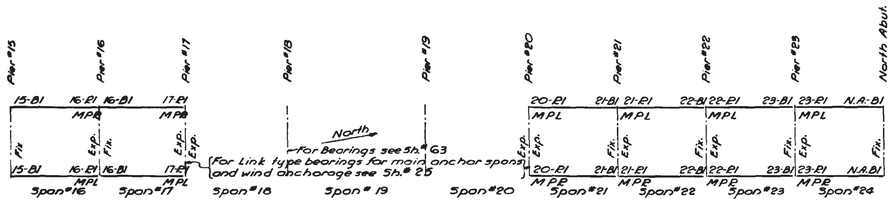

MASONRY PLATE AND BEARING LAYOUT

COMPUTED WEIGHTS

②	Cast Steel	16682 lbs.
①	Structural Steel	10400 lbs.
	Sheet Lead	670 lbs.

① Computed Weight - 5% as per M.H.D 2407.421a is added in summary on sheet 47.
② Includes allowance for finishing - See Note Z.
Four copies of the reports enumerated in 2407.311 will be required.

Paint same as structural steel, except pins and pin holes, which shall receive a coat of hot white lead and tallow.

STATE OF MINNESOTA
DEPARTMENT OF HIGHWAYS

BRIDGE No 5900
MISSISSIPPI RIVER CROSSING AT WINONA
BEARINGS FOR DECK TRUSS SPANS
Approved Nov 7, 1940.
E. J. Miller
Bridge Engineer

S.P. 8503-05 (T.H. 43 & 75) F.A.P. 912-A(3)

SHEET 36 OF SHEETS

5900

Dr. I. M.
Tr. M.C.A.
Ck. D.C.A.

Rail Post Anchorage Units on both sides of bridge to be set in concrete. For location and details see Sheets 72 and 74.

Order of Placing:
Middle section in each span to be placed first over both halves of roadway. After middle section is placed in two adjoining spans, the expansion device over the pier between shall be adjusted to proper elevation to avoid any sag in the final profile. End sections adjacent to the adjusted expansion device may then be placed in any desired order, except that upper end panels of Spans 17 & 21 shall be postponed until devices over piers 17 & 20 are adjusted as noted on sheet #31. No sidewalk runs to be placed in any span until roadway slab in that span is fully completed. In Spans 17 & 21, the lower seven panels may be fully completed if the upper end panels are delayed as noted above.
Sidewalk slab shall be placed in sections not exceeding 32 feet in length, which may be placed in any order desired.
Construction Joints must be located so as to miss Rail Posts and Hub Guard Standards.

Concrete fill under expansion device at top of parapet wall of north abutment is included in yardage shown for superstructure and shall be paid for as Grade "A" Concrete. See sketch below for details.

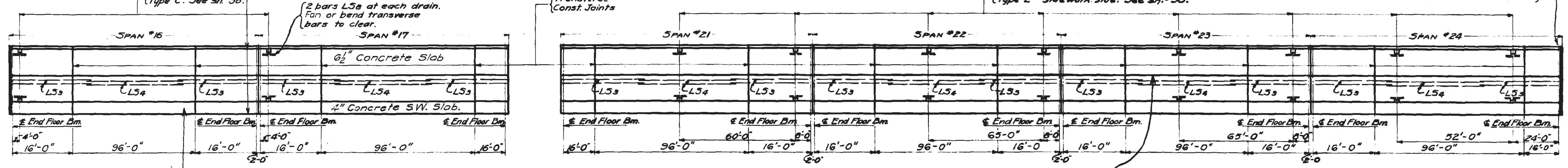

NOTE: Longitudinal dimensions shown are nominal measured along grade. Do not use for exact purposes.

Hub Guard Anchorage Units to be set in concrete. For location and details, see Sheets 40, 41, and 42.

Deck Plan - Spans 16, 17, 21, 22, 23 & 24

Bill Of Reinforcing Bars For 128 Ft. Deck Truss Spans					
Bar	No.	Size	Length	Shape	Location
LS1	1956	⅝"φ	28'-9"	Strt.	Roadway Slab, Transverse
LS2	978	⅝"φ	32'-0"	Bent	" " "
LS3	936	½"φ	41'-6"	Strt.	" " Sdwk. Longit.
LS4	468	½"φ	50'-0"	"	" " " "
LS5	192	½"φ	15'-9"	"	Curb, Longitudinal
LS6	240	½"φ	4'-3"	"	Transv. Joints, Interm. panels
LS7	48	½"φ	3'-9"	"	" " , Curb panel
LS8	40	⅝"φ	5'-0"	"	Floor Drains
LC1	528	½"φ	6'-0"	Bent	Curb, Ties - Rdwy Side
LC2	510	½"φ	4'-2"	"	Sdwk. "
LC3	48	½"φ	33'-0"	"	Sdwk. to Floor Slab Dowels
LC4	216	½"φ	5'-2"	"	Transverse Joints, Ties
* LC5	1	7'-2" x 775'-0"	Bend in field		6"x12"-2/2 Wire Mesh in Sdwk.
LC6	6	¼"φ	20'-0"	Strt.	All Splash Slabs as noted, Sh. 39.

* Length given does not allow for laps. Area for payment = 7'-2" x 775'-0" = 5555 Sq. Ft.
Estimated weight = 3278 Lbs. (Based on .59 #/□').
Weight included in total weight shown for Reinforcement Bars.
Welded Wire Fabric will be paid for at same pound price as Reinforcement Bars.

NOTE: Above bill of bars is complete total for all 6 Deck Truss Spans.

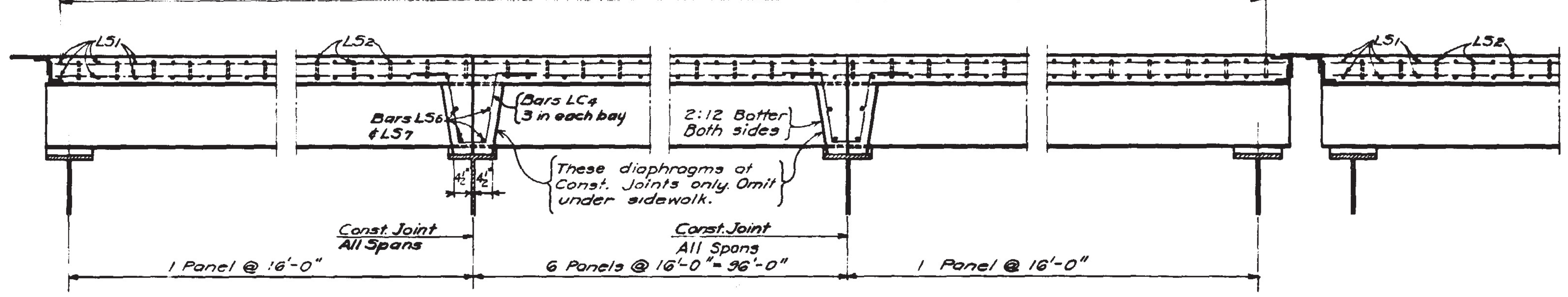

Part Longitudinal Section Near ℄ Roadway of Typical Span

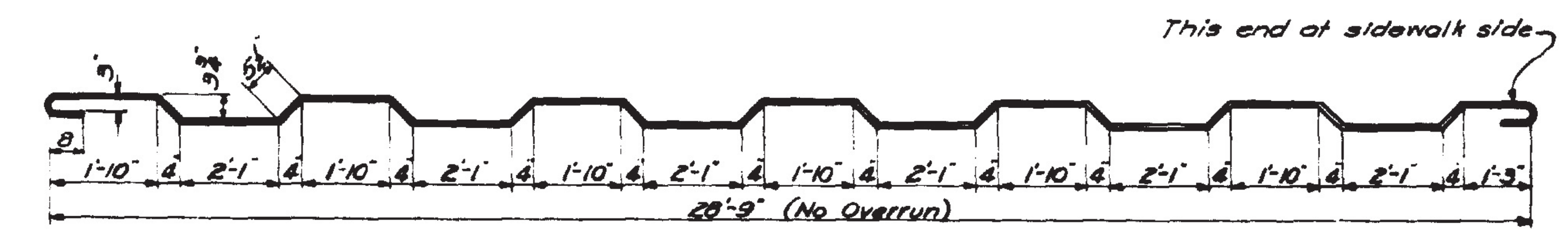

Bars LS2

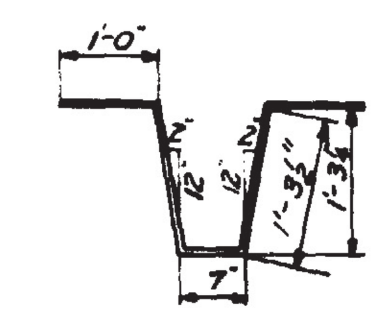

Bars LC4

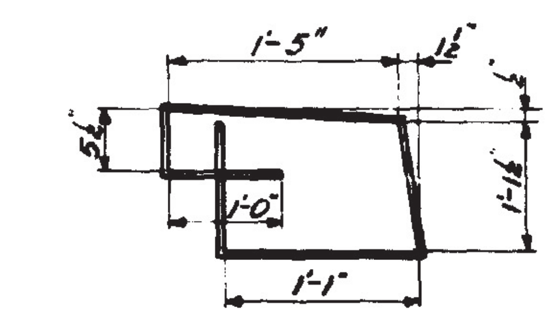

Bars LC1

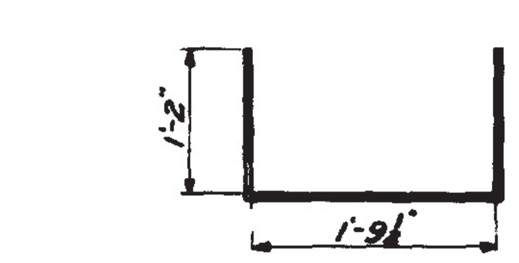

Bars LC2

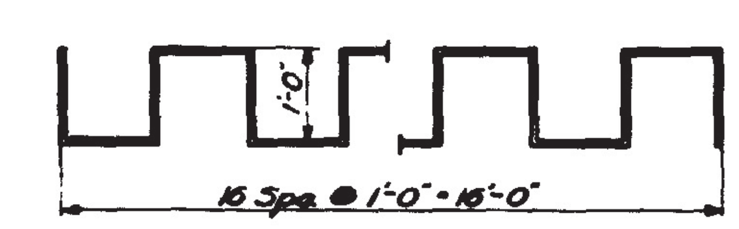

Bars LC3

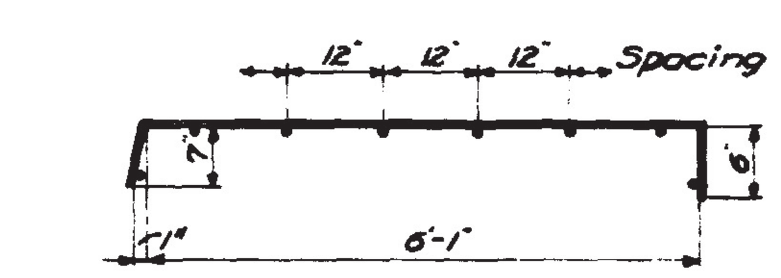

Welded Wire Fabric 6"x12"-2/2 Mark LC5

Ship flat and bend in field

Grade "A" Concrete shall be required throughout.

Construction joints to be placed in curb to top of floor slab over interm. floor beams, except at the three places (per span) where rail post anchorages occur. Joint to be formed by placing sheet of #16 ga metal, oiled or painted, which shall be removed after concrete has reached its initial setting. No reinf. thru these joints.

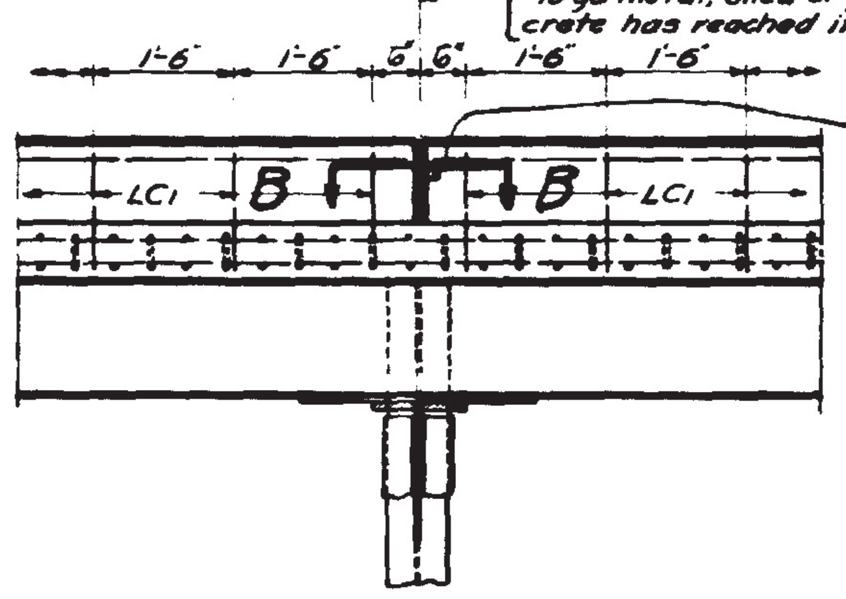

Section A-A

Showing Const. Joint thru curb over intermediate floor beams, at roadway curb only.

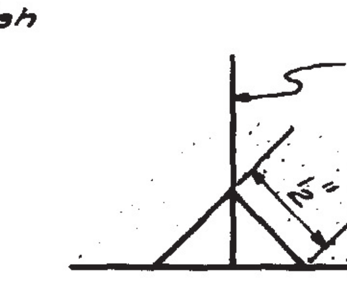

Section B-B

For Profile of finished roadway surface, see Sh. #45.

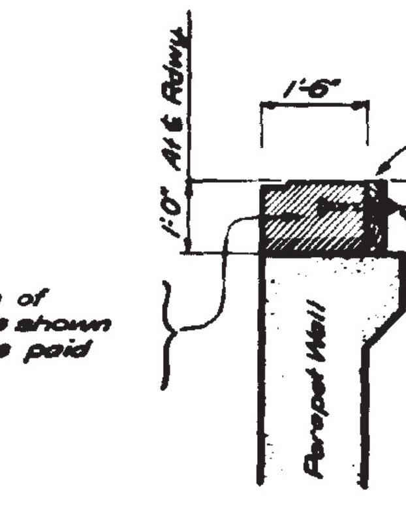

Shaded portion of concrete at top of parapet wall included in yardage shown for superstructure and shall be paid for as Grade "A" concrete.

Section Showing Top Of Parapet Wall Of North Abut.

Estimated Quantities		
Grade "A" Concrete	682.0	Cu. Yds.
Reinforcement Bars	144,340	Lbs.
Structural Steel (Bolts in parapet)	20	Lbs.

NOTE "A": Forms to be built to elevations sufficiently above true grade to allow for deflections due to slab dead load as specified by the Engineer.

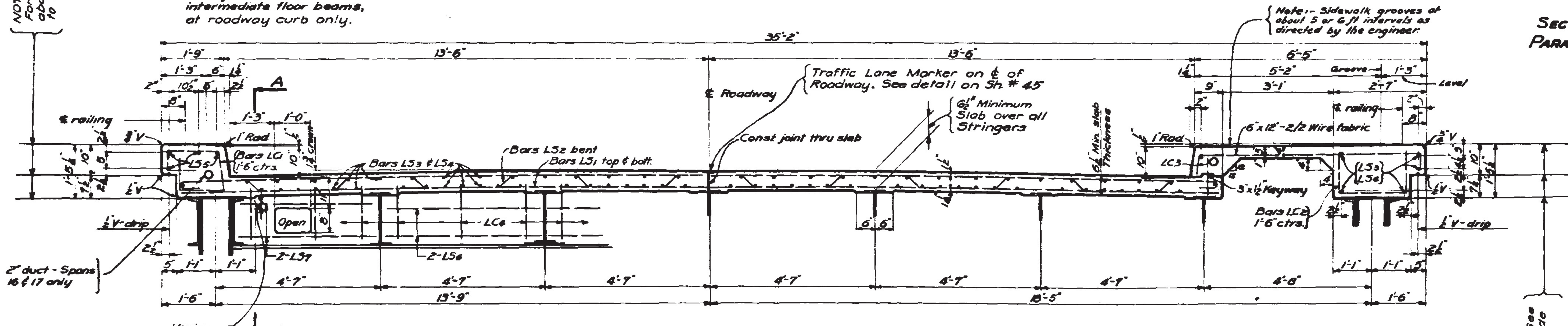

Transverse Section Thru Deck

Total number of lines of longitudinal bars = 82 (78 LS3 or LS4 and 4 LS5)
All to be ½"φ bars, lapped as shown in plan.

State Of Minnesota
Department Of Highways

Bridge No. 5900
Mississippi River Crossing At Winona
Deck Details
Spans 16, 17, 21, 22, 23 & 24
Approved Nov. 7, 1940.

E. J. Miller
Bridge Engineer

S.P. 8503-05 (T.H. 43 = 75) F.A.P. 912-A(3)

5900

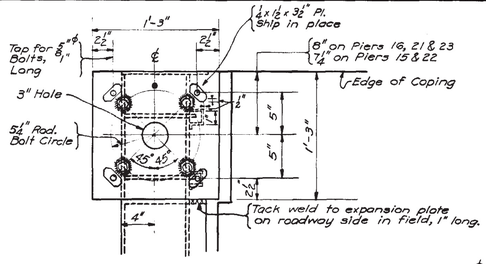

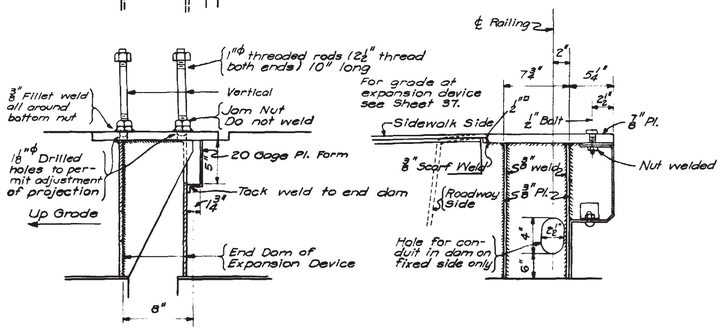

Modification of Expansion Devices for Light Standard Mounting

East Side of Piers 16, 21 and 23.
West Side of Piers 15 and 22.
Devices detailed and billed on Sheet # 37.
Weight includes above details.

Quantity Summaries for Structural Steel, Cast Iron, and Cast Steel

Span 15

Structural Steel	
Main Framing (Sh. 31)	135,500
Bearings (Sh. 32)	2,060
Expansion Devices (Sh. 37)	3,300
Total "Computed" Weight	140,860
5% as per M. H. D. 2407.4Z1a	7,043
Pay Weight	147,903
For Bidding Purposes Use	148,000#
Cast Iron Class 30	
Bearings (Sh. 32)	1,157
10% of net dimensions as per	
M. H. D. 2407.4Z1b	106
Pay Weight	1,263
For Bidding Purposes Use	1,250#

Spans 16, 17, 21, 22, 23 & 24

Structural Steel	
Span 16 (Sh. 33)	166,312
Span 17 (Sh. 33)	188,538
Span 21 (Sh. 33)	188,538
Span 22 (Sh. 33)	186,768
Span 23 (Sh. 33)	188,768
Span 24 (Sh. 33)	184,816
Expansion Devices (Sh. 37)	16,387
Bearings (Sh. 36)	10,400
Anchor Bolts at No. Abut. (Sh. 44)	20
Total "Computed" Weight	1,148,547
5% as per M.H.D. 2407.4Z1a	57,427
Pay Weight	1,205,974
For Bidding Purposes Use	1,206,000#
Cast Steel Grade B_2	
Bearings (Sh. 36)	16,682
10% of net dimensions as per	
M.H.D. 2407.4Z1b	1,637
Pay Weight	18,319
For Bidding Purposes Use	18,350#

Spans 18, 19 & 20

Structural Steel	
Main Framing	3,371,608
Ladders at U_0L_{10}-No.¢So. & $U_{16}L_{18}$-So.	13,372
Wind Anchorage (Sh. 25)	14,188
Railing Connections & Shims	81,415
Misc. Material & Pipe Drains	38,275
"Computed" Weight	3,518,858
5% as per M. H. D. 2407.4Z1a	175,943
Steel Forgings (Shs. 63 & 66)	6215
Pay Weight	3,701,016
For Bidding Purposes, Use	3,700,000#
Cast Steel Grade B_2	
Bearings (Sh. 63)	24,024
Expansion Devices (Shs. 51 & 52)	22,490
Total "Computed" Weight	46,514
10% of net dimensions as per	
M. H. D. 2407.4Z1b	4,518
Pay Weight	51,032
For Bidding Purposes Use	51,050#

Miscellaneous

Structural Steel	
Ladders & Manholes (Sh. 46)	3,100
Service Platform (Sh. 47)	1,850
Total "Computed" Weight	4,950
5% as per M. H. D. 2407.4Z1a	248
Pay Weight	5,198
For Bidding Purposes Use	5,200#
Cast Iron Class 25	
Floor Drains (Sh. 38)	11,186
10% of net dimensions as per	
M. H. D. 2407.4Z1b	1,106
Pay Weight	12,292
For Bidding Purposes Use	12,300#

Summary of Grade "A" Concrete

Deck of Span 15 (Sh. 43)		86 cu. yds.
Deck of Spans 16, 17, 21-24 (Sh. 44)	660	
Fill over Backwall of North Abutment (Sh. 44)	2	662
Deck of Spans 18, 19 & 20 (Sh. 45)		643
Splash Slabs (Sh. 39)	1	
4 Lamp Standard Bases on Hyd. Fill	3	4
Total		1415 cu. yds.

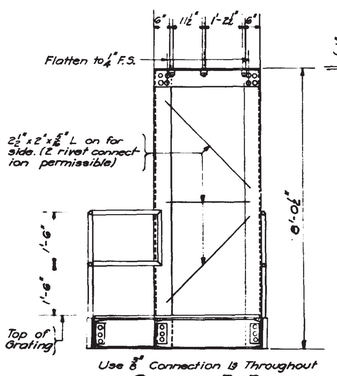

Section B-B

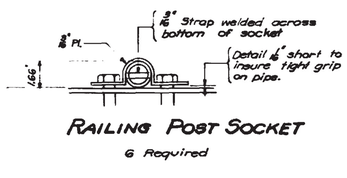

Railing Post Socket

6 Required

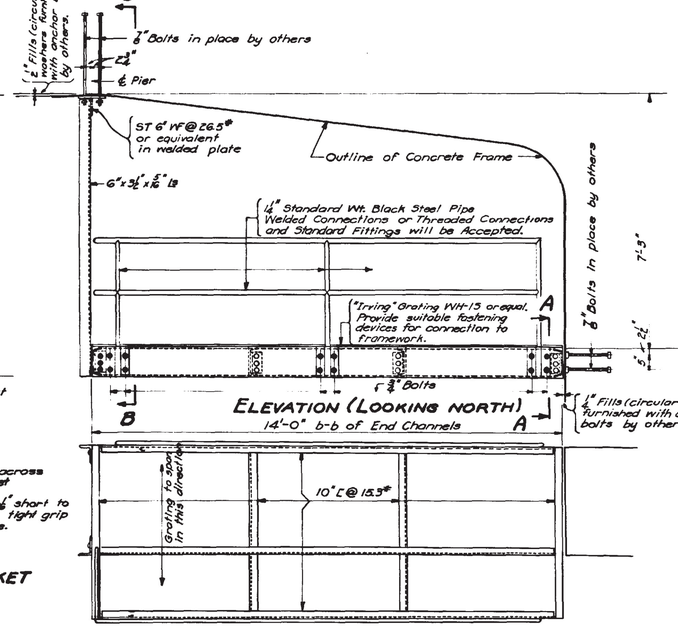

Elevation (Looking North)

Plan

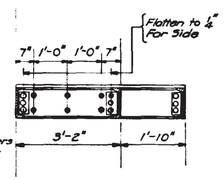

Section A-A

Detail of Service Platform on Pier 14

Included in Schedule III

Note:
All rivets ⅞"ϕ
All holes for ⅞"ϕ rivets and bolts
2 1"ϕ holes for ¾"ϕ bolts
Paint same as other structural steel
Grating included with and paid for at same unit pound price as structural steel.

State Of Minnesota
Department Of Highways

Bridge No. 5900
Mississippi River Crossing At Winona

Miscellaneous Details And Summaries

Approved Nov. 7, 1940.

E. G. Miller
Bridge Engineer

5900

Dr. B.C.R.
Tr. J.A.
Ck. W.H.S.

Inspector:
Inspection Date: 5/2018

Bridge Inspection Report

STRUCTURE TYPE AND MATERIAL

(43) STRUCTURE TYPE, MAIN:		(45) NUMBER OF SPANS IN MAIN UNIT:	3
(A) KIND OF MATERIAL/DESIGN:	4 - Steel continuous	(46) NUMBER OF APPROACH SPANS:	21
(B) TYPE OF DESIGN/CONSTR:	10 - Truss (thru)	(107) DECK STRUCTURE TYPE:	1 - Concrete Cast-in-Place
(44) STRUCTURE TYPE, APPROACH SPANS:		(108) WEARING SURFACE/PROT SYS:	
(A) KIND OF MATERIAL/DESIGN:	3 - Steel	(A) WEARING SURFACE:	1 - Monolithic Concrete
(B) TYPE OF DESIGN/CONSTR:	9 - Truss (deck)	(B) DECK MEMBRANE:	0 - None
		(C) DECK PROTECTION:	1 - Epoxy Coated Reinforcing

AGE OF SERVICE

(27) YEAR BUILT:	1941	(28) LANES:	
(106) YEAR RECONSTRUCTED:	1985	(A) ON BRIDGE:	2
(42) TYPE OF SERVICE:		(B) UNDER BRIDGE:	6
(A) ON BRIDGE:	5 - Highway-pedestrian	(29) AVERAGE DAILY TRAFFIC:	17500
(B) UNDER BRIDGE:	8 - Higway-waterway-railroad	(30) YEAR OF AVERAGE DAILY TRAFFIC:	2004
		(109) AVERAGE DAILY TRUCK TRAFFIC:	10%
		(19) BYPASS DETOUR LENGTH:	65 MI.

GEOMETRIC DATA

(48) LENGTH OF MAX SPAN:	450 FT	(35) STRUCTURE FLARED:	0 - No flare
(49) STRUCTURE LENGTH:	2281 FT	(10) INV RTE, MIN VERT CLEARANCE:	18 FT
(50) CURB/SIDEWALK WIDTHS:		(47) TOT HORIZ CLEARANCE:	9.4 FT
A) LEFT:	4.9 FT	(53) VERT CLEAR OVER BR RDWY:	17.9 FT
B) RIGHT:	4.6 FT	(54) MIN VERTICAL UNDERCLEARANCE:	
(51) BRDG RDWY WIDTH CURB-TO-CURB:	27 FT	A) REFERENCE FEATURE:	H
(52) DECK WIDTH, OUT-TO-OUT:	35.2 FT	B) MIN VERT UNDERCLEAR:	13.9 FT
(32) APPROACH ROADWAY:	9.4 FT.	(55) LATERAL UNDERCLEARANCE RIGHT:	
(33) BRIDGE MEDIAN:	0 - No median	A) REFERENCE FEATURE:	H
(34) SKEW:	0 DEG	B) MIN LATERAL UNDERCLEAR:	8.9 FT
		(56) MIN LATERAL UNDERCLEAR ON LEFT:	0 FT

INSPECTIONS

(90) INSPECTION DATE	6/16	(91) DESIGNATED INSPECTION FREQUENCY:	12
(92) CRITICAL FEATURE INSPECTION:		(93) CRITICAL FEATURE INSPECTION DATE:	
A) FRACTURE CRITICAL REQUIRED/FREQUENCY:	Y24	A) FRACTURE CRTICAL DATE:	6/16
B) UNDERWATER INSPECTION REQUIRED/FREQUENCY:	Y60	B) UNDERWATER INSP DATE:	8/12
C) OTHER SPECIAL INSPECTION REQUIRED/FREQUENCY:	N	C) OTHER SPECIAL INSP DATE:	

CONDITION

(58) DECK:	5 - Fair Condition	(60) SUBSTRUCTURE:	5 - Fair Condition
(59) SUPERSTRUCTURE:	4 - Poor Condition	(61) CHANNEL/CHANNEL PROTECTION:	4 - Bank and embankment protection is severely undermined
		(62) CULVERTS:	N - Not Applicable

CONDITION COMMENTS

(58) DECK: 5 - Fair Condition

Comments:

There are transverse cracks with efflorescence with a 10' to 20' spacing on the underside of the deck.

There are large longitudinal spalls up to 2" deep in spans 17 and 23. The spall in span 17 is about 8' x 5' in area with 1 exposed rebar and the spall in span 23 is 12' x 10' in area with 3 exposed rebars.

(58.01) WEARING SURFACE: 4 - Poor Condition

Comments:

The wearing surface is rough. There are areas of map cracking, spalling, and patching.
Spalling deeper than 2" in spans 15 (1.5'x1') and 16 (1'x1').

(59) SUPERSTRUCTURE: 4 - Poor Condition

Comments:

Crevice corrosion is common at gusset plates and in seams of built-up members in deck trusses, with section loss and distortion in primary members. See attached sheets for thickness measurements.
Section loss has led to crack formation in a few locations. Areas of pitting and minor section loss along the flanges of the truss members.

(60) SUBSTRUCTURE: 5 - Fair Condition

Comments:

There are some cracks and spalls on the piers.

Deteriorated concrete with exposed rebars on Piers 14 and 15. Pier 22 has cracking and spalling with exposed rebar.

(61) CHANNEL/CHANNEL PROTECTION: 4 - Bank and embankment protection is severely undermined

Comments:
Bank and embankment protection is severely undermined. River control devices have severe damage.

(62) CULVERTS: N - Not Applicable

Comments:

CLASSIFICATION

(20) TOLL:	3 - On Free Road	(21) MAINT. RESPONSIBILITY:	1 - State Highway Agency
(22) OWNER:	1 - State Highway Agency	(26) FUNCTION CLASS OF INVENTORY RTE:	14 - Other Principal Arterial
(37) HISTORICAL SIGNIFICANCE:	2 - Eligible for the National Register of Historic Places	(100) STRAHNET HIGHWAY:	0 - Not a STRAHNET route
(101) PARALLEL STRUCTURE:	N - No parallel structure	(102) DIRECTION OF TRAFFIC:	2 - 2-way traffic
(103) TEMPORARY STRUCTURE:	0 - Not applicable	(104) HIGHWAY SYSTEM OF INVENTORY BRIDGE:	1 - Structure/route is on the NHS
(105) FEDERAL LANDS HIGHWAYS:		(110) DESIGNATED NATIONAL NETWORK:	0 - Inventory route not on network
(112) NBIS BRIDGE LENGTH:	Y		

NAVIGATION DATA

(38) NAVIGATION CONTROL:	1 - Navigation control on waterway	(39) NAVIAGATION VERTICAL CLEAR:	63 FT
		(116) MINIMUM NAVIGATION VERT. CLEARANCE, VERT. LIFT BRIDGE:	N/A
(111) PIER OF ABUTMENT PROTECTION:	1 - Navigation protection not required	(40) NAV HORIZONTAL CLEARANCE:	438 FT

Photo 1: Elevation View of Approach Span 16

Photo 2: Bottom Truss Chord (Member L2-L4)

Photo 3: General condition of web plate and channels (looking from L2 to L4)

Photo 4: General condition of exterior face of channels (Channel A)

Photo 5: General condition of batten plates

Photo 6: Crack in web plate near top (similar in a few locations)

Photo 7: Cross Section 1 (129" from L2)

Photo 8: Cross Section 1 (129" from L2)

Photo 9: Channel A at Cross Section 1 (top)

Photo 10: Channel B at Cross Section 1 (top)

Photo 11: Small crack in web plate of Channel B at Cross Section 1

Photo 12: Channel A at Cross Section 1 (bottom)

Photo 13: Cross Section 2 (113" from L4)

Photo 14: Channel A at Cross Section 2 (top)

Photo 15: Channel B at Cross Section 2 (top)

Photo 16: Channel A at Cross Section 2 (bottom)

Photo 17: Channel B at Cross Section 2 (bottom)

Photo 18: Small holes in web plate of Channel B near Cross Section 2

Photo 19: Cross Section 3 (18" from L2)

Photo 20: Cross Section 3 (18" from L2)

Photo 21: Bottom batten plate at Cross Section 3

Photo 22: Web and splice plates on Channel B at Cross Section 3

Inspector:

Inspection Date: 5/2018

Bridge Inspection Report -
METALWORK LOSSES

CROSS SECTION NO.	SPAN/ MEMBER	SIDE	DESCRIPTION
1	16/L2 - L4	A	157" from C/L of L2 - crevice corrosion between channel and web pl. 1-9/16" of distortion at top, 1-1/4" of distortion at bottom Appears to be worst case along the length of the member
1	16/L2 - L4	B	157" from C/L of L2 - crevice corrosion between channel and web pl. 1-7/8" of distortion at top, 0" of distortion at bottom Small crack forming due to section loss at top of web plate Appears to be worst case along the length of the member

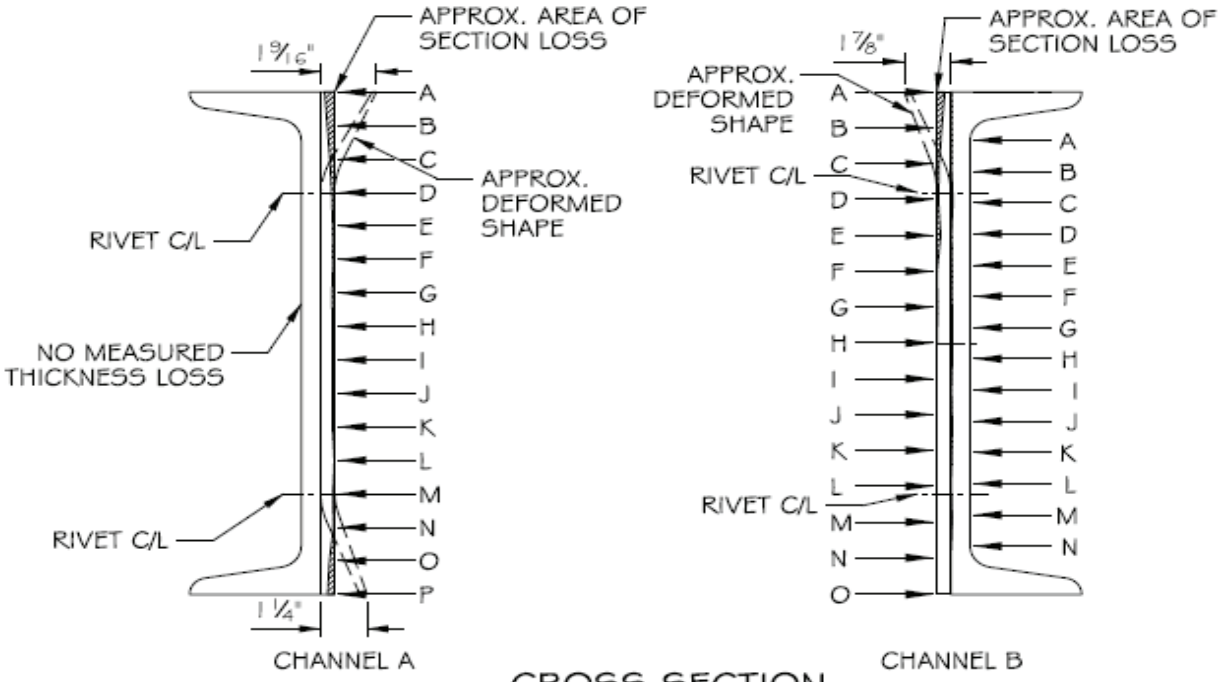

CROSS SECTION (LOOKING FROM L4 TO L2)

NOTES:
1. MEASUREMENTS EQUALLY SPACED.
2. MEASUREMENTS TAKEN 1 29" FROM EDGE OF GUSSET PLATE AT JOINT L2.
3. MEASURED THICKNESS OF WEB PLATE IN AN UNDETERIORATED REGION IS 0.39".

CHANNEL A, WEB PLATE	
LOCATION	MEASUREMENT
A	0.11"
B	0.18"
C	0.25"
D	0.3"
E	0.33"
F	0.34"
G	0.31"
H	0.32"
I	0.32"
J	0.32"
K	0.32
L	0.37"
M	0.33"
N	0.35"
O	0.24"
P	0.19"

CHANNEL B, WEB PLATE	
LOCATION	MEASUREMENT
A	0.16"
B	0.24"
C	0.31"
D	0.33"
E	0.27"
F	0.37"
G	0.35"
H	0.37"
I	
J	
K	
L	
M	
N	
O	

CHANNEL B, CHANNEL	
LOCATION	MEASUREMENT
A	0.5"
B	0.5"
C	0.46"
D	0.5"
E	0.49"
F	0.49"
G	0.47"
H	0.48"
I	0.5"
J	0.48"
K	0.49"
L	0.52"
M	0.49"
N	0.52"

Inspector:

Inspection Date: 5/2018

Bridge Inspection Report -
METALWORK LOSSES

CROSS SECTION NO.	SPAN/ MEMBER	SIDE	DESCRIPTION
2	16/L2 - L4	A	140" from C/L of L4 - crevice corrosion between channel and web pl. 1-1/16" of distortion at top, 15/16" of distortion at bottom Section occurs at rivet holes
2	16/L2 - L4	B	140" from C/L of L4 - crevice corrosion between channel and web pl. 1-5/8" of distortion at top, 3/4" of distortion at bottom Section occurs at rivet holes, small holes in web plate near top edge

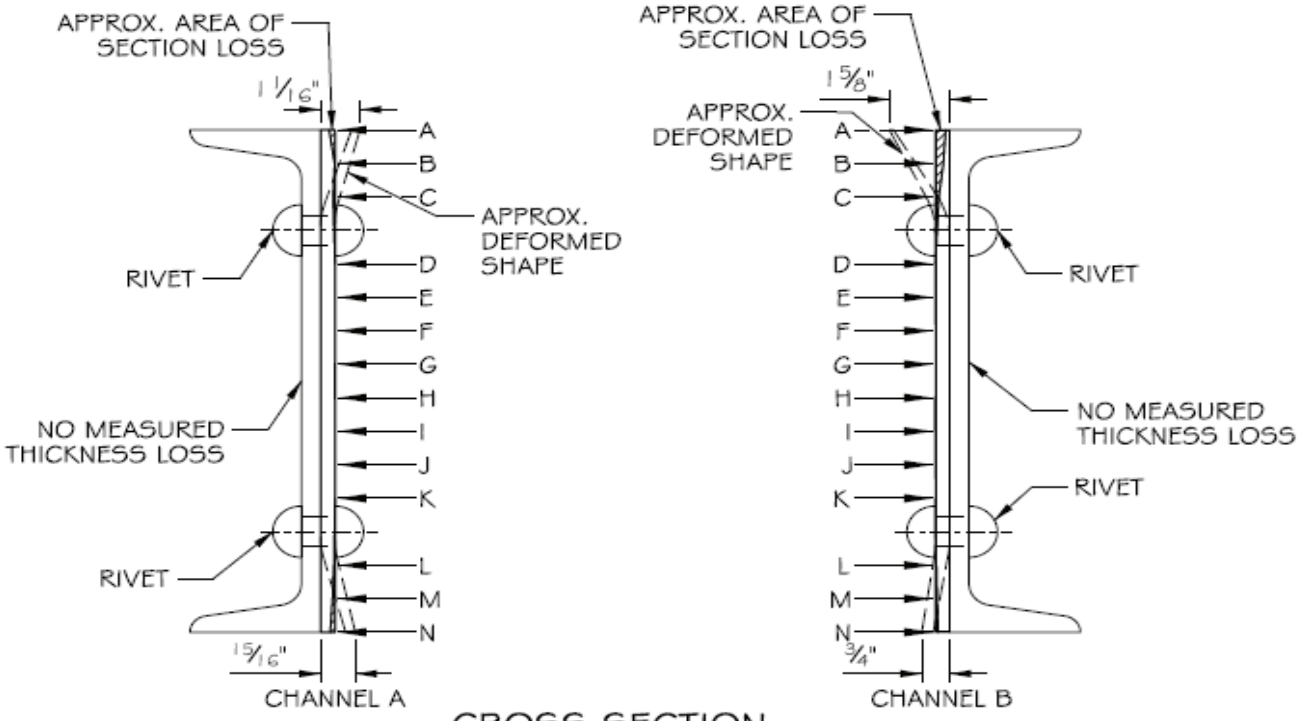

CROSS SECTION (LOOKING FROM L4 TO L2)

NOTES:
1. MEASUREMENTS EQUALLY SPACED.
2. MEASUREMENTS TAKEN 1 1/3" FROM EDGE OF GUSSET PLATE AT JOINT L4.
3. MEASURED THICKNESS OF WEB PLATE IN AN UNDETERIORATED REGION IS 0.39".

CHANNEL A, WEB PLATE	
LOCATION	MEASUREMENT
A	0.23"
B	0.28"
C	0.34"
D	0.39"
E	
F	
G	
H	
I	
J	
K	
L	0.36"
M	0.32"
N	0.26"

CHANNEL B, WEB PLATE	
LOCATION	MEASUREMENT
A	0.11"
B	0.17"
C	0.29"
D	0.39"
E	0.39"
F	0.38"
G	0.39"
H	0.39"
I	0.38"
J	0.38"
K	0.39
L	0.36"
M	0.34"
N	0.31"

Inspector:

Inspection Date: 5/2018

Bridge Inspection Report -
METALWORK LOSSES

CROSS SECTION NO.	SPAN/ MEMBER	SIDE	DESCRIPTION
3	16/L2 - L4	A	45.5" from C/L of L2, at outside edge of L2 joint (before splice plate) Web plate in good condition, minor thickness loss along bottom batten plate
3	16/L2 - L4	B	45.5" from C/L of L2, at outside edge of L2 joint (before splice plate) Near complete loss of top 1.5" of web plate Distortion/thickness loss in top batten plate at edge of Channel B

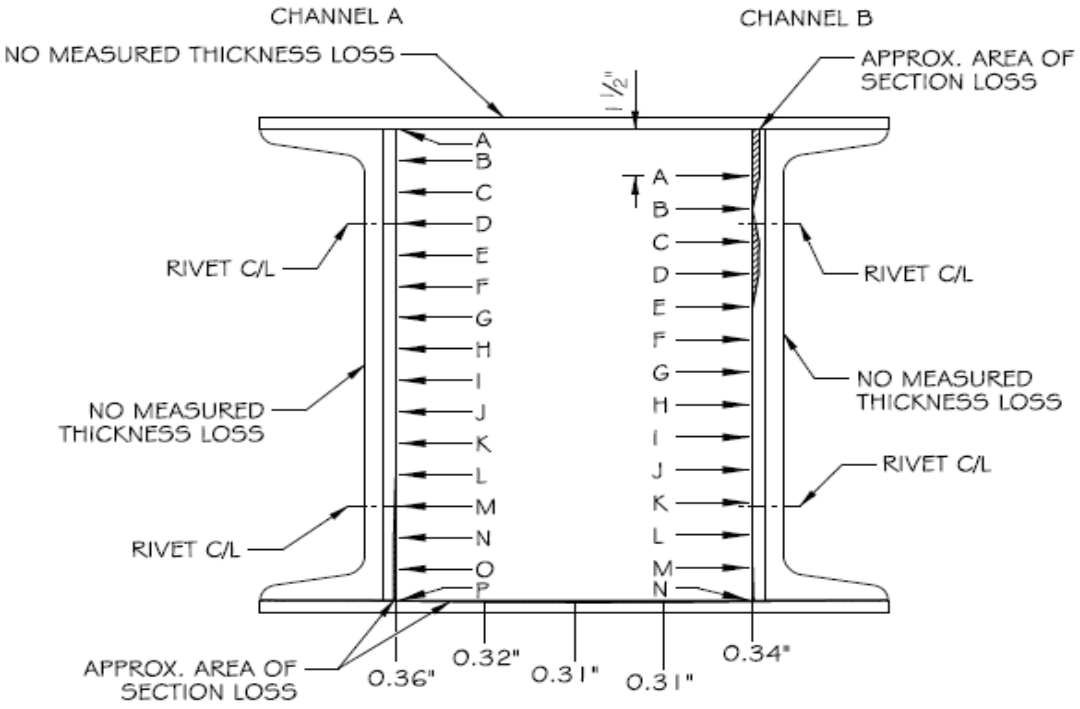

CROSS SECTION
(LOOKING FROM L4 TO L2)

NOTES:
1. MEASUREMENTS EQUALLY SPACED.
2. MEASUREMENTS TAKEN 17.5" FROM EDGE OF GUSSET PLATE AT JOINT L2.
3. MEASURED THICKNESS OF WEB PLATE IN AN UNDETERIORATED REGION IS 0.39".

CHANNEL A, WEB PLATE	
LOCATION	MEASUREMENT
A	0.37"
B	
C	
D	
E	
F	
G	
H	
I	
J	
K	
L	
M	0.34"
N	0.31"
O	
P	

CHANNEL B, WEB PLATE	
LOCATION	MEASUREMENT
A	0.16"
B	0.37"
C	0.18"
D	0.19"
E	0.37"
F	
G	
H	
I	
J	
K	
L	
M	
N	0.34"

Load Rating Round Robin
Load Rater Information

Please complete the following form. All information collected is used for research purposes only.

Name:_____ Date of Load Rating:_____
Employer: _____ Years of Load Rating Experience:_____
Age:_____

1) Please list the references, if any, you consulted while performing this load rating.

2) Please list the computer programs, if any, you used to perform this load rating.

3) Have you previously load rated a steel truss bridge?

Yes No

4) Approximately how long did it take you to complete this load rating? Round to the nearest quarter hour.

5) Is there any additional information regarding the bridge structure that you wish had been provided?

6) Approximately how many bridge load ratings have you completed in the last 12 months? What percentage of these were performed on steel bridges?

7) Approximately what percentage of your work time (on a per week basis) is spent performing bridge load ratings?

8) Please indicate which inspection training courses you have completed and the date of completion (estimates are acceptable for the dates):

Fundamentals of LRFR and Applications of LRFR for Bridge Superstructures (FHWA/NHI): _____
Load and Resistance Factor Rating for Highway Bridges (FHWA/NHI): _____
Load Rating of Steel Truss Bridges (FHWA Webinar): _____
Implementation of the LRFR Method (FHWA Webinar): _____
State Specific Bridge Load Rating Training: _____

Other:

9) Have you received any training specific to evaluating corrosion or section loss in steel members?

Yes No

If yes, please provide a brief description.

10) Are you a registered professional engineer or engineer-in-training?

Yes No

If yes, please indicate your license below.

SE PE (civil) PE (other) FE (civil) FE (other) Other

11) What is the highest level of education that you have completed?

_____ High School degree or equivalent

_____ Trade School Degree

_____ Associate's Degree

_____ Bachelor's Degree in CIVIL ENGINEERING? Or OTHER? (circle one)

_____ Master's Degree in CIVIL ENGINEERING? Or OTHER? (circle one)

_____ PhD in CIVIL ENGINEERING? Or OTHER? (circle one)

12) Do you have experience performing routine or hands-on inspections of steel bridges?

Yes No

If so, how many years of inspection experience do you have?

13) Do you have experience designing steel bridges for new construction?

Yes No

If yes, have you designed a steel truss bridge?

Load Rater:	LEC
Date:	June 2018
Rating Method:	Load and resistance factor

IDENTIFCATION

Structure Type:	Steel deck truss (approach span)
Description:	Two (2) parallel trusses/simple span
Year Built:	1941

GEOMETRY

Span Number:	16 (approach span)	O-to-O Coping:	35'-2"
Span Length:	128'-0"	Clear Roadway:	27'-0"
Truss Spacing:	32'-2"	Skew:	0°

STEEL SUPERSTRUCTURE

Structural Steel:

Steel Fy:	33	ksi	(Actual material properties not known, assumed values based on MBE Table 6A.6.2.1-1 for construction in 1941)
Steel Fu:	66	ksi	

DESIGN LOADS (unfactored)

Dead Load:		
P_{DC}	335	kips
P_{DW}	0	kips
Live Load: Strength I		
P_{LL+IM}	322	kips
Live Load: Fatigue		
P_{LL+IM}	134	kips

STRENGTH I RATING (as-built condition)

Vehicle Configuration:	HL-93	
Member Capacity:	978	kips
Inventory Rating Factor:	0.99	

STRENGTH I RATING (as-inspected condition)

Vehicle Configuration:	HL-93	
Member Capacity:	866	kips
Inventory Rating Factor:	0.79	

FATIGUE ANALSYIS (as-inspected condition)

Vehicle Configuration:	HL-93 (Fatigue Truck)	
Governing Fatigue Category:	D	
Effective Stress Range:	3.6	ksi
Remaining Fatigue Life:	32	years

*If infinite fatigue life remains, indicate such here.

References:
1. AASHTO LRFD Bridge Design Specifications, 7th Edition
2. AASHTO Manual for Bridge Evaluation, 2nd Edition (with 2016 revisions)

Step 1: Determine the net area and the gross area of the member in the as-built and as-inspected conditions (see page 4)

$A_{g\_asbuilt} := 34.65\ in^2$

$A_{n\_asbuilt} := 28.95\ in^2$

$A_{g\_asinspected} := 32.5\ in^2$ (at cross section 1)

$A_{n\_asinspected} := 27.91\ in^2$ (at cross section 3)

Step 2: Detemine member capacity considering yielding on the gross section (AASHTO LRFD BDS 6.8.2.1)

$$P_{n\_yield} = \phi_y \cdot A_g \cdot F_y$$

$\phi_y := 0.95$ (AASHTO LRFD BDS Section 6.5.4.2)
$F_y := 33\ ksi$ (Assumed yield strength based on AASHTO MBE Table 6A.6.2.1-1)

As-built condition:

$P_{n\_yield\_asbuilt} := \phi_y \cdot A_{g\_asbuilt} \cdot F_y = 1086.28\ kip$

As-inspected condition:

$P_{n\_yield\_asinspected} := \phi_y \cdot A_{g\_asinspected} \cdot F_y = 1018.88\ kip$

Step 3: Determine member capacity considering fracture on the net section (AASHTO LRFD BDS 6.8.2.1)

$$P_{n\_fracture} = \phi_u \cdot A_n \cdot U \cdot Rp \cdot F_u$$

$\phi_u := 0.8$ (AASHTO LRFD BDS Section 6.5.4.2)
$U := 1$ (not end connected)
$R_p := 1$ (holes were reamed per note on Sheet 33 of the construction plans)
$F_u := 66\ ksi$ (assumed ultimate strength based on AASHTO MBE Table 6A.6.2.1-1)

As-built condition:

$P_{n\_fracture\_asbuilt} := \phi_u \cdot A_{n\_asbuilt} \cdot U \cdot R_p \cdot F_u = 1528.56\ kip$

As-inspected condition:

$P_{n\_fracture\_asinspected} := \phi_u \cdot A_{n\_asinspected} \cdot U \cdot R_p \cdot F_u = 1473.65\ kip$

Step 4: Determine inventory load rating factor for Strength I limit state (AASHTO MBE 6A.4.2)

$$RF = \frac{Capacity - (\gamma_{DC})\ (DC) - (\gamma_{DW})\ (DW)}{(\gamma_{LL})\ (LL + IM)}$$

Dead Load:	$DC := 335\ kip$	$\gamma_{DC} := 1.25$	(AASHTO MBE Table 6A.4.2.2-1)
Wearing Surface:	$DW := 0\ kip$	$\gamma_{DW} := 1.5$	
Live Load (incl. impact):	$LL := 322\ kip$	$\gamma_{LL} := 1.75$	

$$Capacity = \phi_c \cdot \phi_s \cdot \phi \cdot R_n \qquad \text{(AASHTO MBE Eq. 6A.4.2.1-2)}$$

$\phi_c := 0.85$ (Poor condition, AASHTO MBE Section 6A.4.2.3)
$\phi_s := 0.9$ (Riveted members in two girder truss bridge, AASHTO MBE Section 6A.4.2.4)

Note: $\phi_c \cdot \phi_s > 0.85$ per Section AASHTO MBE Section 6A.4.2.1-3, therefore $\phi_c \phi_s := 0.85$

$C_{asbuilt} := \phi_s \cdot min\left(P_{n\_yield\_asbuilt}, P_{n\_fracture\_asbuilt}\right) = \boxed{977.65\ kip}$ (Note, condition factor not included in as-built rating)

$C_{asinspected} := \phi_c \phi_s \cdot min\left(P_{n\_yield\_asinspected}, P_{n\_fracture\_asinspected}\right) = \boxed{866.04\ kip}$

Note: yielding on the gross section governs in both cases

As-built condition:

$$RF_{asbuilt} := \frac{C_{asbuilt} - (\gamma_{DC})\ (DC) - (\gamma_{DW})\ (DW)}{(\gamma_{LL})\ (LL)} = \boxed{0.99}$$

As-inspected condition:

$$RF_{asinspected} := \frac{C_{asinspected} - (\gamma_{DC})\ (DC) - (\gamma_{DW})\ (DW)}{(\gamma_{LL}) \cdot (LL)} = \boxed{0.79}$$

Step 5: Estimate effective stress range for determing fatigue life (AASHTO MBE 7.2.2, 2015 revision)

$$\Delta f_{eff} = R_p \cdot R_s \cdot \Delta f$$

Live load from fatigue truck (incl. impact):	$LL_{fatigue} := 134\ kip$	$\gamma_{fatigueI} := 1.5$ $\gamma_{fatigueII} := 0.75$	(AASHTO LRFD BDS Table 3.4.1-1)
Span length:	$L := 128\ ft$		
Number of lanes:	$n_L := 2$		
Single lane average daily truck traffic:	$ADTT_{SL} := 1500$		
Structure age:	$age := 2018 - 1941 = 77$		

Note: the load factors have been increased to 1.75 and 0.8 in the 8th edition of the specifications

$R_p := 0.988 + 6.87\ 10^{-5} \cdot \left(\frac{L}{ft}\right) + 4.01 \cdot 10^{-6} \cdot \left(ADTT_{SL}\right) + \frac{0.0107}{n_L}$

$R_p = 1.01$ (Multiple presense factor, AASHTO MBE Eq. 7.2.2.1-1)

$R_s := 1.0$ (Stress-range estimate partial load factor, AASHTO MBE Section 7.2.2.1.1)

$\Delta f := \frac{LL_{fatigue}}{A_{n\_asinspected}} \cdot \gamma_{fatigueII} = 3.6\ \frac{kip}{in^2}$ (factored caculated stress range for Fatigue II load combination)

$\Delta f_{eff} := R_p \cdot R_s \cdot \Delta f = \boxed{3.63\ \frac{kip}{in^2}}$

Note: with updated load factors, effective stress range is = 3.87 ksi

Step 6: Determine remaining fatigue life

$\Delta F_{TH} := 7\ ksi$ (Constant amplitude fatigue threshold for Fatigue Category D, AASHTO LRFD BDS Table 6.6.1.2.5-3 - reasonable due to deteriorated condition)

- Infitinite Life Check (AASHTO MBE 7.2.4, 2015 revisions)

$\Delta f_{max} := \frac{\gamma_{fatigueI}}{\gamma_{fatigueII}} \cdot \Delta f \cdot R_p = 7.26\ \frac{kip}{in^2}$

Since $\Delta f_{max} > \Delta F_{TH}$, finite fatigue life remains

- Finite Life Check (AASHTO MBE 7.2.5, 2015 revisions)

$$Years_{remaining} = \frac{N_{available} - N_{used}}{365 \cdot n \cdot ADTT_{SL}}$$

$A := 22 \cdot 10^8\ ksi^3$ (Detail category constant, AASHTO LRFD BDS Table 6.6.1.2.5-1)
$n := 1$ (Cycles per truck passage, AASHTO LRFD BDS Table 6.6.1.2.5-2)
$R_R := 1.3$ (Resistance factor for evaluation, AASHTO MBE Table 7.2.5.1-1 for Category D Evaluation 1 Life)

$N_{available} := \frac{R_R \cdot A}{\left(\Delta f_{eff}\right)^3} = 59780670$ (AASHTO MBE Eq. 7.2.5.1-1)

$N_{used} := 365 \cdot n \cdot ADTT_{SL} \cdot age = 42157500$

$N_{remaining} := N_{available} - N_{used} = 17623170.23$

$Y_{remaining} := \frac{N_{remaining}}{365 \cdot n \cdot ADTT_{SL}} = \boxed{32.19}$ (AASHTO MBE Eq. 7.2.5.1-1)

Note: with updated load factors, remaining life is 13 years

ELEMENT	GROSS AREA (SQ. IN.)	NET AREA (SQ. IN.)
CHANNEL A, WEB PLATE	5.63	4.92
CHANNEL A, CHANNEL	11.7	9.55
CHANNEL B, WEB PLATE	5.63	4.92
CHANNEL B, CHANNEL	11.7	9.55
TOTAL	34.65	28.95

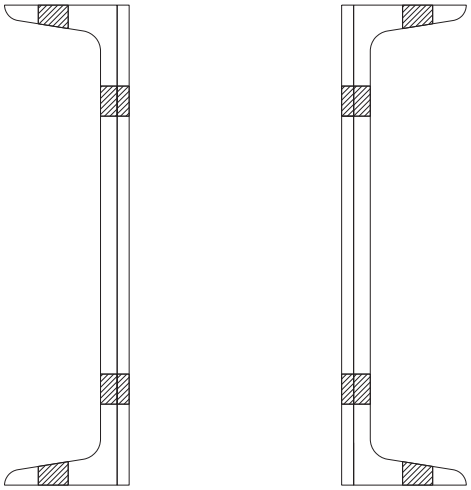

AS-BUILT

ELEMENT	GROSS AREA (SQ. IN.)	NET AREA (SQ. IN.)
CHANNEL A, WEB PLATE	4.43	3.84
CHANNEL A, CHANNEL	11.7	10.73
CHANNEL B, WEB PLATE	5.06	4.41
CHANNEL B, CHANNEL	11.31	10.39
TOTAL	32.5	29.36
% LOSS	6.2%	6.1%

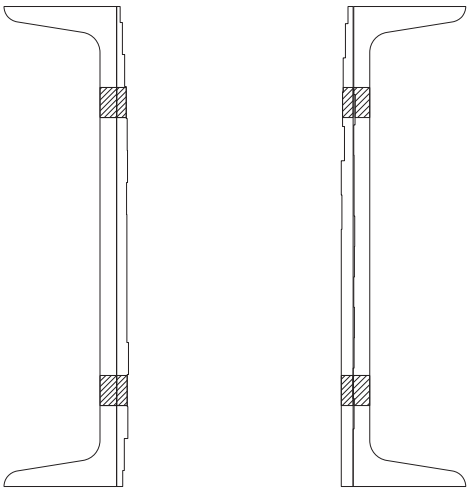

AS-INSPECTED (CROSS SECTION 1)

ELEMENT	GROSS AREA (SQ. IN.)	NET AREA (SQ. IN.)
CHANNEL A, WEB PLATE	5.41	4.71
CHANNEL A, CHANNEL	11.7	10.73
CHANNEL B, WEB PLATE	5.18	4.50
CHANNEL B, CHANNEL	11.7	10.73
TOTAL	33.98	30.67
% LOSS	1.9%	2.0%

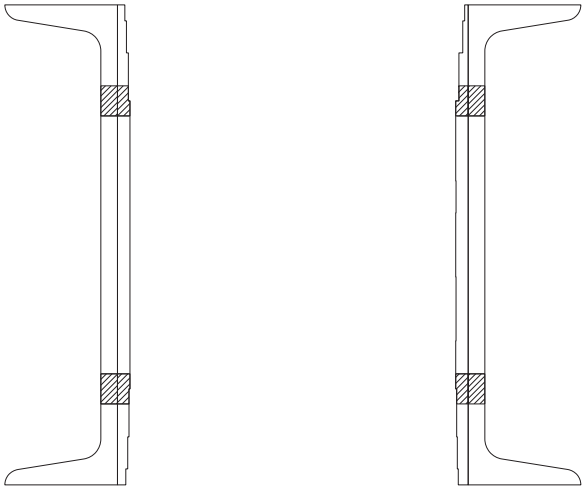

AS-INSPECTED (CROSS SECTION 2)

ELEMENT	GROSS AREA (SQ. IN.)	NET AREA (SQ. IN.)
CHANNEL A, WEB PLATE	5.37	4.70
CHANNEL A, CHANNEL	11.7	9.55
CHANNEL B, WEB PLATE	4.73	4.11
CHANNEL B, CHANNEL	11.7	9.55
TOTAL	33.5	27.91
% LOSS	3.3%	3.6%

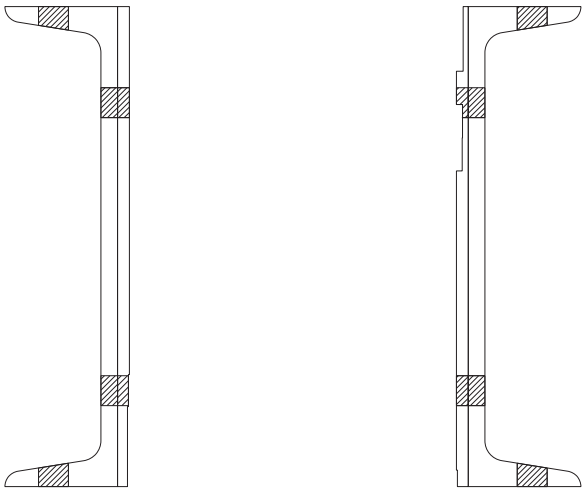

AS-INSPECTED (CROSS SECTION 3)

As-Built Web Plate			
Label	Depth (in)	Thickness (in)	Area (in^2)
Plate	15	0.375	5.625
Hole	0.9375	0.375	0.351563

Gross Area	**5.625**	in^2
Net Area (2 holes)	**4.922**	in^2

As-Built Web Channel			
Label	Depth (in)	Thickness (in)	Area (in^2)
Channel	-	-	11.7
Web Hole	0.9375	0.52	0.4875
Flange Hole	0.9375	0.625	0.585938

Gross Area	**11.7**	in^2
Net Area (2 web, 2 flange)	**9.553**	in^2
Net Area (2 web, 0 flange)	**10.725**	in^2

Web Plate A1				
Label	Distance along member (in.)	Thickness Measurement (in.)	Increment (in.)	Area (in^2)
A	0	0.11	0.5	0.055
B	1	0.18	1	0.18
C	2	0.25	1	0.25
D	3	0.3	1	0.3
E	4	0.33	1	0.33
F	5	0.34	1	0.34
G	6	0.31	1	0.31
H	7	0.32	1	0.32
I	8	0.32	1	0.32
J	9	0.32	1	0.32
K	10	0.32	1	0.32
L	11	0.37	1	0.37
M	12	0.33	1	0.33
N	13	0.35	1	0.35
O	14	0.24	1	0.24
P	15	0.19	0.5	0.095

Gross Area	**4.43** in^2
Area of Hole 1 (Measured in Auto Cad)	0.281 in^2
Area of Hole 2 (Measured in Auto Cad)	0.309 in^2
New Area	**3.839** in^2

Web Plate B1				
Label	Distance along member (in.)	Thickness Measurement (in.)	Increment (in.)	Area (in^2)
A	0	0.16	0.54	0.085714
B	1.07	0.24	1.07	0.257143
C	2.14	0.31	1.07	0.332143
D	3.21	0.33	1.07	0.353571
E	4.29	0.27	1.07	0.289286
F	5.36	0.37	1.07	0.396429
G	6.43	0.35	1.07	0.375
H	7.50	0.37	1.07	0.396429
I	8.57	0.37	1.07	0.396429
J	9.64	0.37	1.07	0.396429
K	10.71	0.37	1.07	0.396429
L	11.79	0.37	1.07	0.396429
M	12.86	0.37	1.07	0.396429
N	13.93	0.37	1.07	0.396429
O	15.00	0.37	0.54	0.198214

Gross Area	**5.063** in^2
Area of Hole 1 (Measured in Auto Cad)	0.306 in^2
Area of Hole 2 (Measured in Auto Cad)	0.347 in^2
New Area	**4.409** in^2

Channel A1			
Distance along member (in.)	Thickness Measurement (in.)	Increment (in.)	Area (in^2)
NO THICKNESS LOSS			

Gross Area	**11.7** in^2
Area of Web Holes	0.488 in^2
Area of Flange Holes	0 in^2
Net Area	**10.725** in^2

Channel B1					
Label	Distance along member (in.)	Thickness Measurement (in.)	Increment (in.)	Lost Material	Area Lost (in^2)
A	0	0.5	0.662	0.02	0.013
B	1.324	0.5	1.137	0.02	0.023
C	2.274	0.5	0.950	0.02	0.019
D	3.224	0.46	0.950	0.06	0.057
E	4.174	0.5	0.950	0.02	0.019
F	5.124	0.49	0.950	0.03	0.029
G	6.075	0.49	0.950	0.03	0.029
H	7.025	0.47	0.950	0.05	0.048
I	7.975	0.48	0.950	0.04	0.038
J	8.925	0.5	0.950	0.02	0.019
K	9.876	0.48	0.950	0.04	0.038
L	10.826	0.49	0.950	0.03	0.029
M	11.776	0.52	0.950	0	0.000
N	12.726	0.49	0.950	0.03	0.029
O	13.677	0.52	0.475	0	0.000

Total Area Lost	0.388 in^2

Gross Area	**11.312** in^2
Area of Hole 1 (Measured in Auto Cad)	0.44 in^2
Area of Hole 2 (Measured in Auto Cad)	0.481 in^2
Net Area	**10.391** in^2

Web Plate A2				
Label	Distance along member (in.)	Thickness Measurement (in.)	Increment (in.)	Area (in^2)
A	0	0.23	0.5	0.115
B	1	0.28	1	0.28
C	2	0.34	1.5	0.51
D	4	0.39	1.50	0.585
E	5	0.39	1.00	0.39
F	6	0.39	1.00	0.39
G	7	0.39	1.00	0.39
H	8	0.39	1.00	0.39
I	9	0.39	1.00	0.39
J	10	0.39	1.00	0.39
K	11	0.39	1.50	0.585
L	13	0.36	1.5	0.54
M	14	0.32	1	0.32
N	15	0.26	0.5	0.13

Gross Area	**5.405** in^2
Area of Hole 1 (Measured in Auto Cad)	0.342 in^2
Area of Hole 2 (Measured in Auto Cad)	0.352 in^2
Net Area	**4.711** in^2

Channel A2			
Distance along member (in.)	Thickness Measurement (in.)	Increment (in.)	Area (in^2)
NO THICKNESS LOSS			

Gross Area	**11.7** in^2
Area of Web Holes	0.488 in^2
Area of Flange Holes	0 in^2
Net Area	**10.725** in^2

Web Plate B2				
Label	Distance along member (in.)	Thickness Measurement (in.)	Increment (in.)	Area (in^2)
A	0	0.11	0.5	0.055
B	1	0.17	1	0.17
C	2	0.29	1.5	0.435
D	4	0.39	1.50	0.585
E	5	0.39	1.00	0.39
F	6	0.38	1.00	0.38
G	7	0.39	1.00	0.39
H	8	0.39	1.00	0.39
I	9	0.38	1.00	0.38
J	10	0.38	1.00	0.38
K	11	0.39	1.50	0.585
L	13	0.36	1.5	0.54
M	14	0.34	1	0.34
N	15	0.31	0.5	0.155

Gross Area	**5.175** in^2
Area of Hole 1 (Measured in Auto Cad)	0.319 in^2
Area of Hole 2 (Measured in Auto Cad)	0.352 in^2
Net Area	**4.505** in^2

Channel B2			
Distance along member (in.)	Thickness Measurement (in.)	Increment (in.)	Area (in^2)
NO THICKNESS LOSS			

Gross Area	**11.7** in^2
Area of Web Holes	0.488 in^2
Area of Flange Holes	0 in^2
Net Area	**10.725** in^2

Web Plate A3				
Label	Distance along member (in.)	Thickness Measurement (in.)	Increment (in.)	Area (in^2)
A	0	0.37	0.5	0.185
B	1	0.37	1	0.37
C	2	0.37	1	0.37
D	3	0.37	1	0.37
E	4	0.37	1	0.37
F	5	0.37	1	0.37
G	6	0.37	1	0.37
H	7	0.37	1	0.37
I	8	0.37	1	0.37
J	9	0.37	1	0.37
K	10	0.37	1	0.37
L	11	0.37	1	0.37
M	12	0.34	1	0.34
N	13	0.31	1	0.31
O	14	0.31	1	0.31
P	15	0.31	0.5	0.155

Gross Area	**5.37** in^2
Area of Hole 1 (Measured in Auto Cad)	0.347 in^2
Area of Hole 2 (Measured in Auto Cad)	0.319 in^2
Net Area	**4.704** in^2

Web Plate B3				
Label	Distance along member (in.)	Thickness Measurement (in.)	Increment (in.)	Area (in^2)
A	1.5	0.16	2.02	0.32
B	2.54	0.37	1.04	0.38
C	3.58	0.18	1.04	0.19
D	4.62	0.19	1.04	0.20
E	5.65	0.37	1.04	0.38
F	6.69	0.37	1.04	0.38
G	7.73	0.37	1.04	0.38
H	8.77	0.37	1.04	0.38
I	9.81	0.37	1.04	0.38
J	10.85	0.37	1.04	0.38
K	11.88	0.37	1.04	0.38
L	12.92	0.37	1.04	0.38
M	13.96	0.37	1.04	0.38
N	15.00	0.34	0.52	0.18

Gross Area	**4.726** in^2
Area of Hole 1 (Measured in Auto Cad)	0.269 in^2
Area of Hole 2 (Measured in Auto Cad)	0.347 in^2
Net Area	**4.110** in^2

Channel A3			
Distance along member (in.)	Thickness Measurement (in.)	Increment (in.)	Area (in^2)
NO THICKNESS LOSS			

Gross Area	**11.7** in^2
Area of Web Holes	0.488 in^2
Area of Flange Holes	0.586 in^2
Net Area	**9.553** in^2

Channel B3			
Distance along member (in.)	Thickness Measurement (in.)	Increment (in.)	Area (in^2)
NO THICKNESS LOSS			

Gross Area	**11.7** in^2
Area of Web Holes	0.488 in^2
Area of Flange Holes	0.586 in^2
Net Area	**9.553** in^2

Dead Load Analysis:

- Determine dead load effects and compare to original design plans
- No wearing surface

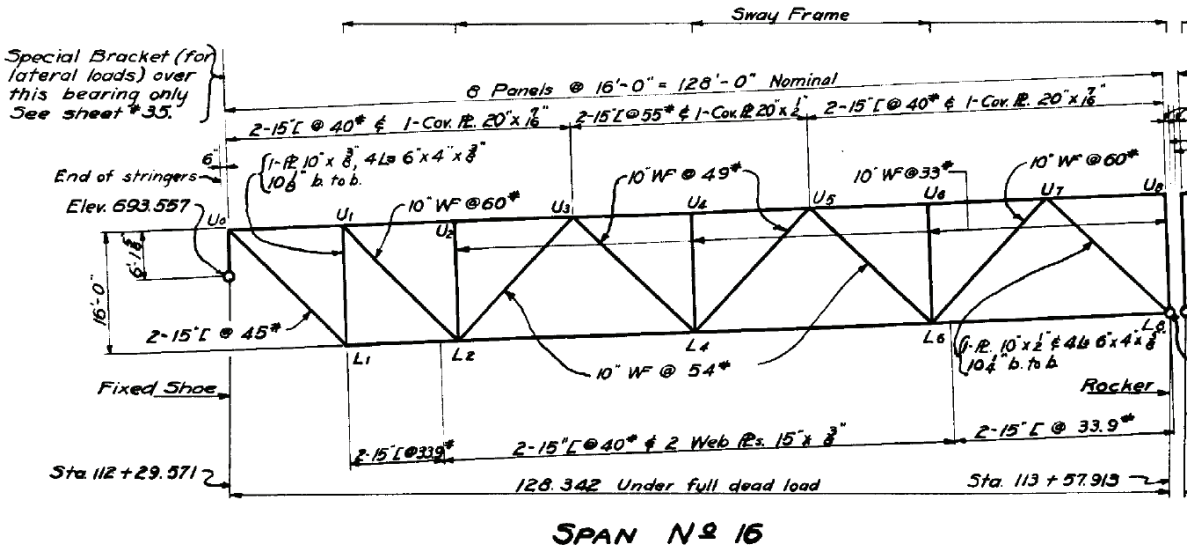

SPAN Nº 16

Joint Loads (see attached spreadsheet):

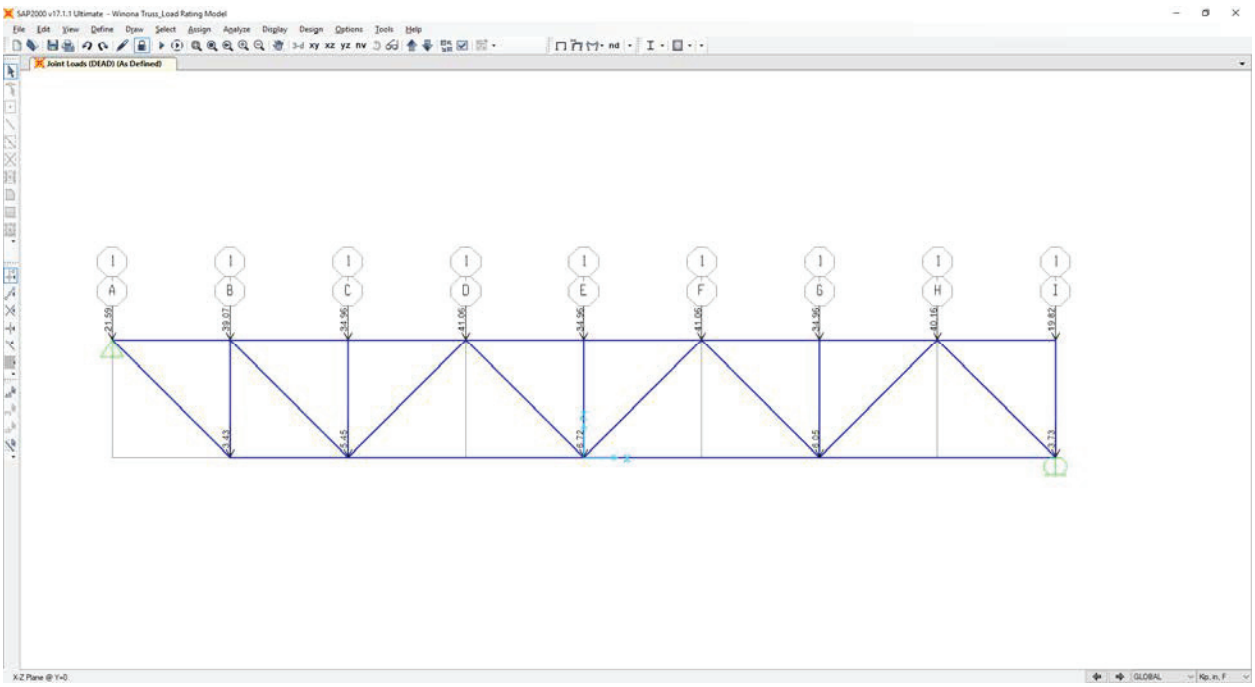

Distributed Load (see attached spreadsheet):

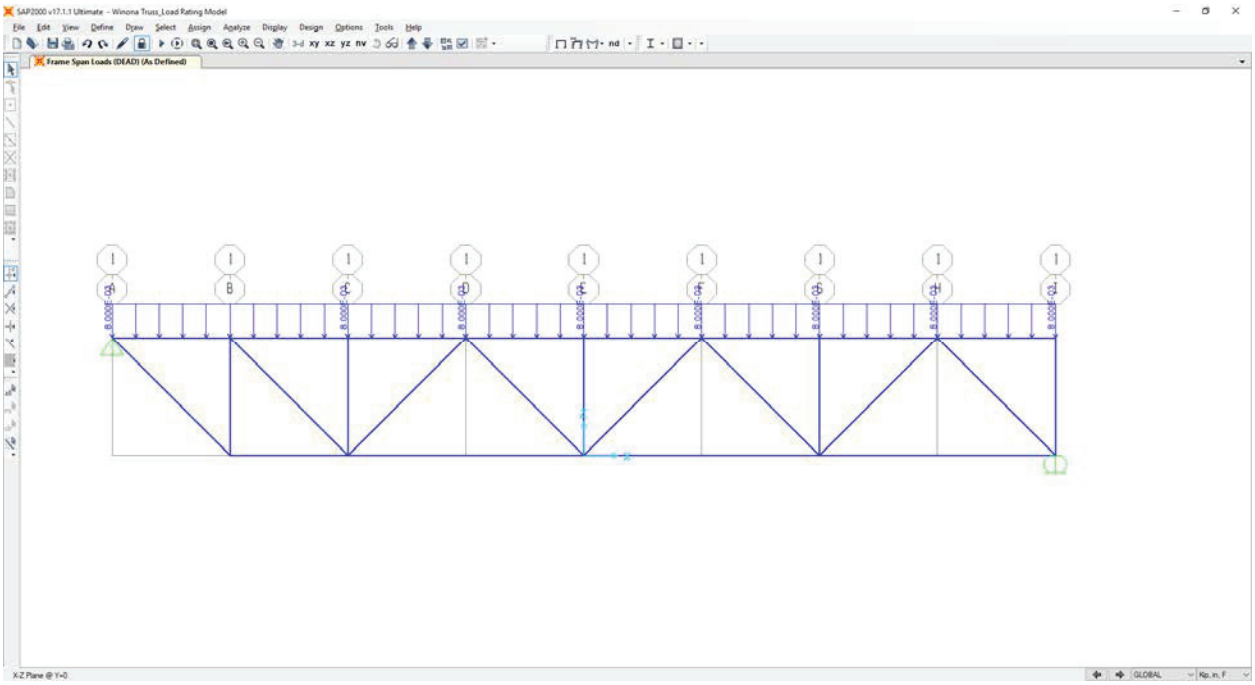

Member Forces:

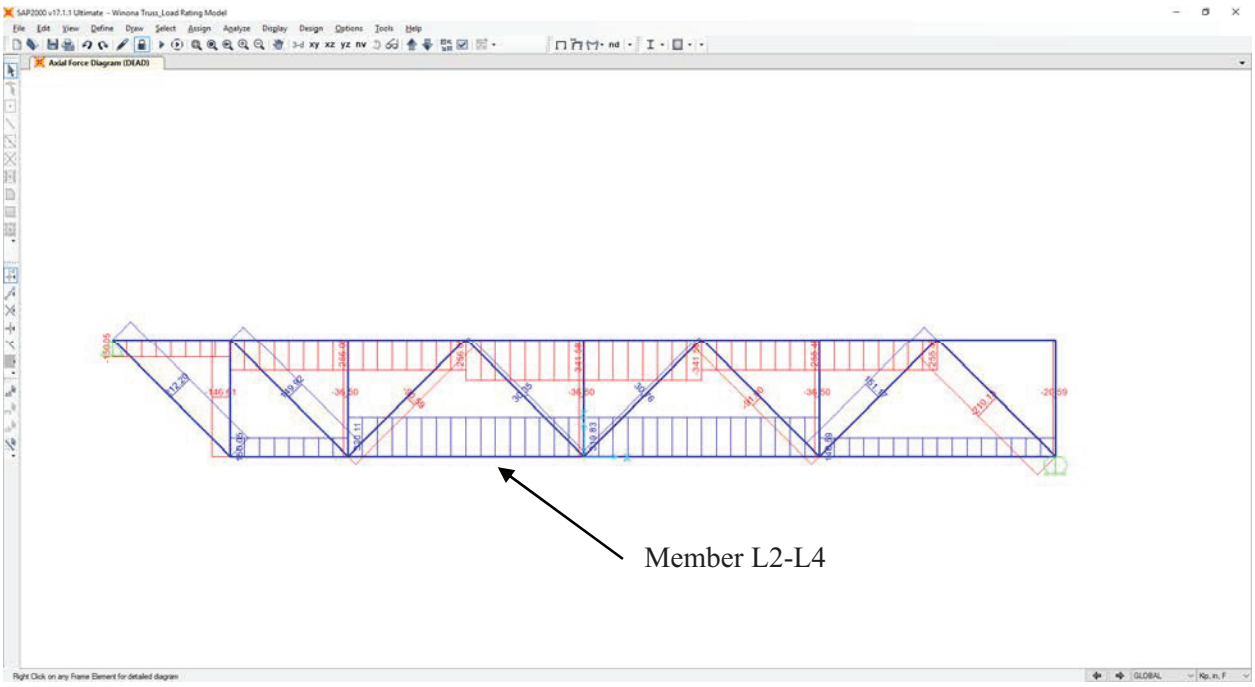

Summary of Member Forces (+ Tension, - Compression)		
Member	SAP2000 (kips)	Original Plans (kips)
U0U1	-150.05	-156.45
U1U3	-256.05	-268.2
U3U5	-341.58	-357.6
U5U7	-255.45	-268.2
U7U8	0	0
L1L2	150.05	156.45
L2L4	**320.11**	**335.25**
L4L6	319.85	335.25
L6L8	148.59	156.45
U0L1	212.5	221.25
U1L1	-146.61	-156.45
U1L2	149.92	158.03
U2L2	-36.5	-44.7
U3L2	-90.59	-94.82
U3L4	30.35	31.61
U4L4	-36.5	-44.7
L4U5	30.76	31.61
U5L6	-91	-94.82
U6L6	-36.5	-44.7
L6U7	151.17	158.03
U7L8	-210.13	-221.25
U8L8	-20.59	-22.55

Dead Load Force Effects (DC = Component, DW = Wearing Surface)

P_{DC} = 335 kips (NOTE: DEAD LOAD FROM ORIGINAL CONSTRUCTION PLANS GOVERNS)

P_{DW} = 0 kips

Dead Load - Determine joint and uniform load

Primary Truss Members

Unit Weight of Steel **490** pcf

Member	Gross Area (in^2)	Adjusting Coeff*	Adjusted Area (in^2)	Weight (klf)	Length (ft.)	Quantity	Self Weight (kips)
L1L2	9.96	1.1	10.956	0.037	16	2	1.19
L2L4	11.8	1.1	12.98	0.044	32	2	2.83
	5.625	1.1	6.1875	0.021	32	2	1.35
L4L6	11.8	1.1	12.98	0.044	32	2	2.83
	5.625	1.1	6.1875	0.021	32	2	1.35
L6L8	9.96	1.1	10.956	0.037	32	2	2.39
U0U1	11.8	1.1	12.98	0.044	16	2	1.41
	8.75	1.05	9.1875	0.031	16	1	0.50
U1U3	11.8	1.1	12.98	0.044	32	2	2.83
	8.75	1.05	9.1875	0.031	32	1	1.00
U3U5	16.11	1.1	17.721	0.060	32	2	3.86
	10	1.05	10.5	0.036	32	1	1.14
U5U7	11.8	1.1	12.98	0.044	32	2	2.83
	8.75	1.05	9.1875	0.031	32	1	1.00
U7U8	11.8	1.1	12.98	0.044	16	2	1.41
	8.75	1.05	9.1875	0.031	16	1	0.50
U0L1	13.17	1.1	14.487	0.049	22.627417	2	2.23
U1L2	17.6	1.05	18.48	0.063	22.627417	1	1.42
L2U3	15.8	1.05	16.59	0.056	22.627417	1	1.28
U3L4	14.4	1.05	15.12	0.051	22.627417	1	1.16
L4U5	14.4	1.05	15.12	0.051	22.627417	1	1.16
U5L6	15.8	1.05	16.59	0.056	22.627417	1	1.28
L6U7	17.6	1.05	18.48	0.063	22.627417	1	1.42
U7L8	5	1.05	5.25	0.018	22.627417	1	0.40
	5.86	1.05	6.153	0.021	22.627417	4	1.90
U1L1	3.75	1.05	3.9375	0.013	17.25	1	0.23
	3.61	1.05	3.7905	0.013	17.25	4	0.89
U2L2	9.71	1.05	10.1955	0.035	17.25	1	0.60
U4L4	9.71	1.05	10.1955	0.035	17.25	1	0.60
U6L6	9.71	1.05	10.1955	0.035	17.25	1	0.60
U8L8	9.71	1.05	10.1955	0.035	17.25	1	0.60
End Post	17.6	1.1	19.36	0.066	7.1667	1	0.47

*Adjusting coefficient used to account for rivets, batten plates, splice plates, etc.

TOTAL 44.66 kips

Member	Area (in^2)*	Thickness (in)	Gross Volume (in^3)	Adjusting Coeff**	Adjusted Volume (in^3)	Quantity	Self Weight (kips)
L1 Gusset Plate	1130	0.4375	494.375	1.05	519.09375	2	0.29
L2 Gusset Plate	1128	0.375	423	1.05	444.15	2	0.25
L4 Gusset Plate	957	0.375	358.875	1.05	376.81875	2	0.21
L6 Gusset Plate	1128	0.375	423	1.05	444.15	2	0.25
L8 Gusset Plate	950	0.375	356.25	1.1	391.875	2	0.22
U0 Gusset Plate	2059	0.375	772.125	1.1	849.3375	2	0.48
U1 Gusset Plate	1130	0.4375	494.375	1.05	519.09375	2	0.29
U3 Gusset Plate	2736	0.375	1026	1.05	1077.3	2	0.61
	17.6	36	633.6	1.05	665.28	1	0.19
U5 Gusset Plate	2736	0.375	1026	1.05	1077.3	2	0.61
	17.6	36	633.6	1.05	665.28	1	0.19
U7 Gusset Plate	2736	0.375	1026	1.05	1077.3	2	0.61
	17.6	36	633.6	1.05	665.28	1	0.19
						TOTAL	4.41

*Area estimated based on joint geometry; gusset plate dimensions not provided on the plans

**Adjusting coefficient used to account for stiffening elements, rivets, fill plates, etc.

Sway Frames - Full Depth

Unit Weight of Steel **490** pcf

Member	Gross Area (in^2)	Adjusting Coeff	Adjusted Area (in^2)	Weight (klf)	Length (ft.)	Quantity	Self Weight (kips)
Horizontal Member	9.54	1.05	10.017	0.034	31.33333333	1	1.07
Diagonal Member	5	1.05	5.25	0.018	16.65	2	0.59

Member	Length (in)*	Width (in)*	Thickness	Gross Volume (in^3)	Adjusting Coeff	Adjusted Volume (in^3)	Quantity	Self Weight (kips)
Stiffener Plates	5.455	5.805	0.375	5.937426563	1.05	6.234297891	8	0.01
Edge Gusset Plate	15	12	0.3125	56.25	1.05	59.0625	2	0.03
Center Gusset Plate	20.5	12	0.3125	76.875	1.05	80.71875	1	0.02
						TOTAL (per truss)		4.33

*Area estimated based on joint geometry; gusset plate dimensions not provided on the plans

Total Per Frame	1.73	kips

Lateral Bracing

Unit Weight of Steel **490** pcf

Member	Gross Area (in^2)	Adjusting Coeff	Adjusted Area (in^2)	Weight (klf)	Length (ft.)	Quantity	Self Weight (kips)
Diagonal Member	2.32	1	2.32	0.008	45.25	1	0.36

Member	Length (in)*	Width (in)*	Thickness	Gross Volume (in^3)	Adjusting Coeff	Adjusted Volume (in^3)	Quantity	Self Weight (kips)
Center Plate (at U1, U3, U5, U7)	28	28	0.3125	245	1.05	257.25	1	0.07
Edge Plate (U2, U4, U6)	28	26	0.3125	227.5	1.05	238.875	1	0.07
Edge Plate (U0, U8)	20	14	0.3125	87.5	1.05	91.875	1	0.03
*Dimensions estimated based on joint geometry; plate dimensions not provided on the plans							TOTAL (per truss)	1.83

Floor System

Unit Weight of Steel	**490**	pcf
Unit Weight of Concrete	**150**	pcf

Member	Gross Area (in^2)	Adjusting Coeff	Adjusted Area (in^2)	Weight (klf)	Length (ft.)	Quantity	Self Weight (kips)
Floorbeam	44.2	1.05	46.41	0.158	31.33333333	1	4.948251389
Stringer	10.6	1.05	11.13	0.038	16	3	1.8179
Deck	3442.5	1.05	3614.625	3.765234375	16	1	60.24375
						TOTAL (steel per truss)	36.81033125
						TOTAL (concrete per truss)	240.975

Railing and Misc. Utilities

Unit Weight of Steel	**490**	pcf
Uniform Weight of Utilitites	**3**	psf

Member	Gross Area (in^2)	Adjusting Coeff	Adjusted Area (in^2)	Weight (klf)	Length (ft.)	Quantity	Weight (kips)
SS-3/RS-3 Railing						3	1.535
Vertical Posts	0.938	1.05	0.984	0.003	3.0416	12	0.122
Vertical Posts	0.938	1.05	0.984	0.003	1.53125	12	0.062
Horizontal post	0.938	1.05	0.984	0.003	1.3125	12	0.053
Top Rail				0.012	10.625	1	0.129
Bottom Channel				0.014	10.625	1	0.147
SS-2/RS-2 Railing						9	4.606
Vertical Posts	0.938	1.05	0.984	0.003	3.0416	12	0.122
Vertical Posts	0.938	1.05	0.984	0.003	1.53125	12	0.062
Horizontal post	0.938	1.05	0.984	0.003	1.3125	12	0.053
Top Rail				0.012	10.625	1	0.129
Bottom Channel				0.014	10.625	1	0.147
Utilities				0.097	128.000	1	12.352
						TOTAL (per truss)	12.317

Summary of Loads

Dead loads assumed to be evenly split between right and left trusses

Where applicable, loads are assumed to be split evenly between upper and lower chords

Joint	Primary Member	Percentage	Sway Frame	Percentage	Lateral Bracing	Percentage	Floor System	Percentage	Vertical Load (kip)
L1	L1L2	0.5							0.596
	U1L1	0.5							0.561
	U0L1	0.5							1.115
	Gusset Plate	1							0.294
			Sway Frame	0.5					0.867
					Diagonal Member	0			0
					Gusset Plate	0			0
							FB	0.5	0
							Stringer	0.5	0
							Deck	0	0
L2	L1L2	0.5							0.596
	L2L4	0.5							2.087
	U1L2	0.5							0.711
	L2U3	0.5							0.639
	U2L2	0.5							0.299
	Gusset Plate	1							0.252
			Sway Frame	0.5					0.867
					Diagonal Member	0			0
					Gusset Plate	0			0
							FB	0	0
							Stringer	0	0
							Deck	0	0
L4	L2L4	0.5							2.087
	L4L6	0.5							2.087
	U3L4	0.5							0.582
	L4U5	0.5							0.582
	U4L4	0.5							0.299
	Gusset Plate	1							0.214
			Sway Frame	0.5					0.867
					Diagonal Member	0			0
					Gusset Plate	0			0
							FB	0	0
							Stringer	0	0
							Deck	0	0
	L4L6	0.5							2.087
	L6L8	0.5							1.193
	U5L6	0.5							0.639

L6	L6U7	0.5						0.711
	U6L6	0.5						0.299
	Gusset Plate	1						0.252
			Sway Frame	0.5				0.867
					Diagonal Member	0		0
					Gusset Plate	0		0
							FB 0	0
							Stringer 0	0
							Deck 0	0
L8	L6L8	0.5						1.193
	U7L8	0.5						1.150
	U8L8	0.5						0.299
	Gusset Plate	1						0.222
			Sway Frame	0.5				0.867
					Diagonal Member	0		0
					Gusset Plate	0		0
							FB 0	0
							Stringer 0	0
							Deck 0	0
Pier Support	End Post	0.5						0.236
					Diagonal Member	0		0
					Gusset Plate	0		0
							FB 0	0
							Stringer 0	0
							Deck 0	0
U0	U0U1	0.5						0.957
	U0L1	0.5						1.115
	End Post	0.5						0.236
	Gusset Plate	1						0.482
			Sway Frame	0				0.000
					Diagonal Member	0.25		0.089
					Gusset Plate	1		0.026
							FB 0.5	2.474
							Stringer 0.5	0.909
							Deck 0.25	15.061
U1	U0U1	0.5						0.957
	U1U3	0.5						1.914
	U1L1	0.5						0.561
	U1L2	0.5						0.711
	Gusset Plate	1						0.294
			Sway Frame	0				0.000
					Diagonal Member	0.25		0.089
					Diagonal Member	0.25		0.089
					Gusset Plate	0.5		0.036

						FB	0.5	2.474
						Stringer	0.5	0.909
						Stringer	0.5	0.909
						Deck	0.25	15.061
						Deck	0.25	15.061
	U2L2	0.5						0.299
			Sway Frame	0				0
				Diagonal Member	0.25			0.089
				Diagonal Member	0.25			0.089
				Gusset Plate	1			0.068
U2						FB	0.5	2.474
						Stringer	0.5	0.909
						Stringer	0.5	0.909
						Deck	0.25	15.061
						Deck	0.25	15.061
	U1U3	0.5						1.914
	U3U5	0.5						2.501
	L2U3	0.5						0.639
	U3L4	0.5						0.582
	Gusset Plate	1						0.800
				Diagonal Member	0.25			0.089
U3				Diagonal Member	0.25			0.089
				Gusset Plate	0.5			0.036
						FB	0.5	2.474
						Stringer	0.5	0.909
						Stringer	0.5	0.909
						Deck	0.25	15.061
						Deck	0.25	15.061
	U4L4	0.5						0.299
			Sway Frame	0				0
				Diagonal Member	0.25			0.089
				Diagonal Member	0.25			0.089
				Gusset Plate	1			0.068
U4						FB	0.5	2.474
						Stringer	0.5	0.909
						Stringer	0.5	0.909
						Deck	0.25	15.061
						Deck	0.25	15.061
	U3U5	0.5						2.501
	U5U7	0.5						1.914
	L4U5	0.5						0.582
	U5L6	0.5						0.639
	Gusset Plate	1						0.800
				Diagonal Member	0.25			0.089

U5				Diagonal Member	0.25			0.089
				Gusset Plate	0.5			0.036
						FB	0.5	2.474
						Stringer	0.5	0.909
						Stringer	0.5	0.909
						Deck	0.25	15.061
						Deck	0.25	15.061
	U6L6	0.5						0.299
			Sway Frame	0				0
				Diagonal Member	0.25			0.089
				Diagonal Member	0.25			0.089
				Gusset Plate	1			0.068
U6								
						FB	0.5	2.474
						Stringer	0.5	0.909
						Stringer	0.5	0.909
						Deck	0.25	15.061
						Deck	0.25	15.061
	U5U7	0.5						1.914
	U7U8	0.5						0.957
	L6U7	0.5						0.711
	U7L8	0.5						1.150
	Gusset Plate	1						0.800
				Diagonal Member	0.25			0.089
U7				Diagonal Member	0.25			0.089
				Gusset Plate	0.5			0.036
						FB	0.5	2.474
						Stringer	0.5	0.909
						Stringer	0.5	0.909
						Deck	0.25	15.061
						Deck	0.25	15.061
	U7U8	0.5						0.957
	U8L8	0.5						0.299
			Sway Frame	0				0
				Diagonal Member	0.25			0.089
U8				Gusset Plate	1			0.026
						FB	0.5	2.474
						Stringer	0.5	0.909
						Deck	0.25	15.061

Notes: 1. Compare calculated steel weight (184.081 kips) to design steel weight (186.312 kips) on Sheet 47.

2. Compare calculated concrete volume (119 cu. yds) to design concrete volume (113.3 cu. yds) on Sheet 47.

Total (steel per truss)	92.04
Total (concrete per truss)	240.975
Total	333.02

Summary (by joint)		
L1	3.434	kip
L2	5.452	kip
L4	6.718	kip
L6	6.048	kip
L8	3.731	kip
U0	21.585	kip
U1	39.066	kip
U2	34.96	kip
U3	41.06	kip
U4	34.96	kip
U5	41.06	kip
U6	34.96	kip
U7	40.16	kip
U8	19.82	kip
Dist. On Top Chord	0.0080	k/in
TOTAL	345.333	kip

Live Load Analysis:

- Determine live load effects for HL-93 loading (AASHTO LRFD BDS, 7th ed.) and H-20 loading (AASHO BDS, 1st edition).

1. Determine distribution factors using the lever rule

For One Lane Loaded -

Multiple Presence Factor (m) = 1.2

Distribution Factor (g) $= \frac{32.167 \text{ ft.} - 0.5 \text{ ft.} - 5 \text{ ft.}}{32.167 \text{ ft.}} = 0.84$

mg = 1.2 x 0.84 = 1.0

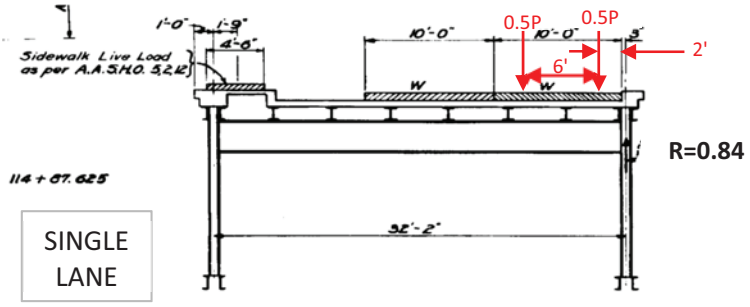

SINGLE LANE

For Two Lanes Loaded -

Multiple Presence Factor (m) = 1.0

Distribution Factor (g) $= (29.917 \text{ ft.} + 16.917 \text{ ft.}) \times \frac{1}{32.167 \text{ft}} = 1.36$

mg = 1.0 x 1.36 = 1.36

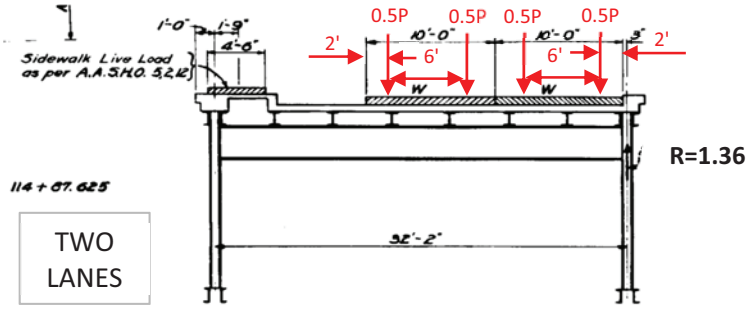

TWO LANES

2. Determine load effects using influence line analysis (undistributed, no impact)

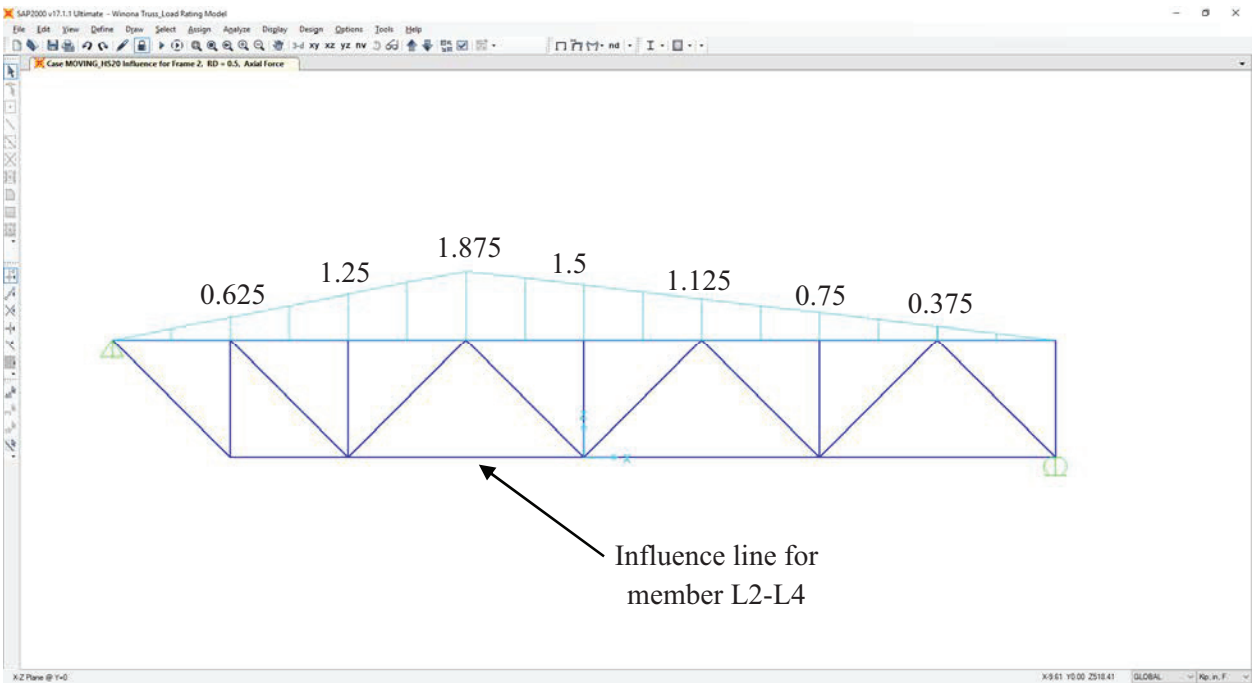

HL-93 Loading (AASHTO LRFD BDS 7th edition)

Design Lane Load	= 0.64k/LF x 0.5(1.875 x 128') = 77 kips
HL-93 Design Truck	= 8k x (1.328) + 32k x (1.875) + 32k x (1.547) = 120 kips
Design Tandem	= 25k x (1.875) + 25k x (1.781) = 91 kips
Fatigue Truck	= 8k x (1.328) + 32k x (1.875) + 32k x (1.172) = 108 kips

H-20 Loading (AASHO 1st edition)

H-20 Truck	= 8k x (1.547) + 32k x (1.875) = 72 kips
Alternate	= 18k x (1.875) + 0.64k/LF x 0.5(1.875 x 128') = 111 kips

3. Determine total load effects (apply distribution and impact factors)

Impact factors

Dynamic Load Allowance, HL-93 Strength = 33%
Dynamic load Allowance, HL-93 Fatigue = 15%
Dynamic Load Allowance, H-20 = 20%

Strength I Live Load

P_{LL+IM} = 77 kips + (120 kips x 1.33)
= 237 kips

mg x P_{LL+IM} = 1.36 x 237 kips
= 322 kips

Fatigue Live Load

P_{LL+IM} = (108 kips x 1.15)
= 124 kips

g x P_{LL+IM} = 0.84 x 124 kips
= 104 kips

H-20 Live Load

P_{LL+IM} = (111 kips) x 1.2
= 133 kips

mg x P_{LL+IM} = 1.36 x 133 kips
= 181 kips (compared to 180 kips on design plans)

Live Load Force Effects (DC = Component, DW = Wearing Surface)

P_{LL+UM} (Strength I) = 322 kips
P_{LL+UM} (Fatigue I) = 134 kips (NOTE: THIS LOAD WAS INCREASED FROM THE VALUE CALCULATED ABOVE TO PRODUCE A FIINITE FATIGUE LIFE)

S-BRITE Center

As infrastructure continues to age, the engineers who designed and had first-hand knowledge of the then new structures (e.g., the Interstate era) eventually exit the workforce. Further, the vast majority of the infrastructure comprises structures built with older materials, design philosophies, and construction practices that are no longer discussed in the classroom. To successfully maintain the existing steel bridge inventory, expertise is needed in the areas of deterioration, fatigue, fracture, corrosion, repair/retrofit, coatings, materials, NDE, riveting, welding, and fabrication. Using Purdue's existing strengths in education and research, the Steel Bridge Research, Inspection, Training, and Engineering (S-BRITE) Center fills a growing need in the transportation industry as it relates to existing and aging steel bridges.

Additional information about the S-BRITE Center is available at https://engineering.purdue.edu/CAI/SBRITE.

Publication

This report was published by the S-BRITE Center at Purdue University. The full content of this technical report (in pdf and e-book formats) is available for download at https://doi.org/10.5703/1288284316925.

Open Access and Collaboration with Purdue University

The Indiana legislature established the Joint Highway Research Project in 1937. In 1997, this collaborative venture between the Indiana Department of Transportation and Purdue University was renamed as the Joint Transportation Research Program (JTRP) to reflect state and national efforts to integrate the management and operation of various transportation modes. Since 1937, the JTRP program has published more than 1,600 technical reports. In 2010, the JTRP partnered with the Purdue University Libraries to incorporate these technical reports in the University's open access digital repository and to develop production processes for rapidly disseminating new research reports via this repository. Affiliated publications have since been added to the JTRP collection, which has exceeded 1.8 million downloads.